THE DEVELOPMENT OF BRAIN STRUCTURE AND CONNECTIVITY

LARA MARISE WIERENGA

thesis_LW_V3.indb 1 06/06/16 07:38

The studies described in this thesis were performed at the Brain Center Rudolf Magnus, Department of Psychiatry, University Medical Center Utrecht, Utrecht, The Netherlands. This thesis was accomplished with financial support from the Netherlands Organisation for Scientific Research (NWO) VICI 453-10-005 to prof. dr. Sarah Durston

Cover design by	Max Unger
Layout by	Lara Wierenga
Printed by	Proefschriftmaken.nl || Uitgeverij BOXPress
Published by	Uitgeverij BOXPress, Vianen
ISBN	978-90-393-6589-2

All rights reserved. No parts of this publication may be reproduced, stored in a retrieval system of any nature, or transmitted in any form or by any means, electronic, mechanical, photocopying, recording or otherwise, without prior permission of the author or, when appropriate, the publishers of the papers.

THE DEVELOPMENT OF BRAIN STRUCTURE AND CONNECTIVITY

De ontwikkeling van hersenstructuur en -verbindingen

PROEFSCHRIFT

ter verkrijging van de graad van doctor aan de Universiteit Utrecht op gezag van de rector magnificus, prof.dr. G.J. van der Zwaan, ingevolge het besluit van het college voor promoties in het openbaar te verdedigen op
maandag 27 juni 2016 des middags te 2.30 uur

door
LARA MARISE WIERENGA
geboren op 10 mei 1986
te Groningen

thesis_LW_V3.indb 3 06/06/16 07:38

Promotor: Prof. dr. S. Durston

Copromotor: Dr. B. Oranje

thesis_LW_V3.indb 4 06/06/16 07:38

Table of contents

Chapter 1	Introduction: Typical and atypical brain development	9
	Part I: Typical development	
Chapter 2	Unique developmental trajectories of cortical thickness and surface area	31
Chapter 3	Typical development of basal ganglia, hippocampus, amygdala and cerebellum from age 7 to 24	67
Chapter 4	The development of brain network architecture	89
	Part II: Atypical development	
Chapter 5	Cortical development in Attention-Deficit/Hyperactivity Disorder: What can it tell us about early developmental mechanisms?	119
Chapter 6	Brain development in adolescents at ultra-high risk for psychosis: longitudinal changes related to resilience	151
Chapter 7	Summary and general discussion	181
	Nederlandse samenvatting	207
	Acknowledgements - dankwoord	217
	List of publications	223
	About the author	226

thesis_LW_V3.indb 5 06/06/16 07:38

thesis_LW_V3.indb 6 06/06/16 07:38

In theory there is no difference between theory and practice

but in practice, there is

-Jan L.A. van de Snepscheut

thesis_LW_V3.indb 7 06/06/16 07:38

thesis_LW_V3.indb 8 06/06/16 07:38

INTRODUCTION
TYPICAL AND ATYPICAL BRAIN DEVELOPMENT

Parts of this chapter are based on a bookchapter (Brain and behavioral development. In The Cambridge Encyclopedia of Child Development. Cambridge, U.K.: Cambridge University Press)
By Lara M Wierenga, Bob Oranje and Sarah Durston

What is this thesis about?

The human brain undergoes profound structural changes with development. It does not mature by simply growing, rather the transition to adulthood is a dynamic process with regionally specific patterns. From as early as two weeks after conception neural connections are formed and consequently neural circuitries shaped. Postnatal brain development shows a complex pattern, with structures increasing and later decreasing in size and connections between some brain regions strengthening while others weaken. Although general patterns have been observed, no two individuals have identical brain developmental trajectories. Hence, in order to fully understand brain development it is essential to study the same individuals over time. This thesis aims to do so; we map the maturation of brain structure and connectivity in longitudinal cohorts of typically and atypically developing children.

Individual variation in brain development is regulated by the interplay between intrinsic genetic programs and environmental exposure. This interplay works in both directions: the environment may trigger genetic programs, and vice versa, genetic programs may make the brain more sensitive to environmental effects, such as learning experiences. An example of such a timing-dependent experience is musical training. Although musical training affects brain structure at all ages, the long-term effects of this experience varies as a function of the age at which training is initiated. This is illustrated by a study of Baharloo et al (2012) who showed that early musical training seems to be essential (but not assured) for the development of absolute pitch. Such early experience are shown to have profound influences on brain structure; musicians who were trained from an early age had higher levels of organization in the corpus callosum than late-trained musicians, independent of the total duration of musical training (Steele, Bailey, Zatorre, & Penhune, 2013).

Studying the timing and pattern of brain development in typically and atypically developing children and adolescents may improve our understanding of what mechanisms shape neural circuitries. For example, we might be able to detect sensitive windows, when plasticity is heightened and consequently experiences have an unusually strong and lasting effect on the formation of brain circuits.

There is no consensus on the timing and shape of growth trajectories of brain structures. This is related to a number of challenges that developmental imaging research faces. One

thesis_LW_V3.indb 10 06/06/16 07:38

complicating factor is the substantial variability in structural size and shape between individuals. Hence, longitudinal study designs are preferred, as these designs permit us to study growth trajectories of brain structures within the same individual rather than comparing them between age groups. Another challenge in studying the development of the human brain is the regional variability in developmental trajectories. This is further complicated by the observation that growth trajectories are non-linear, that could be taken to suggest that the brain is organized differently in childhood, adolescence and adulthood. Hence, it may be the interplay between brain regions, rather than the size of individual brain structures that is crucial to healthy brain function. It is therefore essential to not only study single brain regions, but to compare their development within the context of the whole brain network. In addition, most studies have focused on isolated features of brain regions, for example cortical thickness. However, capturing the multidimensional nature of brain structures (e.g. cortical thickness and surface area) may show important aspects of brain development that would otherwise have been obscured. In this thesis we capitalize on advances in multimodal MRI and use longitudinal study designs to address these issues. This permitted us to map structural brain maturation and connectivity in typical and atypical children and adolescents.

Imaging the developing brain

Pioneering studies in the 1990s observed that the brain is far from fully developed in children and adolescents (Giedd et al., 2015; 1996; Jernigan, Trauner, & Hesselink, 1991; Pfefferbaum et al., 1994). These reports have had a great impact on the scientific approach to and thinking about the relationship between brain and behavioral development in important ways. First, they have shown us that the brain is not fully mature in adolescence. Second, they indicated that brain development is a non-linear process, with periods of rapid growth followed by relative stability. And third, these studies underscore that greater volume does not necessarily imply more efficient functioning. Rather, the brain matures by becoming more specialized and changing the organization of its connectivity. The following paragraphs describe these earlier findings on brain maturation in more detail.

thesis_LW_V3.indb 11 06/06/16 07:38

Volume is relative

A consistent finding in developmental research of the last decade is the inverted U-shaped developmental pattern of the cerebral cortex. However, the exact timing of this pattern differs between studies. Some studies estimated peak volume at age 7 (Aubert-Broche et al., 2013; Steele et al., 2013), while others have estimated volume peaks to occur later (Giedd et al., 1996; 2015; Jernigan et al., 1991; Ostby et al., 2009; Pfefferbaum et al., 1994; Raznahan et al., 2011). Mapping developmental trajectories is complicated by regional heterogeneity in development where, again, not all studies agree upon the patterns observed. For example, peak grey matter volume of the frontal cortex has been estimated as early as age 7 and as late as age 11 (Aubert-Broche et al., 2013; Brain Development Cooperative Group, 2011; Giedd, Blumenthal, & Jeffries, 1999; Lenroot et al., 2007). These discrepancies may be related to methodological factors such as differences between samples or statistical curve fitting methods. Another methodological challenge is related to the inter-individual variability in brain structure and size. Total cortical volume can vary up to 50% between typically developing subjects. The way researchers adjust for this difference highly influences the shape of estimated developmental trajectory. We further discuss this issue in Chapter 2 and Chapter 7. The large variation in brain volume highlights the need for longitudinal cohorts that permit us to map developmental trajectories per individual. To date, a limited number of longitudinal studies have been conducted. The data cohorts used in the present thesis are among the few longitudinal cohorts that are currently available worldwide.

Cortical dimensions

A further challenge in studying the development of the cerebral cortex is its complex shape. The cerebral cortex is essentially a densely folded sheet lying on the pial surface, with a certain surface area and thickness. As such, measuring only its volume does not do the complexity of the structure justice. Recent studies have suggested that there are both overlapping and unique features to the development of different cortical dimensions. For example, a longitudinal study by Raznahan and colleagues showed that most cortical thinning takes place between childhood and early adulthood (2011). In contrast to this decrease in cortical thickness, cortical surface area showed a curvilinear developmental

thesis_LW_V3.indb 12 06/06/16 07:38

trajectory: in early childhood, surface area expanded, while a gradual decrease was observed throughout adolescence.

The developmental pattern of cortical thickness has been investigated in more detail; thickness showed the earliest declines in primary sensory regions followed by higher order association regions, and lastly, the superior temporal cortex (see e.g. Gogtay et al., 2006; Sowell et al., 2004; Shaw et al., 2008). Whether surface area shows a similar regional heterogeneous pattern as observed for cortical thickness is addressed in Chapter 2.

These differences in developmental trajectories of cortical thickness and surface area suggest that there may be different underlying biological mechanisms involved in their development. This has important implications for brain imaging in clinical groups, as one aspect of cortical morphometry may be affected while the other is not. Literature on clinical populations in which developmental trajectories of surface area and thickness are directly compared is scarce. Hence, this thesis also addresses developmental trajectories of multiple cortical dimensions in a longitudinal cohort of children with ADHD and a sample of adolescents at ultra high risk for psychosis in Chapters 5 and 6 respectively.

Subcortical structures

Subcortical structures have often been suggested to show changes in developmental disorders. However, only few studies cover the typical development or inter-individual variation of these structures with contradicting results, perhaps related to different methods used. Knowledge on the typical course and trajectories of subcortical structures is particularly relevant for the interpretation of studies on clinical populations. Hence, we investigate the typical development of subcortical structures in Chapter 3. In the next section we outline what is currently known about the development of the subcortical structures that were assessed in this thesis.

Hippocampus

The hippocampus plays a critical role in memory processes such as the formation of episodic memories. Although it was long believed that the hippocampal formation was near complete at birth, there is increasing evidence of prolonged hippocampal plasticity. It has

thesis_LW_V3.indb 13 06/06/16 07:38

even been suggested that it is the most plastic brain structure throughout life. First, it is one of only two brain structures to show continued neurogenesis through adulthood, the other being the olfactory bulb. But also external stimuli showed to have a direct effect on hippocampus morphology throughout life (DeMaster, Pathman, Lee, & Ghetti, 2014). Such plasticity contrasts with other brain structures, which are reported to become less plastic with age.

Protracted development of the hippocampus is also reflected in early prenatal processes. For example, neural migration in the hippocampus is delayed compared to the neocortex. Postnatally, there is little increase in hippocampus volume in the first two years (Tottenham, Hare, & Quinn, 2010). Although some basic functions, such as relational memory, are already intact at this early age, other processes, such as episodic memory, are not yet fully developed. This is illustrated by the phenomenon of infantile amnesia, where children younger than two years old have a very limited ability to form or store episodic memories for recall later in life. Some studies report substantial structural changes in the hippocampus even throughout early adulthood (e.g. Goddings et al., 2014; Tottenham et al., 2010) while others observed earlier peaks in hippocampal volume (Gogtay et al., 2006; Tamnes et al., 2013). We investigate the developmental trajectory of the hippocampus in Chapter 3.

Amygdala

The amygdala also showed protracted development. However, in contrast to hippocampal development a rapid increase in amygdala volume was observed in the first two years of life (Tottenham et al., 2009). Some studies showed continued changes in amygdala volume throughout adolescence until early adulthood (Goddings et al., 2014; Ostby et al., 2009), while others did not support this finding (Dennison et al., 2013; Koolschijn & Crone, 2013). The amygdala is highly connected with numerous cortical and subcortical regions. As such, it appears to integrate and modulate information across a wide range of domains (Scherf, Smyth, & Delgado, 2013). Given the degree of its connectivity, small changes in amygdala function may have widespread consequences. This structure has been hypothesized to play a central role in the behaviors typically observed in adolescence (Scherf et al., 2013), such as increased interactions with peers. If this is true, this might be reflected in its developmental trajectory, and volumetric changes are expected to continue into adolescence (see Chapter 3).

thesis_LW_V3.indb 14 06/06/16 07:38

Striatum

The striatum is a major relay station in subcortical-cortical circuitry, linking the thalamus and cortex. Its role in voluntary movement is long established, as damage to this structure causes major movement problems. However, more recent studies have also shown its involvement in higher-order cognition. This is reflected in its reciprocal connections with the frontal cortex, where three distinct frontal-striatal circuitries can be identified: the lateral orbito-frontal circuit, dorsolateral prefrontal circuit and anterior cingulate circuit. These circuits are involved in different aspects of cognition: motivation and reward, cognitive control and attention, respectively. Changes in these circuits have been associated with cognitive deficits in almost all developmental disorders, stressing the importance of the striatum for cognitive functioning.

Furthermore, these fronto-striatal circuitries showed heterogeneous developmental patterns that have been hypothesized to be related to behaviors typical of certain developmental stages. For example, the typically adolescent behavior of increased risk seeking has been hypothesized to relate to an imbalance between the cortical and sub-cortical brain regions: sensitivity to reward (related to the orbito-frontal circuit) follows in an inverted U-shaped developmental pattern, with a peak in reward sensitivity between age 14 and 16 years of age (Somerville & Casey, 2010). In contrast, the behavioral development of cognitive control (related to the dorsolateral circuit) appeared to show a linear trajectory. Together, this may result in an imbalance between the frontal-striatal circuitries where reward seeking peaks before cognitive control is fully mature. This is supported by functional imaging studies that showed imbalances in responsiveness of these neural circuitries. Different subparts of the striatum showed different developmental trajectories, although large discrepancies between studies exist: some studies show mainly linear decreases in the nucleus accumbens, caudate and putamen volumes (Goddings et al., 2014; Ostby et al., 2009; Tamnes et al., 2013) others did not find any significant changes during the same age period (Koolschijn & Crone, 2013; Lenroot et al., 2007). We investigate the heterogeneous pattern of striatal development in Chapter 3 using a longitudinal study design. In addition, the close relationship with the frontal cortex underlines the importance of studying connectivity between these structures, which we address in Chapter 4.

thesis_LW_V3.indb 15 06/06/16 07:38

Cerebellum

Although the cerebellum contains approximately 80% of neurons in the brain, surprisingly few studies have investigated the development of this structure. This neglect may arise from the long-standing belief that the cerebellum was primarily involved in motor functions including balance, fine tuning of movements, and complex motor sequences. However, there is increasing evidence showing that this structure also plays a critical role in higher order cognitive functions: first, functional imaging studies showed activity in the cerebellum during the performance of a wide range of cognitive tasks. Second, the cerebellum is both functionally and structurally connected to prefrontal regions that are critically involved in complex tasks, e.g. selection of appropriate verbs (Diamond, 2000). Furthermore, the cerebellum showed a protracted developmental trajectory (as is reviewed by Hibi & Shimizu, 2012) similar to prefrontal regions that are critical for cognition (Tiemeier et al., 2010). This supports the notion that cerebellum may be closely involved in the development of cognitive functions. However, its protracted developmental pattern may also render the cerebellum more vulnerable to environmental factors such as nutrient restriction. The cerebellum has indeed been shown to be one of the least heritable brain structures and its development may therefore be relatively more influenced by experience and environmental factors than other structures (Giedd et al., 2015). Additionally, the cerebellum is the brain structure that has most consistently been reported to show changes in autism and ADHD. Children with these disorders often show abnormalities in motor development in addition to cognitive abnormalities. This further stresses the close relationship between the function and development of cerebellum and prefrontal regions. We will address its developmental trajectory in Chapter 3.

thesis_LW_V3.indb 16 06/06/16 07:38

Brain connectivity

No single brain region operates in isolation. Rather complex behaviors emerge from a network of neural interactions. Functional imaging studies show that during the performance of a cognitive task a distributed network of brain regions are activated. However, it is likely that these tasks tap into multiple cognitive processes making it challenging to assess the organization of these neural brain systems solely based on task activation (Mesulam, 1990). Methods that assess the infrastructure that supports connectivity may provide novel insights in to the organization and development of these distributed brain systems.

The importance of healthy structural connectivity is reflected in the fine-tuning process of the frontal-striatal circuitry; risky behavior that is so typical for adolescents has been associated with a developmental imbalance between the striatum and prefrontal cortex. Thus, it is the timing and integration of these structures within the brain network rather than their individual developmental trajectories that is crucial to behavioral maturation. Deviations in timing may cause (temporary) imbalances in these functional circuitries leading to abnormal behavior. This underlines the importance of studying the development of brain structures within the context of the brain network.

Development of connectivity

Axonal fiber bundles connecting one region to another can be visualized using diffusion weighted imaging (DWI). Changes in diffusion measures inform us on the integrity of white matter bundles and are thought to capture changes in myelination, among other factors (see general discussion for further details). Myelinated axons can transmit signals up to three hundred times faster than unmyelinated axons (Walhovd, Johansen-Berg, & Káradóttir, 2014). Myelination is therefore crucial to the increase in speed of information processing in the brain. Axon myelination continues into mid-adulthood. By 20 years of age, males have a total of 176.000 km of myelinated axons compared to 149.000 km in females. This constitutes approximately half the distance to the moon. A peak in total myelin volume has been observed around age 30, decreasing 10% per decade thereafter (Dennis & Thompson, 2013). The developmental increase in myelination before age 30 years was found to be heterogeneous with different fiber tracts maturing at different ages.

thesis_LW_V3.indb 17 06/06/16 07:38

For example, the corticospinal tract is one of the first bundles to mature, and is thought to contribute to the relatively early maturation of sensations and most motor functions (Dennis & Thompson, 2013). A major challenge in information processing in the brain is to synchronize signal input from axons of different lengths. Consequently, a tight coordination of the myelination process across the brain is critical to healthy development. However, unraveling the developmental pattern and timing of this process is challenging.

Graph theory

Rather than investigating the development of single tracts, an integrative approach including all connections in the brain allows for the assessment of the topological organization of the brain network. By using graph theory, the brain can be represented as a network of nodes (brain regions) and edges (connections or correlations). Edges can be weighted, where the weight represent the quality of that connection often thought to reflect some aspect of communication strength. This method allows us to describe the organization of complex networks such as the brain. Commonly used features are path length, node strength and clustering. Path length is defined as the number of edges that need to be crossed to get from any given node i to any other node j. The global path length of the brain is the average path length for all nodes in the network. Shorter global path length permits more efficient information transfer in the network. Node strength is the sum of weighted edges in a given node i, reflecting how strongly that brain region is wired within the brain. Clustering is an indicator of how well neighbors of a given node i are also connected to each other. These properties may differ per brain region.

An increasing number of studies used graph theory to address the development of the brain network. However, findings have been inconsistent. For instance, both developmental increases and decreases in global network efficiency have been reported; Hagmann and colleagues (2010) showed a linear increase in global efficiency of structural brain connectivity, while Dennis and colleagues (2013) could not replicate this finding. This discrepancy may be related to differences in methodology, sample size and age ranges included. Longitudinal cohorts that are covering a wide age range are essential for a better understanding of the complex heterogeneous developmental pattern of the structural brain network, such as in Chapter 4.

thesis_LW_V3.indb 18 06/06/16 07:38

Atypical brain development

A better understanding of typical brain development can also be gained from studying atypical brain development. This approach shows parallels with the classic method of lesion studies, where knowledge about brain function is derived from examining patients with lesions in specific brain regions. We used a variation on this approach by deriving lessons on typical brain development by studying brain developmental patterns in developmental disorders. This allows us to investigate complex cognitive functions from a developmental perspective. We studied both a childhood onset and adolescent onset developmental disorder, in Chapter 5 and 6 respectively. In line with the "moving parts get broken" idea, we hypothesize that symptoms that emerge at certain ages are associated with brain regions that show important developmental processes during that age period.

Childhood onset

The most frequently diagnosed childhood onset developmental disorder is ADHD, with a worldwide prevalence of five percent (Polanczyk & Rohde, 2007). Although the main behavioral symptoms are related to inattention, hyperactivity and impulsivity, cognitive domains are often affected. These include deficits in response inhibition, reward processing and timing (Durston, van Belle, & de Zeeuw, 2011). Studies on brain structure showed consistently smaller total brain volumes in children with ADHD compared to typically developing children (Durston et al., 2011; Friedman & Rapoport, 2015). These reductions are most pronounced in the prefrontal cortex, basal ganglia and cerebellum. Not only does the cortex show reductions in volume, the developmental trajectory of both cortical thickness and surface area have been shown to lag behind those of typically developing children (Shaw et al., 2007; 2012). Yet the developmental trajectories of thickness and surface area have not been directly compared. Hence, we assessed longitudinal changes in both cortical thickness and surface area in a cohort of children with and without ADHD in Chapter 5.

thesis_LW_V3.indb 19 06/06/16 07:38

Adolescent onset

Many psychiatric disorders including anxiety disorder, bipolar disorder, depression, eating disorders, substance use disorders and psychosis commonly emerge in adolescence (Kessler et al., 2005). Interestingly, these disorders have been linked to abnormalities in the prefrontal cortex, one of the structures showing substantial change during adolescence (Paus, Keshavan, & Giedd, 2008). However, whether brain changes in psychiatric disorders are related to the onset of disease or are already present at an early age is hard to unravel as these individuals are usually monitored after disease onset.

Psychosis is one of the most disabling and costly disorders for society, affecting 1,2% of the European population (Zdanowicz, Mees, Jacques, Tordeurs, & Reynaert, 2014). Hence, a lot of research has focused on early detection of this disorder. Individuals who show sub-threshold clinical symptoms can be considered to be at "ultra high risk" of developing psychosis later in life. Hence, studying these individuals may be particularly useful for investigating the role of the prefrontal cortex in the onset of psychosis during adolescence.

Individuals at ultra high risk have been shown to have reductions in frontal and temporal grey matter volume as well as in anterior cingulate gyrus and hippocampal regions (Bois et al., 2014; Fusar-Poli, Radua, McGuire, & Borgwardt, 2012). About 30 to 40 percent of these individuals had a psychotic episode within two years, but also approximately half of these patients fully remitted from their subclinical symptoms within two years. The classification of individuals at high risk allows us to closely monitor brain changes before onset of psychosis. Most studies to date have used cross-sectional data and results have been contradictory. In order to study brain changes related to the onset of disease we follow individuals at "ultra high risk" before onset of psychosis and compare developmental trajectories of individuals with good and poor clinical outcome in Chapter 6.

thesis_LW_V3.indb 20 06/06/16 07:38

Outline of this thesis

In Chapter 2, we map typical developmental patterns of the cortex. We focus on the regional patterns of the development of cortical surface area, cortical volume and thickness. In Chapter 3, we investigate the typical development of subcortical structures. We study regions that have often been indicated to show changes in clinical populations including the thalamus, amygdala, hippocampus, caudate, globus pallidum, nucleus accumbens and cerebellum. The focus of Chapter 4 is how connectivity between cortical and subcortical structures changes with development. We address the development of connectivity by comparing maturational changes for different fiber classes (projection, inter hemispheric and association fibers) in addition to global changes in network topology using graph theory. In Chapters 5 and 6 we focus on brain development in children with attention deficit/hyperactivity disorder (ADHD) and individuals at "ultra high risk" for psychosis. We discuss the implications of our findings in Chapter 7.

thesis_LW_V3.indb 21 06/06/16 07:38

References

Andersen, S. L., & Teicher, M. H. (2008). Stress, sensitive periods and maturational events in adolescent depression. Trends in Neurosciences.

Aubert-Broche, B., Fonov, V. S., García-Lorenzo, D., Mouiha, A., Guizard, N., Coupé, P., et al. (2013). A new method for structural volume analysis of longitudinal brain MRI data and its application in studying the growth trajectories of anatomical brain structures in childhood. NeuroImage, 82, 393–402. http://doi.org/10.1016/j.neuroimage.2013.05.065

Bois, C., Levita, L., Ripp, I., Owens, D. C. G., Johnstone, E. C., Whalley, H. C., & Lawrie, S. M. (2014). Longitudinal changes in hippocampal volume in the Edinburgh High Risk Study of Schizophrenia. Schizophrenia Research. http://doi.org/10.1016/j.schres.2014.12.003

Brain Development Cooperative Group. (2011). Total and Regional Brain Volumes in a Population-Based Normative Sample from 4 to 18 Years: The NIH MRI Study of Normal Brain Development. Cerebral Cortex, 22(1), 1–12. http://doi.org/10.1093/cercor/bhr018

Brown, T. T., & Jernigan, T. L. (2012). Brain Development During the Preschool Years. Neuropsychology Review, 22(4), 313–333. http://doi.org/10.1007/s11065-012-9214-1

DeMaster, D., Pathman, T., Lee, J. K., & Ghetti, S. (2014). Structural development of the hippocampus and episodic memory: developmental differences along the anterior/posterior axis. Cerebral Cortex, 24(11), 3036–3045. http://doi.org/10.1093/cercor/bht160

Dennis, E. L., & Thompson, P. M. (2013). Typical and atypical brain development: a review of neuroimaging studies. Dialogues in Clinical Neuroscience, 15(3), 359–384.

Dennis, E. L., Jahanshad, N., McMahon, K. L., de Zubicaray, G. I., Martin, N. G., Hickie, I. B., et al. (2013). Development of brain structural connectivity between ages 12 and 30: A 4-Tesla diffusion imaging study in 439 adolescents and adults. NeuroImage, 64, 671–684. http://doi.org/10.1016/j.neuroimage.2012.09.004

Dennison, M., Whittle, S., Yücel, M., Vijayakumar, N., Kline, A., Simmons, J., & Allen, N.

thesis_LW_V3.indb 22 06/06/16 07:38

B. (2013). Mapping subcortical brain maturation during adolescence: evidence of hemisphere- and sex-specific longitudinal changes. Developmental Science, 16(5), 772–791. http://doi.org/10.1111/desc.12057

Diamond, A. (2000). Close interrelation of motor development and cognitive development and of the cerebellum and prefrontal cortex. Child Development, 71(1), 44–56.

Durston, S., van Belle, J., & de Zeeuw, P. (2011). Differentiating frontostriatal and fronto-cerebellar circuits in attention-deficit/hyperactivity disorder. Biological Psychiatry, 69(12), 1178–1184. http://doi.org/10.1016/j.biopsych.2010.07.037

Friedman, L. A., & Rapoport, J. L. (2015). Brain development in ADHD. Current Opinion in Neurobiology, 30, 106–111. http://doi.org/10.1016/j.conb.2014.11.007

Fusar-Poli, P., Radua, J., McGuire, P., & Borgwardt, S. (2012). Neuroanatomical maps of psychosis onset: voxel-wise meta-analysis of antipsychotic-naive VBM studies. Schizophrenia Bulletin, 38(6), 1297–1307. http://doi.org/10.1093/schbul/sbr134

Giedd, J. N., Blumenthal, J., & Jeffries, N. O. (1999). Brain development during childhood and adolescence: a longitudinal MRI study. Nature Neuroscience 2, 861 – 863. doi:10.1038/13158

Giedd, J. N., Raznahan, A., Alexander-Bloch, A., Schmitt, E., Gogtay, N., & Rapoport, J. L. (2015). Child psychiatry branch of the National Institute of Mental Health longitudinal structural magnetic resonance imaging study of human brain development. Neuropsychopharmacology : Official Publication of the American College of Neuropsychopharmacology, 40(1), 43–49. http://doi.org/10.1038/npp.2014.236

Giedd, J. N., Snell, J. W., Lange, N., Rajapakse, J. C., Casey, B. J., Kozuch, P. L., et al. (1996). Quantitative Magnetic Resonance Imaging of Human Brain Development: Ages 4–18. Arch Dis Child 2002;87:279-283 doi:10.1136/adc.87.4.279

Goddings, A.-L., Mills, K. L., Clasen, L. S., Giedd, J. N., Viner, R. M., & Blakemore, S.J. (2014). The influence of puberty on subcortical brain development. NeuroImage, 88, 242–251. http://doi.org/10.1016/j.neuroimage.2013.09.073

Gogtay, N., Nugent, T. F., Herman, D. H., Ordonez, A., Greenstein, D., Hayashi, K. M., et al. (2006). Dynamic mapping of normal human hippocampal development. Hippocampus,

thesis_LW_V3.indb 23 06/06/16 07:38

16(8), 664–672. http://doi.org/10.1002/hipo.20193

Hagmann, P., Sporns, O., Madan, N., Cammoun, L., Pienaar, R., Wedeen, V. J., et al. (2010). White matter maturation reshapes structural connectivity in the late developing human brain. Proceedings of the National Academy of Sciences, 107(44), 19067–19072. http://doi.org/10.1073/pnas.1009073107

Herculano-Houzel, S. (2009). The human brain in numbers: a linearly scaled-up primate brain. Frontiers in Human Neuroscience, 3, 31. http://doi.org/10.3389/neuro.09.031.2009

Hibi, M., & Shimizu, T. (2012). Development of the cerebellum and cerebellar neural circuits. Developmental Neurobiology, 72(3), 282–301. http://doi.org/10.1002/dneu.20875

Jernigan, T. L., Trauner, D. A., & Hesselink, J. R. (1991). Maturation of human cerebrum observed in vivo during adolescence. Brain : a Journal of Neurology. http://doi.org/10.1093/brain/114.5.2037

Kessler, R. C., Berglund, P., Demler, O., Jin, R., Merikangas, K. R., & Walters, E. E. (2005). Lifetime prevalence and age-of-onset distributions of DSM-IV disorders in the National Comorbidity Survey Replication. Archives of General Psychiatry, 62(6), 593–602. http://doi.org/10.1001/archpsyc.62.6.593

Koolschijn, P. C. M. P., & Crone, E. A. (2013). Sex differences and structural brain maturation from childhood to early adulthood. Developmental Cognitive Neuroscience, 5, 106–118. http://doi.org/10.1016/j.dcn.2013.02.003

Lenroot, R. K., Gogtay, N., Greenstein, D. K., Wells, E. M., Wallace, G. L., Clasen, L. S., et al. (2007). Sexual dimorphism of brain developmental trajectories during childhood and adolescence. NeuroImage, 36(4), 1065–1073. http://doi.org/10.1016/j.neuroimage.2007.03.053

Mesulam, M. M. (1990). Large scale neurocognitive networks and distributed processing for attention. Annals of Neurology, 28(5), 597–613. http://doi.org/10.1002/ana.410280502

Ostby, Y., Tamnes, C. K., Fjell, A. M., Westlye, L. T., Due-Tonnessen, P., & Walhovd, K. B. (2009). Heterogeneity in Subcortical Brain Development: A Structural Magnetic Resonance Imaging Study of Brain Maturation from 8 to 30 Years. The Journal of

thesis_LW_V3.indb 24 06/06/16 07:38

Neuroscience : the Official Journal of the Society for Neuroscience, 29(38), 11772–11782. http://doi.org/10.1523/JNEUROSCI.1242-09.2009

Paus, T., Keshavan, M., & Giedd, J. N. (2008). Why do many psychiatric disorders emerge during adolescence? Nature Reviews. Neuroscience, 9(12), 947–957. http://doi.org/10.1038/nrn2513

Pfefferbaum, A., Mathalon, D. H., Sullivan, E. V., Rawles, J. M., Zipursky, R. B., & Lim, K. O. (1994). A Quantitative Magnetic Resonance Imaging Study of Changes in Brain Morphology From Infancy to Late Adulthood. Archives of Neurology, 51(9), 874–887. http://doi.org/10.1001/archneur.1994.00540210046012

Polanczyk, G., & Rohde, L. A. (2007). Epidemiology of attention-deficit/hyperactivity disorder across the lifespan. Current Opinion in Psychiatry, 20(4), 386–392. http://doi.org/10.1097/YCO.0b013e3281568d7a

Raznahan, A., Shaw, P., Lalonde, F., Stockman, M., Wallace, G. L., Greenstein, D., et al. (2011). How does your cortex grow? The Journal of Neuroscience : the Official Journal of the Society for Neuroscience, 31(19), 7174–7177. http://doi.org/10.1523/JNEUROSCI.0054-11.2011

Scherf, K. S., Smyth, J. M., & Delgado, M. R. (2013). The amygdala: An agent of change in adolescent neural networks. Hormones and Behavior, 64(2), 298–313. http://doi.org/10.1016/j.yhbeh.2013.05.011

Shaw, P., Eckstrand, K., Sharp, W., Blumenthal, J., Lerch, J. P., Greenstein, D., et al. (2007). Attention-deficit/hyperactivity disorder is characterized by a delay in cortical maturation. Proceedings of the National Academy of Sciences, 104(49), 19649–19654. http://doi.org/10.1073/pnas.0707741104

Shaw, P., Kabani, N. J., Lerch, J. P., Eckstrand, K., Lenroot, R., Gogtay, N., et al. (2008). Neurodevelopmental trajectories of the human cerebral cortex. The Journal of Neuroscience : the Official Journal of the Society for Neuroscience, 28(14), 3586–3594. http://doi.org/10.1523/JNEUROSCI.5309-07.2008

Shaw, P., Malek, M., Watson, B., Sharp, W., Evans, A., & Greenstein, D. (2012). Development of cortical surface area and gyrification in attention-deficit/hyperactivity disorder. Biological Psychiatry, 72(3), 191–197. http://doi.org/10.1016/j.biopsych.2012.01.031

thesis_LW_V3.indb 25 06/06/16 07:38

Somerville, L. H., & Casey, B. J. (2010). Developmental neurobiology of cognitive control and motivational systems. Current Opinion in Neurobiology, 20(2), 236–241. http://doi.org/10.1016/j.conb.2010.01.006

Sowell, E. R., Thompson, P. M., Leonard, C. M., Welcome, S. E., Kan, E., & Toga, A. W. (2004). Longitudinal Mapping of Cortical Thickness and Brain Growth in Normal Children. The Journal of Neuroscience : the Official Journal of the Society for Neuroscience, 24(38), 8223–8231. http://doi.org/10.1523/JNEUROSCI.1798-04.2004

Steele, C. J., Bailey, J. A., Zatorre, R. J., & Penhune, V. B. (2013). Early Musical Training and White-Matter Plasticity in the Corpus Callosum: Evidence for a Sensitive Period. The Journal of Neuroscience : the Official Journal of the Society for Neuroscience, 33(3), 1282–1290. http://doi.org/10.1523/JNEUROSCI.3578-12.2013

Tamnes, C. K., Walhovd, K. B., Dale, A. M., Østby, Y., Grydeland, H., Richardson, G., et al. (2013). Brain development and aging: Overlapping and unique patterns of change. NeuroImage, 68, 63–74. http://doi.org/10.1016/j.neuroimage.2012.11.039

Tiemeier, H., Lenroot, R. K., Greenstein, D. K., Tran, L., Pierson, R., & Giedd, J. N. (2010). Cerebellum development during childhood and adolescence: a longitudinal morphometric MRI study. NeuroImage, 49(1), 63–70. http://doi.org/10.1016/j.neuroimage.2009.08.016

Tottenham, N., Hare, T. A., & Quinn, B. T. (2010). Prolonged institutional rearing is associated with atypically large amygdala volume and difficulties in emotion regulation. Developmental Science, 13(1), 46–61. http://doi.org/10.1111/j.1467-7687.2009.00852

Walhovd, K. B., Johansen-Berg, H., & Káradóttir, R. T. (2014). Unraveling the secrets of white matter – Bridging the gap between cellular, animal and human imaging studies. Neuroscience, 276, 2–13. http://doi.org/10.1016/j.neuroscience.2014.06.058

Zdanowicz, N., Mees, L., Jacques, D., Tordeurs, D., & Reynaert, C. (2014). Assessment and treatment of the risk of psychosis in adolescents--a review. Psychiatria Danubina, 26(2), 115–121.

Zhao, T., Cao, M., Niu, H., Zuo, X.-N., Evans, A., He, Y., et al. (2015). Age-related changes in the topological organization of the white matter structural connectome across the human lifespan. Human Brain Mapping. http://doi.org/10.1002/hbm.22877

thesis_LW_V3.indb 26 06/06/16 07:38

thesis_LW_V3.indb 27 06/06/16 07:38

PART I

Typical development

thesis_LW_V3.indb 29 06/06/16 07:38

UNIQUE DEVELOPMENTAL TRAJECTORIES OF CORTICAL THICKNESS AND SURFACE AREA

Lara M Wierenga
Marieke Langen
Bob Oranje
Sarah Durston

NeuroImage 2014: 87, 120–126

thesis_LW_V3.indb 31 06/06/16 07:38

Abstract

There is evidence that the timing of developmental changes in cortical volume and thickness varies across the brain, although the processes behind these differences are not well understood. In contrast to volume and thickness the regional developmental trajectories of cortical surface area have not yet been described. The present study used a combed cross-sectional and longitudinal design with 201 MRI-scans (acquired at 1.5-T) from 135 typically developing children and adolescents. Scans were processed using FreeSurfer software and the Desikan–Killiany atlas. Developmental trajectories were estimated using mixed model regression analysis. Within most regions cortical thickness showed linear decreases with age, whereas both cortical volume and surface area showed curvilinear trajectories. On average, maximum surface area occurred later in development than maximum volume. Global gender differences were more pronounced in cortical volume and surface area than in average thickness. Our findings suggest that developmental trajectories of surface area and thickness differ across the brain, both in their pattern and their timing, and that they also differ from the developmental trajectory of global cortical volume. Taken together, these findings indicate that the development of surface area and thickness is driven by different processes, at least in part.

thesis_LW_V3.indb 32 06/06/16 07:38

Introduction

The human brain undergoes dynamic structural changes during development that continue into early adulthood and beyond. Interestingly, factors such as gender, cognitive ability, or psychiatric disorders are often more related to changes in the developmental trajectories of brain areas than to differences in brain structure at any time point in development (Lenroot et al., 2007; Shaw et al., 2006; 2012; Tamnes et al., 2011). Furthermore, different tissue types, brain structures, and neural circuits follow distinct developmental trajectories: whereas white matter increases monotonously until early adulthood, gray matter volume follows an inverted U-shaped trajectory, peaking in late childhood (Giedd and Rapoport, 2010; Lenroot et al., 2007; Reiss et al., 1996; Sowell et al., 1999; 2002; Wilke et al., 2007). The volume of cortical gray matter is likely to reflect numerous characteristics of the underlying neural architecture, such as the number of columns and cells (Panizzon et al., 2009; Rakic, 1995). In turn, these microstructural characteristics may be reflected differentially in its two composite dimensions: cortical thickness and cortical surface area.

The global pattern of early increases in cortical volume and thickness followed by decreases in adolescence is seen throughout the cortex. However, there are regional differences in the timing of this pattern (Giedd et al., 1999; Gogtay et al., 2004; Sowell et al., 2001). Studies have suggested that primary sensory areas show peak volume and thickness first. This is then followed by peaks in higher order association areas in parietal and prefrontal regions (Shaw et al., 2008; Sowell et al., 2004). Although cortical volume is defined as the product of cortical thickness and surface area, very few studies have actively investigated surface area. One recent study by Raznahan et al. (2011) showed curvilinear development of total surface area, with the peak occurring later in males than in females. Most studies have investigated only one of these three measures (cortical volume, thickness or surface area). However, it is not necessarily the case that developmental changes observed in only one dimension give the best assessment of maturation, as other biological factors may contribute to the changes in cortical thickness and surface area (cortical volume is the product of the two). Furthermore, it is unclear to what degree the developmental trajectories of cortical thickness and surface area vary locally, both in terms of their patterns and their timing. Therefore we set out to investigate regional developmental

thesis_LW_V3.indb 33 06/06/16 07:38

changes in cortical volume, thickness and surface area in typically developing children. We used a surface based method to compare these developmental trajectories in a combined cross- sectional and longitudinal study design. More than 200 MRI scans from 135 typically developing children and adolescents were included. We hypothesized that the developmental trajectories of cortical thickness and surface area would not be parallel, but would differ both in their onset and timing. Second, we hypothesized that the developmental patterns of cortical thickness and surface area would differ between cortical regions.

Materials and methods

Participants

The present study included a total of 201 MRI-scans from 135 typically developing individuals (92 males; 43 females); 49 participants were scanned twice or more, with an average interval of two years, and an interval range from 1.5 to 5.5 years. Participants were aged between 7.0 and 23.3 years, with above average intellectual levels (see Table 1 for

Table 1 Demographic details

	Group	
Characterstics	Male	Female
Number of individuals, n	92	43
Handedness, n		
Right-handed	73	39
Not Right-handed	19	4
Height, mean (SD)	163.6 (20.9)	155.2 (17.2)
Weight, mean (SD)	53.66 (19.3)	49.09 (16.2)
IQ, mean (SD)	113.2 (16.2)	123.5 (14.2)
Sibling, n	30	6
Total number of scans, n	145	56
Number of scans, n		
1	52	34
2	28	5
≥3	12	4
Age at scan, years		
Mean (SD)	12.6 (4.0)	12.5 (4.2)
Range	7.0 - 23.3	7.0 - 23.0

SD, standard deviation; IQ, intelligence quotient.

thesis_LW_V3.indb 34 06/06/16 07:38

participant characteristics). Participants were recruited through schools and educational centers in the area. For all participants under 18 years of age, a parent participated in a semi-structured interview session with a trained rater to confirm the absence of any psychiatric diagnosis (Diagnostic Interview Schedule for Children [DISC-P])(Costello et al., 1985). In older subjects, the Mini-International Neuropsychiatric Interview (MINI) was conducted to confirm the absence of psychopathology (Sheehan et al., 1998). Individuals with a psychiatric diagnosis (current or prior), major physical illness of the cardiovascular, the endocrine, the pulmonary or the gastrointestinal system, neurological illness, a history of head trauma with unconsciousness, organic brain damage or disease, alcohol or other drug dependence, or full-scale IQ below 75 were excluded from participation. In addition, individuals with a first-degree relative suffering from a psychiatric illness were excluded.

Written informed consent was obtained from all participants. For children under 18 years of age, a parent signed for consent. All individuals participated in at least one or more MRI scanning session and a neuropsychological assessment (Wechsler Adult Intelligence Scale/ Wechsler Adult Intelligence Scale-Third Edition [WAIS/WAIS -III] (Wechsler and Wechsler, 2000); Wechsler Intelligence Scale for Children-Revised/ Wechsler Intelligence Scale for Children-Third Edition [WISC-R/WISC -III] (Van Haasen et al., 1986). Furthermore, participants and their parents filled out a questionnaire on hand preference (van Strien, 2003) and a questionnaire related to major physical or neurological illness. Children under 13 years of age were acclimated to the scanning procedure in a dummy-scan session prior to the actual MRI session (Durston et al., 2009). An independent clinical neuroradiologist evaluated all MRI scans. No gross abnormalities were reported for any of the participants. The procedure was approved by the Institutional Review Board of the University Medical Center Utrecht, The Netherlands.

Image acquisition

Magnetic resonance imaging (MRI) scans were acquired on two identical Philips Achieva 1.5 Tesla scanners, using identical 6 element SENSE receiver head coils (Philips, Best, The Netherlands). For definition of all brain measures, a whole brain T1-weighted three-dimensional fast field echo scan with 160–180; 1 mm × 1 mm × 1.2 mm contiguous coronal slices was acquired (256 × 256 matrix, FoV = 256 mm, echo time (TE) = 4.6

thesis_LW_V3.indb 35 06/06/16 07:38

ms, repetition time (TR) = 30 ms, flip angle = 30°). There were no significant differences between scanners on any measures.

Image processing
Cortical reconstruction and volumetric segmentation

All MRI scans were coded to ensure rater blindness to subject identity. Scans were processed and analyzed using the neuroimaging computer network of the department of Psychiatry, University Medical Center Utrecht. Cortical thickness and surface area were estimated using FreeSurfer v5.1.0 software. This is a well-validated and well-documented software program that is freely available for download online (http://surfer.nmr.mgh.harvard.edu/). Technical details of the automated reconstruction scheme are described elsewhere (e.g. Dale et al., 1999; Fischl et al., 1999).

In short, the automated reconstruction involves motion correction, removal of non-brain tissue using a hybrid watershed/surface deformation procedure (Clarkson et al., 2011; Segonne et al., 2004), Talairach transformation (affine registration), segmentation of subcortical white matter, deep gray matter structures and cerebellar structures (Fischl et al., 2004a,b; Hutton et al., 2009; Salat, 2004), intensity normalization (Sled et al., 1998); tessellation of gray white matter boundary automated topology correction (Fischl et al., 2001; Segonne et al., 2007), and surface deformation.

Thickness measurements for each vertex on the tessellated surface were obtained by calculating the closest distance between representations of the cortical surface and the gray/white matter border (Fischl and Dale, 2000). Because the maps are not restricted to the voxel resolution of the original data, this vertex wise surface reconstruction is a powerful method to detect sub-millimeter change. The morphometric procedures have been demonstrated to show good test–retest reliability across scanner manufacturers and across field strengths (Han et al., 2006; Reuter et al., 2012).

For each individual scan, surface-based maps were constructed for analysis. Thirty-four cortical structures were labeled per hemisphere using the Desikan–Killiany atlas (Desikan et al., 2006). This labeling process involved surface inflation (Fischl et al., 1999) and registration to a spherical atlas based on subject specific cortical folding patterns (Fischl et al., 2004a,b). As information from multiple morphological properties was used to

thesis_LW_V3.indb 36 06/06/16 07:38

define anatomical landmarks, the accuracy was larger than for volume-based registration approaches in children (Ghosh et al., 2010). For each labeled cortical structure, average thickness (in mm) surface area (in mm^2) and volume (in mm^3) was calculated (as is illustrated in Figure 1).

Third, TBV was not equally related to volume in all cortical regions, meaning that the extent of overcorrection would also have differed between regions. Therefore, we chose to explore uncorrected measures of cortical volume, thickness and surface area.

Before quantitative analyses could be performed, output required qualitative inspection (Dewey et al., 2010). Surface reconstruction, cortical parcellation and white matter segmentation were therefore evaluated for accuracy by three experienced raters. Manual edits were performed where needed. Edits included removal of non-brain tissue and perfecting the white matter mask. For these manual interventions standard procedures, documented on the FreeSurfer website, were used.

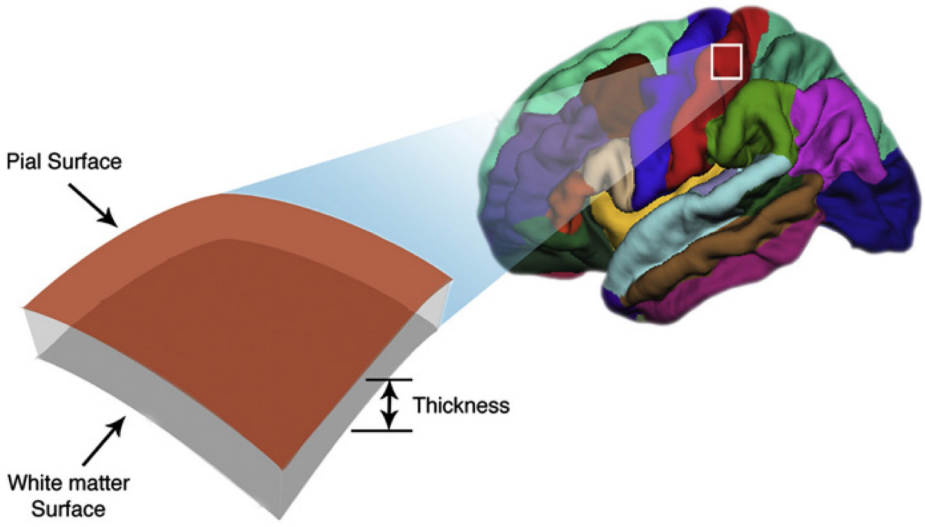

Figure 1 Graphical representation of cortical thickness and surface area. Cortical thickness was estimated as the distance between the white and pial surfaces, averaged over all vertices (in mm). Surface area is the area of the white matter surface (in cm^2), whereas cortical volume was calculated as the product of thickness and surface area (in cm^3).

thesis_LW_V3.indb 37 06/06/16 07:38

Longitudinal processing

In order to reduce within subject scan session variability, a longitudinal stream was developed for FreeSurfer by Reuter and Fischl (2011). This method increases repeatability and statistical power (Reuter et al., 2010). All scans in the longitudinal series (n = 49) were processed using this procedure. An unbiased within-subject template and an average image were created, using inverse consistent registration. This reduced the potential over-regularization of longitudinal image processing (Reuter et al., 2012).

Statistical analyses

We used a linear mixed model procedure to examine the relation between age and cortical gray volume, thickness and surface area. This procedure accounts for irregular intervals between measures, missing data and within person dependence (Fox, 2002). Each dependent measure of the ith family, jth individual and kth time-point was modeled as described by Raznahan et al. (2011). Several models including linear age terms, quadratic age terms, cubic age terms or gender terms were fit. The full model is represented by the following formula:

$$\text{Measurement}_{ijk} = \text{Intercept} + d_{ij} + ß_1(\text{gender}) + ß_2(\text{age}) + ß_3(\text{age}^2) + ß_4(\text{age}^3) + ß_5(\text{gender}*\text{age}) + ß_6(\text{gender}*\text{age}^2) + ß_7(\text{gender}*\text{age}^3) + e_{ijk}$$

The e_{ijk} term represents the normally distributed residual error. Each ß represents a parameter estimate; for example the quadratic age effect is represented by $ß_3$. Furthermore, the interaction effects of gender and age were included in the model. The full model was tested against models including linear or quadratic age terms only. Intercept, gender and age effects were fixed, while within person dependence, nested within family (d_{ij}), was modeled as a random effect. All possible developmental models were run using mean-centered age terms (age 13.7 years).

The best-fit model was selected in three basic steps. First, a developmental model was determined using a step-down model selection procedure. Cubic, quadratic and linear age effects were fit. If the cubic age effect was not significant at $p < 0.05$, we stepped

thesis_LW_V3.indb 38 06/06/16 07:38

down to the quadratic developmental model, etc. Second, we investigated whether the developmental model differed between genders. Hence, a full model, containing both main effects of age and gender, as well as interaction effects, was compared to a model including best-fit age terms only using the Bayesian Information Criterion (BIC). Third, if no significant interaction effect was observed, we investigated whether measures significantly differed between genders at mean age. Hence, a model including the fixed gender effect was compared to the best-fit developmental model, selected in step one. The best-fit model was selected using BIC values. If two models had similar BIC values, we used a step-down procedure starting with the full model. We then selected the full regression model if the interaction term was significant at $p < 0.05$. If not, we stepped down to the simpler model with a significant main effect of gender. If no significant effect of gender was present in any of the solutions, we chose the model that included age terms only.

The present study did not correct for total brain volume (TBV) or intra cranial volume (ICV) for several reasons: first, this would have violated the important statistical assumption that the covariate (in this case TBV) should be unrelated to the independent variable (in this case gender). This was clearly not the case as gender was associated with TBV, with larger volumes for males than females. Second, correcting two-dimensional (surface area) and one-dimensional measures (cortical thickness) with a three dimensional measure (TBV) would result in overcorrection, and the extent of overcorrection would vary between these measures. Third, TBV was not equally related to volume in all cortical regions, meaning that the extent of overcorrection would also have differed between regions. Therefore, we chose to explore uncorrected measures of cortical volume, thickness and surface area.

Results

Overall cortical volume, average thickness and total surface area

The developmental trajectories of overall cortical volume, average thickness and total surface area are shown in Figure 2 (regression coefficients in Table 2). There was a main effect of gender and a quadratic effect of age on overall cortical volume: Males had larger overall cortical volume than females, and therwas no interaction between age and gender. No peak in development was observed. The two composite determinants of cortical volume had distinct developmental trajectories: Average cortical thickness showed a linear decrease

thesis_LW_V3.indb 39 06/06/16 07:38

Table 2 Paramters for developmental trajectories

Anatomical structure	Model fit	Intercept (s.e.)		Gender (s.e.)		Age (s.e.)		Age2 (s.e.)		Age3 (s.e.)	
Cerebral Cortical Volume (in cm3)	Quadratic	575.744	(8.14)**	44.917	(9.45)**	-6.269	(6.93)**	-0.266	(0.12)**	0.000	(0.00)
Total Surface Area (in cm2)	Cubic	1822.430	(24.19)**	157.577	(28.93)**	-12.544	(1.54)**	-0.892	(0.23)**	0.115	(0.04)**
Total Average Thickness (in mm)	Linear	2.817	(0.00)**	0.000	(0.00)	-0.021	(0.00)**	0.000	(0.00)	0.000	(0.00)

Intercept is the predicted value at the average age of the sample, s.e.=standard error, ** = significant level p<0.01

thesis_LW_V3.indb 40 06/06/16 07:38

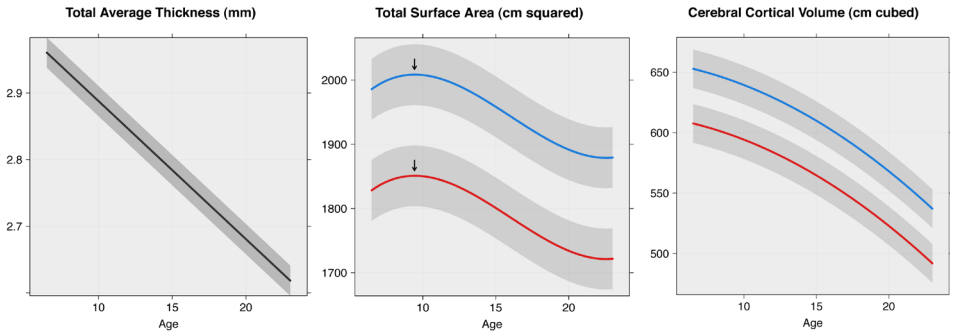

Figure 2 The developmental trajectories of average cortical thickness (in mm), total surface area (in cm^2) and overall cortical volume (in cm^3). The developmental trajectories are shown in blue for males and in red for females. The arrows in the graph indicate peak values.

with age, and no effect of gender. In contrast, overall cortical surface area had a cubic relationship with age, and males had greater overall surface area than females. Overall surface area peaked at age 9 for both genders.

Developmental trajectories within distinct cortical regions

The developmental curves of cortical volume, surface area and average thickness were estimated for 34 distinct ROIs from the Desikan-Killiany atlas for each hemisphere (see Supplementary material, Tables 1 to 6). For all three measures (cortical volume, thickness and surface area) peak values were estimated for those ROIs where their trajectories showed a quadratic or cubic relationship with age. These are shown in Figure 3. Cortical thickness showed linear decreases with age in most ROIs. Therefore no peak values were observed for this measure within the age range studied. Cortical volume showed a quadratic relationship with age, with a developmental peak in most ROIs, where in general the latest peaks were found in frontal areas. The earliest peaks were observed at age 8 years and the latest at 11 years (see Figure 3). Cortical surface area also had a curvilinear relation with age in most ROIs that followed a similar (but not identical pattern) with the estimated peak age varying from 8 to 13 years (see Figure 3).

thesis_LW_V3.indb 41 06/06/16 07:38

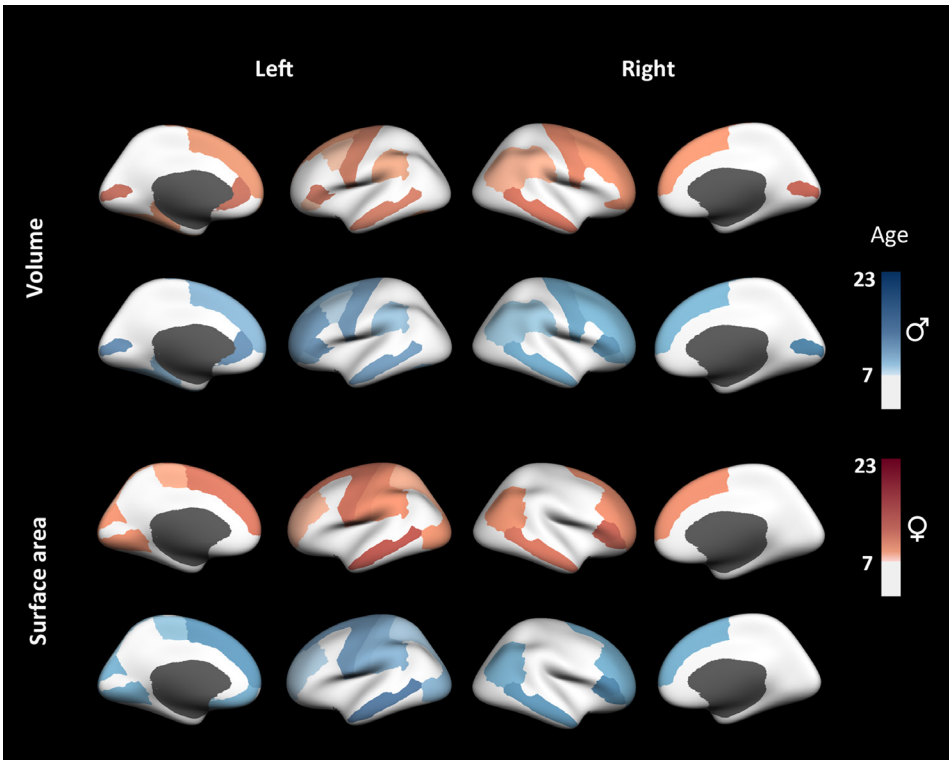

Figure 3 Peak ages for cortical volume and surface area for boys (blue) and girls (red). The darker the color, the later the peak occurs. For white areas, the estimated peak age did not occur within the age range of this study.

Gender effects

In nearly all regions, males had greater cortical volume and surface area than females. Although the development of surface area did not show any age x gender interactions, the development of volume showed such interactions in the left superior parietal and lateral occipital region and right insula, lingual and superior temporal regions: here, females showed a steeper decline than males. Also, peak volume occurred earlier for females than males in the pars triangularis. In contrast to the data on cortical volume and surface area, the data on cortical thickness showed very few gender effects: we found greater average thickness for males bilaterally in medial orbitofrontal cortex and visual cortex. Cortical thickness of left paracentral cortex was greater in females. In addition, we found age x gender interactions in left somatosensory cortex and left lingual gyrus where females showed a steeper thickness decline than males (Figure 4).

thesis_LW_V3.indb 42 06/06/16 07:38

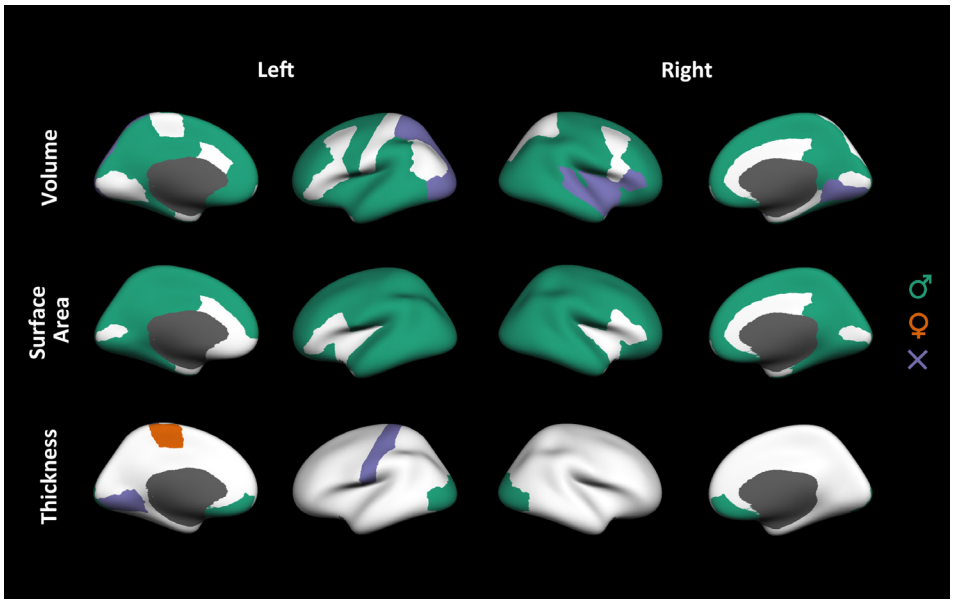

Figure 4 Gender differences in cortical morphometry for the left and right hemispheres. Green indicates greater values in males than females, orange indicates greater values for females than males, and purple indicates age*gender interactions.

Discussion

In this study, we investigated whether the regional developmental patterns of cortical surface area and thickness differ from the developmental trajectory of cortical volume. We found that they do: the developmental trajectories of cortical surface area and cortical thickness differ from one another and the timing of development varies over the cortex. These findings suggest that the development of these two composite dimensions of cortical volume are driven by different processes, at least in part.

In our study, developmental decreases in cortical volume were best described by a quadratic curve, whereas its two composite dimensions, cortical thickness and surface area, either decreased linearly (cortical thickness) or followed a cubic curve (surface area). As such, the developmental patterns of cortical thickness and surface area differed from one another and from the developmental trajectory of cortical volume. Further support for this finding comes from the observation that some cortical regions reached maximum surface area later in time than maximum volume. This suggests that the cortex may still be expanding laterally in some areas, even after maximum volume has been reached. This

thesis_LW_V3.indb 43 06/06/16 07:38

phenomenon would have been masked if we had only studied measures of volume. Our results confirm earlier findings by Raznahan et al. (2011) who showed that not all cortical dimensions develop at the same rate. Similarly to Shaw et al. (2012), we found that overall surface area peaked later in time than average thickness.

In all regions, males and females showed similar developmental trajectories for surface area, although males generally had larger surface area than females, as has been previouslyobserved (Raznahan et al., 2011; Salinas et al., 2012). In contrast, thickness showed similar values in most regions over the whole age range, confirming previous findings (Nopoulos et al., 2000; Salat, 2004). Only few regions showed gender differences in cortical thickness, with greater thickness in females than in males, particularly in early childhood. Greater thickness for females than in males has been reported before in similar regions (Luders et al., 2006; Sowell et al., 2006). However, these studies also reported gender effects in thickness in other cortical regions. This discrepancy is likely to be related to the correction for total brain volume applied in these earlier studies: as the brain is smaller on average in females than males, scaling may exaggerate the increase in cortical thickness in females (as described by Luders et al., 2006). Indeed, applying such a correction to our own data introduced similar, artifactual differences with greater cortical thickness for females than males in a number of regions (see supplementary Tables 7 to 12). The findings in the present study indicate that gender differences in the development of cortical volume are driven mostly by differences in surface area rather than in thickness, as has been suggested before (Raznahan et al., 2011). However, we did not confirm findings of overall sexually dimorphic developmental trajectories for global volume and surface area (Lenroot et al., 2007; Raznahan et al., 2011). This is likely to be related to the limited number of female subjects in our sample and our choice to use uncorrected measures, rather than to apply a correction for total brain volume. We chose not to apply such a correction, as its use may amplify gender differences, as described above. Furthermore, correcting one or two dimensional measures (cortical thickness and surface area) for a three dimensional one (total brain volume) would result in overcorrection.

The discrepancy between the gender effects on the various cortical dimensions further supports the notion that the development of cortical thickness and surface area are different

thesis_LW_V3.indb 44 06/06/16 07:38

processes. This is in line with the radial unit hypothesis of early development by Rakic (1995) that also suggests separate processes may drive the development of these features. This hypothesis poses that the number of radial columns determines the size of the cortical surface, where the number of columns is determined by the number of founder cells in the ventricular zone. In contrast, cortical thickness is determined by the number of cells within a column. Animal lesion studies further suggest that surface area expansion, but not change in cortical thickness, is dependent on afferent input from subcortical structures during early development (Rakic, 1995). This suggests that while development of cortical surface area is dependent on input from subcortical structures, development of cortical thickness may be more dependent on local or intrinsic factors. The development of surface area may also be related to changes in gyrification. However, the direction of causality between developmental changes in these two measures is unclear: Does expanding surface area cause increases in gyrification or is it the other way around? Furthermore, studies on the development of gyrification have reported contradicting results: on the one hand an increase in folding complexity has been reported (Blanton et al., 2001), while Hill et al. (2010) showed that the sulcal pattern is mostly in place at birth. In addition, one aspect that complicates interpretation of developmental changes in gyrification is that changes in curvature could be related to both changes in folding frequency or changes in folding magnitude (sulcal depth). Furthermore, from a genetic perspective, cortical thickness and surface area appear to be modulated by different genes (Jansen, 2005; Panizzon et al., 2009; Piao et al., 2004). In addition, Lenroot et al. (2009) observed that the sensitivity of cortical thickness to genetic factors is dependent on age and gender, suggesting that at different ages, different genes may contribute to cortical change. This underlines the complexity of cortical changes across development and emphasizes the importance of studying the development of its composite dimensions in longitudinal designs.

The findings of the present study should be considered in the light of certain limitations. First, in contrast to previous studies we did not find sexually dimorphic developmental trajectories for cortical volume and surface area (Raznahan et al., 2011). This is likely related to the uneven number of males and females in our study (2:1) and to the limited amount of longitudinal female data. However, we chose to investigate gender effects despite of this skewed distribution, as strong gender effects on these measures have

thesis_LW_V3.indb 45 06/06/16 07:38

been previously reported and reporting on males and females together would not permit comparison of our data to the extant literature (e.g., Lenroot et al., 2007). Second, we chose not to apply a correction for total brain volume and together with the aforementioned limited female sample size this may also have contributed to the lack of gender differences in our developmental trajectories. Third, we did not observe peaks in the development of cortical volume in the age range. However, the model fit is less reliable at the boundary of the age range and this may have led to us not detecting a peak.

In conclusion, the present study shows that the development of cortical surface area and thickness are different from one another and that they also differ from the developmental trajectory of cortical volume. Furthermore, the timing of their developmental patterns varies by anatomical region. Therefore, important developmental aspects may be missed if only one of the cortical components is investigated. This is of particular importance during late childhood where thickness and surface area show diverging developmental patterns. These findings suggest that there are likely different processes driving the development of these two cortical measures.

thesis_LW_V3.indb 46 06/06/16 07:38

thesis_LW_V3.indb 47 06/06/16 07:38

Supplementary Table 1 Parameters for developmental trajectories of cortical thickness in the right hemisphere

Anatomical structure	Best fitting model	Intercept (s.e.)	Gender (s.e.)	Age (s.e.)	Age^2 (s.e.)	Age^3 (s.e.)	Gender x Age (s.e.)	Gender x Age^2 (s.e.)	Gender x Age^3 (s.e.)
bankssts	quadratic	3.044 (0.022)**		-0.046 (0.006)**	-0.001 (0.001)n.s.	0.001 (0.001)**			
caudalanteriorcingulate	linear	2.906 (0.021)**		-0.016 (0.004)**					
caudalmiddlefrontal	linear	2.977 (0.018)**		-0.017 (0.004)**					
cuneus	quadratic	1.994 (0.016)**		-0.024 (0.002)**	0.001 (0.001)**				
entorhinal	n.s.	3.547 (0.034)**		0.01 (0.005)n.s.					
fusiform	linear	2.962 (0.014)**		-0.02 (0.003)**					
inferiorparietal	quadratic	2.926 (0.020)**		-0.04 (0.005)**	-0.001 (0.001)n.s.	0.001 (0.001)**			
inferiortemporal	linear	2.972 (0.015)**		-0.018 (0.003)**					
isthmuscingulate	linear	2.949 (0.019)**		-0.028 (0.003)**					
lateraloccipital	quadratic	2.302 (0.023)**	0.069 (0.026)*	-0.021 (0.002)**	0.001 (0.001)**				
lateralorbitofrontal	linear	3.032 (0.019)**		-0.021 (0.003)**					
lingual	quadratic	2.151 (0.015)**		-0.016 (0.002)**	0.001 (0.001)*				
medialorbitofrontal	linear	2.697 (0.037)**	0.129 (0.044)**	-0.027 (0.004)**					
middletemporal	linear	3.356 (0.018)**		-0.02 (0.003)**					
parahippocampal	linear	2.955 (0.024)**		-0.013 (0.004)**					
paracentral	linear	2.635 (0.014)**		-0.025 (0.003)**					
parsopercularis	linear	3.075 (0.016)**		-0.019 (0.003)**					
parsorbitalis	linear	3.218 (0.026)**		-0.02 (0.005)**					
parstriangularis	linear	3.052 (0.016)**		-0.018 (0.003)**					
pericalcarine	quadratic	1.572 (0.015)**		-0.004 (0.004)n.s.	0.002 (0.001)**	0.001 (0.001)*			
postcentral	linear	2.236 (0.013)**		-0.016 (0.002)**					
posteriorcingulate	quadratic	3.011 (0.021)**		-0.016 (0.003)**	-0.002 (0.001)**				
precentral	linear	2.629 (0.015)**		-0.012 (0.003)**					
precuneus	linear	2.777 (0.014)**		-0.032 (0.003)**					
rostralanteriorcingulate	linear	3.278 (0.023)**		-0.016 (0.005)**					
rostralmiddlefrontal	linear	2.856 (0.014)**		-0.022 (0.003)**					
superiorfrontal	linear	3.209 (0.017)**		-0.019 (0.003)**					
superiorparietal	linear	2.483 (0.016)**		-0.028 (0.003)**					
superiortemporal	linear	3.169 (0.016)**		-0.013 (0.003)**					
supramarginal	linear	2.967 (0.019)**		-0.026 (0.003)**					
frontalpole	linear	3.065 (0.037)**		-0.017 (0.006)*					
temporalpole	linear	4.100 (0.027)**		0.02 (0.005)**					
transversetemporal	linear	2.812 (0.023)**		-0.016 (0.004)**					
insula	linear	3.400 (0.014)**		-0.02 (0.003)**					

Intercept is the predicted value at the average age of the sample, s.e.=standard error, n.s.=not significant, *=significant level p<0.05, **=significant level p<0.01

thesis_LW_V3.indb 48 06/06/16 07:38

Supplementary Table 2 Parameters for developmental trajectories of cortical thickness in the left hemisphere

Anatomical structure	Best fitting model	Intercept (s.e.)	Gender (s.e.)	Age (s.e.)	Age^2 (s.e.)	Age^3 (s.e.)	Gender x Age (s.e.)	Gender x Age^2 (s.e.)	Gender x Age^3 (s.e.)
bankssts	quadratic	2.953 (0.021)**		-0.045 (0.005)**	0.000 (0.001)n.s.	0.001 (0.001)*			
caudalanteriorcingulate	linear	3.029 (0.024)**		-0.027 (0.004)**					
caudalmiddlefrontal	linear	2.976 (0.016)**		-0.02 (0.003)**					
cuneus	quadratic	2.027 (0.018)**		-0.014 (0.004)**	0.002 (0.001)**	0.001 (0.001)*			
entorhinal	n.s.	3.527 (0.032)**		-0.001 (0.005)n.s.					
fusiform	linear	3.023 (0.013)**		-0.02 (0.003)**					
inferiorparietal	linear	2.875 (0.017)**		-0.026 (0.003)**					
inferiortemporal	quadratic	3.023 (0.019)**		-0.027 (0.005)**	-0.002 (0.001)*	0.001 (0.001)*			
isthmuscingulate	linear	2.982 (0.019)**		-0.026 (0.003)**					
lateraloccipital	quadratic	2.223 (0.021)**	0.056 (0.024)*	-0.017 (0.002)**	0.001 (0.000)*				
lateralorbitofrontal	linear	3.113 (0.019)**		-0.022 (0.004)**					
lingual	linear	2.202 (0.020)**	-0.006 (0.030)n.s.	-0.026 (0.000)**			0.013 (0.000)**		
medialorbitofrontal	linear	2.746 (0.034)**	0.115 (0.041)*	-0.025 (0.004)**					
middletemporal	linear	3.285 (0.017)**		-0.023 (0.003)**					
parahippocampal	linear	3.070 (0.028)**		-0.018 (0.005)**					
paracentral	linear	2.716 (0.029)**	-0.082 (0.035)*	-0.026 (0.003)**					
parsopercularis	linear	3.051 (0.015)**		-0.022 (0.003)**					
parsorbitalis	linear	3.262 (0.027)**		-0.021 (0.005)**					
parstriangularis	linear	2.995 (0.018)**		-0.023 (0.004)**					
pericalcarine	linear	1.725 (0.016)**		-0.007 (0.003)**					
postcentral	linear	2.243 (0.020)**	0.004 (0.030)n.s.	-0.027 (0.000)**			0.015 (0.010)**		
posteriorcingulate	linear	3.002 (0.017)**		-0.022 (0.003)**					
precentral	linear	2.642 (0.014)**		-0.013 (0.003)**					
precuneus	linear	2.786 (0.013)**		-0.034 (0.002)**					
rostralanteriorcingulate	linear	3.287 (0.020)**		-0.021 (0.004)**					
rostralmiddlefrontal	linear	2.847 (0.017)**		-0.03 (0.003)**					
superiorfrontal	linear	3.216 (0.016)**		-0.022 (0.003)**					
superiorparietal	quadratic	2.471 (0.019)**		-0.029 (0.003)**	0.001 (0.001)*				
superiortemporal	linear	3.138 (0.017)**		-0.016 (0.003)**					
supramarginal	linear	2.974 (0.017)**		-0.024 (0.003)**					
frontalpole	n.s.	3.105 (0.040)**		-0.004 (0.007)n.s.					
temporalpole	linear	4.031 (0.025)**		0.011 (0.005)*					
transversetemporal	linear	2.717 (0.022)**		-0.012 (0.004)**					
insula	linear	3.433 (0.014)**		-0.02 (0.003)**					

Intercept is the predicted value at the average age of the sample, s.e.=standard error, n.s.=not significant, *=significant level p<0.05, **=significant level p<0.01

thesis_LW_V3.indb 49 06/06/16 07:38

Supplementary Table 3 Parameters for developmental trajectories of cortical surface area in the right hemisphere

Anatomical structure	Best fitting model	Intercept (s.e.)	Gender (s.e.)	Age (s.e.)	Age^2 (s.e.)	Age^3 (s.e.)	Gender x Age (s.e.)	Gender x Age^2 (s.e.)	Gender x Age^3 (s.e.)
bankssts	linear	10.125 (0.235)**	0.940 (0.284)**	-0.092 (0.010)**					
caudalanteriorcingulate	n.s.	7.883 (0.132)**		-0.015 (0.011)n.s.					
caudalmiddlefrontal	linear	23.071 (0.719)**	2.524 (0.870)**	-0.175 (0.032)**					
cuneus	linear	15.96 (0.289)**	1.230 (0.349)**	-0.069 (0.020)**					
entorhinal	n.s.	4.007 (0.087)**		-0.006 (0.011)n.s.					
frontalpole	n.s.	3.109 (0.050)**		-0.011 (0.010)n.s.					
fusiform	linear	33.766 (0.605)**	2.821 (0.732)**	-0.142 (0.035)**					
inferiorparietal	quadratic	59.587 (1.116)**	5.293 (1.336)**	-0.535 (0.070)**	-0.03 (0.011)**	0.004 (0.002)*			
inferiortemporal	linear	33.273 (0.684)**	3.586 (0.824)**	-0.227 (0.043)**					
insula	n.s.	24.697 (0.250)**		-0.022 (0.031)n.s.					
isthmuscingulate	linear	9.482 (0.258)**	0.856 (0.312)*	-0.05 (0.012)**					
lateraloccipital	linear	50.804 (0.980)**	6.057 (1.187)**	-0.316 (0.042)**					
lateralorbitofrontal	linear	25.774 (0.542)**	2.115 (0.656)**	-0.108 (0.036)**					
lingual	linear	32.067 (0.517)**	1.731 (0.615)*	-0.132 (0.032)**					
medialorbitofrontal	linear	17.558 (0.362)**	1.365 (0.438)**	-0.078 (0.026)**					
middletemporal	quadratic	36.533 (0.682)**	3.355 (0.82)**	-0.099 (0.027)**	-0.021 (0.004)**				
paracentral	linear	15.863 (0.384)**	1.510 (0.465)**	-0.098 (0.027)**					
parahippocampal	linear	6.885 (0.158)**	0.766 (0.185)**	-0.03 (0.009)**					
parsopercularis	linear	15.809 (0.227)**		-0.073 (0.013)**					
parsorbitalis	quadratic	8.257 (0.177)**	0.676 (0.206)**	-0.021 (0.013)n.s.	-0.006 (0.002)**				
parstriangularis	quadratic	17.052 (0.248)**		-0.069 (0.026)**	-0.022 (0.004)**	0.002 (0.001)*			
pericalcarine	n.s.	16.073 (0.206)**		-0.016 (0.016)n.s.					
postcentral	linear	44.534 (0.759)**	4.577 (0.918)**	-0.364 (0.055)**					
posteriorcingulate	linear	12.636 (0.171)**		-0.076 (0.015)**					
precentral	quadratic	52.833 (0.893)**	5.742 (1.043)**	-0.274 (0.094)**	-0.038 (0.015)*	0.005 (0.002)*			
precuneus	linear	41.358 (0.822)**	5.491 (0.996)**	-0.352 (0.032)**					
rostralanteriorcingulate	n.s.	7.053 (0.125)**		0.011 (0.012)n.s.					
rostralmiddlefrontal	quadratic	62.962 (1.283)**	6.080 (1.537)**	-0.474 (0.080)**	-0.031 (0.012)*	0.004 (0.002)*			
superiorfrontal	quadratic	75.854 (1.273)**	7.021 (1.521)**	-0.218 (0.066)**	-0.039 (0.011)**				
superiorparietal	linear	59.887 (1.033)**	3.614 (1.246)**	-0.54 (0.070)**					
superiortemporal	linear	39.873 (0.636)**	2.172 (0.772)*	-0.123 (0.027)**					
supramarginal	linear	39.95 (0.919)**	4.662 (1.115)**	-0.27 (0.037)**					
temporalpole	n.s.	4.409 (0.057)**		0.004 (0.010)n.s.					
transversetemporal	linear	3.414 (0.082)**	0.380 (0.100)**	-0.025 (0.006)**					

Intercept is the predicted value at the average age of the sample, s.e.=standard error, n.s.=not significant, *=significant level p<0.05, **=significant level p<0.01

thesis_LW_V3.indb 50 06/06/16 07:38

Supplementary Table 4 Parameters for developmental trajectories of cortical surface area in the left hemisphere

Anatomical structure	Best fitting model	Intercept (s.e.)	Gender (s.e.)	Age (s.e.)	Age^2 (s.e.)	Age^3 (s.e.)	Gender x Age (s.e.)	Gender x Age^2 (s.e.)	Gender x Age^3 (s.e.)
bankssts	quadratic	11.552 (0.293)**	1.024 (0.352)**	-0.141 (0.017)**	-0.002 (0.003)n.s.	0.001 (0.000)*			
caudalanteriorcingulate	linear	6.987 (0.143)**		-0.02 (0.009)*					
caudalmiddlefrontal	linear	25.862 (0.707)**	2.055 (0.856)*	-0.193 (0.036)**					
cuneus	linear	14.709 (0.342)**	1.439 (0.407)**	-0.124 (0.025)**	-0.006 (0.004)n.s.	0.001 (0.001)*			
entorhinal	n.s.	4.602 (0.076)**		-0.014 (0.011)n.s.					
frontalpole	n.s.	2.305 (0.038)**		-0.005 (0.008)n.s.					
fusiform	linear	34.908 (0.643)**	2.435 (0.778)**	-0.125 (0.036)**					
inferiorparietal	quadratic	52.513 (1.087)**	3.315 (1.295)*	-0.375 (0.06)**	-0.021 (0.010)*				
inferiortemporal	linear	35.431 (0.763)**	3.710 (0.924)**	-0.257 (0.04)**					
insula	n.s.	24.271 (0.231)**		-0.009 (0.036)n.s.					
isthmuscingulate	linear	9.911 (0.279)**	1.391 (0.338)**	-0.074 (0.018)**					
lateraloccipital	quadratic	53.745 (0.96)**	4.442 (1.147)**	-0.485 (0.064)**	-0.027 (0.010)**	0.004 (0.002)*			
lateralorbitofrontal	linear	25.326 (0.492)**	1.795 (0.596)**	-0.122 (0.033)**					
lingual	quadratic	31.268 (0.614)**	2.198 (0.732)**	-0.245 (0.044)**	-0.012 (0.007)n.s.	0.003 (0.001)*			
medialorbitofrontal	n.s.	19.872 (0.232)**		-0.062 (0.034)n.s.					
middletemporal	quadratic	33.603 (0.674)**	2.808 (0.805)**	-0.02 (0.036)n.s.	-0.024 (0.006)**				
paracentral	quadratic	14.230 (0.281)**	1.247 (0.33)**	-0.156 (0.026)**	-0.004 (0.004)n.s.	0.001 (0.001)*			
parahippocampal	linear	6.760 (0.233)**	0.996 (0.282)**	-0.039 (0.009)**					
parsopercularis	n.s.	18.654 (0.263)**		-0.04 (0.021)n.s.					
parsorbitalis	linear	6.816 (0.073)**		-0.026 (0.011)*					
parstriangularis	quadratic	14.171 (0.192)**		0.025 (0.018)n.s.	-0.007 (0.003)*				
pericalcarine	n.s.	14.295 (0.185)**		-0.031 (0.016)n.s.					
postcentral	quadratic	47.577 (0.876)**	3.247 (1.036)**	-0.497 (0.077)**	-0.033 (0.012)**	0.006 (0.002)**			
posteriorcingulate	linear	11.375 (0.25)**	1.165 (0.303)**	-0.074 (0.015)**					
precentral	quadratic	53.095 (0.955)**	4.989 (1.099)**	-0.361 (0.119)**	-0.053 (0.019)**	0.006 (0.003)*			
precuneus	linear	39.175 (0.71)**	4.618 (0.861)**	-0.27 (0.031)**					
rostralanteriorcingulate	n.s.	8.976 (0.145)**		0.013 (0.016)n.s.					
rostralmiddlefrontal	quadratic	62.191 (1.217)**	5.882 (1.446)**	-0.306 (0.071)**	-0.026 (0.012)*				
superiorfrontal	quadratic	78.576 (1.293)**	6.402 (1.542)**	-0.17 (0.071)*	-0.033 (0.012)**				
superiorparietal	quadratic	59.879 (1.014)**	4.644 (1.199)**	-0.683 (0.088)**	-0.021 (0.014)n.s.	0.005 (0.002)*			
superiortemporal	linear	40.966 (0.657)**	3.100 (0.796)**	-0.132 (0.036)**					
supramarginal	quadratic	40.947 (0.9)**	6.641 (1.079)**	-0.411 (0.052)**	-0.022 (0.008)**	0.004 (0.001)**			
temporalpole	n.s.	5.060 (0.059)**		0.009 (0.01)n.s.					
transversetemporal	linear	4.475 (0.122)**	0.477 (0.148)**	-0.038 (0.009)**					

Intercept is the predicted value at the average age of the sample, s.e.=standard error, n.s.=not significant, *=significant level p<0.05, **=significant level p<0.01

thesis_LW_V3.indb 51 06/06/16 07:38

Supplementary Table 5 Parameters for developmental trajectories of cortical volume in the right hemisphere

Anatomical structure	Best fitting model	Intercept (s.e.)	Gender (s.e.)	Age (s.e.)	Age^2 (s.e.)	Age^3 (s.e.)	Gender x Age (s.e.)	Gender x Age^2 (s.e.)	Gender x Age^3 (s.e.)
bankssts	linear	3.051 (0.082)**	0.287 (0.100)**	-0.058 (0.005)**					
caudalanteriorcingulate	linear	2.634 (0.053)**		-0.017 (0.003)**					
caudalmiddlefrontal	quadratic	8.465 (0.145)**		-0.092 (0.015)**	-0.009 (0.002)**				
cuneus	quadratic	3.442 (0.082)**	0.273 (0.097)*	-0.053 (0.005)**	0.002 (0.001)*				
entorhinal	n.s.	2.017 (0.044)**		-0.002 (0.006)n.s.					
frontalpole	linear	1.415 (0.027)**		-0.014 (0.005)**					
fusiform	linear	11.371 (0.241)**	0.955 (0.292)**	-0.135 (0.018)**					
inferiorparietal	cubic	20.177 (0.398)**	1.811 (0.466)**	-0.483 (0.041)**	-0.016 (0.006)*	0.003 (0.001)**			
inferiortemporal	linear	12.092 (0.298)**	1.042 (0.361)**	-0.127 (0.018)**					
insula	linear	8.039 (0.150)**	0.921 (0.181)**	-0.099 (0.021)**			0.064 (0.024)*		
isthmuscingulate	linear	3.095 (0.088)**	0.317 (0.107)**	-0.049 (0.004)**					
lateraloccipital	linear	12.747 (0.264)**	1.822 (0.319)**	-0.153 (0.017)**					
lateralorbitofrontal	linear	8.811 (0.192)**	0.694 (0.232)**	-0.091 (0.015)**					
lingual	linear	7.41 (0.159)**	0.334 (0.190)n.s.	-0.145 (0.02)**			0.086 (0.022)*		
medialorbitofrontal	linear	5.659 (0.124)**	0.678 (0.150)**	-0.072 (0.013)**					
middletemporal	quadratic	15.741 (0.299)**	1.208 (0.355)**	-0.099 (0.018)**	-0.013 (0.003)**				
paracentral	linear	4.524 (0.122)**	0.376 (0.147)*	-0.069 (0.008)**					
parahippocampal	quadratic	2.512 (0.000)**		-0.021 (0.004)**	0.001 (0.001)**				
parsopercularis	quadratic	5.648 (0.078)**		-0.059 (0.008)**	-0.004 (0.001)**				
parsorbitalis	quadratic	3.547 (0.091)**	0.261 (0.106)*	-0.030 (0.007)**	-0.004 (0.001)**				
parstriangularis	quadratic	5.807 (0.164)**	0.448 (0.197)*	-0.116 (0.019)**	0.002 (0.002)n.s.		0.082 (0.021)*	-0.01 (0.003)**	
pericalcarine	cubic	2.32 (0.038)**		0.010 (0.007)n.s.	0.003 (0.001)*	-0.001 (0.001)**			
postcentral	linear	11.226 (0.229)**	0.994 (0.277)**	-0.163 (0.020)**					
posteriorcingulate	quadratic	4.239 (0.057)**		-0.050 (0.006)**	-0.002 (0.001)*				
precentral	quadratic	15.396 (0.272)**	1.183 (0.318)**	-0.079 (0.021)**	-0.011 (0.004)**				
precuneus	linear	12.784 (0.242)**	1.337 (0.293)**	-0.257 (0.017)**					
rostralanteriorcingulate	n.s.	2.769 (0.050)**		-0.010 (0.006)n.s.					
rostralmiddlefrontal	quadratic	21.777 (0.451)**	2.243 (0.521)**	-0.221 (0.040)**	-0.022 (0.007)**				
superiorfrontal	quadratic	29.232 (0.518)**	1.768 (0.599)**	-0.246 (0.043)**	-0.036 (0.008)**				
superiorparietal	linear	17.678 (0.180)**		-0.331 (0.025)**					
superiortemporal	linear	14.751 (0.284)**	0.917 (0.344)*	-0.212 (0.037)**			0.132 (0.043)*		
supramarginal	cubic	13.67 (0.304)**	1.229 (0.357)**	-0.266 (0.028)**	-0.012 (0.004)**	0.002 (0.001)*			
temporalpole	n.s.	2.663 (0.037)**		0.010 (0.007)n.s.					
transversetemporal	linear	1.117 (0.034)**	0.106 (0.041)*	-0.015 (0.002)**					

Intercept is the predicted value at the average age of the sample, s.e.=standard error, n.s.=not significant, *=significant level p<0.05, **=significant level p<0.01

thesis_LW_V3.indb 52 06/06/16 07:38

Supplementary Table 6 Parameters for developmental trajectories of cortical volume in the left hemisphere

Anatomical structure	Best fitting model	Intercept (s.e.)	Gender (s.e.)	Age (s.e.)	Age^2 (s.e.)	Age^3 (s.e.)	Gender x Age (s.e.)	Gender x Age^2 (s.e.)	Gender x Age^3 (s.e.)
bankssts	cubic	3.406 (0.100)**	0.349 (0.119)**	-0.088 (0.008)**	-0.001 (0.001)n.s.	0.001 (0.000)**			
caudalanteriorcingulate	linear	2.354 (0.058)**		-0.028 (0.004)**					
caudalmiddlefrontal	quadratic	9.155 (0.140)**		-0.111 (0.014)**	-0.009 (0.002)**				
cuneus	quadratic	3.258 (0.089)**	0.274 (0.106)*	-0.047 (0.006)**	0.002 (0.001)*				
entorhinal	n.s.	2.254 (0.039)**		-0.006 (0.005)n.s.					
frontalpole	n.s.	1.049 (0.024)**		-0.006 (0.004)n.s.					
fusiform	cubic	12.292 (0.250)**	0.755 (0.294)*	-0.181 (0.026)**	-0.009 (0.004)*	0.001 (0.001)*			
inferiorparietal	cubic	17.993 (0.222)**		-0.370 (0.042)**	-0.015 (0.006)*	0.002 (0.001)*			
inferiortemporal	cubic	12.935 (0.304)**	1.413 (0.359)**	-0.180 (0.029)**	-0.013 (0.004)**	0.002 (0.001)*			
insula	linear	8.097 (0.145)**	0.663 (0.175)**	-0.044 (0.012)**					
isthmuscingulate	linear	3.274 (0.083)**	0.453 (0.101)**	-0.050 (0.005)**					
lateraloccipital	linear	12.629 (0.269)**	1.483 (0.326)**	-0.238 (0.037)**			0.122 (0.042)**		
lateralorbitofrontal	linear	8.978 (0.174)**	0.748 (0.212)**	-0.115 (0.015)**					
lingual	linear	7.697 (0.092)**		-0.085 (0.011)**					
medialorbitofrontal	linear	5.955 (0.134)**	0.820 (0.162)**	-0.079 (0.013)**					
middletemporal	quadratic	14.038 (0.306)**	1.068 (0.366)**	-0.077 (0.018)**	-0.013 (0.003)**				
paracentral	linear	4.412 (0.054)**		-0.068 (0.007)**					
parahippocampal	cubic	2.495 (0.083)**	0.296 (0.099)**	-0.039 (0.007)**	-0.002 (0.001)n.s.	0.001 (0.001)*			
parsopercularis	quadratic	6.728 (0.099)**		-0.074 (0.009)**	-0.005 (0.002)**				
parsorbitalis	quadratic	3.051 (0.046)**		-0.026 (0.006)**	-0.003 (0.001)**				
parstriangularis	quadratic	5.020 (0.076)**		-0.031 (0.009)**	-0.006 (0.001)**				
pericalcarine	cubic	2.244 (0.038)**		0.012 (0.006)n.s.	0.002 (0.001)*	0.001 (0.001)**			
postcentral	linear	12.529 (0.152)**		-0.157 (0.019)**					
posteriorcingulate	linear	3.815 (0.088)**	0.392 (0.107)**	-0.051 (0.005)**					
precentral	quadratic	15.520 (0.292)**	1.156 (0.339)**	-0.083 (0.025)**	-0.013 (0.004)**				
precuneus	linear	12.325 (0.228)**	1.287 (0.277)**	-0.231 (0.017)**					
rostralanteriorcingulate	quadratic	3.348 (0.100)**	0.275 (0.118)*	-0.014 (0.008)n.s.	-0.003 (0.001)*				
rostralmiddlefrontal	quadratic	21.231 (0.437)**	2.272 (0.508)**	-0.292 (0.037)**	-0.028 (0.006)**				
superiorfrontal	quadratic	29.735 (0.482)**	1.884 (0.558)**	-0.271 (0.042)**	-0.030 (0.008)**				
superiorparietal	linear	17.012 (0.294)**	1.050 (0.356)**	-0.453 (0.051)**			0.148 (0.059)*		
superiortemporal	linear	14.918 (0.269)**	1.312 (0.326)**	-0.129 (0.019)**					
supramarginal	cubic	13.983 (0.320)**	2.270 (0.376)**	-0.316 (0.034)**	-0.016 (0.005)**	0.002 (0.001)*			
temporalpole	n.s.	3.051 (0.039)**		0.011 (0.007)n.s.					
transversetemporal	linear	1.371 (0.045)**	0.138 (0.055)*	-0.019 (0.003)**					

Intercept is the predicted value at the average age of the sample, s.e.=standard error, n.s.=not significant, *=significant level p<0.05, **=significant level p<0.01

thesis_LW_V3.indb 53 06/06/16 07:38

Supplementary Table 7 Parameters for developmental trajectories of cortical thickness in the right hemisphere TBV included in model

Anatomical structure	Intercept (s.e.)	TotalGrayVolume (s.e.)	Gender (s.e.)	Age (s.e.)	Age^2 (s.e.)	Age^3 (s.e.)	Gender x Age (s.e.)	Gender x Age^2 (s.e.)	Gender x Age^3 (s.e.)
bankssts	2.254 (0.192)**	0.001 (2.29e-04)**		-0.042 (0.005)**	0.001 (8.32e-04)n.s.	0.001 (0.001)**			
caudalanteriorcingulate	2.441 (0.211)**	0.001 (2.56e-04)*		-0.013 (0.004)**					
caudalmiddlefrontal	1.906 (0.194)**	0.001 (2.47e-04)**	-0.173(0.039)**	-0.009 (0.004)*					
cuneus	1.207 (0.139)**	0.001 (1.67e-04)**		-0.018 (0.002)**	0.002 (3.81e-04)*				
entorhinal	2.048 (0.331)**	0.002 (4.21e-04)**	-0.245(0.071)**	0.023 (0.006)**					
fusiform	1.928 (0.145)**	0.001(1.82e-04)**	-0.095(0.029)**	-0.014 (0.003)**	0.001 (4.52e-04)*				
inferiorparietal	1.692 (0.176)**	0.002 (2.21e-04)**	-0.101(0.037)*	-0.033 (0.004)**	0.001 (6.18e-04)n.s.	0.001 (0.001)**			
inferiortemporal	1.677 (0.165)**	0.002 (2.08e-04)**	-0.113(0.033)**	-0.011 (0.003)**	0.001 (4.81e-04)*				
isthmuscingulate	2.292 (0.199)**	0.001 (2.41e-04)**		-0.024 (0.003)**					
lateraloccipital	1.691 (0.133)**	0.001 (1.59e-04)*		-0.017 (0.002)**	0.002 (4.48e-04)*				
lateralorbitofrontal	2 (0.186)**	0.001 (2.26e-04)*		-0.013 (0.004)**					
lingual	1.219 (0.125)**	0.001 (1.50e-04)*		-0.005 (0.003)n.s.	0.002 (4.54e-04)*	0.001 (0.001)*			
medialorbitofrontal	1.661 (0.221)**	0.001 (2.68e-04)*		-0.019 (0.004)**					
middletemporal	2.31 (0.18)**	0.001 (2.27e-04)*	-0.092 (0.039)*	-0.014 (0.003)**	0.001 (4.70e-04)*				
parahippocampal	2.956 (0.024)**			-0.012 (0.004)**					
paracentral	1.748 (0.156)**	0.001 (1.88e-04)*		-0.02 (0.003)**					
parsopercularis	1.877 (0.171)**	0.002 (2.17e-04)*	-0.119 (0.036)**	-0.011 (0.003)**					
parsorbitalis	3.218 (0.026)**			-0.02 (0.005)**					
parstriangularis	2.23 (0.161)**	0.001 (1.95e-04)*		-0.012 (0.003)**					
pericalcarine	1.439 (0.132)**	0 (1.58e-04)n		-0.004 (0.004)n.s.	0.002 (6.42e-04)*	0.001 (0.001)*			
postcentral	1.29 (0.141)**	0.001 (1.80e-04)*	-0.105 (0.03)**	-0.008 (0.002)**					
posteriorcingulate	2.441 (0.203)**	0.001 (2.43e-04)*		-0.013 (0.003)**	-0.001 (5.37e-04)*				
precentral	2.629 (0.015)**			-0.012 (0.003)**					
precuneus	1.64 (0.16)**	0.001 (2.01e-04)*	-0.118 (0.033)**	-0.026 (0.003)**	0.001 (4.28e-04)*				
rostralanteriorcingulate	1.64 (0.16)**	0.001 (2.01e-04)*	-0.118 (0.033)**	-0.026 (0.003)**	0.001 (4.28e-04)*				
rostralmiddlefrontal	2.027 (0.152)**	0.001 (1.84e-04)*		-0.016 (0.003)**					
superiorfrontal	2.105 (0.174)**	0.001 (2.21e-04)*	-0.164 (0.035)**	-0.011 (0.003)**					
superiorparietal	1.234 (0.16)**	0.002 (2.01e-04)*	-0.128 (0.034)**	-0.022 (0.003)**	0.002 (4.08e-04)*				
superiortemporal	3.169 (0.016)**			-0.013 (0.003)**					
supramarginal	1.589 (0.184)**	0.002 (2.33e-04)*	-0.114 (0.041)*	-0.016 (0.003)**					
frontalpole	3.065 (0.037)**			-0.017 (0.006)*					
temporalpole	2.985 (0.292)**	0.001 (3.54e-04)*		0.027 (0.005)**					
transversetemporal	2.812 (0.023)**			-0.016 (0.004)**					
insula	2.478 (0.143)**	0.001 (1.72e-04)*		-0.015 (0.003)**	0.001 (4.55e-04)*				

Intercept is the predicted value at the average age of the sample, s.e. = standard error, n.s. = not significant, * = significant level p<0.05, ** = significant level p<0.01

thesis_LW_V3.indb 54 06/06/16 07:38

Supplementary Table 8 Parameters for developmental trajectories of cortical thickness in the left hemisphere TBV included in model

Anatomical structure	Intercept (s.e.)	TotalGrayVolume (s.e.)	Gender (s.e.)	Age (s.e.)	Age^2 (s.e.)	Age^3 (s.e.)	Gender x Age (s.e.)	Gender x Age^2 (s.e.)	Gender x Age^3 (s.e.)
bankssts	1.767 (0.188)**	0.002 (2.36e-04)*	-0.108 (0.038)*	-0.038 (0.005)**	0.001 (7.31e-04)n.s.	0.001 (0.001)**			
caudalanteriorcingulate	2.296 (0.249)**	0.001 (3.02e-04)*		-0.022 (0.004)**					
caudalmiddlefrontal	2.272 (0.19)**	0.001 (2.42e-04)*	-0.111 (0.038)**	-0.015 (0.003)**					
cuneus	1.334 (0.159)**	0.001 (1.90e-04)*		-0.009 (0.004)*	0.002 (5.43e-04)*	0.001 (0.001)*			
entorhinal	3.527 (0.032)**			-0.001 (0.005)n.s.					
fusiform	2.223 (0.138)**	0.001 (1.76e-04)*	-0.071 (0.028)*	-0.014 (0.003)**					
inferiorparietal	1.846 (0.183)**	0.001 (2.30e-04)*	-0.115 (0.037)**	-0.021 (0.003)**	0.001 (5.74e-04)*				
inferiortemporal	1.845 (0.16)**	0.001 (2.01e-04)*	-0.077 (0.032)*	-0.02 (0.004)**	-0.001 (6.25e-04)n.s.	0.001 (0.001)*			
isthmuscingulate	1.845 (0.16)**	0.001 (2.01e-04)*	-0.077 (0.032)*	-0.02 (0.004)**	-0.001 (6.25e-04)n.s.	0.001 (0.001)*			
lateraloccipital	1.407 (0.114)**	0.001 (1.36e-04)*		-0.011 (0.002)**	0.001 (3.78e-04)*				
lateralorbitofrontal	2.244 (0.21)**	0.001 (2.55e-04)*		-0.016 (0.004)**					
lingual	1.298 (0.131)**	0.001 (1.65e-04)*	-0.083 (0.026)**	-0.011 (0.002)**	0.001 (3.85e-04)*				
medialorbitofrontal	2.083 (0.21)**	0.001 (2.54e-04)*		-0.02 (0.004)**					
middletemporal	2.162 (0.163)**	0.001 (2.07e-04)*	-0.091 (0.035)*	-0.015 (0.003)**					
parahippocampal	2.057 (0.294)**	0.001 (3.73e-04)*	-0.152 (0.064)*	-0.01 (0.005)*					
paracentral	1.599 (0.174)**	0.001 (2.21e-04)*	-0.176 (0.035)**	-0.017 (0.003)**					
parsopercularis	2.151 (0.158)**	0.001 (2.01e-04)*	-0.082 (0.032)*	-0.015 (0.003)**					
parsorbitalis	2.146 (0.299)**	0.001 (3.63e-04)*		-0.013 (0.005)*					
parstriangularis	2.213 (0.2)**	0.001 (2.42e-04)*		-0.017 (0.004)**					
pericalcarine	1.725 (0.016)**			-0.007 (0.003)**					
postcentral	1.22 (0.145)**	0.001 (1.82e-04)*	-0.085 (0.03)*	-0.009 (0.002)**	0.001 (3.97e-04)*				
posteriorcingulate	1.22 (0.145)**	0.001 (1.82e-04)*	-0.085 (0.03)*	-0.009 (0.002)**	0.001 (3.97e-04)*				
precentral	2.642 (0.014)**			-0.013 (0.003)**					
precuneus	1.761 (0.15)**	0.001 (1.88e-04)*	-0.104 (0.03)**	-0.029 (0.002)**	0.001 (4.13e-04)*				
rostralanteriorcingulate	2.362 (0.223)**	0.001 (2.84e-04)*	-0.109 (0.045)*	-0.014 (0.004)**					
rostralmiddlefrontal	1.935 (0.173)**	0.001 (2.10e-04)*		-0.024 (0.003)**					
superiorfrontal	2.239 (0.182)**	0.001 (2.32e-04)*	-0.111 (0.037)**	-0.015 (0.003)**					
superiorparietal	1.197 (0.174)**	0.002 (2.19e-04)*	-0.129 (0.036)**	-0.021 (0.003)**	0.002 (4.82e-04)*				
superiortemporal	2.037 (0.155)**	0.001 (1.88e-04)*		-0.008 (0.003)**					
supramarginal	1.963 (0.18)**	0.001 (2.18e-04)*		-0.019 (0.003)**					
frontalpole	3.105 (0.04)**			-0.004 (0.007)n.s.					
temporalpole	3.248 (0.254)**	0.001 (3.09e-04)*		0.017 (0.005)**					
transversetemporal	2.717 (0.022)**			-0.012 (0.004)**					
insula	2.597 (0.13)**	0.001 (1.58e-04)*		-0.014 (0.003)**					

Intercept is the predicted value at the average age of the sample, s.e. = standard error, n.s. = not significant, * = significant level p<0.05, ** = significant level p<0.01

thesis_LW_V3.indb 55 06/06/16 07:38

Supplementary Table 9 Parameters for developmental trajectories of cortical surface area in the left hemisphere TBV included in model

Anatomical structure	Intercept (s.e.)	TotalGrayVolume (s.e.)	Gender (s.e.)	Age (s.e.)	Age^2 (s.e.)	Age^3 (s.e.)	Gender x Age (s.e.)	Gender x Age^2 (s.e.)	Gender x Age^3 (s.e.)
bankssts	4.84 (1.175)**	0.009 (0.001)**		-0.066 (0.015)**	0.005 (0.002)*				
caudalanteriorcingulate	6.987 (0.143)**			-0.02 (0.009)*					
caudalmiddlefrontal	27.234 (0.423)**			-0.191 (0.036)**					
cuneus	9.942 (1.565)**	0.006 (0.002)**	1.05 (0.414)*	-0.049 (0.022)*					
entorhinal	4.602 (0.076)**			-0.014 (0.011)n.s.					
fusiform	36.57 (0.374)**			-0.122 (0.036)**					
inferiorparietal	31.432 (5.05)**	0.028 (0.006)**		-0.232 (0.071)**					
inferiortemporal	18.662 (3.426)**	0.022 (0.004)**	2.302 (0.891)*	-0.12 (0.048)*					
isthmuscingulate	-1.136 (1.356)n.s.	0.014 (0.002)**		0.008 (0.021)n.s.	0.008 (0.003)*				
lateraloccipital	34.637 (4.078)**	0.024 (0.005)**	2.888 (1.11)*	-0.238 (0.057)**					
lateralorbitofrontal	26.538 (0.29)**			-0.119 (0.033)**					
lingual	20.677 (2.759)**	0.015 (0.003)**		-0.077 (0.038)*					
medialorbitofrontal	19.872 (0.232)**			-0.062 (0.034)n.s.					
middletemporal	14.407 (3.115)**	0.025 (0.004)**		0.127 (0.044)**	-0.013 (0.007)n.s.				
parahippocampal	7.439 (0.137)**			-0.039 (0.009)**					
paracentral	5.835 (1.326)**	0.011 (0.002)**		-0.038 (0.021)n.s.					
parsopercularis	18.654 (0.263)**			-0.04 (0.021)n.s.					
parsorbitalis	6.816 (0.073)**			-0.026 (0.011)*					
parstriangularis	6.985 (1.484)**	0.009 (0.002)**		0.07 (0.021)**					
pericalcarine	14.295 (0.185)**			-0.031 (0.016)n.s.					
postcentral	22.699 (4.32)**	0.033 (0.005)**		-0.279 (0.091)**	-0.016 (0.013)n.s.	0.004 (0.002)*			
posteriorcingulate	12.17 (0.148)**			-0.074 (0.015)**					
precentral	55.799 (0.547)**			-0.204 (0.081)*					
precuneus	24.373 (2.855)**	0.019 (0.004)**	3.36 (0.81)**	-0.15 (0.039)**					
rostralanteriorcingulate	1.774 (1.209)n.s.	0.009 (0.001)**		0.067 (0.018)**					
rostralmiddlefrontal	65.743 (0.715)**			-0.335 (0.072)**					
superiorfrontal	25.723 (5.421)**	0.069 (0.007)**		0.211 (0.083)*					
superiorparietal	44.517 (5.055)**	0.019 (0.006)**	3.42 (1.209)*	-0.427 (0.075)**					
superiortemporal	43.096 (0.389)**			-0.129 (0.036)**					
supramarginal	30.028 (3.865)**	0.014 (0.005)**	5.785 (1.064)**	-0.312 (0.066)**	-0.014 (0.009)n.s.	0.003 (0.001)*			
frontalpole	2.305 (0.038)**			-0.005 (0.008)n.s.					
temporalpole	1.852 (0.538)**	0.004 (0.001)**		0.035 (0.011)**					
transversetemporal	4.794 (0.074)**			-0.037 (0.009)**					
insula	5.843 (1.967)**	0.022 (0.002)**		0.149 (0.036)**					

Intercept is the predicted value at the average age of the sample, s.e. = standard error, n.s. = not significant, * = significant level p<0.05, ** = significant level p<0.01

thesis_LW_V3.indb 56 06/06/16 07:38

Supplementary Table 10 Parameters for developmental trajectories of cortical surface area in the right hemisphere TBV included in model

Anatomical structure	Intercept (s.e.)	TotalGrayVolume (s.e.)	Gender (s.e.)	Age (s.e.)	Age^2 (s.e.)	Age^3 (s.e.)	Gender x Age (s.e.)	Gender x Age^2 (s.e.)	Gender x Age^3 (s.e.)
bankssts	5.988 (0.964)**	0.006 (0.001)**		-0.055 (0.013)**					
caudalanteriorcingulate	7.883 (0.132)**			-0.015 (0.011)n.s.					
caudalmiddlefrontal	12.389 (3.082)**	0.015 (0.004)**		-0.072 (0.041)n.s.					
cuneus	16.788 (0.175)**			-0.067 (0.02)**					
entorhinal	0.296 (0.84)n.s.	0.004 (0.001)**		0.015 (0.013)n.s.	0.004 (0.002)*				
fusiform	35.691 (0.358)**			-0.141 (0.036)**					
inferiorparietal	32.565 (4.743)**	0.034 (0.006)**	3.099 (1.213)*	-0.206 (0.067)**					
inferiortemporal	35.671 (0.43)**			-0.225 (0.043)**					
isthmuscingulate	2.488 (1.116)*	0.009 (0.001)**		0.001 (0.015)n.s.	0.005 (0.002)*				
lateraloccipital	34.376 (3.956)**	0.021 (0.005)**	4.677 (1.149)**	-0.182 (0.053)**					
lateralorbitofrontal	27.215 (0.316)**			-0.107 (0.036)**					
lingual	33.211 (0.324)**			-0.132 (0.032)**					
medialorbitofrontal	18.49 (0.21)**			-0.077 (0.026)**					
middletemporal	20.304 (2.53)**	0.021 (0.003)**	2.004 (0.746)*	0.021 (0.032)n.s.	-0.013 (0.005)**				
parahippocampal	7.391 (0.107)**			-0.031 (0.009)**					
paracentral	16.875 (0.232)**			-0.098 (0.027)**					
parsopercularis	10.442 (1.251)**	0.007 (0.002)**		-0.033 (0.015)*					
parsorbitalis	8.592 (0.104)**			-0.028 (0.013)*					
parstriangularis	8.785 (1.731)**	0.01 (0.002)**		0.033 (0.022)n.s.	-0.011 (0.003)**				
pericalcarine	16.073 (0.206)**			-0.016 (0.016)n.s.					
postcentral	22.039 (3.998)**	0.029 (0.005)**	2.691 (0.883)**	-0.196 (0.062)**					
posteriorcingulate	12.636 (0.171)**			-0.076 (0.015)**					
precentral	56.256 (0.533)**			-0.153 (0.066)*					
precuneus	27.108 (3.201)**	0.018 (0.004)**	4.36 (0.934)**	-0.24 (0.043)**					
rostralanteriorcingulate	1.828 (1.026)n.s.	0.006 (0.001)**		0.049 (0.015)**					
rostralmiddlefrontal	66.7 (0.758)**			-0.372 (0.058)**					
superiorfrontal	79.907 (0.782)**			-0.258 (0.069)**					
superiorparietal	36.203 (5.099)**	0.032 (0.006)**		-0.336 (0.082)**					
superiortemporal	41.373 (0.369)**			-0.121 (0.027)**					
supramarginal	23.465 (3.435)**	0.021 (0.004)**	3.299 (1.082)**	-0.14 (0.045)**					
frontalpole	3.109 (0.05)**			-0.011 (0.01)n.s.					
temporalpole	1.859 (0.568)**	0.003 (0.001)**		0.023 (0.011)*					
transversetemporal	3.673 (0.049)**			-0.025 (0.006)**					
insula	7.471 (1.997)**	0.02 (0.003)**	1.375 (0.418)**	0.141 (0.034)**					

Intercept is the predicted value at the average age of the sample, s.e. = standard error, n.s. = not significant, * = significant level p<0.05, ** = significant level p<0.01

thesis_LW_V3.indb 57 06/06/16 07:38

Supplementary Table 11 Parameters for developmental trajectories of cortical volume in the right hemisphere TBV included in model

Anatomical structure	Intercept (s.e.)	TotalGrayVolume (s.e.)	Gender (s.e.)	Age (s.e.)	Age^2 (s.e.)	Age^3 (s.e.)	Gender x Age (s.e.)	Gender x Age^2 (s.e.)	Gender x Age^3 (s.e.)
bankssts	-0.09 (0.353)n.s.	0.004 (4.24e-04)*		-0.037 (0.005)**	0.003 (7.01eT 04)**				
caudalanteriorcingulate	2.634 (0.053)**			-0.017 (0.003)**					
caudalmiddlefrontal	8.313 (0.138)**			-0.101 (0.015)**					
cuneus	0.498 (0.371)n.s.	0.004 (4.45e-04)*		-0.031 (0.005)**	0.004 (7.44eT 04)**				
entorhinal	-0.762 (0.4)n.s.	0.003 (4.80e-04)*		0.015 (0.006)*	0.002 (9.76eT 04)*				
fusiform	-1.975 (1.002)n.s.	0.017 (1.20e-03)*		-0.045 (0.015)**	0.009 (2.28eT 03)**				
inferiorparietal	-3.861 (1.311)**	0.03 (1.57e-03)*		-0.283 (0.026)**	0.001 (3.85eT 03)n.s.	0.002 (0.001)**			
inferiortemporal	12.798 (0.176)**			-0.126 (0.019)**					
isthmuscingulate	0.052 (0.313)n.s.	0.004 (3.74e-04)*		-0.026 (0.004)**	0.001 (5.46eT 04)*				
lateraloccipital	1.331 (1.218)n.s.	0.015 (1.53e-03)*	0.892 (0.286)**	-0.074 (0.017)**	0.009 (2.58eT 03)**				
lateralorbitofrontal	9.285 (0.111)**			-0.091 (0.015)**					
lingual	0.798 (0.719)n.s.	0.008 (8.61e-04)*		-0.019 (0.014)n.s.	0.008 (1.97eT 03)**	0.001 (0.001)*			
medialorbitofrontal	6.123 (0.075)**			-0.072 (0.013)**					
middletemporal	0.331 (0.997)n.s.	0.02 (1.19e-03)*		0.015 (0.013)n.s.	-0.004 (1.85e-03)*				
parahippocampal	2.513 (0.037)**			-0.021 (0.004)**					
paracentral	0.076 (0.545)n.s.	0.006 (6.61e-04)*		-0.033 (0.008)**					
parsopercularis	-0.925 (0.46)*	0.008 (5.54e-04)*		-0.014 (0.006)*					
parsorbitalis	3.659 (0.051)**			-0.034 (0.007)**					
parstriangularis	6.046 (0.095)**			-0.055 (0.009)**					
pericalcarine	0.978 (0.34)**	0.002 (4.07e-04)*		0.019 (0.008)*	0.004 (1.13eT 03)**	0.001 (0.001)**			
postcentral	-1.565 (1.057)n.s.	0.016 (1.28e-03)*		-0.057 (0.016)**					
posteriorcingulate	0.11 (0.402)n.s.	0.005 (4.86e-04)*		-0.022 (0.005)**					
precentral	-1.118 (0.995)n.s.	0.021 (1.21e-03)*		0.034 (0.015)*					
precuneus	-1.699 (0.898)n.s.	0.019 (1.08e-03)*		-0.153 (0.012)**	0.01 (1.79e-03)*				
rostralanteriorcingulate	-0.757 (0.423)n.s.	0.004 (5.12e-04)*		0.016 (0.006)*					
rostralmiddlefrontal	22.91 (0.263)**			-0.247 (0.041)**					
superiorfrontal	-6.748 (1.782)**	0.046 (2.23e-03)*	-1.23 (0.407)**	0.016 (0.025)n.s.	-0.019 (3.90e-03)*				
superiorparietal	-1.317 (1.394)n.s.	0.024 (1.75e-03)*	-0.883 (0.331)*	-0.206 (0.02)**	0.012 (2.95e-03)*				
superiortemporal	15.392 (0.164)**			-0.111 (0.019)**					
supramarginal	-2.2 (1.013)*	0.02 (1.23e-03)*		-0.097 (0.014)**					
frontalpole	1.415 (0.027)**			-0.014 (0.005)**					
temporalpole	0.616 (0.364)n.s.	0.002 (4.41e-04)*		0.025 (0.007)**					
transversetemporal	0.026 (0.16)n.s.	0.001 (1.92e-04)*		-0.008 (0.002)**	0.001 (3.33e-04)*				
insula	-0.576 (0.613)n.s.	0.011 (7.36e-04)*		0.025 (0.01)*	0.004 (1.73e-03)*				

Intercept is the predicted value at the average age of the sample, s.e. = standard error, n.s. = not significant, * = significant level p<0.05, ** = significant level p<0.01

thesis_LW_V3.indb 58 06/06/16 07:38

Supplementary Table 12 Parameters for developmental trajectories of cortical volume in the left hemisphere TBV included in model

Anatomical structure	Intercept (s.e.)	TotalGrayVolume (s.e.)	Gender (s.e.)	Age (s.e.)	Age^2 (s.e.)	Age^3 (s.e.)	Gender x Age (s.e.)	Gender x Age^2 (s.e.)	Gender x Age^3 (s.e.)
bankssts	-0.78 (0.383)*	0.005 (4.59e-04)*		-0.043 (0.005)**	0.004 (7.28e-04)*				
caudalanteriorcingulate	0.516 (0.341)n.s.	0.002 (4.11e-04)*		-0.014 (0.004)**					
caudalmiddlefrontal	-2.386 (0.748)**	0.014 (9.23e-04)*	-0.655 (0.241)*	-0.034 (0.009)**	-0.003 (1.28e-03)*				
cuneus	0.46 (0.419)n.s.	0.004 (5.02e-04)*		-0.025 (0.006)**	0.004 (8.41e-04)*				
entorhinal	-0.423 (0.314)n.s.	0.003 (3.80e-04)*		0.013 (0.005)*					
fusiform	-0.338 (0.961)n.s.	0.016 (1.16e-03)*		-0.049 (0.014)**					
inferiorparietal	-2.605 (1.547)n.s.	0.026 (1.93e-03)*	-0.936 (0.372)*	-0.215 (0.029)**	0.002 (4.17e03)n.s.	0.002 (0.001)*			
inferiortemporal	13.721 (0.177)**			-0.141 (0.02)**					
isthmuscingulate	-0.064 (0.327)n.s.	0.004 (3.96e-04)*		-0.022 (0.005)**					
lateraloccipital	-0.85 (1.068)n.s.	0.017 (1.28e-03)*		-0.041 (0.015)**	0.009 (2.14e-03)*				
lateralorbitofrontal	-0.668 (0.714)n.s.	0.012 (8.67e-04)*		-0.036 (0.013)**					
lingual	-0.018 (0.664)n.s.	0.009 (7.96e-04)*		-0.034 (0.009)**	0.006 (1.25e-03)*				
medialorbitofrontal	-1.091 (0.649)n.s.	0.009 (7.87e-04)*		-0.021 (0.012)n.s.					
middletemporal	-0.556 (1.02)n.s.	0.019 (1.22e-03)*		0.034 (0.013)*	-0.006 (1.83e-03)*				
parahippocampal	0.193 (0.347)n.s.	0.003 (4.20e-04)*		-0.01 (0.005)*					
paracentral	-0.617 (0.402)n.s.	0.006 (5.10e-04)*	-0.218 (0.094)*	-0.03 (0.006)**					
parsopercularis	0.127 (0.626)n.s.	0.008 (7.58e-04)*		-0.031 (0.009)**					
parsorbitalis	0.374 (0.389)n.s.	0.003 (4.67e-04)*		-0.007 (0.006)n.s.	-0.002 (8.92e-04)*				
parstriangularis	-0.379 (0.536)n.s.	0.007 (6.43e-04)*		0.005 (0.007)n.s.	-0.004 (1.02e-03)*				
pericalcarine	1.204 (0.325)**	0.001 (3.89e-04)*		0.02 (0.007)**	0.003 (1.04e-03)*	0 (0.001)**			
postcentral	-1.68 (1.121)n.s.	0.017 (1.35e-03)*		-0.059 (0.016)**	0.007 (2.44e-03)**				
posteriorcingulate	0.55 (0.376)n.s.	0.004 (4.54e-04)*		-0.025 (0.005)**					
precentral	-1.748 (1.191)n.s.	0.022 (1.43e-03)*		0.078 (0.027)**	0.001 (4.04 e-03)n.s.	0.001 (0.001)*			
precuneus	-0.644 (0.901)n.s.	0.017 (1.08e-03)*		-0.135 (0.012)**	0.008 (1.83 e-03)**				
rostralanteriorcingulate	-1.562 (0.423)**	0.006 (5.12e-04)*		0.019 (0.006)**					
rostralmiddlefrontal	-8.094 (1.496)**	0.037 (1.79e-03)*		-0.093 (0.023)**	-0.013 (3.63e-03)*				
superiorfrontal	-4.079 (1.671)*	0.043 (2.10e-03)*	-0.878 (0.371)*	-0.034 (0.025)n.s.	-0.013 (3.96e-03)*				
superiorparietal	-0.3 (1.333)n.s.	0.022 (1.60e-03)*		-0.229 (0.021)**	0.013 (3.37e-03)*				
superiortemporal	-1.948 (0.902)*	0.022 (1.08e-03)*		0.026 (0.017)n.s.	0.007 (2.42e-03)*	-0.001 (0)*			
supramarginal	-3.906 (1.253)**	0.023 (1.56e-03)*	0.789 (0.304)*	-0.162 (0.024)**	-0.003 (3.40e-03)n	0.001 (0.001)*			
frontalpole	1.049 (0.024)**			-0.006 (0.004)n.s.					
temporalpole	0.622 (0.373)n.s.	0.003 (4.52e-04)*		0.029 (0.007)**					
transversetemporal	-0.208 (0.203)n.s.	0.002 (2.43e-04)*		-0.009 (0.003)**	0.002 (4.09e-04)*				
insula	0.201 (0.614)n.s.	0.01 (7.45e-04)*		0.024 (0.011)*					

Intercept is the predicted value at the average age of the sample, s.e. = standard error, n.s. = not significant, * = significant level p<0.05, ** = significant level p<0.01

thesis_LW_V3.indb 59 06/06/16 07:38

References

Blanton, R.E., Levitt, J.G., Thompson, P.M., Narr, K.L., Capetillo-Cunliffe, L., Nobel, A., et al., 2001. Mapping cortical asymmetry and complexity patterns in normal children. Psychiatry Res. 107 (1), 29–43.

Clarkson, M.J., Cardoso, M.J., Ridgway, G.R., Modat, M., Leung, K.K., Rohrer, J.D., Fox, N.C., Ourselin, S., 2011. A comparison of voxel and surface based cortical thickness estimation methods. NeuroImage 57, 856–865.

Costello, E.J., Edelbrock, C.S., Costello, A.J., 1985. Validity of the NIMH diagnostic interview schedule for children: a comparison between psychiatric and pediatric referrals. J. Abnorm. Child Psychol. 13, 579–595.

Dale, A., Fischl, B., Sereno, M.I., 1999. Cortical surface-based analysis: i. segmentation and surface reconstruction. NeuroImage 9, 179–194.

Desikan, R.S., Ségonne, F., Fischl, B., Quinn, B.T., Dickerson, B.C., Blacker, D., Buckner, R.L., Dale, A.M., Maguire, R.P., Hyman, B.T., Albert, M.S., Killiany, R.J., 2006. An automated labeling system for subdividing the human cerebral cortex on MRI scans into gyral based regions of interest. NeuroImage 31, 968–980.

Dewey, J., Hana, G., Russell, T., Price, J., McCaffrey, D., Harezlak, J., Sem, E., Anyanwu, J.C., Guttmann, C.R., Navia, B., Cohen, R., Tate, D.F., HIV Neuroimaging Consortium, 2010. Reliability and validity of MRI-based automated volumetry software relative to auto-assisted manual measurement of subcortical structures in HIV-infected patients from a multisite study. NeuroImage 51, 1334–1344.

Durston, S., Nederveen, H., van Dijk, S., van Belle, J., de Zeeuw, P., Langen, M., van Dijk, A., 2009. Magnetic resonance simulation is effective in reducing anxiety related to magnetic resonance scanning in children. J. Am. Acad. Child Adolesc. Psychiatry 48, 206–207.

Fischl, B., Dale, A.M., 2000. Measuring the thickness of the human cerebral cortex from magnetic resonance images. Proc. Natl. Acad. Sci. U. S. A. 97, 11050–11055.

Fischl, B., Sereno, M.I., Dale, A., 1999. Cortical surface-based analysis: II: inflation, flattening, and a surface-based coordinate system. NeuroImage 9, 195–207.

thesis_LW_V3.indb 60 06/06/16 07:38

Fischl, B., Liu, A., Dale, A.M., 2001. Automated manifold surgery: constructing geometrically accurate and topologically correct models of the human cerebral cortex. IEEE Med. Imaging 20, 70–80.

Fischl, B., Salat, D.H., van der Kouwe, A.J.W., Makris, N., Ségonne, F., Quinn, B.T., Dale, A.M., 2004a. Sequence-independent segmentation of magnetic resonance images. NeuroImage 23, S69–S84.

Fischl, B., van der Kouwe, A., Destrieux, C., Halgren, E., Ségonne, F., Salat, D.H., Busa, E., Seidman, L.J., Goldstein, J., Kennedy, D., Caviness, V., Makris, N., Rosen, B., Dale, A.M., 2004b. Automatically parcellating the human cerebral cortex. Cereb. Cortex 14, 11–22.

Fox, J., 2002. Linear mixed models-appendix to an R and S-PLUS companion to applied regression. Relation 10, 5261.

Giedd, J.N., Rapoport, J.L., 2010. Structural MRI of pediatric brain development: what have we learned and where are we going? Neuron 67, 728–734.

Giedd, J.N., Blumenthal, J., Jeffries, N.O., Castellanos, F.X., Liu, H., Zijdenbos, A., Paus, T., Evans, A.C., Rapoport, J.L., 1999. Brain development during childhood and adolescence: a longitudinal MRI study. Nat. Neurosci. 2, 861–863.

Gogtay, N., Giedd, J., Lusk, L., Hayashi, K., Greenstein, D., Vaituzis, A., Nugent, T., Herman, D., Clasen, L., Toga, A., Rapoport, J., Thompson, P., 2004. Dynamic mapping of human cortical development during childhood through early adulthood. Proc. Natl. Acad. Sci. U. S. A. 101, 8174–8179.

Ghosh, S.S., Kakunoori, S., Augustinack, J., Nieto-Castanon, A., Kovelman, I., Gaab, N., et al., 2010. Evaluating the validity of volume-based and surface-based brain image registration for developmental cognitive neuroscience studies in children 4 to 11 years of age. NeuroImage 53 (1), 85–93.

Han, X., Jovicich, J., Salat, D., van der Kouwe, A., Quinn, B., Czanner, S., Busa, E., Pacheco, J., Albert, M., Killiany, R., Maguire, P., Rosas, D., Makris, N., Dale, A., Dickerson, B., Fischl, B., 2006. Reliability of MRI-derived measurements of human cerebral cortical thickness: the effects of field strength, scanner upgrade and manufacturer. NeuroImage 32, 180–194.

thesis_LW_V3.indb 61 06/06/16 07:38

Hill, J., Inder, T., Neil, J., Dierker, D., Harwell, J., Van Essen, D., 2010. Similar patterns of cortical expansion during human development and evolution. Proc. Natl. Acad. Sci. 107 (29), 13135–13140.

Hutton, C., Draganski, B., Ashburner, J., Weiskopf, N., 2009. A comparison between voxel based cortical thickness and voxel-based morphometry in normal aging. NeuroImage 48, 371–380.

Jansen, A., 2005. Genetics of the polymicrogyria syndromes. J. Med. Genet. 42, 369–378. Lenroot, R.K., Gogtay, N., Greenstein, D.K., Wells, E.M., Wallace, G.L., Clasen, L.S.,

Blumenthal, J.D., Lerch, J., Zijdenbos, A.P., Evans, A.C., Thompson, P.M., Giedd, J.N., 2007. Sexual dimorphism of brain developmental trajectories during childhood and adolescence. NeuroImage 36, 1065–1073.

Lenroot, R.K., Schmitt, J.E., Ordaz, S.J., Wallace, G.L., Neale, M.C., Lerch, J.P., Kendler, K.S., Evans, A.C., Giedd, J.N., 2009. Differences in genetic and environmental influences on the human cerebral cortex associated with development during childhood and adolescence. Hum. Brain Mapp. 30, 163–174.

Luders, E., Narr, K.L., Thompson, P.M., Rex, D.E., Woods, R.P., DeLuca, H., Jancke, L., Toga, A.W., 2006. Gender effects on cortical thickness and the influence of scaling. Hum. Brain Mapp. 27, 314–324.

Nopoulos, P., Flaum, M., O'Leary, D., Andreasen, N.C., 2000. Sexual dimorphism in the human brain: evaluation of tissue volume, tissue composition and surface anatomy using magnetic resonance imaging. Psychiatry Res. Neuroimaging 98, 1–13.

Panizzon, M.S., Fennema-Notestine, C., Eyler, L.T., Jernigan, T.L., Prom-Wormley, E., Neale, M., Jacobson, K., Lyons, M.J., Grant, M.D., Franz, C.E., Xian, H., Tsuang, M., Fischl, B., Seidman, L., Dale, A., Kremen, W.S., 2009. Distinct genetic influences on cortical surface area and cortical thickness. Cereb. Cortex 19, 2728–2735.

Piao, X., Hill, R.S., Bodell, A., Chang, B.S., Basel-Vanagaite, L., Straussberg, R., Dobyns, W.B., Qasrawi, B., Winter, R.M., Innes, A.M., Voit, T., Ross, M.E., Michaud, J.L., Descarie, J.-C., Barkovich, A.J., Walsh, C.A., 2004. G protein-coupled receptor-dependent development of human frontal cortex. Sci. Signal. 303, 2033–2036.

thesis_LW_V3.indb 62 06/06/16 07:38

Rakic, P., 1995. A small step for the cell, a giant leap for mankind: a hypothesis of neocortical expansion during evolution. Trends Neurosci. 18, 383–388.

Raznahan, A., Shaw, P., Lalonde, F., Stockman, M., Wallace, G.L., Greenstein, D., Clasen, L., Gogtay, N., Giedd, J.N., 2011. How does your cortex grow? J. Neurosci. 31, 7174–7177.

Reiss, A.L., Abrams, M.T., Singer, H.S., Ross, J.L., Denckla, M.B., 1996. Brain development, gender and IQ in children. A volumetric imaging study. Brain 119, 1763–1774.

Reuter, M., Fischl, B., 2011. Avoiding asymmetry-induced bias in longitudinal image processing. NeuroImage 57, 19–21.

Reuter, M., Rosas, H.D., Fischl, B., 2010. Highly accurate inverse consistent registration: a robust approach. NeuroImage 53, 1181–1196.

Reuter, M., Schmansky, N.J., Rosas, H.D., Fischl, B., 2012. Within-subject template estimation for unbiased longitudinal image analysis. NeuroImage 61, 1402–1418.

Salat, D.H., 2004. Thinning of the cerebral cortex in aging. Cereb. Cortex 14, 721–730. Salinas, J., Mills, E.D., Conrad, A.L., Koscik, T., Andreasen, N.C., Nopoulos, P., 2012. Sex differences in parietal lobe structure and development. Gend. Med. 9, 44–55.

Segonne, F., Dale, A.M., Busa, E., Glessner, M., Salat, D., Hahn, H.K., Fischl, B., 2004. A hybrid approach to the skull stripping problem in MRI. NeuroImage 22 (3), 1060–1075. Segonne, F., Pacheco, J., Fischl, B., 2007. Geometrically accurate topology-correction of cortical surfaces using nonseparating loops. IEEE Trans. Med. Imaging 26, 518–529.

Shaw, P., Greenstein, D., Lerch, J., Clasen, L., Lenroot, R., Gogtay, N., Evans, A., Rapoport, J., Giedd, J., 2006. Intellectual ability and cortical development in children and adolescents. Nature 440, 676–679.

Shaw, P., Kabani, N.J., Lerch, J.P., Eckstrand, K., Lenroot, R., Gogtay, N., Greenstein, D., Clasen, L., Evans, A., Rapoport, J.L., Giedd, J.N., Wise, S.P., 2008. Neurodevelopmental trajectories of the human cerebral cortex. J. Neurosci. 28, 3586–3594.

Shaw, P., Malek, M., Watson, B., Sharp, W., Evans, A., Greenstein, D., 2012. Development of cortical surface area and gyrification in attention-deficit/hyperactivity disorder. Biol.

thesis_LW_V3.indb 63 06/06/16 07:38

Psychiatry 72, 191–197.

Sheehan, D.V., Lecrubier, Y., Sheehan, K.H., Amorim, P., Janavs, J., Weiller, E., Hergueta, T., Baker, R., Dunbar, G.C., 1998. The mini-international neuropsychiatric interview (M.I.N.I.): the development and validation of a structured diagnostic psychiatric interview for DSM-IV and ICD-10. J. Clin. Psychiatry 59 (Suppl. 20), 22–33 (quiz 34–57).

Sled, J.G., Zijdenbos, A.P., Evans, A.C., 1998. A nonparametric method for automatic correction of intensity nonuniformity in MRI data. IEEE Trans. Med. Imaging 17, 87–97.

Sowell, E.R., Thompson, P.M., Holmes, C.J., Jernigan, T.L., Toga, A.W., 1999. In vivo evidence for post-adolescent brain maturation in frontal and striatal regions. Nat. Neurosci. 2, 859–861.

Sowell, E.R., Thompson, P.M., Tessner, K.D., Toga, A.W., 2001. Mapping continued brain growth and gray matter density reduction in dorsal frontal cortex: inverse relationships during postadolescent brain maturation. J. Neurosci. 21, 8819–8829.

Sowell, E.R., Trauner, D.A., Gamst, A., Jernigan, T.L., 2002. Development of cortical and subcortical brain structures in childhood and adolescence: a structural MRI study. Dev. Med. Child Neurol. 44 (1), 4–16.

Sowell, E., Thompson, P., Leonard, C., Welcome, S., Kan, E., Toga, A., 2004. Longitudinal mapping of cortical thickness and brain growth in normal children. J. Neurosci. 24, 8223–8231.

Sowell, E.R., Peterson, B.S., Kan, E., Woods, R.P., Yoshii, J., Bansal, R., Xu, D., Thompson, P.M., Toga, A.W., 2006. Sex differences in cortical thickness mapped in 176 healthy individuals between 7 and 87 years of age. Cereb. Cortex 17, 1550–1560.

Strien, J.W.V., 2003. The Dutch Handedness Questionnaire.

Tamnes, C.K., Fjell, A.M., Ostby, Y., Westlye, L.T., Due-Tonnessen, P., Bjornerud, A., Walhovd, K.B., 2011. The brain dynamics of intellectual development: waxing and waning white and gray matter. Neuropsychologia 49, 3605–3611.

Van Haasen, P.P., De Bruyn, E.E.J., Pijl, Y.J., Poortinga, Y.H., Lutje-Spelberg, H.C., Vander

thesis_LW_V3.indb 64 06/06/16 07:38

Steene, G., et al., 1986. Wechsler Intelligence Scale for Children-Revised, Dutch Version.

Wechsler, D., Wechsler, D., 2000. wechsler adult intelligence scale-third edition (WAIS-III): Nederlandstalige Bewerking. Technische Handleiding. (Dutch Version Technical Manual).

Wilke, M., Krägeloh-Mann, I., Holland, S.K., 2007. Global and local development of gray and white matter volume in normal children and adolescents. Exp. Brain Res. 178, 296–307.

thesis_LW_V3.indb 65 06/06/16 07:38

TYPICAL DEVELOPMENT OF BASAL GANGLIA, HIPPOCAMPUS, AMYGDALA AND CEREBELLUM FROM AGE 7 TO 24

Lara M Wierenga
Marieke Langen
Sara Ambrosino
Sarai van Dijk
Bob Oranje
Sarah Durston

NeuroImage 2014: 96, 67–72

thesis_LW_V3.indb 67 06/06/16 07:38

Abstract

Developmental imaging studies show that cortical grey matter decreases in volume during childhood and adolescence. However, considerably less research has adressed the development of subcortical regions (caudate, putamen, pallidum, accumbens, thalamus, amygdala, hippocampus and the cerebellar cortex), in particular not in longitudinal designs. We used the automatic labeling procedure in FreeSurfer to estimate the developmental trajectories of the volume of these subcortical structures in 147 participants (age 7.0-24.3 years old, 94 males; 53 females) of whom 53 participants were scanned twice or more. A total of 223 magnetic resonance imaging (MRI) scans (acquired at 1.5-T) were analyzed. Substantial diversity in the developmental trajectories was observed between the different subcortical gray matter structures: the volume of caudate, putamen and nucleus accumbens decreased with age, whereas volume of hippocampus, amygdala, pallidum and cerebellum showed an inverted U-shaped developmental trajectory. The thalamus showed an initial small increase in volume followed by a slight decrease. All structures had larger volume in males than females over the whole age range, except for the cerebellum that had a sexually dimorphic developmental trajectory. Thus, subcortical structures appear to not yet be fully developed in childhood, similar to the cerebral cortex, and continue to show maturational changes into adolescence. In addition, there is substantial heterogeneity between the developmental trajectories of these structures.

thesis_LW_V3.indb 68 06/06/16 07:38

Introduction

Brain development is an extremely complex process that is guided by genetic programs, environmental exposure and experiences (Tau and Peterson, 2009). Its course is protracted, continuing into adolescence and adulthood: for example, overall gray matter volume shows an inverted U-shaped trajectory, peaking in early adolescence (Dennison et al., 2013; Giedd and Rapoport, 2010; Goddings et al., 2013; Koolschijn and Crone, 2013; Lenroot et al., 2007; Ostby et al., 2009; Reiss et al., 1996; Sowell et al., 1999; 2002; Tau and Peterson, 2009; Wilke et al., 2007). White matter, in contrast, continues to increase in volume into adulthood (Paus, 2010a; Paus et al., 2001; Walhovd et al., 2005). However, the developmental patterns of other structures, such as the striatum, limbic structures and the cerebellum, have been studied less frequently and findings have often been inconsistent: for example, both increases and decreases in caudate volume have been reported in children and adolescents (Giedd and Rapoport, 2010; Giedd et al., 1996; Goddings et al., 2013; Koolschijn and Crone, 2013; Lenroot et al., 2007; Ostby et al., 2009; Reiss et al., 1996; Sowell et al., 2002; 1999; Tau and Peterson, 2009; Wilke et al., 2007). In addition, most studies of such structures have investigated only one single structure, or a few, making it difficult to address the dynamic interplay between subcortical structures as they develop. Furthermore, differences in methodology or sample characteristics between studies complicate direct comparisons between reported findings. It is therefore pivotal to investigate multiple structures in the same sample (as in Dennison et al., 2013; Goddings et al., 2013; Koolschijn and Crone, 2013; Ostby et al., 2009). Furthermore, most studies to date have used cross-sectional designs, thus limiting their ability to draw inferences about development. Particularly given the large inter-individual variation, it is important to use longitudinal designs to investigate brain development. Therefore, we set out to investigate the dynamic changes in subcortical structures with development, as well as the relationship between them in the present longitudinal study. We investigated changes in the volume of caudate nucleus, putamen, pallidum, accumbens, thalamus, amygdala, hippocampus and cerebellum. We were particularly interested in these structures, as they play an important role in cognitive development (Bunge, 2009; Diamond, 2000; Ito, 2008; Lavenex and Banta Lavenex, 2013; Scherf et al., 2013) and because they have been implicated in

thesis_LW_V3.indb 69 06/06/16 07:38

various developmental disorders, such as autism (Langen et al., 2013; Philip et al., 2012), attention deficit/hyperactivity disorder (Carmona et al., 2009; Krain and Castellanos, 2006), schizophrenia (Ballmaier et al., 2008; Mamah et al., 2008), and substance use disorders (Berman et al., 2008; Koob, 2006; Volkow et al., 2007). Interestingly, many of these disorders first manifest themselves during childhood or adolescence (Paus et al., 2010, Durston et al., 2001), underlining that brain development in this period is pivotal in healthy development.

Recently, we reported on the development of cortical volume, thickness and surface area in a large cohort of typically developing children, using a combined cross-sectional and longitudinal study design (Wierenga et al. 2013). Here, we report on the development of eight subcortical structures in a larger cohort. We focused on those subcortical structures that have been implicated most frequently in developmental disorders (caudate nucleus, putamen, pallidum, accumbens, thalamus, amygdala, hippocampus and the cerebellum). A total of 223 MRI scans from 147 typical developing children and adolescents (64% males) were included, where more than one third of the participants was scanned twice or more. On average, the time interval between two successive scans was two years (ranging from 1.5 to 5.6 years). We aimed to describe the developmental trajectories of these subcortical structures. In addition, we investigated gender differences, as some studies have reported sexually dimorphic developmental trajectories (e.g. Dennison et al., 2013). We explored developmental change in the volume of amygdala and hippocampus, striatum and cerebellum.

Materials and methods

The Institutional Review Board of the University Medical Center Utrecht, the Netherlands approved this study and its procedures. Subjects aged 18 years and older signed for their own consent. For children under 18 years of age, a parent signed for consent.

Participants

The present study included a total of 223 MRI-scans from 147 typically developing individuals (94 males; 53 females); 53 participants were scanned twice or more (41 males; 12 females). Scans were acquired with a average interval of two years (ranging from 1.5

thesis_LW_V3.indb 70 06/06/16 07:38

to 5.6 years). Participants were aged between 7.0 and 23.3 years old, with above average intellectual levels (see Table 1 for participant characteristics).

Participants were recruited through schools and other educational centers in the area. For all participants under 18 years of age, a parent participated in a semi-structured interview session with a trained rater to confirm absence of any psychiatric diagnosis (Diagnostic Interview Schedule for Children; DISC). Older subjects participated in the Mini-International Neuropsychiatric Interview (M.I.N.I) to confirm absence of psychopathological symptoms (Sheehan et al., 1998). Individuals with a psychiatric diagnosis (current or prior), major physical illness of the cardiovascular, the endocrine, the pulmonic or the gastrointestinal system, neurological illness, a history of unconsciousness, organic brain damage or disease, alcohol or other drug dependence, or full IQ below 75 were excluded from participation. In addition, individuals with a first-degree relative suffering from a psychiatric illness were excluded.

Table 1 Participant characteristics

	Group			
Characterstics	Male		Female	
Number of individuals, n	94		53	
Hand preference, n				
Right handed	74		48	
Other	20		5	
Height, mean (SD)	163.2 (20.6)		155.6 (17.4)	
Weight, mean (SD)	52.5 (19.0)		48.7 (15.5)	
IQ, mean (SD)	113.2 (16.1)		112.6 (13.8)	
Sibling, n	30		9	
Total number of scans, n	153		70	
Scan Nr.	n	Mean age (SD)	n	Mean age (SD)
1	94	12.6 (4.0)	53	12.5 (3.9)
2	41	15.0 (4.0)	12	14.2 (4.1)
≥3	18	16.2 (2.7)	5	18.7 (2.9)

SD=standard deviation

thesis_LW_V3.indb 71 06/06/16 07:38

Written informed consent was obtained for all participants. All individuals participated in at least one or more MRI scanning sessions and intelligence testing (children older than 16 years of age: Wechsler Adult Intelligence Scale/Wechsler Adult Intelligence Scale-Third Edition [WAIS/WAIS-III] (Stinissen et al., 1980; Wechsler D, 2000); children of 16 years or younger: Wechsler Intelligence Scale for Children-Revised/Wechsler Intelligence Scale for Children-Third Edition [WISC-R/WISC-III] (Van Haasen et al., 1986; Lisse et al., 2005). Furthermore, participants and their parents filled out a short questionnaire on hand preference and a questionnaire related to major physical or neurological illness. Children under 13 years of age were acclimated to the scanning procedure in a dummy-scan session prior to the actual MRI session (Durston et al., 2009; Mega and Cummings, 1994). An independent clinical neuroradiologist evaluated all MRI-scans. No gross abnormalities were reported for any of the participants.

Image acquisition

Magnetic resonance imaging (MRI) scans were acquired on a 1.5-T scanner (Philips, Best, The Netherlands). For definition of all brain measures, a whole brain T1-weighted three-dimensional fast field echo scan with 160-180; 1 mm × 1 mm × 1.2 mm contiguous coronal slices was acquired (256 × 256 matrix, FoV = 256 mm, echo time (TE) = 4.6 ms, repetition time (TR) = 30 ms, flip angle = 30°).

Image processing
Cortical reconstruction and volumetric segmentation

All MRI scans were coded to ensure rater blindness to subject identity. Scans were processed and analyzed using the neuroimaging computer network of the Department of Psychiatry, Brain Center Rudolf Magnus, University Medical Center Utrecht. FreeSurfer v 5.1.0 software was used to estimate the volume of our regions of interest (ROIs): caudate nucleus, putamen, pallidum, accumbens, thalamus, amygdala, hippocampus and the cerebellar cortex. This is a well-validated and well-documented software program that is freely available for download online (http://surfer.nmr.mgh.harvard.edu/). Technical details of the automated reconstruction scheme are described elsewhere (Carmona et al., 2009; Dale et al., 1999; Fischl et al., 1999).

In short, neuroanatomical labels are automatically assigned to each voxel based on

thesis_LW_V3.indb 72 06/06/16 07:38

probabilistic information from a manually labeled set. This automatic labeling method shows similar results to manual labeling, and low reproducibility errors (Fischl et al., 2002; Tae et al. 2008; Jovicich et al., 2009). Before quantitative analyses can be performed, output requires qualitative inspection (Dewey et al., 2010). Manual edits were performed where needed by three experienced raters (LW, SA, SvD). Edits included the removal of non-brain tissue and perfecting the white matter mask. The standardized procedures, documented on the FreeSurfer website, were used for these manual edits.

Total CSF volume was calculated as the sum of all ventricles. Total cerebral subcortical gray volume was calculated as the sum of all subcortical ROIs, excluding the cerebellum (caudate nucleus, putamen, pallidum, accumbens, thalamus, amygdala and hippocampus). The brain stem was not included as its volume depends on the field of view at acquisition.

Longitudinal processing

In order to reduce within subject variability between scan sessions, a longitudinal analysis method was developed for FreeSurfer (Gogtay et al., 2006; Reuter and Fischl, 2011). This method increases repeatability and statistical power (Gogtay et al., 2006; Lenroot et al., 2007; Reuter et al., 2010; Wilke et al., 2007). All second, third and fourth scans (n = 53) were processed using this procedure. An unbiased within-subject template and an average image were created, using inverse consistent registration. This reduces the potential over-regularization of longitudinal image processing (Reuter et al., 2012).

Statistical analyses

In order to investigate the relation between age and the volume of our ROIs, we used a linear mixed model procedure. This procedure accounts for irregular intervals between measures, missing data and within person dependence (Fox, 2002; Neufang et al., 2009; Ostby et al., 2009; Shaw et al., 2011). Each dependent measure of the ith family, jth individual and kth time-point was modeled as described by Raznahan and colleagues (2011). Several models including linear age terms, quadratic age terms, cubic age terms or gender terms were fit.

thesis_LW_V3.indb 73 06/06/16 07:38

The full model is represented by the following formula:

$$\text{Measurement}_{ijk} = \text{Intercept} + d_{ij} + ß_1(\text{gender}) + ß_2(\text{age}) + ß_3(\text{age}^2) + ß_4(\text{age}^3) + ß_5(\text{gender*age}) + ß_6(\text{gender*age}^2) + ß_7(\text{gender*age}^3) + e_{ijk}$$

The e_{ijk} term represents the normally distributed residual error. Each ß represents a parameter estimate; for example the quadratic age effect parameter is represented by $ß_3$. Furthermore, interaction effects of gender and age are modeled. The full model was tested against models including linear or quadratic age terms only. Intercept, gender and age effects were fixed, while within person dependence, nested within family (dij), was modeled as a random effect. All possible developmental models were run using mean-centered age terms (age 13.5).

The choice of the best model fit was based on three steps: first, cubic, quadratic and linear age effects were fitted on the volumes of each ROI (region of interest). If the cubic age effect was not significant at $p < 0.05$, we stepped down to the quadratic developmental model, etc. Second, we investigated whether the developmental trajectories differed between genders. Hence, using the Bayesian Information Criterion (BIC), a full model containing both main effects of age and gender, as well as interaction effects, was compared to a simpler model including main effects of age and gender only. We tested whether the full model allowing for differences in growth trajectories between genders explained more variance than the simpler model. Third, if this was not the case the simpler model including main effects of age and gender was compared to the best-fit developmental model selected in step one including age terms only. Again the best-fit model was selected using BIC values, resulting in the model that explained most variance accounting for the amount of parameters included in the model and herewith minimize the effects of overfitting the data. Confidence intervals for intercepts were estimated using a bootstrap method with 1000 case resamples. Sampling with replacement was used to reestimate the intercept parameter. Furthermore, age at peak volume was calculated from the first-order derivative of non-linear growth curves. Confidence intervals of age at peak volume were calculated using the above-mentioned bootstrap method.

thesis_LW_V3.indb 74 06/06/16 07:38

Table 2 Best fit regression model for each structure volume in cm^3

Parameters for developmental trajectories

Anatomical structure	Best fitting model	Intercept (s.e.)	Gender(s.e.)	Age coefficient β2 (s.e.)	Age^2 coefficient β3 (s.e.)	Age*gender coefficient β5 (s.e.)	Age^2 * gender coefficient β6 (s.e.)
TotalGrayVol	Quadratic	779.617 (9.013)**	65.549 (10.974)7.69x10^6	-5.702 (0.673)1.69e-12	-0.401 (0.11)**	n.s.	n.s.
Caudate	Linear	7.935 (0.147)**	0.598 (0.183)**	-0.042 (0.009)8.59x10^6	n.s.	n.s.	n.s.
Putamen	Linear	11.157 (0.164)**	1.104 (0.203)2.46x10^5	-0.053 (0.01)1.04x10^6	n.s.	n.s.	n.s.
Pallidum	Quadratic	3.73 (0.057)**	0.32 (0.068)**	0.024 (0.004)6.47x10^7	-0.003 (0.001)2.88x10^5	n.s.	n.s.
Accumbensarea	Linear	1.135 (0.023)**	0.111 (0.028)**	-0.006 (0.002)*	n.s.	n.s.	n.s.
CerebellumCortex	Quadratic	125.385 (1.689)**	14.147 (2.104)1.52x10^6	-0.565 (0.218)*	-0.024 (0.027)n.s.	1.271 (0.245)1.93x10^6	-0.107 (0.034)**
ThalamusProper	Quadratic	15.881 (0.208)**	1.251 (0.255)8.46x10^5	0.003 (0.012)n.s.	-0.006 (0.002)**	n.s.	n.s.
Amygdala	Quadratic	3.109 (0.045)**	0.281 (0.055)5.14x10^5	0.024 (0.004)1.39x10^8	-0.002 (0.001)**	n.s.	n.s.
Hippocampus	Quadratic	8.727 (0.115)**	0.502 (0.141)**	0.045 (0.007)9.86x10^9	-0.006 (0.001)7.62x10^7	n.s.	n.s.

Intercept is the predicted value at the average age of the sample, s.e.=standard error, ** = significant level p<0.01, * = significant level p<0.05

thesis_LW_V3.indb 75 06/06/16 07:38

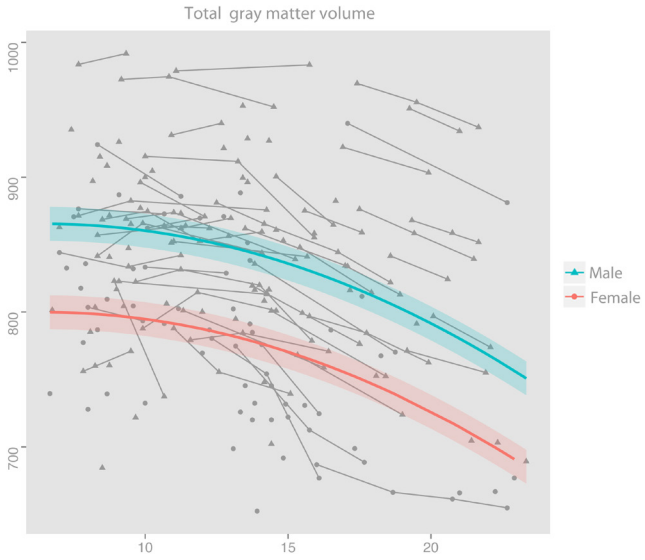

Figure 1 Developmental trajectories for total gray matter volume: Age 7.0-23.3 years old. Mean volume in cm^3 (y-axis) by age in years (x-axis) is shown for males (n= 94, blue) and females (n=53, red). The shade around the regression lines represents the 95% confidence interval of the intercept.

Results

Developmental trajectories

Results of the regression models for each ROI are shown in Figure 1 and Table 2. Total brain volume decreased in a curvilinear fashion, peaking at age 7.0 for both males and females. There was no interaction between age and gender, but there was a main effect of gender, where total brain volume was larger for males than females over the entire age range. All subcortical structures also showed an association with age, as well as a main effect of gender, with larger gray matter volumes for males than females. There were linear decreases with age in the volume of caudate nucleus, putamen and accumbens, whereas the volume of pallidum showed a quadratic developmental trajectory with a peak at age 17.2 years. The volume of thalamus, hippocampus and amygdala also followed inverted-U shaped developmental trajectories, with peaks at age 13.8, 17.3 and 19.7 years respectively (see Table 3). The cerebellar cortex was the only ROI to show an age * gender interaction: for males there was a quadratic relationship between age and volume with a peak at age 15.6 years, whereas for females cerebellar gray matter decreased quadratically over the age range.

thesis_LW_V3.indb 76 06/06/16 07:38

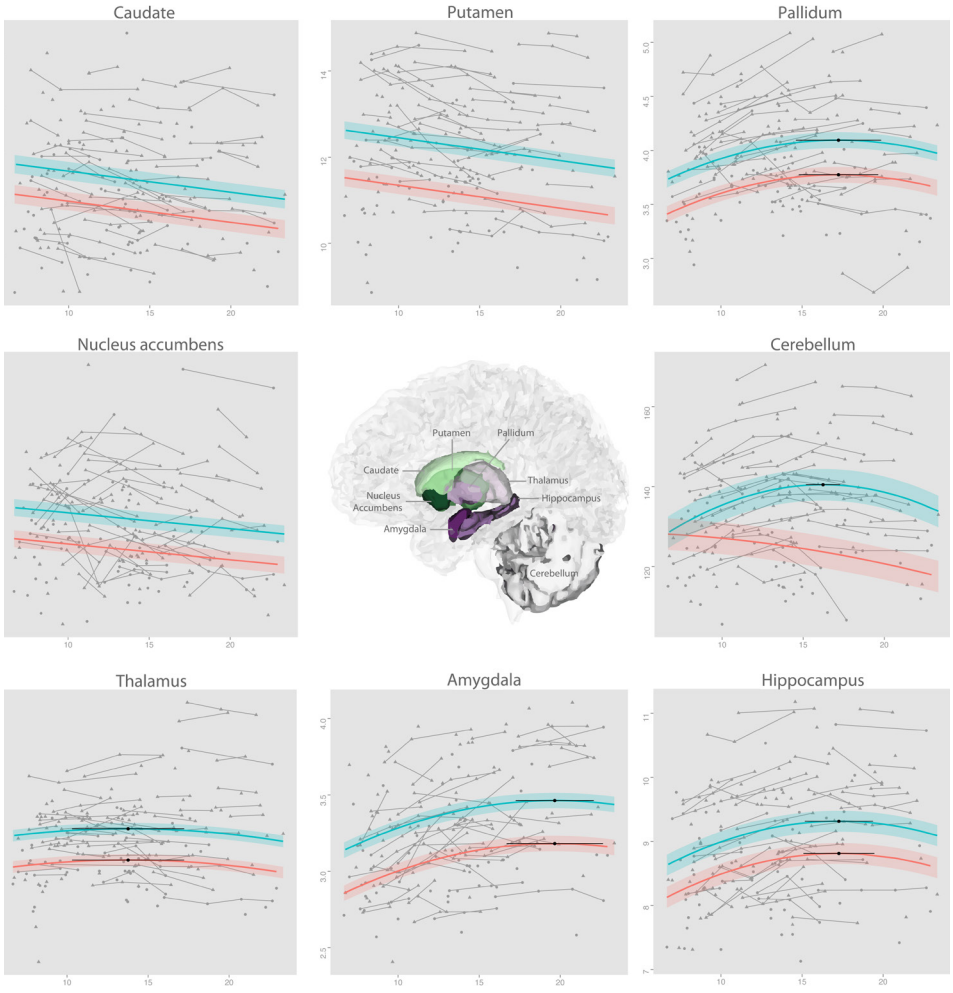

Figure 2 Developmental trajectories of subcortical gray matter volumes: Age 7.0-23.3 years old. Mean volume in cm^3 (y-axis) by age in years (x-axis) is shown for males (n= 94, blue) and females (n=53, red). The shade around the regression lines represents the 95% confidence interval of the intercept. Caudate nucleus, Putamen, Pallidum, Nucleus accumbens, Cerebellum cortex, Thalamus, Amygdala and Hippocampus.

Discussion

We investigated the development of subcortical brain structures in typically developing children, using a mixed cross-sectional and longitudinal design. Subcortical structures showed developmental patterns that were markedly different from the global decrease in cortical volume that has been described during childhood and adolescence (Dennison et al., 2013; Giedd and Rapoport, 2010; Goddings et al., 2013; Koolschijn and Crone, 2013;

thesis_LW_V3.indb 77 06/06/16 07:38

Table 3 Age at peak volume for each structure that showed a curvilinear developmental trajectory

	Peak volume females		Peak volume males	
Structure	Age	95% CI	Age	95% CI
ThalamusProper	13.8	10.3-17.2	13.8	10.3-17.2
Pallidum	17.2	14.8-19.7	17.2	14.6-19.9
Hippocampus	17.3	15.1-19.4	17.3	15.2-19.4
Amygdala	19.7	16.7-22.6	19.7	17.3-22.1
CerebellumCortex			15.6	14.1-17.2

Age at peak was estimated for curvilinear growth models, CI were estimated using repeated bootstrapping methods with 1000 samples.

Lenroot et al., 2007; Ostby et al., 2009; Reiss et al., 1996; Sowell et al., 1999; 2002; Tau and Peterson, 2009; Wilke et al., 2007; Tamnes et al., 2013). We found inverted U-shaped developmental patterns in gray matter volume across our age range for the hippocampus, amygdala, pallidum, thamalus and cerebellar cortex, while linear decreases were observed in the caudate, putamen and nucleus accumbens. Furthermore, all subcortical structures were larger in males than females over the whole age range. The cerebellum was the only structure to show a sexually dimorphic developmental trajectory, with an earlier peak volume in females than males.

The developmental patterns observed in the present study are broadly consistent with previous findings for the striatum (Dennison et al., 2013; Giedd et al., 1996; Goddings et al., 2013; Ostby et al, 2009; Tamnes et al., 2013) although most of these studies were cross-sectional. However, one of the few longitudinal studies did not observe a decrease in the striatum (Raznahan et al., 2014). They showed substantial heterogeneity in development of subdivisions of the striatum, which may have been obscured in our data. In addition, differences in developmental trajectories between our study and the one by Raznahan and colleagues could partly be attributable to differences in the number of subjects. Furthermore, our results are consistent with previous findings on protracted development of hippocampus and amygdala volumes (e.g.; Goddings et al., 2013; Mosconi et al., 2009; Ostby et al., 2009). Additionally, not all studies observed a protracted development in hippocampal volume, as decreases in a similar age range have also been reported (Mattai et

thesis_LW_V3.indb 78 06/06/16 07:38

al, 2011; Tamnes et al., 2013). However, this discrepancy could be related to our use of raw volumes rather than intracranial corrected volume (as in Mattai et al., 2011). Furthermore, our results are in line with findings on thalamus volume (Brown and Jernigan, 2012; Giedd et al., 1996; Ostby et al., 2009; Schuman et al. 2004; Tamnes et al., 2013), and the cerebellum (Ostby et al., 2009; Tiemeier et al., 2010) However, the observed increase in the volume of the pallidum is not in line with previous literature (Giedd et al., 1998; Goddings et al., 2013; Ostby et al., 2009; Raznahan et al., 2014). This discrepancy may again be attributable to our choice not to correct for overall brain volume, as two earlier studies did report increases in uncorrected pallidum volume (Dennison et al., 2013; Ostby et al.,2009). Also, our study is one of few to capture developmental changes in thalamus volume (Brown and Jernigan, 2012; Dennison et al., 2013; Giedd et al., 1996; Ostby et al., 2009; Reiss et al., 1996). This may be related to the small magnitude of the change (approximately 2%, see Supplementary Figure 1), as this might render it particularly difficult to detect in cross-sectional designs (Giedd et al., 1996; Ostby et al., 2009; Reiss et al., 1996). In addition, the thalamus shows protracted development compared to total grey matter, but peak volume occurs before the hippocampus and amygdala. Hence the thalamus may therefore mature earlier than the hippocampus and amygdala. However, whether the age at peak volume reflects homologue biological processes and hence is a meaningful biological marker in terms of developmental timing, remains unclear. Alternatively, rate of change, which is moderate for thalamus development, may also be an important indicator of developmental timing. Finally, we replicated an earlier report of an age*gender effect on cerebellar gray volume (Tiemeier et al., 2010). The cerebellum plays an important role in cognitive functioning (Ito, 2008). This finding may therefore reflect the role of cerebellum in the development of cognitive functions during adolescence, and possibly gender differences in the rate of development.

We did not replicate previous reports of sexually dimorphic developmental trajectories for thalamus (Dennison et al., 2013; Lenroot et al., 2007, Raznahan et al, 2014), caudate nucleus or putamen (Dennison et al., 2013; Goddings et al., 2013, Raznahan et al, 2014). This may be related to differences in methodology as some of these studies allowed for growth trajectories to vary in shape between males and females early in the model

thesis_LW_V3.indb 79 06/06/16 07:38

selection procedure. While our method selection procedure may have been more strict and herewith perhaps have underestimated the age*gender interaction effects. But also the limited amount of female longitudinal scans in our dataset may have resulted in a lack of a significant gender*age interaction effect. Previous studies have suggested that sexually dimorphic developmental trajectories may relate to differences in pubertal measures, including steroid hormones (Goddings et al., 2013; Peper et al., 2011). Although we did not investigate such measures of puberty, our findings do not support the notion of hormonally driven gender differences in the timing of brain development, with the possible exception of the cerebellum.

The neuroanatomical processes underlying the developmental changes in brain volume remain unclear. The heterogeneity in developmental trajectories between structures suggests that these processes may vary between them and perhaps even over developmental time. They may be related to changes in gray matter, such as changes in the number of oligodendrocytes, that have been associated with developmental changes in amygdala volume (Chareyron et al., 2012). Alternatively, they could also be related to changes in the surrounding white matter, such as increased myelination of axonal projections, that have been related to developmental reductions in striatum (Ostby et al., 2009; Shaw et al., 2011).

Some limitations of the present study should be acknowledged. First, we looked at the whole volume of the subcortical structures, rather than the substructures that form them or at deformations on their surface that may show where in the structure changes are occurring (Raznahan et al., 2014). As such, we may have overlooked any heterogeneity in the development of these substructures (e.g., Gogtay et al., 2006). Second, our dataset included more males than females. As such, we may have been somewhat underpowered to investigate gender differences.

We described the developmental trajectories of a number of subcortical structures using a mixed longitudinal and cross-sectional dataset in a population of typically developing individuals. The observed heterogeneity in the development of subcortical brain structures indicates dynamic developmental changes during development that are likely to be related to changes in behavioral and cognitive development.

thesis_LW_V3.indb 80 06/06/16 07:38

Supplementary information

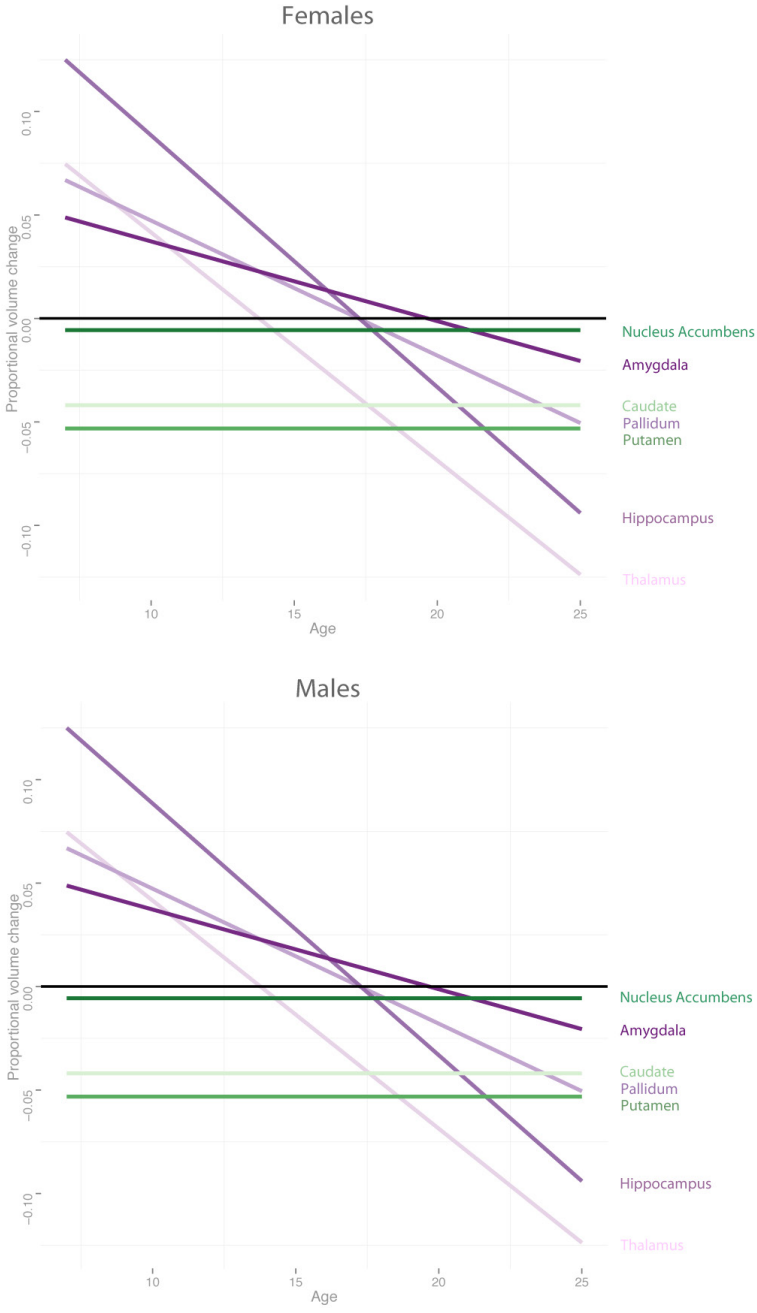

Supplemental Figure 1 Annual change in proportional volume for females (upper panel) and males (lower panel) from the first order derivative of estimated growth trajectories. The age at which zero change (black line) is observed represents a peak in the growth trajectory.

thesis_LW_V3.indb 81 06/06/16 07:38

References

Ballmaier, M., Schlagenhauf, F., Toga, A.W., Gallinat, J., Koslowski, M., Zoli, M., Hojatkashani, C., Narr, K.L., Heinz, A., 2008. Regional patterns and clinical correlates of basal ganglia morphology in non-medicated schizophrenia. 106, 140–147.

Berman, S., O'Neill, J., Fears, S., Bartzokis, G., London, E.D., 2008. Abuse of amphetamines and structural abnormalities in the brain. 1141, 195–220.

Brown, T.T., Jernigan, T.L., 2012. Brain Development During the Preschool Years. Neuropsychol Rev 22, 313–333.

Bunge, S., 2009. Neural correlates of the development of cognitive control. Neuroimaging in developmental clinical neuroscience 22–37

Carmona, S., Proal, E., Hoekzema, E.A., Gispert, J.-D., Picado, M., Moreno, I., Carlos Soliva, J., Bielsa, A., Rovira, M., Hilferty, J., Bulbena, A., Casas, M., Tobena, A., Vilarroya, O., 2009. Ventro-Striatal Reductions Underpin Symptoms of Hyperactivity and Impulsivity in Attention-Deficit/Hyperactivity Disorder. Biological Psychiatry 66, 972–977.

Chareyron, L.J., Lavenex, P.B., Amaral, D.G., Lavenex, P., 2012. Postnatal development of the amygdala: A stereological study in macaque monkeys. J. Comp. Neurol. 520, 1965–1984.

Dale, A., Fischl, B., Sereno, M.I., 1999. Cortical Surface-Based Analysis: I. Segmentation and Surface Reconstruction. NeuroImage 9, 179–194.

Dennison, M., Whittle, S., Yücel, M., Vijayakumar, N., Kline, A., Simmons, J., Allen, N.B., 2013. Mapping subcortical brain maturation during adolescence: evidence of hemisphere- and sex-specific longitudinal changes. Developmental Science 16, 772–791.

Dewey, J., Hana, G., Russell, T., Price, J., McCaffrey, D., Harezlak, J., Sem, E., Anyanwu, J.C., Guttmann, C.R., Navia, B., Cohen, R., Tate, D.F., HIV Neuroimaging Consortium, 2010. Reliability and validity of MRI-based automated volumetry software relative to auto-assisted manual measurement of subcortical structures in HIV-infected patients from a multisite study. NeuroImage 51, 1334–1344.

thesis_LW_V3.indb 82 06/06/16 07:38

Diamond, A., 2000. Close Interrelation of Motor Development and Cognitive Development and of the Cerebellum and Prefrontal Cortex. Child Development 71, 44–56.

Durston, S., Nederveen, H., van Dijk, S., van Belle, J., de Zeeuw, P., Langen, M., van Dijk, A., 2009. Magnetic Resonance Simulation is Effective in Reducing Anxiety Related to Magnetic Resonance Scanning in Children. Journal of the American Academy of Child & Adolescent Psychiatry 48, 206–207.

Durston, S., Hulshoff Pol, H. E., Casey, B. J., Giedd, J. N., Buitelaar, J. K., & van Engeland, H. (2001). Anatomical MRI of the developing human brain: what have we learned? Journal of the American Academy of Child & Adolescent Psychiatry, 40(9), 1012–1020.

Fischl, B., Sereno, M.I., Dale, A., 1999. Cortical Surface-Based Analysis: II: Inflation, Flattening, and a Surface-Based Coordinate System. NeuroImage 9, 195–207.

Fischl, B., Salat, D. H., Busa, E., Albert, M., Dieterich, M., Haselgrove, C., et al. (2002). Whole Brain Segmentation. Neuron, 33(3), 341–355

Fox, J., 2002. Linear Mixed Models-Appendix to An R and S-PLUS Companion to Applied Regression. Relation 10, 5261.

Giedd, J.N., Blumenthal, J., Jeffries, N.O., Castellanos, F.X., Liu, H., Zijdenbos, A., Paus, T., Evans, A.C., Rapoport, J.L., 1999. Brain development during childhood and adolescence: a longitudinal MRI study. Nat Neurosci 2, 861–863.

Giedd, J.N., Rapoport, J.L., 2010. Structural MRI of Pediatric Brain Development: What Have We Learned and Where Are We Going? Neuron 67, 728–734.

Giedd, J.N., Snell, J.W., Lange, N., Rajapakse, J.C., Casey, B.J., Kozuch, P.L., Vaituzis, A.C., Vauss, Y.C., Hamburger, S.D., Kaysen, D., Rapoport, J.L., 1996. Quantitative Magnetic Resonance Imaging of Human Brain Development: Ages 4–18. Cerebral Cortex (New York, N.Y. : 1991), 6(4), 551–560

Giedd, J. N., Vaituzis, A. C., Hamburger, S. D., Lange, N., Rajapakse, J. C., Kaysen, D., et al. (1996). Quantitative MRI of the temporal lobe, amygdala, and hippocampus in normal human development: ages 4–18 years. The Journal of Comparative Neurology, 366(2), 223–230.

thesis_LW_V3.indb 83 06/06/16 07:38

Goddings, A.-L., Mills, K.L., Clasen, L.S., Giedd, J.N., Viner, R.M., Blakemore, S.-J., 2013. The influence of puberty on subcortical brain development. NeuroImage, 88, 242–251

Gogtay, N., Nugent, T.F., Herman, D.H., Ordonez, A., Greenstein, D., Hayashi, K.M., Clasen, L., Toga, A.W., Giedd, J.N., Rapoport, J.L., Thompson, P.M., 2006. Dynamic mapping of normal human hippocampal development. Hippocampus 16, 664–672.

Van Haasen PP, De Bruyn EEJ, Pijl YJ, Poortinga YH, Lutje-Spelberg HC, Vander Steene G, et al. (1986): Wechsler Intelligence Scale for Children- Revised, Dutch Version. Lisse: Swets and Zeitlinger.

Ito, M., 2008. Control of mental activities by internal models in the cerebellum. Nat Rev Neurosci 9, 304–313.

Koob, G.F., 2006. The neurobiology of addiction: a neuroadaptational view relevant for diagnosis. 101 Suppl 1, 23–30.

Jovicich, J., Czanner, S., Greve, D., Haley, E., van der Kouwe, A., Gollub, R., et al. (2006). Reliability in multi-site structural MRI studies: Effects of gradient non-linearity correction on phantom and human data. NeuroImage, 30(2), 436–443.

Koolschijn, P.C.M.P., Crone, E.A., 2013. Sex differences and structural brain maturation from childhood to early adulthood. Dev Cogn Neurosci 5C, 106–118.

Langen, M., Bos, D., Noordermeer, S. D. S., Nederveen, H., van Engeland, H., & Durston, S. (in press). Changes in the Development of Striatum Are Involved in Repetitive Behavior in Autism. Biological Psychiatry, 76(5), 405–411.

Lavenex, P., Banta Lavenex, P., 2013. Building hippocampal circuits to learn and remember: insights into the development of human memory. Behav. Brain Res. 254, 8–21.

Lenroot, R.K., Gogtay, N., Greenstein, D.K., Wells, E.M., Wallace, G.L., Clasen, L.S., Blumenthal, J.D., Lerch, J., Zijdenbos, A.P., Evans, A.C., Thompson, P.M., Giedd, J.N., 2007. Sexual dimorphism of brain developmental trajectories during childhood and adolescence. NeuroImage 36, 1065–1073.

Mamah, D., Harms, M.P., Wang, L., Barch, D., Thompson, P., Kim, J., Miller, M.I., Csernansky, J.G., 2008. Basal ganglia shape abnormalities in the unaffected siblings of schizophrenia patients. 64, 111–120.

thesis_LW_V3.indb 84 06/06/16 07:38

Mega, M.S., Cummings, J.L., 1994. Frontal-subcortical circuits and neuropsychiatric disorders. J Neuropsychiatry Clin Neurosci 6, 358–370.

Mosconi, M. W., Cody-Hazlett, H., Poe, M. D., Gerig, G., Gimpel-Smith, R., & Piven, J. (2009). Longitudinal study of amygdala volume and joint attention in 2- to 4-year-old children with autism. Archives of General Psychiatry, 66(5), 509–516.

Ostby, Y., Tamnes, C.K., Fjell, A.M., Westlye, L.T., Due-Tonnessen, P., Walhovd, K.B., 2009. Heterogeneity in Subcortical Brain Development: A Structural Magnetic Resonance Imaging Study of Brain Maturation from 8 to 30 Years. J Neurosci 29, 11772–11782.

Paus, T., Keshavan, M., Giedd, J.N., 2010. Why do many psychiatric disorders emerge during adolescence? Nature Reviews. Neuroscience, 9(12), 947–957

Peper, J.S., Hulshoff Pol, H.E., Crone, E.A., van Honk, J., 2011. Sex steroids and brain structure in pubertal boys and girls: a mini-review of neuroimaging studies. 191, 28–37.

Philip, R.C.M., Dauvermann, M.R., Whalley, H.C., Baynham, K., Lawrie, S.M., Stanfield, A.C., 2012. A systematic review and meta-analysis of the fMRI investigation of autism spectrum disorders. 36, 901–942.

Raznahan, A., Shaw, P., Lalonde, F., Stockman, M., Wallace, G.L., Greenstein, D., Clasen, L., Gogtay, N., Giedd, J.N., 2011. How does your cortex grow? J Neurosci 31, 7174–7177.

Reiss, A.L., Abrams, M.T., Singer, H.S., Ross, J.L., Denckla, M.B., 1996. Brain development, gender and IQ in children. A volumetric imaging study. Brain 119 (Pt 5), 1763–1774.

Reuter, M., Fischl, B., 2011. Avoiding Asymmetry-Induced Bias in Longitudinal Image Processing. NeuroImage 57, 19–21.

Reuter, M., Rosas, H.D., Fischl, B., 2010. Highly Accurate Inverse Consistent Registration: A Robust Approach. NeuroImage 53, 1181–1196.

Reuter, M., Schmansky, N.J., Rosas, H.D., Fischl, B., 2012. Within-Subject Template Estimation for Unbiased Longitudinal Image Analysis. NeuroImage 61, 1402–1418.

Scherf, K.S., Smyth, J.M., Delgado, M.R., 2013. The amygdala: an agent of change in adolescent neural networks. Hormones and Behavior 64, 298–313.

thesis_LW_V3.indb 85 06/06/16 07:38

Schumann, C. M., Hamstra, J., Goodlin-Jones, B. L., Lotspeich, L. J., Kwon, H., Buonocore, M. H., et al. (2004). The amygdala is enlarged in children but not adolescents with autism; the hippocampus is enlarged at all ages. Journal of Neuroscience, 24(28), 6392–6401.

Shaw, P., Kabani, N.J., Lerch, J.P., Eckstrand, K., Lenroot, R., Gogtay, N., Greenstein, D., Clasen, L., Evans, A., Rapoport, J.L., Giedd, J.N., Wise, S.P., 2008. Neurodevelopmental trajectories of the human cerebral cortex. J Neurosci 28, 3586–3594.

Sheehan, D.V., Lecrubier, Y., Sheehan, K.H., Amorim, P., Janavs, J., Weiller, E., Hergueta, T., Baker, R., Dunbar, G.C., 1998. The Mini-International Neuropsychiatric Interview (M.I.N.I.): the development and validation of a structured diagnostic psychiatric interview for DSM-IV and ICD-10. J Clin Psychiatry 59 Suppl 20, 22–33–quiz 34–57.

Sowell, E.R., Thompson, P.M., Holmes, C.J., Jernigan, T.L., Toga, A.W., 1999. In vivo evidence for post-adolescent brain maturation in frontal and striatal regions. Nat Neurosci 2, 859–861.

Sowell, E.R., Trauner, D.A., Gamst, A., Jernigan, T.L., 2002. Development of cortical and subcortical brain structures in childhood and adolescence: a structural MRI study. Dev Med Child Neurol 44, 4–16.

Stinissen J, Willems PJ, Coetsier P, Hulsman WLL (1970): Nederlandstalige Bewerking van de Wechsler Adult Intelligence Scale (W.A.I.S.) (Manual). [Manual for the Dutch Translated and Adapted Version of The Wechsler Adult Intelligence Scale (WAIS)]. Lisse: Swets and Zeitlinger.

Tau, G.Z., Peterson, B.S., 2009. Normal Development of Brain Circuits. Neuropsychopharmacology 35, 147–168.

Tiemeier, H., Lenroot, R.K., Greenstein, D.K., Tran, L., Pierson, R., Giedd, J.N., 2010. Cerebellum development during childhood and adolescence: a longitudinal morphometric MRI study. NeuroImage 49, 63–70.

Volkow, N.D., Fowler, J.S., Wang, G.-J., Swanson, J.M., Telang, F., 2007. Dopamine in drug abuse and addiction: results of imaging studies and treatment implications. 64, 1575–1579.

thesis_LW_V3.indb 86 06/06/16 07:38

Walhovd, K. B., Westlye, L. T., Amlien, I., Espeseth, T., Reinvang, I., Raz, N., et al. (2011). Consistent neuroanatomical age-related volume differences across multiple samples. NBA, 32(5), 916–932.

Wechsler D (2000): Wechsler Adult Intelligence Scale-Third Edition (WAIS- III): Nederlandstalige Bewerking. Technische Handleiding. (Dutch Version Technical Manual).

Wierenga, L. M., Langen, M., Oranje, B., & Durston, S. (2014). Unique developmental trajectories of cortical thickness and surface area. NeuroImage 87, 120-126.

Wilke, M., Krägeloh-Mann, I., Holland, S.K., 2007. Global and local development of gray and white matter volume in normal children and adolescents. Exp Brain Res 178, 296–307.

thesis_LW_V3.indb 87 06/06/16 07:38

THE DEVELOPMENT OF BRAIN NETWORK ARCHITECTURE

Lara M Wierenga
Martijn P van den Heuvel
Sarai van Dijk
Yvonne Rijks
Marcel A de Reus
Sarah Durston

Human Brain Mapping 2015: 37-2, 717–729

thesis_LW_V3.indb 89 06/06/16 07:38

Abstract

Brain connectivity shows protracted development over childhood and adolescence, and, as such, the topology of brain networks changes during this period. The complexity of these changes with development is reflected by regional differences in maturation. This study explored age-related changes in network topology and regional developmental patterns during childhood and adolescence. We acquired two sets of Diffusion Weighted Imaging-scans and anatomical T1-weighted scans. The first dataset included 85 typically developing individuals (53 males; 32 females), aged between 7 and 23 years and was acquired on a Philips Achieva 1.5 Tesla scanner. A second dataset (N=38) was acquired on a different (but identical) 1.5 T scanner and was used for independent replication. We reconstructed whole brain networks using tractography. We operationalized fiber tract development as changes in mean diffusivity and radial diffusivity with age. Most fibers showed maturational changes in mean and radial diffusivity values throughout childhood and adolescence, likely reflecting increasing white matter integrity. The largest age-related changes were observed in association fibers within and between the frontal and parietal lobes. Furthermore, there was a simultaneous age-related decrease in average path length ($p < .0001$), increase in node strength ($p < .0001$) as well as network clustering ($p = 0.001$), which may reflect fine-tuning of topological organization. These results suggest a sequential maturational model where connections between unimodal regions strengthen in childhood, followed by connections from these unimodal regions to association regions, while adolescence is characterized by the strengthening of connections between association regions within the frontal and parietal cortex.

thesis_LW_V3.indb 90 06/06/16 07:38

Introduction

It is well established that pronounced changes in white matter structure occur early in life (as reviewed in Dubois et al., 2014, van den Heuvel et al., 2014, Ball et al., 2014, Hagmann et al, 2010). In addition, refinement of brain networks and connectivity network continue throughout childhood and adolescence. This is reflected by increases in total white matter volume, reported in studies using anatomical Magnetic Resonance Imaging (MRI), as well as studies using Diffusion Weighted Imaging (DWI) which show developmental increases in fractional anisotropy (FA) and concurrent decreases in mean diffusion (MD) in white matter bundles. Such relatively late developmental changes are likely to reflect developmental increases in myelination leading to increases in axonal conduction speed (Baumann and Pham-Dinh, 2001) which in turn improve the efficiency of information transfer (van der Knaap et al., 1991). As all fibers in the brain contribute to network topology, even small changes in white matter structure may have large effects on the properties of the network as a whole. Recent advances in network analysis are now permitting us to investigate such aspects of network topology (He et al., 2007; Bullmore and Sporns, 2009; Van den Heuvel and Hulshoff 2010). Studies of brain network development in childhood and adolescence have shown increases in network strength and global efficiency (Hagmann et al., 2010; Dennis et al, 2013; Chen et al., 2013; Van den Heuvel et al. 2014). Furthermore, there is evidence that not all fibers develop at the same rate (Lebel et al., 2008; Tamnes et al., 2010) and may therefore not all contribute equally or simultaneously to global changes in network topology with age.

For example, in newborns, studies have suggested that centrally located white matter develops earlier than in peripheral regions and that occipital white matter develops before that in frontal regions (Gao et al., 2009; Hermoye et al., 2006; Provenzale et al., 2007). Other studies have shown that the maturation of white matter continues into childhood and adolescence, and that the rates of change may differ per region. For example, the association tracts within frontal and temporal lobes continue to mature for longer than the commissural fibers connecting the hemispheres and the projection fibers connecting subcortical to cortical structures (Lebel et al., 2011, Tamnes et al., 2010 and Dennis et al., 2013). Hagmann and colleagues were one of the first to show that these patterns of

thesis_LW_V3.indb 91 06/06/16 07:38

white matter maturation contribute to the development of connectivity. They described a maturational pattern with relatively later maturation of long-distance pathways compared to shorter ones (2010). They showed that this maturational pattern was related to increases in network efficiency, as reflected by a reduction in the number of steps necessary to get from one brain region to another (also reported by Dennis et al., 2013). Studies of age-related change in functional connectivity support this observation as they show age-related increases in functional connectivity between distant regions, with smaller changes, or even decreases, in short range connectivity (Dosenbach et al., 2010; Fair et al., 2009). These results still held after age-related motion effects were removed (Power et al., 2012). Thus, studies on the developmental patterns of structural white matter are essential for our understanding of the development of network topology, yet they are not all in agreement. Therefore, the first aim of the present study is to describe regional patterns of age-related changes within white matter. Second, we explored developmental patterns in global network topology (node strength, path length, and clustering) and investigate their relation to our regional differences in maturation between fiber tracts.

We used two datasets (N=85 and N=38 respectively) of typically developing children and adolescents (aged 7.0-22.9, 61% males). The datasets were acquired on two 1.5 Tesla Philips Achieva MRI-scanners, allowing us to use of second dataset to replicate findings from the first.

Materials and methods

The Institutional Review Board (IRB) of the University Medical Center Utrecht in the Netherlands approved this study and its procedures. Written informed consent was obtained for all subjects. For children under 18 years of age, a parent signed for consent. Subjects aged 18 years and older signed for their own consent.

Participants

Dataset I included 85 typically developing individuals (53 males; 32 females) aged between 7.0 and 22.6 years, with average IQ (see demographic details in Table I). Dataset II included 38 scans in a comparable demographic (23 males; 15 females, aged between 7.4 and 22.9 years). The two datasets were acquired on Philips Achieva 1.5 Tesla MRI

thesis_LW_V3.indb 92 06/06/16 07:38

scanners, we used the second set for independent replication of our findings. Dataset I and II did not differ in terms of gender distribution, IQ, socio-economic status or hand preference and had a similar age range (see Table I).

We recruited all participants through schools and educational centers in the area. For each subject, a parent participated in a semi-structured interview session with a trained rater to confirm the absence of any psychiatric diagnosis (Diagnostic Interview Schedule for Children [DISC]) (Costello et al., 1985). Subjects older than 18 years old participated in the Mini-International Neuropsychiatric Interview (M.I.N.I) to confirm absence of psychopathological symptoms (Sheehan et al., 1998). Participants had no psychiatric diagnosis (current or prior), or first-degree relative suffering from a psychiatric illness, no major physical illness of the cardiovascular, the endocrine, the pulmonic or the gastrointestinal system, neurological illness, a history of head trauma with unconsciousness, organic brain damage or disease, alcohol or other drug dependence, or full-IQ scale below 75.

All subjects participated in a neuropsychological assessment (Wechsler Adult Intelligence Scale/Wechsler Adult Intelligence Scale-Third Edition [WAIS/WAIS-III] (Wechsler D, 2000); Wechsler Intelligence Scale for Children-Revised/Wechsler Intelligence Scale for Children-Third Edition [WISC-R/WISC-III] (Van Haasen et al., 1986). Furthermore, participants and their parents filled out a short questionnaire on hand preference and a questionnaire related to major physical or neurological illness. Subjects acclimated to the scanning procedure in a simulated scan session prior to the actual MRI scan (Durston et al., 2009). An independent clinical neuroradiologist evaluated all MRI-scans and no gross abnormalities were reported for any of the participants.

Image acquisition and processing
Acquisition

MRI scans were acquired using an identical scan protocol on two identical Philips Achieva 1.5 Tesla scanners, with 6-element SENSE receiver head coils (Philips, Best, The Netherlands). The protocol included a DTI scan and a high-resolution T1-weighted scan (used for anatomical reference). First, we acquired a whole brain T1-weighted three-dimensional fast field echo scan of the whole head (flip angle = 30°; 160-180 contiguous coronal slices; 1 mm × 1 mm × 1.2 mm voxel size; 256 × 256 matrix; FoV = 256 mm; TE

thesis_LW_V3.indb 93 06/06/16 07:38

thesis_LW_V3.indb 94

Table 1 Demographic details

	Dataset I				Dataset II			
Characterstics	Male		Female		Male		Female	
Number of individuals, n	53		32		23		15	
Hand preference, n								
Right-handed	42		29		18		13	
Not Right-handed	10		3		5		2	
Height (cm), mean (SD) range	162.2 (21.1)	129.0 -202.0	152.4 (14.9)	121.0 -179.0	175.7 (15.7)	127.0 -204.0	164.2 (10.3)	146.0 -183.0
Weight (kg), mean (SD) range	52.4 (19.0)	26.0 -94.0	44.4(15.2)	20.0 -73.0	65.1 (18.3)	25.0 -100.0	54.8 (13.3)	32.0 -75.0
IQ, mean (SD) range	110.0 (17.9)	75.0 -145.0	114.2 (14.1)	84.0 -124.0	112.0 (12.0)	84.0 -136.0	110.4 (14.2)	87.0 -133.0
Paternal education (years), mean (SD)	13.9 (2.4)		13.9 (2.0)		14.6 (1.9)		13.9 (2.3)	
Maternal education (years), mean (SD)	13.5 (2.3)		13.4 (2.5)		12.6 (2.9)		14.1 (1.7)	
Sibling, n	8		6		5		0	
Age at scan, years								
Mean (SD) range	13.1 (3.8)	7.0 -22.1	12.4 (4.1)	7.0 -22.7	15.8 (3.9)	7.4 -22.3	14.8 (3.2)	10.0 -22.9

SD, standard deviation; IQ, intelligence quotient

06/06/16 07:38

= 4.6 ms; TR = 30 ms; and total scan duration = 405–456 s). For white matter fiber tract reconstruction and computation of the MD and RD (radial diffusivity) values, two transverse DTI-sets were acquired, each consisting of 32 diffusion-weighted volumes with different non-collinear diffusion directions with b-factor = 1,000 s/mm^2 and 8 diffusion-unweighted volumes with b-factor = 0 s/mm^2 (parallel imaging SENSE factor = 2.5; flip angle = 90°; 60 slices; 1. 875 mm × 1.875 mm × 2.5 mm voxel size; no slice gap; 96 x 96 acquisition matrix; reconstruction matrix 128 x 128; FoV = 240 mm; TE = 88 ms; TR = 9822 ms; no cardiac gating; and total scan duration = 296 s).

DTI preprocessing and fiber track reconstruction

The DTI preprocessing pipeline has been described in detail elsewhere (van den Heuvel et al., 2010). In short, it involved the following steps: first, both DWI sets were realigned and corrected for common gradient-induced distortions. Second, diffusion images were corrected for common gradient-induced distortions and realigned to the b = 0 image (Andersson and Skare 2002). Third, we fitted a diffusion profile within each voxel using the two sets of 32 weighted images and the average b = 0 image from each subject. From the resulting tensor, the main diffusion direction in each voxel was selected as the principal eigenvector resulting from the eigenvalue decomposition of the fitted tensor, marking the preferred diffusion direction in each voxel. For each voxel, the FA, indicating the level of anisotropic diffusion, MD and RD values were computed (Basser & Pierpaoli, 1996; Beaulieu & Allen, 1994). Fourth, using the extracted information on the preferred diffusion direction within each voxel in the brain mask, the white matter tracts of the whole brain network were reconstructed using the deterministic fiber tracking, based on the FACT algorithm (fiber assignment by continuous tracking) (Mori & van Zijl, 2002; Mori, Crain, Chacko, & van Zijl, 2001). This enabled the reconstruction of white matter tracts (van den Heuvel et al., 2009; van den Heuvel, et al., 2011). Fibers were reconstructed by starting eight seeds in each voxel and following the main diffusion direction of each voxel (selected as the principal eigenvector) until the fiber tract entered a voxel with a low level of diffusion preference (FA < 0.1), made an unexpected sharp angular turn (angle > 45°), or left the brain mask. All reconstructed fibers included a minimum number of five streamlines. One measure of white matter connectivity strength is the level of myelination, as higher levels

thesis_LW_V3.indb 95 06/06/16 07:38

of myelination have been linked to higher transportation speeds along axonal connections (Wolff & Balaban, 1994). MD and RD have been associated with myelination (Schmierer et al., 2007). Therefore, we labeled the strength of each reconstructed fiber with its corresponding MD and RD value by assigning each point of the fiber tract the MD and RD values of the voxels along the three-dimensional (3D) path of the fiber (see van den Heuvel et al., 2008; 2009; Hagmann et al., 2010). The mean MD and RD of each fiber tract were our measures of interest. One of the greatest challenges in diffusion weighted imaging is partial volume averaging between tissue types and characteristics, e.g. at crossing fibers. This is particularly challenging for the interpretation of FA changes near crossing fibers: FA is particularly sensitive to (age-related) changes in white matter, yet not very specific for the type of microstructural change. Therefore, changes in fiber integrity near crossing fibers may cause both increases and decreases in FA (Alexander et al., 2011; Hagmann et al., 2010; Van den Heuvel et al. 2010). In our data, we found no significant net effect of age on FA, due to these increases and decreases that we did observe (see Supplemental Figure 1 and 2). For this reason, we chose MD and RD as markers of white matter development and not FA, similar to the methods proposed by Hagmann and coworkers (2010).

T1 preprocessing

Within each individual dataset, we used the T1 images for anatomical reference and for the selection of brain network nodes. Tissue classification and anatomical labeling was performed on the basis of the T1-weighted MR image using the well-validated and well-documented Freesurfer v5.1.0 software (http:// surfer.nmr.mgh.harvard.edu/). Technical details of the automated reconstruction scheme are described elsewhere (e.g. (Dale, Fischl, & Sereno, 1999; Fischl, Sereno, & Dale, 1999). Automatic segmentation of subcortical structures (thalamus, pallidum, caudate, putamen, accumbens, hippocampus, amygdala) and parcellation of the reconstructed cortical surface into 68 distinct brain regions was performed using the Desikan-Killiany atlas (Desikan et al., 2006). Visual data inspection was performed by two independent raters (LW, SvD). The nodes of the individual brain networks were therefore represented by a total of 82 brain regions.

thesis_LW_V3.indb 96 06/06/16 07:38

Reconstruction of un-weighted and weighted graphs

Each individual's DTI connectivity dataset was represented as a graph, with 82 brain regions defined as the nodes of the graph and the edges between nodes i and j (i.e., brain region i and region j) reflecting a reconstructed white matter tract. For the un-weighted graphs, fibers that touched both region i and j were selected in the total collection of reconstructed tracts, resulting in a undirected binary matrix G for each individual representing all connections within the brain (van den Heuvel et al., 2008; 2009). Next, MD- and RD-weighted graphs were created by defining the connection strength of each tract as the average level of MD or RD over the whole fiber (inversely reflecting the degree of myelination and/or axonal density (Alexander et al., 2007; Yoshida et al., 2013). This resulted in the undirected weighted connectivity matrix M. As such, the level of MD and RD expressed the strength of each connection.

To effectively reduce the occurrence of falsely positive and falsely negative traced connections, networks were thresholded, retaining only those connections that were present in 60% of all subjects (de Reus & van den Heuvel, 2013). In addition, we computed the graph measures at multiple threshold levels, to address the robustness of our findings. Supplemental Figure 3 shows a connection density matrix of the two datasets, where the number of subjects that share a connection is expressed as a percentage.

Network metrics

For graph theoretical analysis, we used the Brain Connectivity Toolbox (Rubinov & Sporns, 2010). The inverse MD and RD values of each edge in matrix M were used to compute the following measures: average node strength as the average sum of weights of connections to each node; path length as the average minimum number of weighted edges to be traversed to get from one node to another in matrix M (Watts & Strogatz, 1998); and finally, mean clustering coefficient as the ratio of the number of connections between direct neighbors of a node and the total number of possible connections between these neighbors (Watts & Strogatz, 1998).

thesis_LW_V3.indb 97 06/06/16 07:38

Statistical analyses

To analyze age-related changes in the number of connections and mean MD and mean RD, Pearson correlations were calculated. The number of connections in each undirected binary matrix G for each subject was correlated with age. Next, mean MD and mean RD were calculated per subject over all connections in each weighted connectivity matrix M and correlated with age.

Furthermore, we used a linear model procedure to examine the relation between age and MD/RD values on each single connection in the weighted matrix M and network metrics. Note that only connections that were present in more than 60% of the subjects were taken into account. Each dependent measure of the ith individual was modeled as follows:

$$\text{Measurement}_i = \text{Intercept} + ß_{gender}*\text{gender}_i + ß_{age}*\text{age}_i + ß_{ICV}*\text{ICV}_i + e_i$$

with e_i being the normally distributed residual error and intercept, age, gender and intracranial volume (ICV) being fixed effects (Yan et al., 2011). [The possible presence of quadratic age-related curves was investigated by adding an age*age term to the regression model, but this did not improve the model fit]. As the focus was on age-related changes, we estimated $ß_{age}$ values for each connection in the weighted connectivity matrix M. Next, $ß_{age}$ values for each connection were subdivided into the four lobes and four fiber categories: intra-lobe, association (within hemisphere connections between the different lobes), commissural (connecting both hemispheres) and projection fibers (connecting subcortical with cortical structures). Age-related changes were compared between fiber categories using ANOVA and post hoc t-tests (Bonferroni corrected).

Results

Age-related changes in un-weighted graphs G

No changes with age were found in the total amount of (binary) connections in the individual un-weighted graphs (dataset I: R = -0.17, p = 0.11, replication dataset II: R = -0.04, p = 0.81), supporting earlier observations of the majority of tracts being present in the early developing brain (Hagmann et al. 2010; Van den Heuvel et al. 2015).

thesis_LW_V3.indb 98 06/06/16 07:38

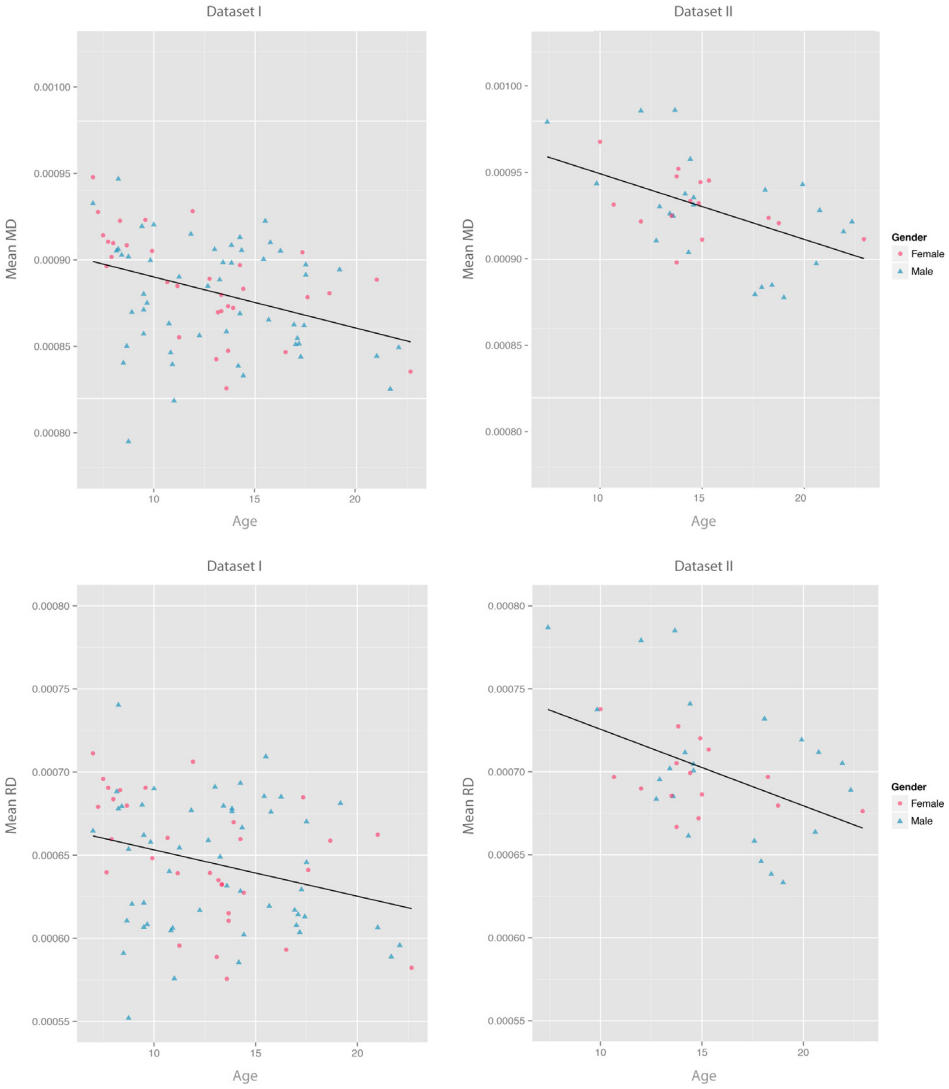

Figure 1 Mean MD and RD decreases with age. Mean MD and RD were calculated per subject by averaging MD and RD values for each connection in the weighted matrix M. Males are shown in blue, females in pink.

Age-related changes in MD- and RD-weighted graphs M

Mean MD decreased with age (dataset I: $R = -0.37$, $p < 0.001$, replication dataset II: $R = -0.52$, $p < 0.001$; Figure 1). Mean RD also decreased with age (dataset I: $R = -0.28$, $p < 0.01$, replication dataset II: $R = -0.47$, $p < 0.01$; Figure 1). We found linear decreases in MD

thesis_LW_V3.indb 99 06/06/16 07:38

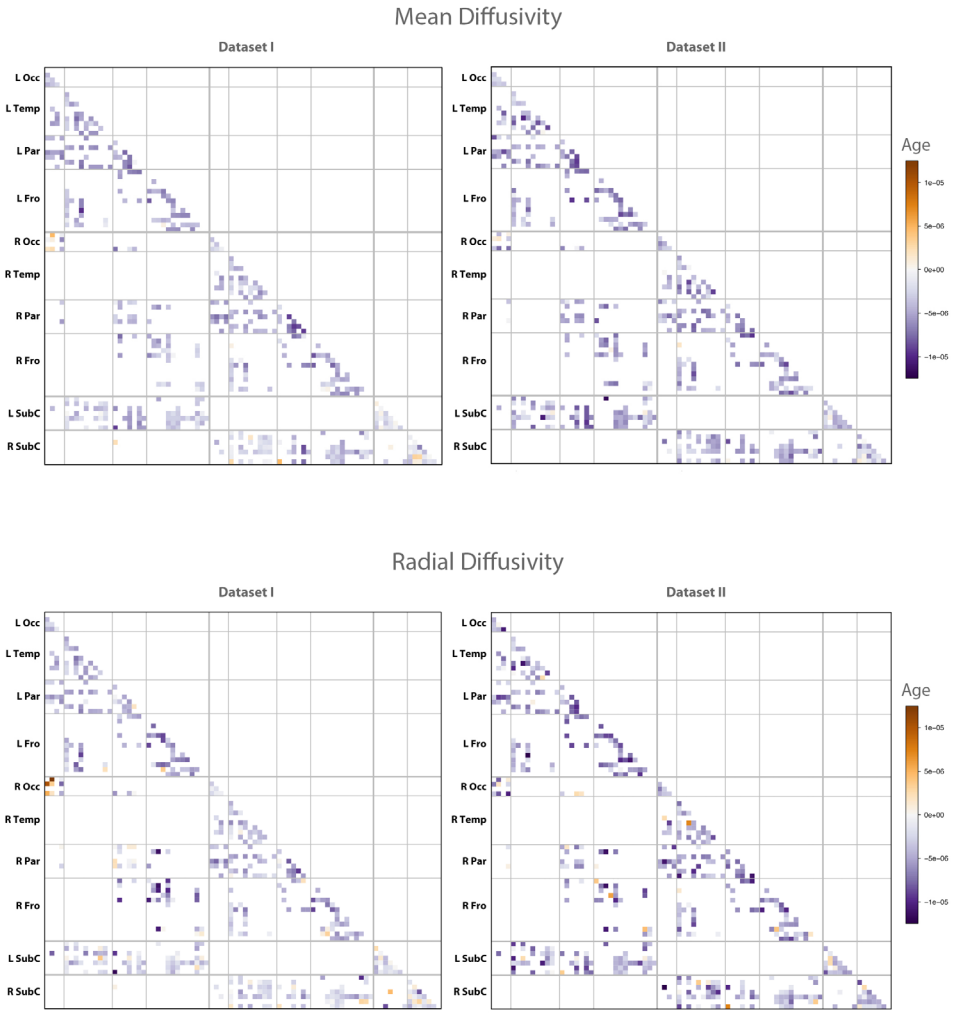

Figure 2 Age-related changes in MD and RD for the connections in the weighted matrix M. Changes are estimated as $ß_{age}$ for all connections that were present in at least 60% of the participants. We found widespread decreases in MD and RD with age (shown in purple) and only limited increases (shown in orange). R SubC=right subcortical structures, L SubC=left subcortical structures, R Fro=right frontal lobe, R Par=right parietal lobe, r Temp=right temporal lobe, R Occ=right occipital lobe, L Fro=left frontal lobe, L Par=left parietal lobe, L Temp=left temporal lobe and L Occ=left occipital lobe.

and RD for almost all connections, reflected by negative $ß_{age}$ values (Figure 2). ANOVA showed that there was variation in the rate of age-related change between fiber groups for both MD (dataset I: $F(3,414) = 42.63$, $p < 0.001$, replication dataset II: $F(3,412) = 17.09$, $p < 0.001$) and RD groups (dataset I: $F(3,427) = 56.29$, $p < 0.001$, replication dataset II: $F(3,420) = 20.72$, $p < 0.001$). The largest changes (i.e. global decreases in MD and RD) were found for

thesis_LW_V3.indb 100 06/06/16 07:38

association and intra-lobe fibers (Figure 3). Post hoc t-tests (Bonferroni corrected) confirmed that the rate of change in these fibers was larger as compared to the class of commissural and projection fibers ($p<0.001$). Furthermore, there was variation between lobes in both MD-weighted graphs (dataset I: $F(4,179) = 33.78$, $p < 0.001$, replication dataset II: $F(4,178) = 13.64$, $p < 0.001$) and RD-weighted graphs (dataset I: $F(4,179) = 13.43$, $p < 0.001$, replication dataset II: $F(4,179) = 6.23$, $p < 0.002$, Figure 4). Here, we found the greatest age-related decreases in parietal lobe, followed by frontal lobe, temporal lobe, occipital lobe and finally subcortical structures (Bonferroni corrected, see Figure 4 and 5).

Age-related changes in network metrics

There were no effects of ICV or gender on any of the network measures therefore these terms were dropped from the model. Age-related changes in inverse MD- and inverse RD-weighted graphs are given in Table II. Average node strength increased with age for both MD and RD-weighted graphs in dataset I (MD: $ß_{age} = 53.506$, $t(80) = 3.802$, $p < .0001$, RD: $ß_{age} = 79.092$, $t(80) = 2.908$, $p = 0.005$) as well as in replication dataset II (MD: $ß_{age} = 39.435$, $t(32) = 2.175$, $p = 0.037$, RD: $ß_{age} = 86.689$, $t(32) = 2.917$, $p = 0.006$). Average path length significantly decreased with age in dataset I (MD: $ß_{age} = -1.113*10\text{-}5$, $t(80) = 5.011$, $p < .0001$, RD: $ß_{age} = -8.052*10\text{-}6$, $t(80) = 3.372$, $p = 0.001$), this result was replicated in replication dataset II (MD: $ß_{age} = -1.112*10\text{-}5$, $t(32) = 3.904$, $p < .0001$, RD: $ß_{age} = -7.866*10\text{-}6$, $t(32) = 2.409$, $p = .022$). Mean clustering coefficient increased with age for MD-weighted graphs in dataset I (MD: $ß_{age} = 2.389$, $t(80) = 3.467$, $p = 0.001$, RD: $ß_{age} = 3.908$, $t(80) = 2.961$, $p = 0.004$) but didn't reach significance in replication dataset II. In order to test the stability of the network reconstruction we tested these age effects over different group threshold levels (20, 40, 60 and 80%). We observed that the age effects were not significantly different between group threshold levels for node strength ($p = 0.965$), average path length ($p = 0.923$) or clustering ($p = 0.992$).

thesis_LW_V3.indb 101 06/06/16 07:38

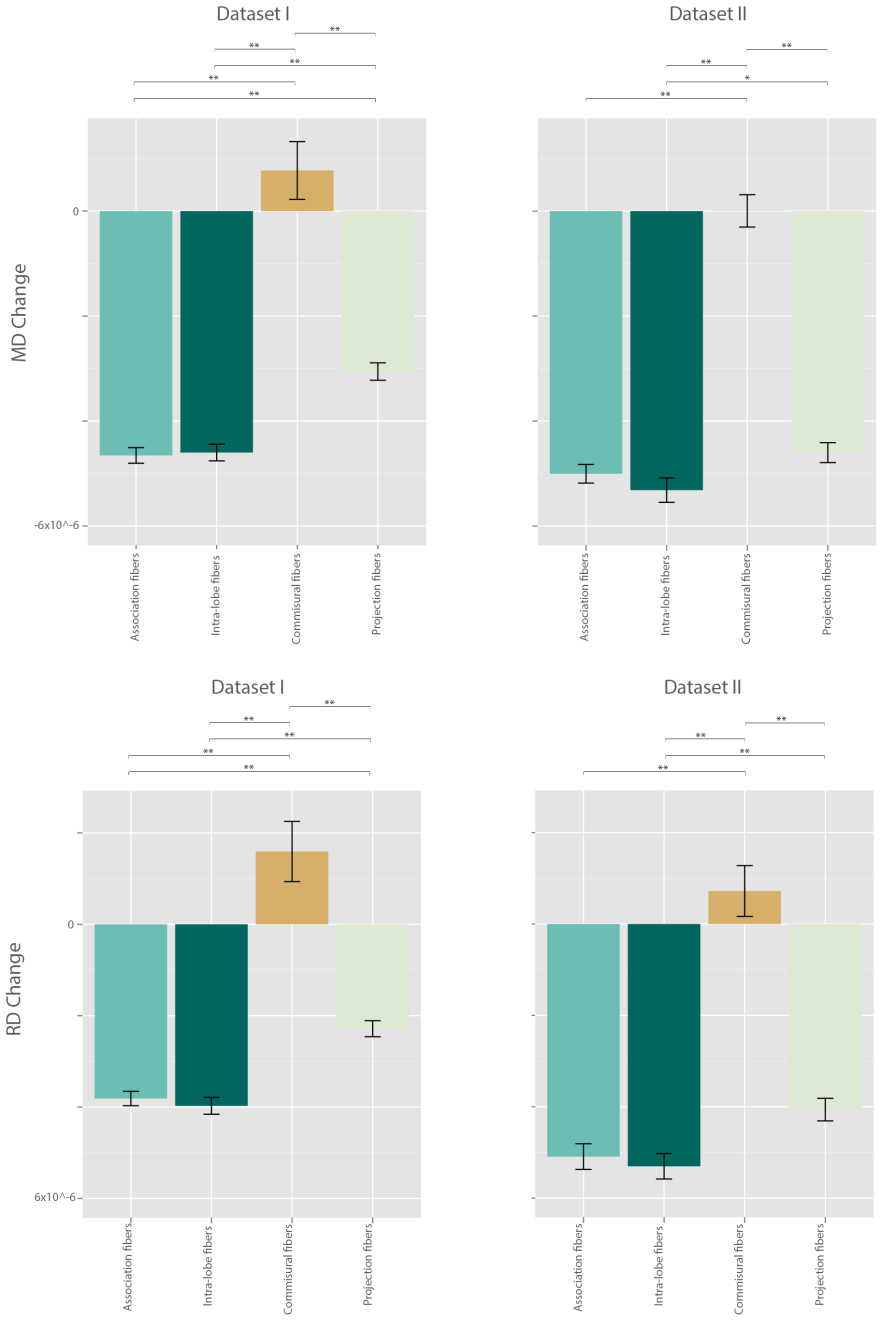

Figure 3 Age-related changes are greatest for association and intra-lobe fibers. The Y-axis shows age-related change (estimated as $ß_{age}$) in MD and RD per connection for each fiber class (x-axis): association, intralobe, commissural and projection fibers. *5P<0.05, **5P<0.01

thesis_LW_V3.indb 102 06/06/16 07:38

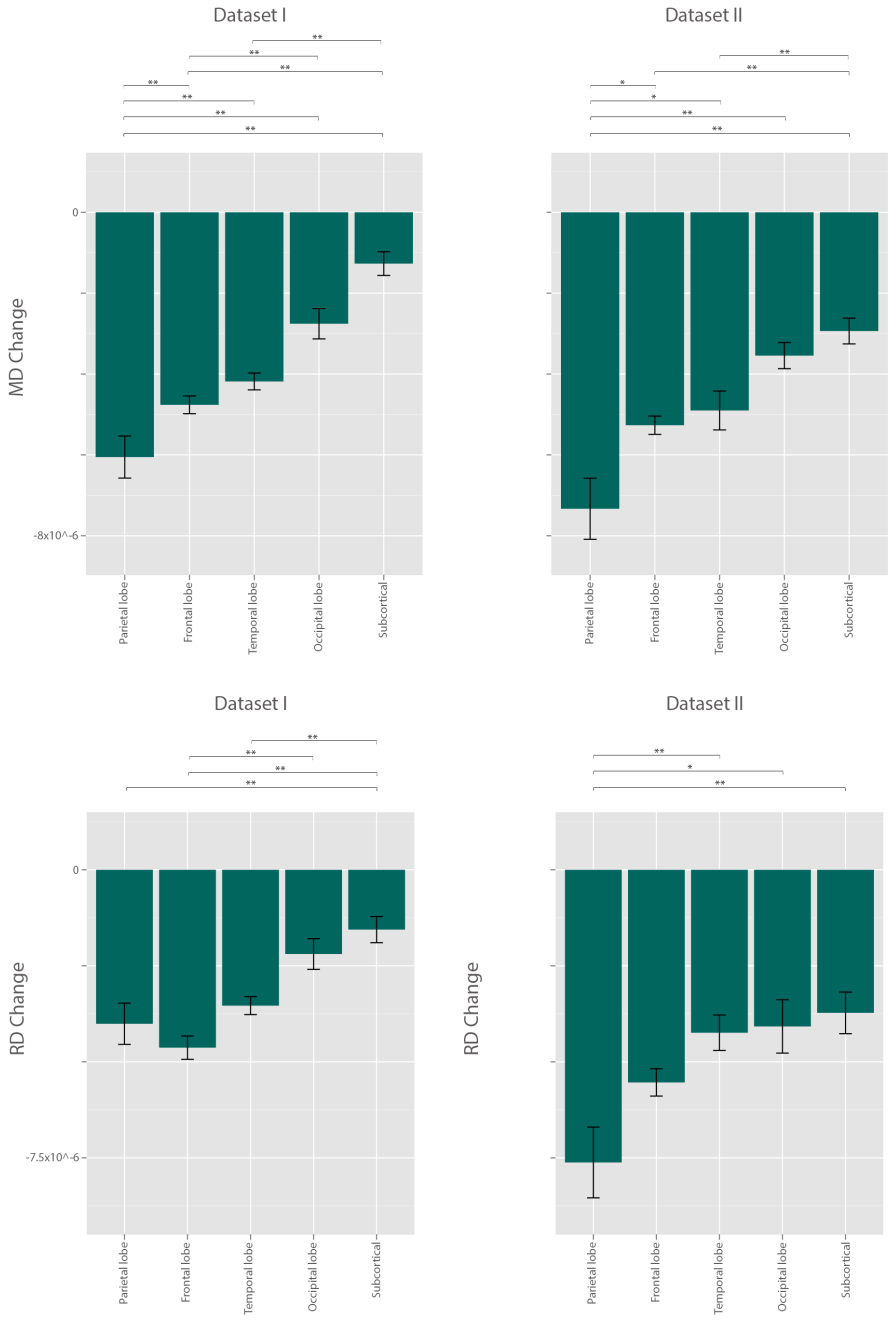

Figure 4 Age-related changes within lobes are greatest for parietal and frontal lobes. The Y-axis shows age-related changes (estimated as β_{age}) in MD and RD for intralobe fibers per lobe (x-axis); parietal lobe, frontal lobe, temporal lobe, occipital lobe, and fibers connecting subcortical structures., *5P<0.05, **5P<0.01.

thesis_LW_V3.indb 103 06/06/16 07:38

Table 2 The effect of age on network metrices

	Age	(s.e.)	p	
Dataset I				
Node strength	2.156	(31.324)	0.945	n.s.
Path length	-5.471×10^{-6}	(2.474×10^{-6})	0.030	*
Clustering	2.281	(0.941)	0.018	*
Dataset II				
Node strength	71.025	(35.087)	0.051	n.s.
Path length	-1.099×10^{-5}	(4.004×10^{-6})	0.010	**
Clustering	2.216	(1.182)	0.070	n.s.

Node strength, global efficiency, path length and clustering coefficient. s.e., standard error; n.s., not significant; *$p < 0.05$; **$p < 0.01$

Discussion

In this study, we show maturation of brain connectivity throughout adolescence. The developmental changes appear not to be uniform, but rather show regional heterogeneity, with greater strengthening of association and intra-lobe connections than commissural and projection fibers. Furthermore, in the age range of 7 and 23, relatively strong developmental changes in intra-lobe connections within the frontal and parietal lobes compared to changes in temporal and occipital lobes and between subcortical structures were observed. Increased node strength and global clustering in addition to decreased average path length accompanied these changes in connection strength.

Our findings on network topology are in agreement with the findings of Dennis and coworkers (2013) and Hagmann and coworkers (2010), who also reported a decrease in overall path length with age and an increase in node strength, respectively. This is in line with previous studies showing maturational increases in efficiency of functional communication over the network (Supekar, et al., 2009). We observed that those connections that are potentially involved with information integration in higher order association frontal and parietal areas, show the largest age related change, suggesting that changes in these fiber pathways contribute most to the observed changes in

thesis_LW_V3.indb 104 06/06/16 07:38

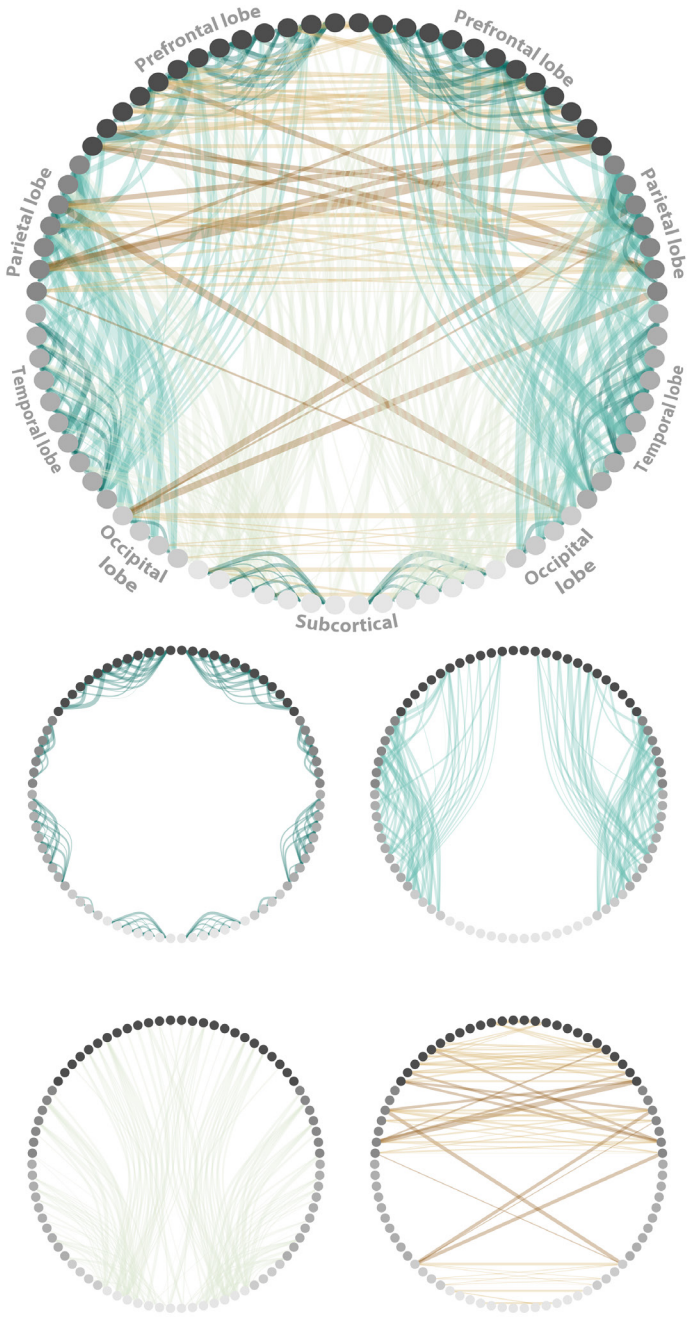

Figure 5 Age-related changes in MD for each connection in the weighted matrix M of dataset I. A link between two structures on the circle indicates the presence of a connection between them. Thicker lines reflect a greater rate of developmental change and therefore indicate protracted development. Color coding indicates the different fiber classes of intra-lobe, association, projection and commisural fibers.

thesis_LW_V3.indb 105 06/06/16 07:38

network topology within this age range. We also replicated an increase in clustering with age, as was previously observed by Dennis and coworkers (2013).

Differences in the rate of age-related changes between fibers could be interpreted as differences in maturational rate: a lower rate of change could be taken to suggest more stable or completed development. Earlier work by Lebel and coworkers (2008) showed that white matter development levels off in adulthood (2008), with maturational rate slowing. If we adhere to this line of interpretation, our results could be taken to suggest that projection and commissural fibers are the first to mature followed by association and intra-lobe fibers. Within the intra lobe fiber category occipital fibers are the first to mature, followed by temporal fibers, whereas parietal and frontal projections show a more protracted development. This is in keeping with the posterior to anterior pattern of white matter development that has been reported in post-mortem studies (Yakovlev and Lecours, 1967;Benes, 1989) and in anatomical MRI-studies of cortical brain development (Gogtay et al., 2004; Sowell et al., 2001; Wierenga, et al., 2013).

Our results complement earlier reports of relatively late maturation of short association-fibers and intra-lobar connections between parietal and frontal regions throughout adolescence and adulthood (Lebel et al., 2011; Chen et al., 2013; Westlye et al., 2010). Taken together with these earlier observations, our findings suggest a sequential developmental pattern, with early strengthening of connections between unimodal regions, followed by the maturation of connections from these regions to association areas, and finally by maturation of connections between association regions.

There are several limitations to this study. First the male to female ratio was uneven (5:3). Given the relatively small number of female subjects, we may have had limited power to detect gender differences. We did include gender in our regression model, as studies have reported differences in brain development between males and females (see e.g. Lenroot et al., 2007; Ruigrok et al. 2014). Less then 2% of the connections showed significant effects of gender. Furthermore, we included intracranial volume to account for the effect of brain size, which improved model fit for 17% of the connections. Second, we could not replicate non-linear age-related changes in white

thesis_LW_V3.indb 106 06/06/16 07:38

matter tracts, as have been previously observed (Lebel et al., 2008). We may not have been able to detect such non-linear changes due to limited power or the age-range included. Sensitivity to such changes could be improved by including longitudinal data.

In sum, our data support the hypothesis that age-related strengthening of white matter fibers is not homogenous throughout the brain during childhood and adolescence. Rather, we find that development seems to be characterized by strengthening of relatively short association fibers, particularly those within and between the frontal and parietal lobes. This suggests that changes in these connections contribute most to changes in network topology during the same developmental time period.

thesis_LW_V3.indb 107 06/06/16 07:38

Supplementary information

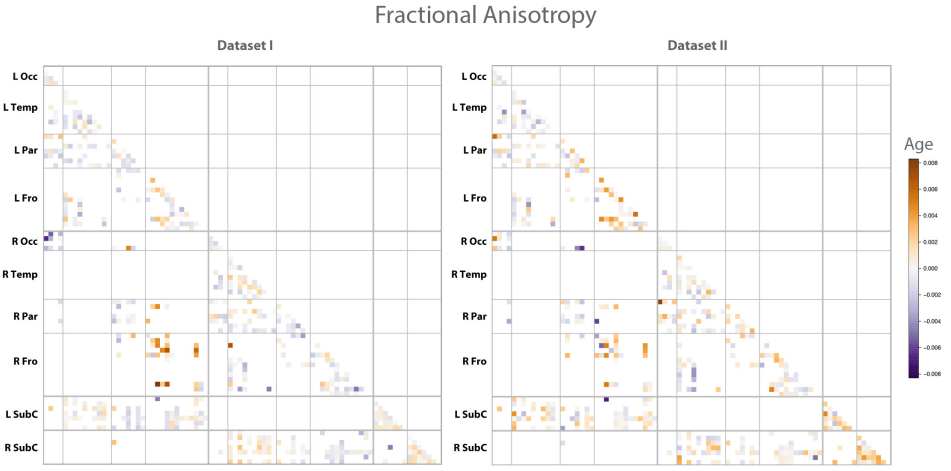

Supplemental Figure 1 Age-related changes in FA for the connections in the weighted matrix M. Changes are estimated as $ß_{age}$ for all connections that were present in at least 60% of the participants. We observed both increases and decreases in FA with age (shown in orange and purple respectively). R SubC =right subcortical structures, L SubC = left subcortical structures, R Fro = right frontal lobe, R Par = right parietal lobe, r Temp = right temporal lobe, R Occ = right occipital lobe, L Fro = left frontal lobe, L Par = left parietal lobe, L Temp = left temporal lobe and L Occ = left occipital lobe

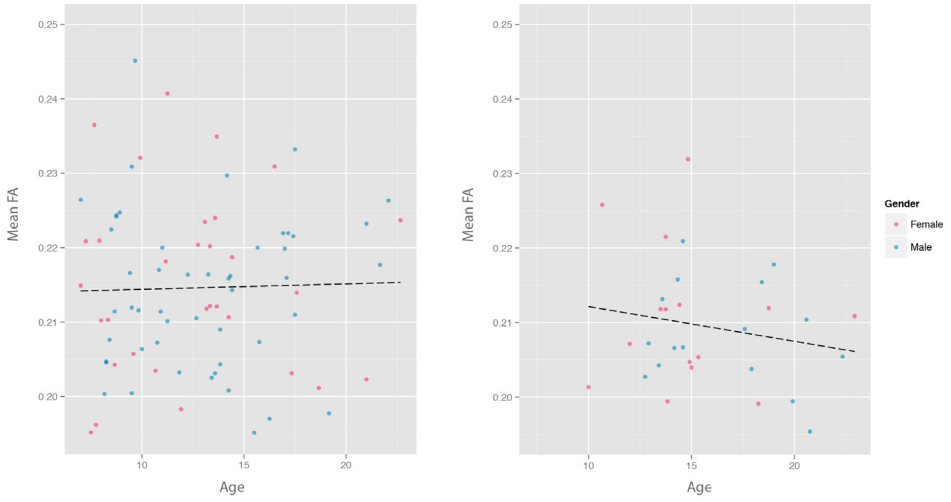

Supplemental Figure 2 Mean FA does not change with age. Mean FA was calculated per subject by averaging FA values for each connection in the weighted matrix M. Males are shown in blue, females in pink. No significant changes in mean FA was observed with age in Dataset I nor Dataset II

thesis_LW_V3.indb 108 06/06/16 07:38

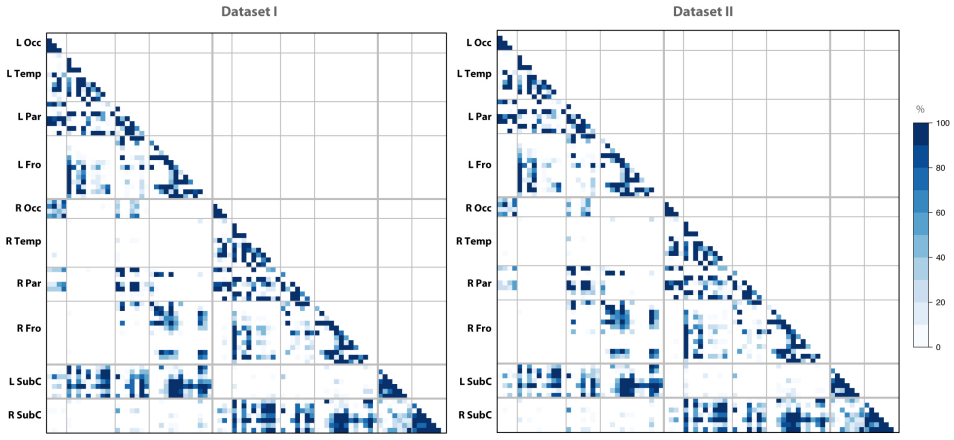

Supplemental Figure 3 Connection density in the un-weighted matrix G. Percentage of subjects that share a connection in the matrix. Connections that were present in over 60% of subjects were included in analysis

thesis_LW_V3.indb 109 06/06/16 07:38

References

Alexander, A. L., Lee, J. E., Lazar, M., & Field, A. S. (2007). Diffusion tensor imaging of the brain. Neurotherapeutics 4, 316-329.

Andersson, J., & Skare, S. (2002). A Model-Based Method for Retrospective Correction of Geometric Distortions in Diffusion-Weighted EPI. NeuroImage, 16(1), 177–199.

Ball, G., Aljabar, P., Zebari, S., Tusor, N., Arichi, T., Merchant, N., et al. (2014). Rich-club organization of the newborn human brain. Proceedings of the National Academy of Sciences of the United States of America, 111(20), 7456–7461.

Basser, P. J., & Pierpaoli, C. (1996). Microstructural and physiological features of tissues elucidated by quantitative-diffusion-tensor MRI. Journal of Magnetic Resonance. Series B, 111(3), 209–219.

Baumann, N., & Pham-Dinh, D. (2001). Biology of oligodendrocyte and myelin in the mammalian central nervous system. Physiological Reviews, 81(2), 871–927.

Beaulieu, C., & Allen, P. S. (1994). Determinants of anisotropic water diffusion in nerves. Magnetic Resonance in Medicine : Official Journal of the Society of Magnetic Resonance in Medicine / Society of Magnetic Resonance in Medicine, 31(4), 394–400.

Benes, F. M. (1989). Myelination of cortical-hippocampal relays during late adolescence. Schizophrenia Bulletin, 15(4), 585.

Bullmore, E., & Sporns, O. (2009). Complex brain networks: graph theoretical analysis of structural and functional systems. Nature Reviews Neuroscience, 10(3), 186–198.

Chen, Z., Liu, M., Gross, D. W., & Beaulieu, C. (2013). Graph theoretical analysis of developmental patterns of the white matter network. Frontiers in human neuroscience, 7, 716.

Costello, E. J., Edelbrock, C. S., & Costello, A. J. (1985). Validity of the NIMH Diagnostic Interview Schedule for Children: A comparison between psychiatric and pediatric referrals. Journal of Abnormal Child Psychology, 13(4), 579–595.

Dale, A., Fischl, B., & Sereno, M. I. (1999). Cortical Surface-Based Analysis: I. Segmentation and Surface Reconstruction. NeuroImage, 9(2), 179–194.

Darki, F., & Klingberg, T. (2014). The Role of Fronto-Parietal and Fronto-Striatal Networks

thesis_LW_V3.indb 110 06/06/16 07:38

in the Development of Working Memory: A Longitudinal Study. Cerebral Cortex, 25(6), 1587–1595

de Reus, M. A., & van den Heuvel, M. P. (2013). Estimating false positives and negatives in brain networks. NeuroImage, 70, 402–409.

Dennis, E. L., Jahanshad, N., McMahon, K. L., de Zubicaray, G. I., Martin, N. G., Hickie, I. B., et al. (2013). Development of brain structural connectivity between ages 12 and 30: A 4-Tesla diffusion imaging study in 439 adolescents and adults. NeuroImage, 64, 671–684.

Desikan, R. S., Ségonne, F., Fischl, B., Quinn, B. T., Dickerson, B. C., Blacker, D., et al. (2006). An automated labeling system for subdividing the human cerebral cortex on MRI scans into gyral based regions of interest. NeuroImage, 31(3), 968–980

Dosenbach, N. U. F., Nardos, B., Cohen, A. L., Fair, D. A., Power, J. D., Church, J. A., et al. (2010). Prediction of individual brain maturity using fMRI. Science, 329(5997), 1358–1361.

Dubois, J., Dehaene-Lambertz, G., Kulikova, S., Poupon, C., Hüppi, P. S., & Hertz-Pannier, L. (2014). The early development of brain white matter: a review of imaging studies in fetuses, newborns and infants. Neuroscience, 276, 48–71.

Durston, S., Nederveen, H., van Dijk, S., van Belle, J., de Zeeuw, P., Langen, M., & van Dijk, A. (2009). Magnetic Resonance Simulation is Effective in Reducing Anxiety Related to Magnetic Resonance Scanning in Children. Journal of the American Academy of Child & Adolescent Psychiatry, 48(2), 206–207.

Fair, D. A., Cohen, A. L., Power, J. D., Dosenbach, N. U. F., Church, J. A., Miezin, F. M., et al. (2009). Functional brain networks develop from a "local to distributed" organization. PLoS Computational Biology, 5(5), e1000381.

Fan, Y., Shi, F., Smith, J. K., Lin, W., Gilmore, J. H., & Shen, D. (2011). Brain anatomical networks in early human brain development. NeuroImage, 54(3), 1862–1871.

Feldman, H. M., Lee, E. S., Yeatman, J. D., & Yeom, K. W. (2012). Language and reading skills in school-aged children and adolescents born preterm are associated with white matter properties on diffusion tensor imaging. Neuropsychologia, 50(14), 3348–3362

thesis_LW_V3.indb 111 06/06/16 07:38

Fischl, B., Sereno, M. I., & Dale, A. (1999). Cortical Surface-Based Analysis: II: Inflation, Flattening, and a Surface-Based Coordinate System. NeuroImage, 9(2), 195–207.

Gao, W., Lin, W., Chen, Y., Gerig, G., Smith, J. K., Jewells, V., & Gilmore, J. H. (2009). Temporal and spatial development of axonal maturation and myelination of white matter in the developing brain. AJNR. American journal of neuroradiology, 30(2), 290–296.

Gogtay, N., Giedd, J., Lusk, L., Hayashi, K., Greenstein, D., Vaituzis, A., et al. (2004). Dynamic mapping of human cortical development during childhood through early adulthood. Proceedings of the National Academy of Sciences of the United States of America, 101(21), 8174–8179.

Hagmann, P., Sporns, O., Madan, N., Cammoun, L., Pienaar, R., Wedeen, V. J., et al. (2010). White matter maturation reshapes structural connectivity in the late developing human brain. Proceedings of the National Academy of Sciences, 107(44), 19067–19072.

He, Y., Chen, Z. J., & Evans, A. C. (2006). Small-World Anatomical Networks in the Human Brain Revealed by Cortical Thickness from MRI. Cerebral Cortex, 17(10), 2407–2419.

Hermoye, L., Saint-Martin, C., Cosnard, G., Lee, S.-K., Kim, J., Nassogne, M.-C., et al. (2006). Pediatric diffusion tensor imaging: normal database and observation of the white matter maturation in early childhood. NeuroImage, 29(2), 493–504.

Knudsen, E. I. (2004). Sensitive periods in the development of the brain and behavior. Journal of Cognitive Neuroscience, 16(8), 1412–1425.

Latora, V., & Marchiori, M. (2001). Efficient Behavior of Small-World Networks. Physical Review Letters, 87(19), 198701.

Lebel, C., Walker, L., Leemans, A., Phillips, L., & Beaulieu, C. (2008). Microstructural maturation of the human brain from childhood to adulthood. NeuroImage, 40(3), 1044–1055.

Lebel, C., & Beaulieu, C. (2011). Longitudinal Development of Human Brain Wiring Continues from Childhood into Adulthood. Journal of Neuroscience, 31(30), 10937–10947.

Lenroot, R. K., Gogtay, N., Greenstein, D. K., Wells, E. M., Wallace, G. L., Clasen, L. S., et al. (2007). Sexual dimorphism of brain developmental trajectories during childhood

thesis_LW_V3.indb 112 06/06/16 07:38

and adolescence. NeuroImage, 36(4), 1065–1073.

Mori, S., & van Zijl, P. C. M. (2002). Fiber tracking: principles and strategies - a technical review. NMR in Biomedicine, 15(7-8), 468–480.

Mori, S., Crain, B. J., Chacko, V. P., & van Zijl, P. C. M. (2001). Three-dimensional tracking of axonal projections in the brain by magnetic resonance imaging. Annals of Neurology, 45(2), 265–269.

Nagy, Z., Westerberg, H., & Klingberg, T. (2004). Maturation of White Matter is Associated with the Development of Cognitive Functions during Childhood. Journal of Cognitive Neuroscience, 16(7), 1227–1233.

Peters, B. D., Ikuta, T., DeRosse, P., John, M., & Burdick, K. E. (2014). Age-Related Differences in White Matter Tract Microstructure Are Associated with Cognitive Performance from Childhood to Adulthood. Biological Psychiatry, 75(3), 248–256

Power, J. D., Barnes, K. A., Snyder, A. Z., Schlager, B. L., & Petersen, S. A. (2012). Spuerious but systematic correlations in functional connectivity MRI networks arise from subject motion. NeuroImage, 59(3), 2142-2154.

Provenzale, J. M., Liang, L., DeLong, D., & White, L. E. (2007). Diffusion tensor imaging assessment of brain white matter maturation during the first postnatal year. American Journal of Roentgenology, 189(2), 476–486.

Rubinov, M., & Sporns, O. (2010). Complex network measures of brain connectivity: Uses and interpretations. NeuroImage, 52(3), 1059–1069.

Ruigrok, A. N. V., Salimi-Khorshidi, G., Lai, M.-C., Baron-Cohen, S., Lombardo, M. V., Tait, R. J., & Suckling, J. (2014). A meta-analysis of sex differences in human brain structure. Neuroscience and Biobehavioral Reviews, 39, 34–50.

Schmierer, K., Wheeler-Kingshott, C. A. M., Boulby, P. A., Scaravilli, F., Altmann, D. R., Barker, G. J., et al. (2007). Diffusion tensor imaging of post mortem multiple sclerosis brain. NeuroImage, 35(2), 467–477.

Sheehan, D. V., Lecrubier, Y., Sheehan, K. H., Amorim, P., Janavs, J., Weiller, E., et al. (1998). The Mini-International Neuropsychiatric Interview (M.I.N.I.): the development and validation of a structured diagnostic psychiatric interview for DSM-IV and ICD-10.

thesis_LW_V3.indb 113 06/06/16 07:38

The Journal of clinical psychiatry, 59 Suppl 20, 22–33;quiz 34–57.

Sowell, E. R., Thompson, P. M., Tessner, K. D., & Toga, A. W. (2001). Mapping continued brain growth and gray matter density reduction in dorsal frontal cortex: Inverse relationships during postadolescent brain maturation. Journal of Neuroscience, 21(22), 8819–8829.

Supekar, K., Musen, M., & Menon, V. (2009). Development of large-scale functional brain networks in children. PLoS Biology, 7(7), e1000157.

Tamnes, C. K., Ostby, Y., Fjell, A. M., Westlye, L. T., Due-Tonnessen, P., & Walhovd, K. B. (2010). Brain Maturation in Adolescence and Young Adulthood: Regional Age-Related Changes in Cortical Thickness and White Matter Volume and Microstructure. Cerebral Cortex, 20(3), 534–548.

Thomas, M. S. C., & Johnson, M. H. (2008). New Advances in Understanding Sensitive Periods in Brain Development. Current Directions in Psychological Science, 17(1), 1–5.

van den Heuvel, M. P., & Hulshoff Pol, H. E. (2010). Exploring the brain network: A review on resting-state fMRI functional connectivity. European Neuropsychopharmacology, 20(8), 519–534.

van den Heuvel, M. P., Mandl, R. C. W., Kahn, R. S., & Hulshoff Pol, H. E. (2009). Functionally linked resting-state networks reflect the underlying structural connectivity architecture of the human brain. Human Brain Mapping, 30(10), 3127–3141.

van den Heuvel, M. P., Mandl, R. C. W., Stam, C. J., Kahn, R. S., & Hulshoff Pol, H. E. (2010). Aberrant frontal and temporal complex network structure in schizophrenia: a graph theoretical analysis. Journal of Neuroscience, 30(47), 15915–15926.

van den Heuvel, M. P., & Sporns, O. (2011). Rich-club organization of the human connectome. Journal of Neuroscience, 31(44), 15775–15786.

van den Heuvel, M. P., Kersbergen, K. J., de Reus, M. A., Keunen, K., Kahn, R. S., Groenendaal, F., et al. (2014). The Neonatal Connectome During Preterm Brain Development. Cerebral Cortex, 25(9), 3000–3013

van der Knaap MS, Valk J, Bakker CJ, Schooneveld M, Faber JA, Willemse J, Gooskens RH

thesis_LW_V3.indb 114 06/06/16 07:38

(1991) Myelination as an expression of the functional maturity of the brain. Dev Med Child Neurol 33(10):849–857.

Van Haasen PP, De Bruyn EEJ, Pijl YJ, Poortinga YH, Lutje-Spelberg HC, Vander Steene G, et al. (1986): Wechsler Intelligence Scale for Children- Revised, Dutch Version.

Wechsler, D., 2000: Wechsler Adult Intelligence Scale-Third Edition (WAIS- III): Nederlandstalige Bewerking. Technische Handleiding. (Dutch Version Technical Manual).

Westlye, L. T., Walhovd, K. B., Dale, A. M., Bjornerud, A., Due-Tonnessen, P., Engvig, A., et al. (2010). Life-Span Changes of the Human Brain White Matter: Diffusion Tensor Imaging (DTI) and Volumetry. Cerebral Cortex, 20(9), 2055–2068.

Wierenga, L. M., Langen, M., Oranje, B., & Durston, S. (2013). Unique developmental trajectories of cortical thickness and surface area. NeuroImage, 87, 120–126.

Wolff, S. D., & Balaban, R. S. (1994). Magnetization transfer imaging: practical aspects and clinical applications. Radiology, 192(3), 593–599.

Yakovlev, P.I., Lecours, A.R., 1967. The myelogenetic cycles of regional maturation of the brain. In: Minkowski, A (Ed.), Regional Development of the Brain Early in Life. Blackwell Scientific Publications Inc., Boston, pp. 3–70. Massachusetts.

Yan, C., Gong, G., Wang, J., Wang, D., Liu, D., Zhu, C., et al. (2011). Sex- and Brain Size-Related Small-World Structural Cortical Networks in Young Adults: A DTI Tractography Study. Cerebral Cortex, 21(2), 449–458.

Yap, Q. J., Teh, I., Fusar-Poli, P., Sum, M. Y., Kuswanto, C., & Sim, K. (2013). Tracking cerebral white matter changes across the lifespan: insights from diffusion tensor imaging studies. Journal of neural transmission (Vienna, Austria : 1996), 120(9), 1369–1395.

Yoshida, S., Oishi, K., Faria, A. V., & Mori, S. (2013). Diffusion tensor imaging of normal brain development. Pediatric Radiology 43, 15-27.

Zatorre, R. J., Fields, R. D., & Johansen-Berg, H. (2012). Plasticity in gray and white: neuroimaging changes in brain structure during learning. Nature Neuroscience, 15(4), 528–536.

thesis_LW_V3.indb 115 06/06/16 07:38

PART II

Atypical development

thesis_LW_V3.indb 117 06/06/16 07:38

CORTICAL DEVELOPMENT IN ATTENTION-DEFICIT/ HYPERACTIVITY DISORDER: WHAT CAN IT TELL US ABOUT EARLY DEVELOPMENTAL MECHANISMS?

Sara Ambrosino
Patrick de Zeeuw
Lara M Wierenga
Sarai van Dijk
Sarah Durston

Submitted

thesis_LW_V3.indb 119 06/06/16 07:38

Abstract

Studies of brain development in Attention-Deficit/Hyperactivity Disorder (ADHD) have shown developmental changes in the cortical mantle. As different aspects of cortical morphology likely relate to different neurodevelopmental mechanisms, studying multiple aspects may inform us about the developmental origins of ADHD. Furthermore, many longitudinal studies to date come from overlapping cohorts. Therefore, we conducted a longitudinal study of brain development in a large independent ADHD sample, and measured multiple markers of cortical morphology that relate to different neurodevelopmental mechanisms. We analyzed 297 longitudinal anatomical MRI-scans from two matched groups of 94 subjects with ADHD and 94 controls, aged 6-28 years. Scans were processed using FreeSurfer pipeline, which provides subcortical volumes and measures of cerebral cortex (volume, surface, thickness and gyrification) as a whole and within 68 regions based on the Desikan-Killiany atlas. We estimated the developmental trajectories for both groups using mixed-effects regression analysis. Subjects with ADHD had smaller overall cortical volume, which was driven by decreases in volume in regions throughout the cortical mantle, but predominately in the frontal lobes. The decreased volume in frontal regions was associated with smaller surface area and sometimes a lower degree of gyrification. Nearly all decreases were stable across development. There were no between-group differences in cortical thickness, nor in subcortical volumes. Our data suggest ADHD is associated with developmentally persistent reductions in cortical volume, surface area, and gyrification, particularly in frontal areas. These findings implicate neurodevelopmental mechanisms that regulate the early stages of cortical expansion and convolution in ADHD.

thesis_LW_V3.indb 120 06/06/16 07:38

Introduction

Studies of brain development in Attention-Deficit/Hyperactivity Disorder (ADHD) have shown developmental changes in the volume of cortical and subcortical regions (Valera et al., 2007; Durston et al., 2009a; Nakao et al., 2011; Frodl & Skokauskas, 2012). However, the pathological processes that may be responsible for these alterations in ADHD remain unclear.

Novel neuroimaging approaches offer a valuable contribution in ADHD research as now permit to examine volumetric alterations in greater detail and a higher degree of specificity with regard to particular neurobiological processes. In fact, distinct dimensions of cortical volume express different cytoarchitectonic properties, which likely relate to partially distinct early neurodevelopmental processes. For example, cortical surface area is related to the number of the columns, which in turn is regulated by the number of progenitor cells formed during early phase of neuronal proliferation. In contrast cortical thickness is affected by the number of intermediate progenitor cells that migrate within a column during embryonic development (Rakic 1995, Rakic 2000). As such, studying these markers has the potential to inform us at which developmental stage cortical changes occur, and therefore they can meaningfully contribute in constructing neuropathological models of ADHD.

The group at National Institute of Mental Health (NIMH) has produced perhaps the largest and most prolific studies. They have reported reductions in cortical thickness (Shaw et al., 2006) that have sometimes been (partially) replicated (Sowell et al., 2003; Narr et al., 2009; Batty et al., 2010) and sometimes not at all (de Zeeuw et al., 2012, Wolosin et al., 2009). The first studies to investigate other important aspects of cortical morphology (surface area and gyrification) have reported either reduced (Wolosin et al., 2009) or delayed (Shaw et al., 2012) cortical surface expansion in ADHD, while results for gyrification were equivocal (Li et al., 2007; Shaw et al., 2012). The findings from NIMH of a simultaneous delay in cortical thickness development (Shaw et al., 2007) and surface area development (Shaw et al., 2012) suggest that there may be a global perturbation of cortical maturation in ADHD (Shaw et al., 2012). To date, no studies have assessed all relevant cortical markers simultaneously (cortical volume, thickness, surface area and gyrification) in a single, longitudinal sample. Doing so may permit a more refined characterization of

thesis_LW_V3.indb 121 06/06/16 07:38

cortical development in ADHD, as it will allow us to assess the interplay between multiple architectonic features that represent different aspects of early development. Furthermore, studies of longitudinal brain development in ADHD are scarce and mainly from overlapping samples at the NIMH (Castellanos et al., 2002; Shaw et al., 2007; Shaw et al., 2012). Therefore it is important that results are confirmed in other, independent longitudinal samples (Horga et al., 2014).

In the current study, we investigated brain development in ADHD, using comprehensive makers of cortical development, in a large, European longitudinal sample. We hypothesized that subjects with ADHD would show decreases in cortical volume, in particular in frontal areas. We had no specific expectations regarding which aspects of cortical morphology would be most affected.

Materials and methods

The Institutional Review Board of the University Medical Center Utrecht, the Netherlands, approved the study and its procedures. For subjects under the age of 18 years, written informed consent was obtained from the parents after full disclosure of the study purpose and procedure. Children provided written and/or verbal assent. Subjects aged 18 years or above gave written informed consent themselves.

Participants and clinical measures

We acquired 410 whole-brain MRI scans from 260 subjects (129 with ADHD and 131 typically developing controls). We used Propensity Score Matching (PSM) to equalize gender, socioeconomic status (SES) and the number of longitudinal scans between groups. We chose not to match the groups for intelligence quotient (IQ) as changes in IQ are intrinsically related to ADHD (Frazier et al., 2004). Therefore matching for IQ would have led to unrepresentative samples of both the ADHD and control populations (i.e., selection bias). Such a bias would likely remove variability in the dependent variables of interest (e.g., brain volume) and possibly generate anomalous findings (Dennis et al., 2009). Propensity score matching resulted in a sample of 188 closely matched subjects (94 in each group), aged between 6 and 28 years. There was a total of 297 MRI-scans available, with 73 participants (34 subjects with ADHD; 39 controls) scanned twice or more. There was no

thesis_LW_V3.indb 122 06/06/16 07:38

Table 1 Demographic and clinical characteristics of the sample

		ADHD (N=94)	Controls (N=94)	Group Differences[e]
Gender	N Male - Female	78 - 16	80 - 14	ns
Age at scan	N scans Wave 1 / years M (SD)	94 / 11.4 (2.9)	94 / 11.2 (4.0)	ns
	N scans Wave 2 / years M (SD)	34 / 15.1 (2.6)	39 / 14.5 (3.4)	ns
	N scans Wave 3+ / years M (SD)	13 / 18.5 (2.7)	23 / 18.1 (2.7)	ns
Hand preference	N Righthanded/Other	70 / 24	77 / 17	ns
SES	Parental education years M (SD)	12.8 (2.2)	13.1 (2.0)	ns
Total IQ	M (SD) at baseline*	100.9 (16.8)	109.8 (16.8)	*
DISC[a]	N ADHD-I	23	0	-
	N ADHD-HI	16	0	-
	N ADHD-C	55	0	-
	N ODD	34	0	-
	N CD	1	0	-
CBCL[b]	Internalising raw score M (SD)	9.3 (5.6)	4.4 (4.9)	**
	Externalising raw score M (SD)	16.6 (9.5)	4.5 (5.0)	**
	Attention problem raw score M (SD)	9.2 (4.0)	3.1 (2.5)	**
TRF[c]	Internalising raw score M (SD)	7.5 (5.9)	3.5 (4.6)	**
	Externalising raw score M (SD)	13.1 (10.6)	3.0 (5.0)	**
	Attention problem raw score M (SD)	16.9 (9.4)	6.0 (7.0)	**
Medication[d]	N Medicated / Unmedicated at			
	Wave 1	64°/20	0 / 94	**
	Wave 2	22/12	0 / 39	**
	Wave 3	6/4	0 / 23	*

Abbreviations: ADHD, Attention-Deficit/Hyperactivity Disorder (I=inattentive type, HI=hyperactive/impulsive type, C=combined type); N, number; M, mean; SD, standard deviation; SES, Socio-Economic Status; IQ, intelligence quotient; DISC, Diagnostic Interview Schedule for Children; ODD, Oppositional Defiant Disorder; CD, Conduct Disorder; CBCL, Child Behavior Checklist; TRF, Teacher Report Form. Note. [a]DISC repeated at follow-up for 36% of the subjects; [b]CBCL unavailable for 9 controls and 13 ADHD subjects; [c]TRF unavailable for 19 controls and 30 ADHD subjects; [d]unavailable for 10 subjects with ADHD; °63 subjects on psychostimulants (59 on methylphenidate, 3 on dexamphetamine, 1 on atomoxetine), 1 subject on desipramine; [e]t-Test for age at scan at each wave of scanning and total IQ; X^2 for Gender and Handedness; nonparametric statistical test for SES, CBCL and TRF; Fisher's exact test for Medication status at each wave of scanning; ns, not significant; *p < .001; **p < .0001.

thesis_LW_V3.indb 123 06/06/16 07:38

difference in mean age between groups at each wave of scanning. Longitudinal scans were acquired with a similar average interval in both groups (ADHD: M(SD) = 3.6(2.0) years, controls: M(SD) = 3.4(2.3) years; p = .739).

The Diagnostic Interview Schedule for Children (DISC, version 2.3 or IV), parent version (Shaffer et al., 2000), was administered to parents in order to confirm the clinical diagnosis of ADHD or to exclude psychiatric comorbidity in controls at study entry. Parents and teachers completed broadband psychiatric screeners at each time point: Child Behavior Checklist (CBCL) and Teacher Report Form (TRF) respectively, to provide a dimensional measure of behavioral symptoms (Verhulst et al., 1996; Verhulst et al., 1997). Total IQ was estimated using a short form of the Dutch version of the Wechsler intelligence scales (WISC-R/WISC-III or WAIS-III as appropriate), including the subtests Vocabulary, Block Design, Similarities and Object Assembly (Wechsler, 2005).

Controls were excluded in case of psychiatric morbidity or first-degree relatives with a history of psychiatric problems. Children with ADHD were excluded if they met DSM criteriar for any co-morbid disorder other than Oppositional Defiant Disorder (ODD) or Conduct Disorder (CD) on the DISC at study entry. In both groups, additional exclusion criteria were IQ below 70, any major physical or neurological illnesses or the presence of metals in the body that precluded the MRI session. Table 1 lists participant characteristics for both samples. Medication status based on parental- and self-report could reliably be assessed at study entry for 89% of ADHD cases. At study entry, 75% of the subjects with ADHD were using psychostimulant medication. The vast majority (94%) was taking methylphenidate preparations. The proportion of medicated subjects declined slightly at follow-up: 73% of subjects with ADHD were medicated at the time of their second scan, 67% were medicated at scan 3.

Prior to the MRI scan, children under 13 years of age were acclimated to the MRI procedure in a practice session using a dummy scanner as described previously (Durston et al., 2009); children over 13 years were also offered the opportunity to do a practice session.

thesis_LW_V3.indb 124 06/06/16 07:38

Propensity Score Matching (PSM)

PSM is a statistical matching technique that pairs cases and controls with similar values on a propensity score (PS) from a pool of participants. The PS is the probability of group membership conditional on a set of observed non-random confounders. PSs were estimated using logistic regression, including gender, SES and a dummy variable for the presence of longitudinal scans as covariates, implemented in SPSS 20.0.0 and R 3.0.2 (Thoemmes, 2012). Subjects were then matched using nearest neighbor matching. The caliper width (maximum permitted difference between two subjects) was set to the recommended value (Austin, 2011) of .20 standard deviations of the logit of the PS.

MRI acquisition

All imaging was performed over the time span of 15 years using a 1.5-T MRI-scanner (Philips, Best, The Netherlands). A T1-weighted three-dimensional fast field echo scan of the whole head was acquired with 130 to 150 1.5-mm contiguous coronal slices (earlier scans; 58 scans from subjects with ADHD and 51 scans from controls) or 160 to 180 1.2-mm contiguous coronal slices (later scans; 83 scans from subjects with ADHD and 105 scans from controls) (echo time 4.6 ms; repetition time 30 ms; flip angle 30°; field of view 256 mm; in-lane voxel size 1mm x 1mm). Groups did not differ with respect to the distribution of MRI protocols (slice thickness 1.5 vs 1.2 mm), for either baseline ($p = .770$) or longitudinal measures ($p = .133$). Independent neuroradiologists evaluated all MRI scans and no gross morphological abnormalities were reported for any of the participants.

MRI processing

All scans were coded in order to ensure rater blindness to subject identity and diagnosis at all times during analysis. The T1-weighted images were processed using FreeSurfer v5.1.0 (Fischl, 2012), a well validated and widely used segmentation and image analysis software package (http://surfer.nmr.mgh.harvard.edu/fswiki).

The package contains a fully automated structural imaging pipeline for the quantitative study of brain anatomy including volumetry of subcortical structures and a complete assessment of cortical morphometry, along the entire surface and with accuracy comparable to manual methods (Fischl et al., 2002) and post-mortem studies (Fischl & Dale, 2000). The brain segmentation and

thesis_LW_V3.indb 125 06/06/16 07:38

cortical reconstruction pipelines in FreeSurfer have been described in more detail elsewhere (Dale et al., 1999; Fischl et al., 1999; Fischl & Dale, 2000; Fischl et al., 2002; Fischl et al., 2004a; Fischl et al., 2004b). In short, brain segmentation consists of registering the brain into Talaraich space (Talairach & Tournoux, 1988), removing non-brain tissue using a deformable template model (skull stripping), and neuroanatomical labeling, based on both voxel intensity values and a probabilistic atlas (Fischl et al., 2002). The reconstruction of cortical surfaces involves the segmentation of white matter, used to derive a surface representing the gray-white matter boundary (white surface). The white surface is then refined and deformed to locate the pial surface (gray matter/cerebrospinal fluid boundary) (Dale et al., 1999). Finally, by incorporating both geometric information derived from the cortical model and standard neuroanatomical conventions (Desikan et al., 2006; Destrieux et al., 2010), the procedure automatically assigns a neuroanatomical label to each location on the cortical surface (cortical parcellation). The automated cortical reconstruction is described in more detail in the Supplemental Material.

The FreeSurfer pipeline requires that output is checked individually at multiple points during the processing stream, in order to correct errors, if necessary. This ensures robustness and reliability of the results across participants (Dewey et al., 2010). Accordingly, we inspected the Talaraich registration, tissue segmentations and cortical parcellation for accuracy. If necessary, manual edits were performed by experienced operators (SA, LW) following the standardized procedures documented on the FreeSurfer website (http://surfer.nmr.mgh.harvard.edu/fswiki). The types of errors that frequently required user editing were incomplete skull stripping and mis-classification of white matter.

We acquired the volume of 24 non-cortical regions, including six subcortical structures per hemisphere (caudate, putamen, pallidum, accumbens, thalamus and amygdala), the corpus callosum (anterior, mid-anterior, central, mid-posterior and posterior segments), bilateral hippocampus, bilateral cerebellar gray and white matter and the brain stem. For simplicity, hereafter we refer to these as 'subcortical' structures.

For the study of cortical morphometry, we analyzed 34 areas per hemisphere from the Desikan-Killiany atlas (Desikan et al., 2006) (see Supplemental Material). The FreeSurfer outputs of interest were: cortical volume (CV, mm3), surface area (CS, mm2), cortical thickness (CT, mm) and local gyrification index (LGI, dimensionless) of the cortex as a whole and within the predefined areas (Figure 1).

thesis_LW_V3.indb 126 06/06/16 07:38

For each area, CS was measured along the white surface; CV and CT were measured as the volume and the average distance, respectively, between the parcellated portions of white and pial surfaces (Fischl & Dale, 2000). LGI is a measure of gyral complexity that is calculated at each point of the pial surface and was averaged across each area. LGI refers to the ratio between the surface of a circular patch of the pial surface and the corresponding patch on the outer smoothed surface of the brain (Schaer et al., 2008).

Total, left (lh) and right (rh) hemisphere values were obtained for cortical volume, surface, thickness and gyrification by summing or averaging each measure across all areas included. Average thickness throughout the cortex was computed applying the formula: Total CT= ((lh.CT * lh.CS) + (rh.CT * rh.CS)) / lh.CS + rh.CS

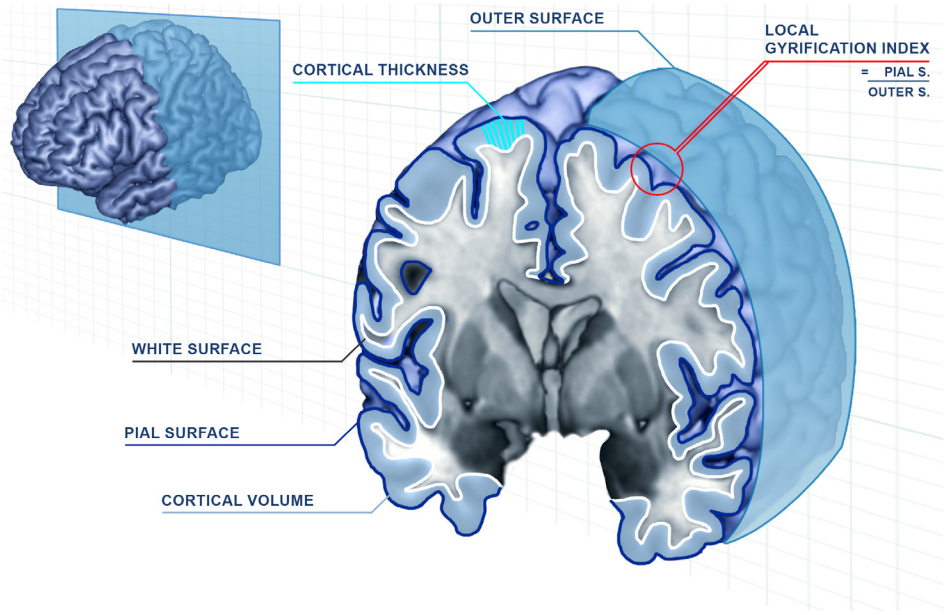

Figure 1 Morphometric parameters of the cerebral cortex.For every defined region of interest, cortical thickness was estimated as the average distance (in mm) between the white and pial surfaces; cortical surface was the area of the white surface (in mm^2); cortical volume was calculated as the volume contained between the white and pial surfaces (in mm^3), whereas local gyrification index (dimensionless) was computed as the ratio between the pial and outer surface.

thesis_LW_V3.indb 127 06/06/16 07:38

Statistical analyses

SPSS Statistics 20.0.0 for Mac OS X (SPSS Inc., Chicago, Illinois) was used to test for between-group differences in demographic and clinical data using parametric or non-parametric tests as appropriate.

The developmental trajectories of each measure were determined using (generalized) Linear Mixed Models as implemented in the lme4 library (Bates et al., 2011) in the R statistical package (R Development Core Team, 2012). This method permits the inclusion of multiple scans per person, to combine both inter- and intra-individual differences in the growth parameters (i.e., intercepts and slopes), while accounting for unbalanced data structure due to irregular time intervals between scans and unequal numbers of scans between subjects.

The best-fit model was determined in two phases following the procedure described previously (Wierenga et al., 2014a, 2014b). First, a growth model was determined using a step-down selection procedure. Each brain measure of the ith individual at the jth time point was modeled using cubic, quadratic and linear age effects (with age centered around the mean of the whole group: 13 years), with gender as covariate, according to the formula:

$$\text{Measurement}_{ij} = \text{Intercept} + d_{ij} + ß_1(\text{gender}) + ß_2(\text{age}) + ß_3(\text{age}^2) + ß_4(\text{age}^3) + e_{ij}$$

where dij represents the within person dependence and the eij term is the residual error. Gender and age effects were fixed, while the intercept and the dij term were modeled as random effects. If the cubic age effect was not significant at $p < .05$, it was removed from the model in order to test the quadratic age effect and so on.

Second, we examined whether the growth model differed between subjects with ADHD and controls. The selected growth model was expanded to include a dichotomous variable "ADHD" and its interaction with the age term(s) as fixed factors.

thesis_LW_V3.indb 128 06/06/16 07:38

For example, measures where the cubic model was appropriate were modelled as:

$$\text{Measurement}_{ij} = \text{Intercept} + d_{ij} + ß_1(\text{gender}) + ß_2(\text{age}) + ß_3(\text{age}^2) + ß_4(\text{age}^3) + ß_5(\text{group}) + ß_6(\text{group*age}) + ß_7(\text{group*age}^2) + ß_8(\text{group*age}^3) + e_{ij}$$

We tested whether the full model fit the data better than a simpler model including only the main effects of the ADHD and age. If it did not (indicating that there was no group by age interaction), the simpler model was compared to the selected growth model including the age terms only (i.e., this would denote that ADHD had no effect at all). Coefficients were estimated using the full Maximum Likelihood criterion and models were compared using the Bayesian Information Criterion (BIC). If the difference between the BIC of two nested models was greater than 2, the model with the lower BIC was selected; if ($\Delta BIC \leq 2$), the simplest model was selected on the grounds of parsimony. This procedure allowed us to achieve a balance between model complexity and goodness of fit (Kass and Raftery, 1995). Finally, since there were only few data points over age 25, we reran the analysis without older participants. Since this did not lead to any meaningful changes in the results and tinterpretation, we report on the results from all participants here.

Results

Total cortical volume, surface, thickness and gyrification

The developmental trajectories of total cortical volume, surface area, thickness and gyrification are provided in Figure 2. The regression coefficients are given in the Supplemental Material (Table S2). There was a quadratic effect of age and a main effect of ADHD on total cortical volume, but no interaction between ADHD and age. Mean total cortical volume was 5% smaller for subjects with ADHD than controls and this difference was stable development. Total cortical surface area followed a cubic trajectory for the entire group; total cortical thickness and total gyrification both showed a linear decrease with age for the whole group. There were no main effects or interaction between age and diagnostic group for these measures.

thesis_LW_V3.indb 129 06/06/16 07:38

Table 2 Group difference for regional measures (baseline values)

Left hemisphere						Right hemishpere					
Volume (mm^3)	Controls M (SD)	ADHD M (SD)	Δ%	t(186)	p value	Volume (mm^3)	Controls M (SD)	ADHD M (SD)	Δ%	t(186)	p value
caudal ant cingulate	2364.17 (620.95)	2131.25 (512.94)	9.85	-2.804	0.006	Caudal m frontal	8693,085 (1611.33)	7785,415 (1416.34)	10.44	-4.102	<.0001
lateralorbitofrontal	9645.06 (1280.61)	9152.60 (1186.19)	5.11	-2.735	0.007	cuneus	3895.93 (588.77)	3591.45 (634.43)	7.82	-3.411	<.001
medialorbitofrontal	6648.14 (942.18)	6231.90 (953.22)	6.26	-3.011	0.003	isthmuscingulate	3460.10 (724.36)	3094.21 (509.83)	10.57	-4.005	<.0001
middletemporal	14873.34 (2070.92)	14144.67 (1836.65)	4.9	-2.552	0.012	lateraloccipital	14491.13 (2097.74)	13229.42 (1734.95)	8.71	-4.494	<.0001
precentral	16023.61 (1836.40)	15349.56 (1794.82)	4.21	-2.545	0.012	lateralorbitofrontal	9458.86 (1279.44)	8952.87 (1146.93)	5.35	-2.855	0.005
precuneus	13796.31 (1792.36)	12977.44 (1730.64)	5.94	-3.187	0.002	medialorbitofrontal	6273.25 (848.37)	5873.16 (829.83)	6.38	-3.269	0.001
rostralmiddlefrontal	23282.65 (3312.90)	21494.06 (2341.65)	7.68	-4.274	<.0001	parsopercularis	5787.43 (963.86)	5300.62 (921.71)	8.41	-3.539	0.001
superiorparietal	18177.81 (2473.67)	16961.56 (2000.78)	6.69	-3.706	<.001	precentral	16002.22 (1931.85)	15119.47 (1740.48)	5.52	-3.291	0.001
superiortemporal	16179.76 (1955.96)	15048.86 (1788.64)	6.99	-4.137	<.0001	precuneus	14164.17 (1972.88)	13387.95 (1859.06)	5.48	-2.776	0.006
supramarginal	15878.93 (2151.64)	14688.31 (2096.45)	7.5	-3.843	<.001	superiorfrontal	30092.40 (3711.68)	28745.44 (2876.46)	4.48	-2.781	0.006
						superiorparietal	18074.09 (2442.41)	17086.73 (2046.77)	5.46	-3.004	0.003
						superiortemporal	15571.57 (1965.54)	14801.53 (1580.31)	4.95	-2.96	0.003
Surface Area (mm^2)	Controls M (SD)	ADHD M (SD)	Δ%	t(186)	p value	Surface Area (mm^2)	Controls M (SD)	ADHD M (SD)	Δ%	t(186)	p value
caudal ant cingulate	705.61 (153.51)	645.12 (153.51)	8.57	-2.908	0.004	Caudal m frontal	2692.20 (539.24)	2407.82 (439.15)	10.56	-3.965	<.001
rostral antcingulate	922.50 (156.31)	857.87 (179.75)	7.01	-2.63	0.009	isthmuscingulate	1044.27 (185.54)	949.76 (174.11)	9.05	-3.601	<.001
rostralmiddlefrontal	6791.60 (909.71)	6341.90 (906.39)	6.62	-3.395	0.001	lateraloccipital	5649.27 (755.85)	5291.44 (682.30)	6.33	-3.407	0.001
superiortemporal	4436.60 (487.06)	4180.88 (472.39)	5.76	-3.654	<.001	parsopercularis	1647.07 (273.67)	2407.82 (278.47)	9.57	-3.916	<.001
Gyrification	Controls M (SD)	ADHD M (SD)	Δ%	t(186)	p value	Gyrification	Controls M (SD)	ADHD M (SD)	Δ%	t(186)	p value
cuneus	3.03 (0.18)	2.99 (0.23)	1.29	-1.298	0.196	parsopercularis	4.80 (0.34)	4.67 (0.32)	2.77	-2.775	0.006
rostralmiddlefrontal	3.01 (0.17)	2.93 (0.17)	2.6	-3.116	0.002	transversetemporal	5.39 (0.36)	5.23 (0.38)	2.97	-2.953	0.004

Abbreviations and symbols: ADHD, Attention-Deficit/Hyperactivity Disorder; M, mean; SD, standard deviation; Δ%, percentage change, determined by dividing the difference of the ADHD and control values by the control value, multplied by 100.

thesis_LW_V3.indb 130 06/06/16 07:38

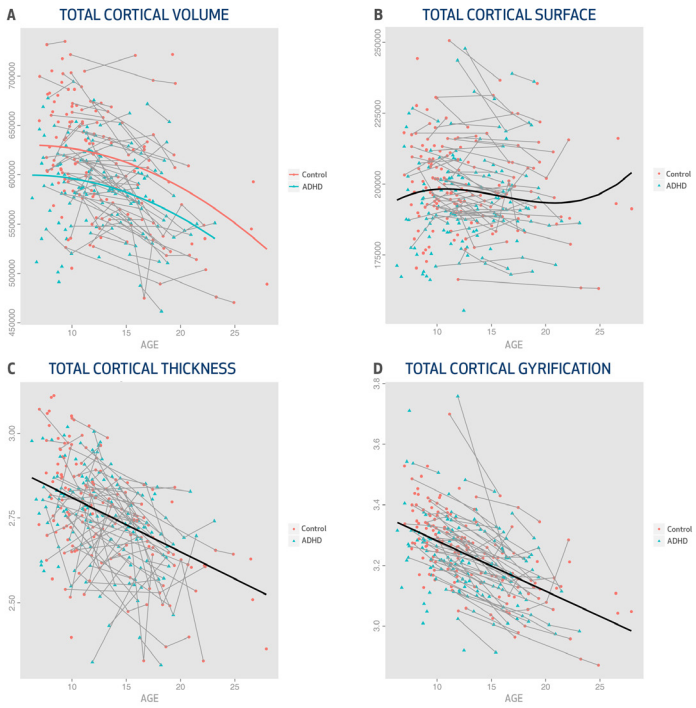

Figure 2 Developmental trajectories of total cortical volume (panel A, mm^3), surface area (panel B, mm^2), thickness (panel C, mm) and gyrification (panel D, dimensionless) Abbreviations: ADHD, Attention-Deficit/ Hyperactivity Disorder.

The analysis for each hemisphere separately showed that there was a reduction of cortical volume in the left hemisphere for ADHD, and a reduction cortical volume and surface area in the right hemisphere (Table S2).

Local differences in cortical volume, surface area, thickness and gyrification

Subjects with ADHD had reduced cortical volume in several areas throughout the cortex, predominantly in frontal lobes (caudal anterior cingulate and rostral middle frontal cortex of the left hemisphere, bilateral medial and lateral orbitofrontal cortex, bilateral precentral cortex, right superior frontal, caudal middle frontal and pars opercularis of the inferior frontal gyrus). There were no ADHD by age interaction effects on regional cortical volumes, indicating

thesis_LW_V3.indb 131 06/06/16 07:38

that the main effects of diagnosis were stable over development. Surface area and gyrification were also reduced in a number of areas. There were no differences in thickness in any cortical area. Table 2 and Figure 3 summarize these differences; parameters for developmental trajectories are provided in the Supplemental Material (Table S3).

Reductions in volumes were particularly pronounced in the caudal middle frontal and isthmus cingulate cortices of the right hemisphere, where volume reductions of more than 10% (>4 SD below the mean of the controls) were found. In many regions, the reduction of surface area occurred together with a reduction of cortical volume (left caudal anterior cingulate, rostral middle frontal and superior temporal cortices; right caudal middle frontal cortex, isthmus cingulate cortex, pars opercularis and lateral occipital cortex). In two regions with decreased cortical volume and surface area, we also found reduced gyrification (left rostral middle frontal cortex and right pars opercularis).

For nearly all areas there were no differences in the shape of developmental trajectories between the ADHD and control groups. As such, the reductions in cortical surface area and gyrification described above were stable over development. We found only two group by age

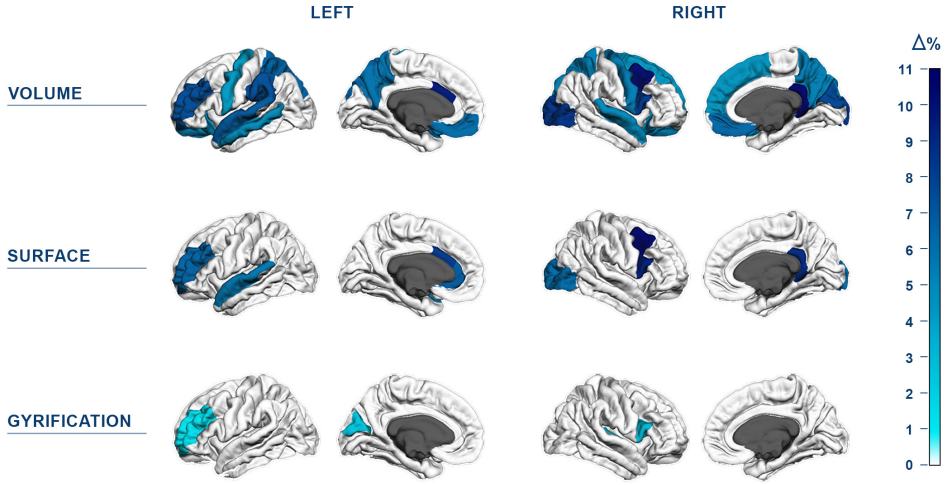

Figure 3 Group differences for regional measures. Note. The darker the color, the greater the reduction in Attention-Deficit/Hyperactivity Disorder compared to controls. References to color in this figure legend are provided in Table 3.

thesis_LW_V3.indb 132 06/06/16 07:38

interactions: for gyrification in the left cuneus and right pars opercularis. In these regions, the gyrification was reduced in the younger age ranges in ADHD, but declined less steeply in subjects with ADHD than controls, which led to convergence of the gyrification index at later age ranges (see: Supplemental Figure S3).

Subcortical areas

There were no differences between groups in the developmental trajectories of any subcortical areas, nor were there any main effects of diagnosis.

Discussion

In this study, we investigated brain development in a large sample of subjects with ADHD and matched, typically developing controls, using a combined cross-sectional and longitudinal design. We found reduced cortical volume in ADHD, predominantly in the frontal lobes, in line with previous studies (Castellanos et al., 2002; Wolosin et al. 2009; Durston et al., 2009a; Batty et al., 2010). More detailed examination of cortical markers suggested that the reductions in volume were primarily driven by a reduction in surface area, rather than thinning of the cortex, and that these differences persisted across development.

We found changes with development in cortical and subcortical areas for both controls and ADHD subjects, reflecting structural maturation of the brain. Furthermore, we found that developmental remodeling of the cortex relied on the unique developmental trajectories of its markers (surface area, thickness and gyrification), supporting earlier studies (Wierenga et al., 2014a; Raznahan et al., 2011) that they are driven, at least in part, by distinct regulatory processes (Panizzon et al., 2009; White et al., 2010).

Our data suggest that ADHD is primarily associated with developmentally stable changes in cortical markers. These changes appear to be particularly associated with less surface expansion, as evidenced by reductions in surface area, and less convolution, as evidenced by reductions in gyrification. This pattern of results particularly implicates the neurodevelopmental mechanisms that govern the tangential growth and sulcation of the cortex in ADHD.

The mature cortex is structurally (and functionally) organized into columns (Mountcastle,

thesis_LW_V3.indb 133 06/06/16 07:38

1997; Jones, 2000). According to the radial unit hypothesis (Rakic, 1995), cortical surface area is determined by the number of columns, which depends on the number of neural progenitors within the proliferative zones. The proliferation phase of brain development is governed by mechanisms that either promote the number of neurons that can migrate to target cortical areas (neurogenesis) or restrict it (cell death) (Rakic, 2000). Therefore, either lower production or excessive loss of cells during proliferation could lead to a lower degree of cortical expansion. Disorders of late neuronal proliferation have been associated with congenital anomalies such as primary mycrocephaly, characterized by small brain sizes with normal to thin cortex and simplified, but grossly conserved, gyral patterning (Barkovich et al., 2012). We speculate that a possible mechanism underlying the pattern reductions in surface area with normal cortical thickness in ADHD could be a minor perturbation of late neuronal proliferation, leading to a subtle but stable reduction of cortical surface area, with largely preserved cortical layering. Any reflection on the pathological mechanisms underlying such a hypothesized perturbation will be, of necessity, speculative. However, it is noteworthy that teratogenic substances targeting neuronal precursors, such as nicotine and alcohol (Banerjee et al., 2007; Linnet et al., 2003), and a number of genetic and molecular factors regulating neuronal proliferation and differentiation (e.g. DIRAS2 (Reif et al., 2011), CDH13 (Rivero et al., 2013; Poelmans et al., 2011), UPF3B (Jolly et al., 2013), BDNF (Shim et al., 2008) and other neurotrophins (Syed et al., 2007)), have been linked to ADHD.

Our results of localized decreases in cortical surface area and gyrification contrast with earlier findings of decreased cortical thickness (Sowell et al., 2003; Shaw et al., 2006; Narr et al., 2009) and smaller striatum volume in ADHD (Durston et al., 2009a; Nakao et al., 2011; Frodl & Skokauskas, 2012). Furthermore, we did not replicate longitudinal results from NIMH showing delays in the maturation of cortical thickness and surface area in their longitudinal ADHD sample (Shaw et al., 2007; Shaw et al., 2012). In the field, there is a call for replication in independent samples, particularly for longitudinal studies. As such, it is important that we do not replicate their findings, but rather report differing ones in this independent sample. It underscores that earlier results do not necessarily generalize to other samples of subjects with ADHD, but that differences between ADHD and controls may vary as a function of sample characteristics. Important differences

thesis_LW_V3.indb 134 06/06/16 07:38

between the NIMH sample and ours are in geographical location, average IQ and SES. The NIMH studies have typically matched groups for IQ and SES (e.g., Shaw et al., 2007), whereas we matched for SES only. Demographic differences within and between studies are increasingly being recognized as an important caveat in conducting and comparing neuroimaging studies in developmental disorders (Horga et al., 2014). Another factor contributing to these differences might be methodology; the NIMH studies investigated between-group differences in the mean age of the peak of their developmental models. We used a stringent statistical procedure to determine the best developmental model for our data, resulting in different models than those used in the NIMH sample. Furthermore, we investigated cortical markers per area, rather than per vertex, to preserve statistical power. In doing so, we may have missed small effects in highly localized cortical areas.

There are some limitations to our study. First, the majority of subjects with ADHD in our sample were using psychostimulants. There was insufficient power to statistically investigate the effects of medication on our results. Second, we were could not examine developmental trajectories in more homogeneous clinical subgroups based on gender, IQ, subtype or severity of the clinical presentation.

In conclusion, our findings show developmentally persistent reductions in cortical volume, surface area, and gyrification in our sample of subjects ADHD, particularly in frontal areas. These findings contrast with other studies in different samples and underline the importance of replication in independent samples, particularly for longitudinal data. Furthermore, they suggest that, at least for some children with ADHD, this disorder may be associated with an early (prenatal) disruption of cortical development leading to changes in surface area and gyrification that are stable across development.

thesis_LW_V3.indb 135 06/06/16 07:38

Supplementary information

MRI processing

The FreeSurfer v5.1.0 package [http://surfer.nmr.mgh.harvard.edu/fswiki] contains a fully automated structural imaging pipeline for the quantitative study of cortical and subcortical neuroanatomy. The cortical surface reconstruction pipeline is complex and consists of several stages for each individual scan. First, the scan is automatically placed in the Talaraich orientation, by registering it to a model brain in Talairach space (1) (Talaraich registration). Next, the intensity variations due to magnetic field inhomogeneities are corrected and a normalized intensity image is created (intensity normalization). The extra-cerebral voxels (skull and meningeal surfaces) are removed using a deformable template model, leaving only the brain and the overlying pial surface (skull stripping). Voxels are then classified as white matter or other tissues based on their intensity and their neighbour constraints (white matter segmentation). Based on the expected Talairach location of the corpus callosum and pons, sagittal and axial cutting planes are computed in order to separate the cerebral hemispheres from each other. This procedure also separates the cerebellum and brain stem from the cerebrum (cutting planes procedure). Any interior cavities inside the white matter volume are filled (ventricles, lacunes) to generate two solid masses of connected voxels, each representing the hemispheric subcortical mass (connected components procedure). These resulting volumes are then covered with a triangular tessellation (approximately 160.000 meshes), representing the surface topology of the corresponding volume (surface tessellation). To reduce metric distortions, this initial jagged surface is refined guided by the local MRI intensity gradients between the white and gray matter: the smoothed reconstructed surface is referred to as the white surface (surface refinement procedure). Next, for the pial surface reconstruction, the white surface is deformed, following a function that specifies the direction of movement of the tessellation towards the gray matter/CSF border (surface deformation) (2). In order to establish a surface-based coordinate system, the reconstructed cortical surface of each hemisphere is morphed (“inflated”) into a spherical surface (spherical transformation). This representation allows identification of the same point on the pial and the white surface of any participant using the same standard spherical coordinates systems (e.g., longitude and colatitude), which increases the accuracy of anatomical localization across scans (3). The distance between the white and pial surfaces at any point on the cortex gives the thickness of the cortical mantle at that location (4). In the final procedure, both geometric information derived from the cortical model and standard neuroanatomical conventions are integrated to automatically assign

thesis_LW_V3.indb 136 06/06/16 07:38

a probabilistic neuroanatomical label to each location on the cortical surface (cortical parcellation). Figure S1 summarizes the main FreeSurfer processing stages.

FreeSurfer performs two distinct parcellations, based on the Desikan-Killiany- and the Destrieux cortical atlases, which differ in the number and designation criteria of regions of interest (ROIs) (34 gyral-based and 74 surface-based areas per hemisphere respectively) (5,6). In the current study, we used the Desikan-Killiany ROIs, listed according to the lobes in Table S1 and depicted in Figure S2.

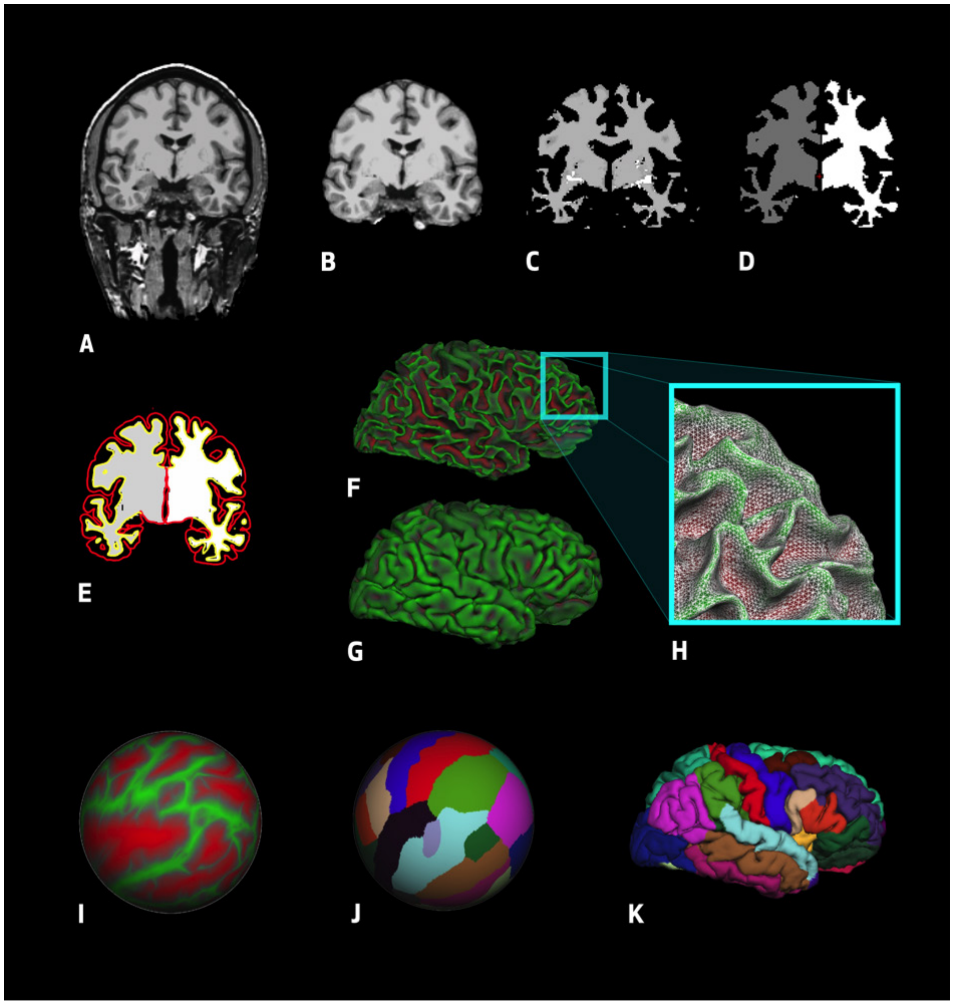

Figure S1. Main FreeSurfer processing stages

Note. A: T1 normalized volume; B: skull stripping; C: white matter segmentation; D: connected components; E yellow line and F: white surface; E red line and G: pial surface; H: surface tessellation I: spherical transformation; J, K: cortical parcellation (Desikan-Killiany atlas) [http://surfer.nmr.mgh.harvard.edu].

thesis_LW_V3.indb 137 06/06/16 07:38

Table S1 List of Desikan-Killiany regions for each lobe

Cerebral Lobes	
Frontal	caudal anterior cingulate, caudal middle frontal, frontal pole, lateral orbitofrontal, medial orbitofrontal, pars opercularis, pars orbitalis, pars triangularis, paracentral, precentral, rostral anterior cingulate, rostral middle frontal, superior frontal
Parietal	inferior parietal, isthmus cingulate, postcentral, precuneus, posterior cingulate, superior parietal, supramarginal
Temporal	banks of the superior temporal sulcus (banks sts), entorhinal, fusiform, inferior temporal, insula, middle temporal, parahippocampal, superior temporal, temporal pole, transverse temporal
Occipital	cuneus, lateral occipital, lingual, pericalcarine

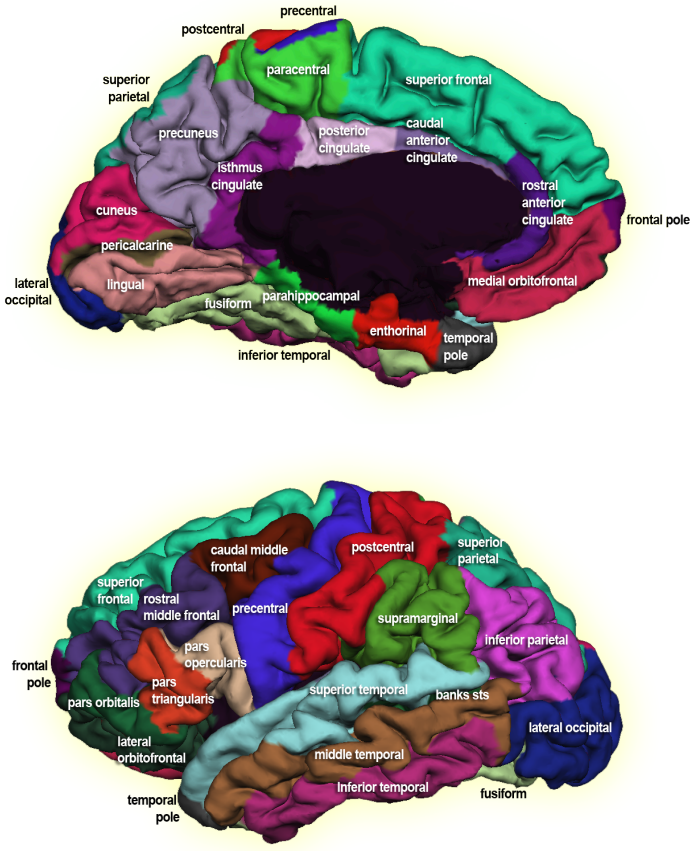

Figure S2 Desikan-Killiany atlas

thesis_LW_V3.indb 138 06/06/16 07:38

1. Talaraich J, Tournoux P. (1988): Co-planar Stereotaxic Atlas of the Human Brain: 3-dimensional Proportional System: An Approach To Cerebral Imaging. Thieme Medical Publishers, Stuttgart.

2. Dale AM, Fischl B, Sereno MI. (1999): Cortical surface-based analysis I. Segmentation and surface reconstruction. NeuroImage 9(2): 179-194.

3. Fischl B, Sereno MI, Dale AM. (1999): Cortical Surface-Based Analysis II: Inflation, Flattening, and a Surface-Based Coordinate System. NeuroImage 9(2): 195-207.

4. Fischl B, Dale AM. (2000): Measuring the Thickness of the Human Cerebral Cortex from Magnetic Resonance Images. Proc Natl Acad Sci U.S.A. 97 (20): 11050-11055.

5. Desikan RS, Segonne F, Fischl B, Quinn BT, Dickerson BC, Blacker D, et al. (2006): An automated labeling system for subdividing the human cerebral cortex on MRI scans into gyral based regions of interest. NeuroImage 31(3): 968-980.

6. Destrieux C, Fischl B, Dale A, Halgren E. (2010): Automatic parcellation of human cortical gyri and sulci using standard anatomical nomenclature. Neuroimage 15, 53(1): 1-15.

thesis_LW_V3.indb 139 06/06/16 07:38

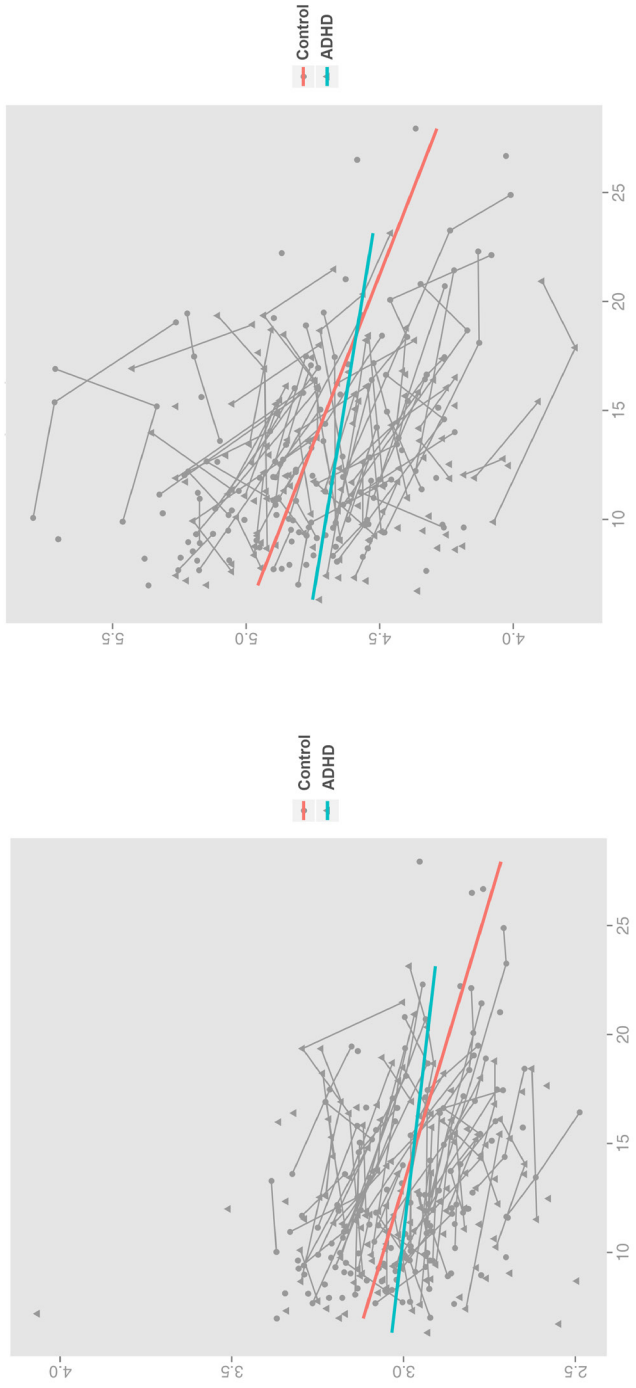

Figure S3 ADHD by age interaction effects on the developmental trajectories of cortical gyrification (panel A, left cuneus; panel B, right pars opercularis)

thesis_LW_V3.indb 140 06/06/16 07:38

thesis_LW_V3.indb 141 06/06/16 07:38

Table S2 Parameters for developmental trajectories of cerebral cortex markers, overall and per hemisphere

	Cortical parameter	Growth model	Intercept (s.e.)	Gender (s.e.)	Age (s.e.)	Age^2 (s.e.)	Age^3 (s.e.)	ADHD (s.e.)
Total	Volume	Quadratic	565660.46 (9692.59) **	53595.44 (9341.07) **	-3044.85 (507.49) **	-221.46 (88.33) **	9.73 (4.32) **	-30378.30(6845.15) **
	Surface	Cubic	174784.82 (3087.81) **	22948.58 (3296.46) **	-495.76 (167.21) **	-83.58 (40.32) **		
	Thickness	Linear	2.80 (.02) **	-.04 (.02)	-.02 (.00) **			
	Gyrification	Linear	3.16 (.02) **	.08 (.02) **	-.02 (.00) **		4.62 (2.23) **	
Left	Volume	Linear	279266.4 (4629.14) **	27914.02 (4649.35) **	-1990.65 (206.02) **			-13911.16(3406.79) **
	Surface	Linear	87014.38 (1465.24) **	11318.41 (1600.21) **	-149.57 (60.01) *			
	Thickness	Linear	2.80 (.02) **	-.04 (.02)	-.02 (.00) **			
	Gyrification	Linear	3.16 (.02) **	.07 (.02) **	-.02 (.00) **			
Right	Volume	Quadratic	282856.88 (4895.91) **	26968.03 (4709.06) **	-1408.72 (264.43) **	-115.17 (45.76) **		-15495.12(3451.47) **
	Surface	Cubic	89458.58 (1697.83) **	11268.54 (1658.71) **	-242.65 (87.19) **	-45.09 (20.83) **		
	Thickness	Linear	2.79 (.02) **	-.03 (.02)	-.02 (.00) **			-3438.28 (1216.87) **
	Gyrification	Quadratic	3.14 (.02) **	.09 (.02) **	-.02 (.00) **	.00 (.00) **		

Note. Cortical volume values in mm^3, surface values in mm^2, thickness values in mm, gyrification values dimensionless; *p < .05; **p < .01. Abbreviations: s.e., standard error; ADHD, Attention-Deficit/Hyperactivity Disorder

thesis_LW_V3.indb 142 06/06/16 07:38

thesis_LW_V3.indb 143

Table S3 Parameters for developmental trajectories of regional cortical measures in the left and right hemispheres

	Volume		Surface Area		Gyrification		
	Growth Model	ADHD (s.e.)	Growth Model	ADHD (s.e.)	Growth Model	ADHD (s.e.)	ADHD*Age (s.e.)
Left Hemisphere							
caudalanteriorcingulate	Quadratic	-247.755 (79.718)**	Linear	-59.018 (19.607)**	Linear		
cuneus	Linear		Linear		Linear		0.012 (.0029)**
lateralorbitofrontal	Linear	-469.482 (161.502)**	Linear		Linear		
medialorbitofrontal	Linear	-359.546 (12.486)**	Linear		Linear		
middletemporal	Quadratic	-74.055 (263.443)**	Linear		Linear		
precentral	Linear	-704.923 (244.695)**	Linear		Linear		
precuneus	Cubic	-723.306 (224.500)**	Linear		Linear		
rostralanteriorcingulate	Quadratic		Linear	-68.469 (23.769)**	Linear		
rostralmiddlefrontal	Quadratic	-1857.419 (38.178)**	Linear	-40.654 (12.725)**	Linear	-0.067 (.0215)*	
superiorparietal	Linear	-1228.321 (295.477)**	Cubic		Linear		
superiortemporal	Cubic	-1122.874 (255.754)**	Linear	-221.665 (64.526)**	Linear		
supramarginal	Cubic	-1172.661 (282.945)**	Cubic		Linear		
Right Hemisphere							
caudalmiddlefrontal	Linear	-921.245 (214.547)**	Linear	-252.481 (66.754)**	Linear		
cuneus	Linear	-279.887 (79.349)**	Linear		Linear		
isthmuscingulate	Linear	-342.842 (83.376)**	Linear	-88.771 (25.320)**	Quadratic		
lateraloccipital	Linear	-1192.241 (245.651)**	Linear	-356.887 (94.855)**	Cubic		
lateralorbitofrontal	Quadratic	-556.099 (165.271)**	Linear		Linear		
medialorbitofrontal	Linear	-366.866 (112.561)**	Linear		Linear		
parsopercularis	Linear	-476.22 (133.735)**	Linear	-155.221 (39.211)**	Linear		0.019 (.0061)**
precentral	Linear	-796.882 (235.315)**	Linear		Linear		
precuneus	Linear	-705.108 (247.449)**	Linear		Quadratic		
superiorfrontal	Quadratic	-1541.425 (437.092)**	Linear		Linear		
superiorparietal	Linear	-887.752 (299.179)**	Linear		Linear		
superiortemporal	Quadratic	-854.851 (248.854)**	Linear		Linear		
transversetemporal	Linear		Linear		Linear	-0.147 (.0504)**	

Note. Cortical volume values in mm^3; Cortical surface area values in mm^2; Cortical gyrification values dimensionless; *p < .05; **p < .01. Abbreviations: s.e., standard error; ADHD, Attention-Deficit/Hyperactivity Disorder

06/06/16 07:38

References

Valera EM, Faraone SV, Murray KE, & Seidman LJ (2007): Meta-analysis of structural imaging findings in attention-deficit/hyperactivity disorder. Biol Psychiatry 61:1361–1369.

Durston S, de Zeeuw P, Staal WG (2009): Imaging genetics in ADHD: a focus on cognitive control. Neurosci Biobehav Rev 33(5):674–689.

Nakao T, Radua J, Rubia K, Mataix-Cols D (2011): Gray matter volume abnormalities in ADHD: voxel-based meta-analysis exploring the effects of age and stimulant medication. Am J Psychiatry 168(11):1154–1163.

Frodl T, Skokauskas N (2012): Meta-analysis of structural MRI studies in children and adults with attention deficit hyperactivity disorder indicates treatment effects. Acta Psych Scand 125:114–126.

Rakic P (1995): A small step for the cell, a giant leap for mankind: a hypothesis of neocortical expansion during evolution. Trends Neurosci 18:383–388.

Rakic P (2000): Radial unit hypothesis of neocortical expansion. Novartis Found Symp 228:30–42; discussion 42–52.

Shaw P, Lerch J, Greenstein D, Sharp W, Clasen L, Evans A, et al. (2006): Longitudinal mapping of cortical thickness and clinical outcome in children and adolescents with attention-deficit/hyperactivity disorder. Arch Gen Psychiatry 63:540–549.

Sowell ER, Thompson PM, Welcome SE, Henkenius AL, Toga AW, Peterson BS (2003): Cortical abnormalities in children and adolescents with attention-deficit hyperactivity disorder. Lancet 362:1699–1707.

Narr KL, Woods RP, Lin J, Kim J, Phillips OR, Del'Homme M, et al. (2009): Widespread cortical thinning is a robust anatomical marker for attention-deficit/hyperactivity disorder. J Am Acad Child Adolesc Psychiatry 48:1014–1022.

Batty MJ, Liddle EB, Pitiot A, Toro R, Groom MJ, Scerif G, et al. (2010): Cortical gray matter in attention-deficit/hyperactivity disorder: a structural magnetic resonance imaging study. J Am Acad Child Adolesc Psychiatry 49(3):229–238.

de Zeeuw P, Schnack HG, Van Belle J, Weusten J, Van Dijk S, Langen M, et al. (2012): Differential brain development with low and high IQ in Attention-Deficit/Hyperactivity Disorder. PLoS One

thesis_LW_V3.indb 144 06/06/16 07:38

7:e35770.

Wolosin SM, Richardson ME, Hennessey JG, Denckla MB, Mostofsky SH (2009): Abnormal cerebral cortex structure in children with ADHD. Hum Brain Mapp 30(1):175–184.

Shaw P, Malek M, Watson B, Sharp W, Evans A, Greenstein D (2012): Development of cortical surface area and gyrification in attention-deficit/hyperactivity disorder. Biol Psychiatry 1;72(3):191–197.

Li X, Jiang J, Zhu W, Yu C, Sui M, Wang Y, Jiang T (2007): Asymmetry of prefrontal cortical convolution complexity in males with attention-deficit/ hyperactivity disorder using fractal information dimension. Brain Dev 29:649–655.

Shaw P, Eckstrand K, Sharp W, Blumenthal J, Lerch JP, Greenstein D, et al. (2007): Attention-deficit/hyperactivity disorder is characterized by a delay in cortical maturation. Proc Natl Acad Sci U S A 4;104(49):19649–19654.

Castellanos FX, Lee PP, Sharp W, Jeffries NO, Greenstein DK, Clasen LS, et al. (2002): Developmental trajectories of brain volume abnormalities in children and adolescents with attention-deficit/ hyperactivity disorder. JAMA 288(14):1740–1748.

Horga G, Kaur T, Peterson BS (2014): Annual Research Review: Current limitations and future directions in MR studies of child- and adult-onset developmental psychopathologies. J Child Psychol Psychiatry 55:659–680.

Frazier TW, Demaree HA, Youngstrom EA (2004): Meta-analysis of intellectual and neuropsychological test performance in attention-deficit/hyperactivity disorder. Neuropsychology 18(3):543–555.

Dennis M, Francis DJ, Cirino PT, Schachar R, Barnes MA, Fletcher JM (2009): Why IQ is not a covariate in cognitive studies of neurodevelopmental disorders. J Int Neuropsychol Soc 15(3):331–343.

Shaffer D, Fisher P, Lucas CP, Dulcan MK, Schwab-Stone ME (2000): NIMH Diagnostic Interview Schedule for Children Version IV (NIMH DISC-IV): description, differences from previous versions, and reliability of some common diagnoses. J Am Acad Child Adolesc Psychiatry 39(1):28–38.

Verhulst F, Van Der Ende J, Koot H (1996): Handleiding voor de CBCL/4-18 (Manual for the CBCL/4-18). Rotterdam: Department of Child and Adolescent Psychiatry, Erasmus Academic Medical Center.

thesis_LW_V3.indb 145 06/06/16 07:38

Verhulst F, Van Der Ende J, Koot H (1997): Handleiding voor de Teacher's Report Form (TRF) (Manual for the Teacher Report Form (TRF)). Rotterdam: Department of Child and Adolescent Psychiatry, Erasmus Academic Medical Center.

Wechsler D (2005): Wechsler Intelligence Scale for Children – Derde Editie NL. Handleiding en Verantwoording. (Wechsler Intelligence Scale for Children – Third Edition, Dutch Version, Manual). London: Harcourt Assessment.

Durston S, Nederveen H, van Dijk S, van Belle J, de Zeeuw P, Langen M, van Dijk A (2009): Magnetic resonance simulation is effective in reducing anxiety related to magnetic resonance scanning in children. J Am Acad Child Adolesc Psychiatry 48(2):206–207.

Thoemmes F (2012): Propensity score matching in SPSS. arXiv:1201.6385.

Austin PC (2011): Optimal caliper widths for propensity-score matching when estimating differences in means and differences in proportions in observational studies. Pharm Stat 10(2):150–161.

Fischl B (2012): FreeSurfer. Neuroimage 15;62(2):774–781.

Fischl B, Salat DH, Busa E, Albert M, Dieterich M, Haselgrove C, et al. (2002): Whole brain segmentation: automated labeling of neuroanatomical structures in the human brain. Neuron 33(3):341–355.

Fischl B, Dale AM (2000): Measuring the thickness of the human cerebral cortex from magnetic resonance images. Proc Natl Acad Sci U S A 97(20):11050–11055.

Dale AM, Fischl B, Sereno MI (1999): Cortical surface-based analysis I. Segmentation and surface reconstruction. NeuroImage 9(2):179–194.

Fischl B, Sereno MI, Dale AM (1999): Cortical surface-based analysis ii: inflation, flattening, and a surface-based coordinate system. NeuroImage 9(2):195–207.

Fischl B, Salat DH, van der Kouwe AJW, Makris N, Ségonne F, Quinn BT, Dale AM (2004): Sequence-independent segmentation of magnetic resonance images. NeuroImage 23 (Suppl 1):S69–S84.

Fischl B, van der Kouwe A, Destrieux C, Halgren E, Ségonne F, Salat DH, et al. (2004): Automatically parcellating the human cerebral cortex. Cereb Cortex 14(1):11–22.

Talaraich J, Tournoux P (1988): Co-planar stereotaxic atlas of the human brain: 3-dimensional proportional system: an approach to cerebral imaging. Stuttgart: Thieme Medical Publishers.

thesis_LW_V3.indb 146 06/06/16 07:38

Desikan RS, Segonne F, Fischl B, Quinn BT, Dickerson BC, Blacker D, et al. (2006): An automated labeling system for subdividing the human cerebral cortex on MRI scans into gyral based regions of interest. NeuroImage 31(3):968–980.

Destrieux C, Fischl B, Dale A, Halgren E (2010): Automatic parcellation of human cortical gyri and sulci using standard anatomical nomenclature. Neuroimage 15;53(1):1–15.

Dewey J, Hana G, Russell T, Price J, McCaffrey D, Harezlak, J, et al. (2010): Reliability and validity of MRI-based automated volumetry software relative to auto-assisted manual measurement of subcortical structures in HIV-infected patients from a multisite study. Neuroimage 15;51(4):1334–1344.

Schaer M, Cuadra MB, Tamarit L, Lazeyras F, Eliez S, Thiran JP (2008): A surface-based approach to quantify local cortical gyrification. IEEE Trans Med Imaging 27(2):161–170.

Bates D, Maechler M, Bolker B (2011): Lme4: Linear Mixed-Effects Models using S4 Classes. R Package Version 0.999375-39.

Wierenga LM, Langen M, Oranje B, Durston S (2014): Unique developmental trajectories of cortical thickness and surface area. Neuroimage 15;87:120–126.

Wierenga L, Langen M, Ambrosino S, van Dijk S, Oranje B, Durston S (2014): Typical development of basal ganglia, hippocampus, amygdala and cerebellum from age 7 to 24. Neuroimage 1;96:67–72.

Kass RE, Raftery AE (1995): Bayes Factors. J Am Statist Assoc 90(430):773–795.

Raznahan A, Shaw P, Lalonde F, Stockman M, Wallace GL, Greenstein D, et al. (2011): How does your cortex grow? J Neurosci 11;31(19):7174–7177.

Panizzon MS, Fennema-Notestine C, Eyler LT, Jernigan TL, Prom-Wormley E, Neale M, et al. (2009): Distinct genetic influences on cortical surface area and cortical thickness. Cereb Cortex 19(11):2728–2735.

White T, Su S, Schmidt M, Kao CY, Sapiro G (2010): The development of gyrification in childhood and adolescence. Brain & Cognition 72(1):36–45.

Mountcastle VB (1997): The columnar organization of the neocortex. Brain 120(Pt 4):701–722.

Jones EG (2000): Microcolumns in the cerebral cortex. Proc Natl Acad Sci U S A 9;97(10):5019–5021.

thesis_LW_V3.indb 147 06/06/16 07:38

Barkovich AJ, Guerrini R, Kuzniecky RI, Jackson GD, Dobyns WB (2012): A developmental and genetic classification for malformations of cortical development: update 2012. Brain 135(Pt 5):1348–1369.

Banerjee TD, Middleton F, Faraone SV (2007): Environmental risk factors for attention-deficit hyperactivity disorder. Acta Paediatr 96(9):1269–1274.

Linnet KM, Dalsgaard S, Obel C, Wisborg K, Henriksen TB, Rodriguez A, et al. (2003): Maternal lifestyle factors in pregnancy risk of attention deficit hyperactivity disorder and associated behaviors: review of the current evidence. Am J Psychiatry 160(6):1028–1040.

Reif A, Nguyen TT, Weissflog L, Jacob CP, Romanos M, Renner TJ, et al. (2011): DIRAS2 is associated with adult ADHD, related traits, and co-morbid disorders. Neuropsychopharmacology. 36(11):2318–2327.

Rivero O, Sich S, Popp S, Schmitt A, Franke B, Lesch KP (2013): Impact of the ADHD-susceptibility gene CDH13 on development and function of brain networks. Eur Neuropsychopharmacol 23(6):492–507.

Poelmans G, Pauls DL, Buitelaar JK, Franke B (2011): Integrated genome-wide association study findings: identification of a neurodevelopmental network for attention deficit hyperactivity disorder. Am J Psychiatry 168(4):365–377.

Jolly LA, Homan CC, Jacob R, Barry S, Gecz J (2013): The UPF3B gene, implicated in intellectual disability, autism, ADHD and childhood onset schizophrenia regulates neural progenitor cell behaviour and neuronal outgrowth. Hum Mol Genet 1;22(23):4673–4687.

Shim SH, Hwangbo Y, Kwon YJ, Jeong HY, Lee BH, Lee HJ, Kim YK (2008): Increased levels of plasma brain-derived neurotrophic factor (BDNF) in children with attention deficit-hyperactivity disorder (ADHD). Prog Neuropsychopharmacol Biol Psychiatry 12;32(8):1824–1828.

Syed Z, Dudbridge F, Kent L (2007): An investigation of the neurotrophic factor genes GDNF, NGF, and NT3 in susceptibility to ADHD. Am J Med Genet B Neuropsychiatr Genet Part B 144B:375–378.

thesis_LW_V3.indb 148 06/06/16 07:38

thesis_LW_V3.indb 149 06/06/16 07:38

BRAIN DEVELOPMENT IN ADOLESCENTS AT ULTRA-HIGH RISK FOR PSYCHOSIS: LONGITUDINAL CHANGES RELATED TO RESILIENCE

Lara M Wierenga*
Sanne de Wit*
Bob Oranje
Tim B Ziermans
Patricia F Schothors
Herman van Engeland
René S Kahn
Sarah Durston

*Both authors contributed equally to the manuscript

NeuroImage Clinical; in press

thesis_LW_V3.indb 151 06/06/16 07:38

Abstract

The main focus of studies of individuals at ultra-high risk for psychosis (UHR) has been identifying brain changes in those individuals who will develop psychosis. However, longitudinal studies showed that up to half of UHR individuals are resilient, with symptomatic remission and good functioning at follow-up. Yet little is known about brain development in resilient individuals. Therefore, the aim of this study was to investigate differences in brain development between resilient and non-resilient individuals. A six-year longitudinal structural MRI study was performed with up to three scans per individual. The final sample consisted of 48 UHR individuals and 48 typically developing controls with a total of 225 MRI-scans, aged 12-20 years at the time of the first MRI-scan and matched for age, gender and number of follow-up scans. At six-year follow-up, 35 UHR individuals were divided in resilient and non-resilient subgroups. We operationalized resilience in two ways as either good functioning or complete remission from UHR criteria at six-year follow-up. The main outcome measures were developmental changes in MR-based measures of cortical and subcortical anatomy. We found widespread differences in volume of frontal, temporal and parietal cortex between resilient and non-resilient individuals. These were already present at baseline and remained stable over development (12-24 years). Furthermore, there were differences in the development of cortical surface area in frontal regions including cingulate gyrus. Developmental differences may reflect compensatory neural mechanisms, where better functioning in resilient individuals leads to less tissue loss over development.

thesis_LW_V3.indb 152 06/06/16 07:38

Introduction

Traditionally, studies of individuals at ultra-high risk (UHR) for psychosis have attempted to identify neurobiological markers to predict which UHR individuals will develop psychosis (i.e. undergo a 'transition to psychosis'). Thus, the field has focused on identifying differences in the brains of those subjects who will worsen over time compared to those who will not. However, transition rates have plummeted since the earliest reports of rates of over 50% (Miller et al. 2002) to an average of 29% in more recent reports (Fusar-Poli et al. 2012a). At the same time, there has been a steady increase in the remission rates reported, of up to 54% (Simon et al. 2011). A recent meta-analysis of eight longitudinal studies (Simon et al. 2013) reported that 73% of 773 UHR subjects did not develop psychosis over a 2-year follow-up and 46% fully remitted from their baseline symptoms. We conducted a longer follow-up, with a mean of six years, and found that 41% of adolescents at UHR fully remitted from their at-risk state (de Wit et al. 2014). Therefore, it is at least as relevant to investigate neurobiological changes in UHR subjects who show resilience and go on to function well, as it is to investigate those who undergo a transition to psychosis.

In addition, the criterion of 'transition to psychosis' has been criticized as a measure to identify which individuals will have a truly poor clinical outcome: the threshold for transition is essentially arbitrary and is based entirely on positive symptoms (Fusar-Poli et al. 2013; Ziermans et al. 2014). There is increasing evidence that negative symptoms and the level of cognitive and social functioning are equally important for the long-term outcome of UHR individuals (Fusar-Poli & Borgwardt 2007; Carrión et al. 2013; Fusar-Poli et al. 2013).

Taken together, decreasing transition rates, high percentages of remitters and the criticism of 'transition to psychosis' as an outcome measure underscore the importance of studying remission as well as other, more comprehensive, measures of outcome. Therefore, in this study we focus on resilience, instead of transition to psychosis, and operationalize resilience as level of functioning. In addition, we conducted a second more traditional operationalization of resilience as the remission of positive symptoms.

Compared to typically developing controls UHR individuals showed reduced grey matter volume in the frontal and temporal lobes, anterior cingulate gyrus and hippocampal regions (Fusar-Poli et al. 2011; Wood et al. 2013; Bois et al. 2014). However, most imaging

thesis_LW_V3.indb 153 06/06/16 07:38

studies on UHR individuals have been cross-sectional study designs and were therefore limited in their ability to show developmental differences between UHR individuals with good and poor outcomes. The few longitudinal studies that have been conducted were only partially successful in predicting transition to psychosis and have reported many inconsistent findings (for review, see Wood et al. 2013). This may in part be related to limited follow-up times and differences in the methods used (Wood et al. 2013), but is likely also related to the diverse clinical outcomes of UHR individuals and the relatively arbitrary criterion of transition to psychosis (de Wit et al. 2014).

We investigated brain development in resilient versus non-resilient UHR individuals over a six year period. We conducted a comprehensive assessment of symptoms and functioning and examined brain development, with MRI scans at three different time points. This is the first study with a long follow-up and more than two MRI scans per individual. This is a promising assessment of outcome and permits non-linear modeling of developmental trajectories.

Materials and methods

Participants

All data were collected at the Department of Psychiatry at the University Medical Center Utrecht, Brain Center Rudolf Magnus in the Netherlands. Participants were between 12 and 18 years of age at the time of recruitment and were included after written informed consent. The study was approved by the Dutch Central Committee on Research Involving Human Subjects.

Recruitment details have been described previously (Sprong et al. 2008; Ziermans et al. 2011). Briefly, adolescents at UHR were referred by general practitioners or other psychiatry clinics. For inclusion at baseline, subjects in the UHR group had to fulfill at least one of the following criteria: 1) attenuated positive symptoms, 2) brief, limited, or intermittent psychotic symptoms, 3) genetic risk for psychosis combined with a deterioration in overall level of social, occupational/school, and psychological functioning in the past year or 4) two or more of nine basic symptoms of mild cognitive disturbances. The first three inclusion criteria were assessed using the Structured Interview for Prodromal Syndromes

thesis_LW_V3.indb 154 06/06/16 07:38

Table 1 Demographic data for typically developing controls (TDC) and UHR individuals

	TDC	UHR	UHR vs. TDC
Number of individuals, n (males)	48 (29)	48 (29)	n.s.
Hand preference, n, right/non-right	40/8	44/4	n.s.
Parental education, years, mean (SD)			
Mother	13.45 (2.39)	12.96 (2.16)	n.s.
Father	14.22 (2.17)	13.74 (2.18)	n.s.
Premorbid IQ, mean (SD)	107.04 (13.12)	100.40 (11.97)	t = 2.85, p = 0.01
Age at baseline scan, years			
Mean (SD)	15.72 (1.54)	15.43 (2.11)	n.s.
Range	12.19-18.76	12.28-19.64	
Age at 6-year FU scan, years			
Mean (SD)	21.40 (1.57)	21.16 (2.42)	n.s.
Range	17.57-24.54	16.84-25.79	
Intra Cranial Volume (mm^3)	1621000 (148220)	1586000 (167740)	n.s.
Number of scans, n			n.a.
Total number of scans, n	103	122	
1	48	48	
2	24	39	
3	31	35	

Notes: TDC = typically developing controls; UHR = Individuals at ultra-high risk for psychosis; IQ = intelligence quotient; SD = standard deviation; FU = follow-up

(McGlashan et al. 2001) and the Family Interview for Genetic Studies (Maxwell 1982). The fourth inclusion criterion was assessed using the Bonn Scale for the Assessment of Basic Symptoms-Prediction List (Schultze-Lutter & Klosterkötter 2002). Exclusion criteria consisted of a past or present psychotic episode lasting more than one week, traumatic brain injury or any known neurological disorder, and verbal intellectual IQ < 75. The control group consisted of typically developing adolescents recruited through secondary schools in the region of Utrecht. They were excluded if they met one of the UHR-criteria, if they or any first degree relative had a history of a psychiatric illness, or if they had a second-degree relative with a psychotic disorder.

At baseline 64 UHR individuals and 62 typically developing controls completed the clinical assessment and an MRI scan. These groups were then matched for gender, age,

thesis_LW_V3.indb 155 06/06/16 07:38

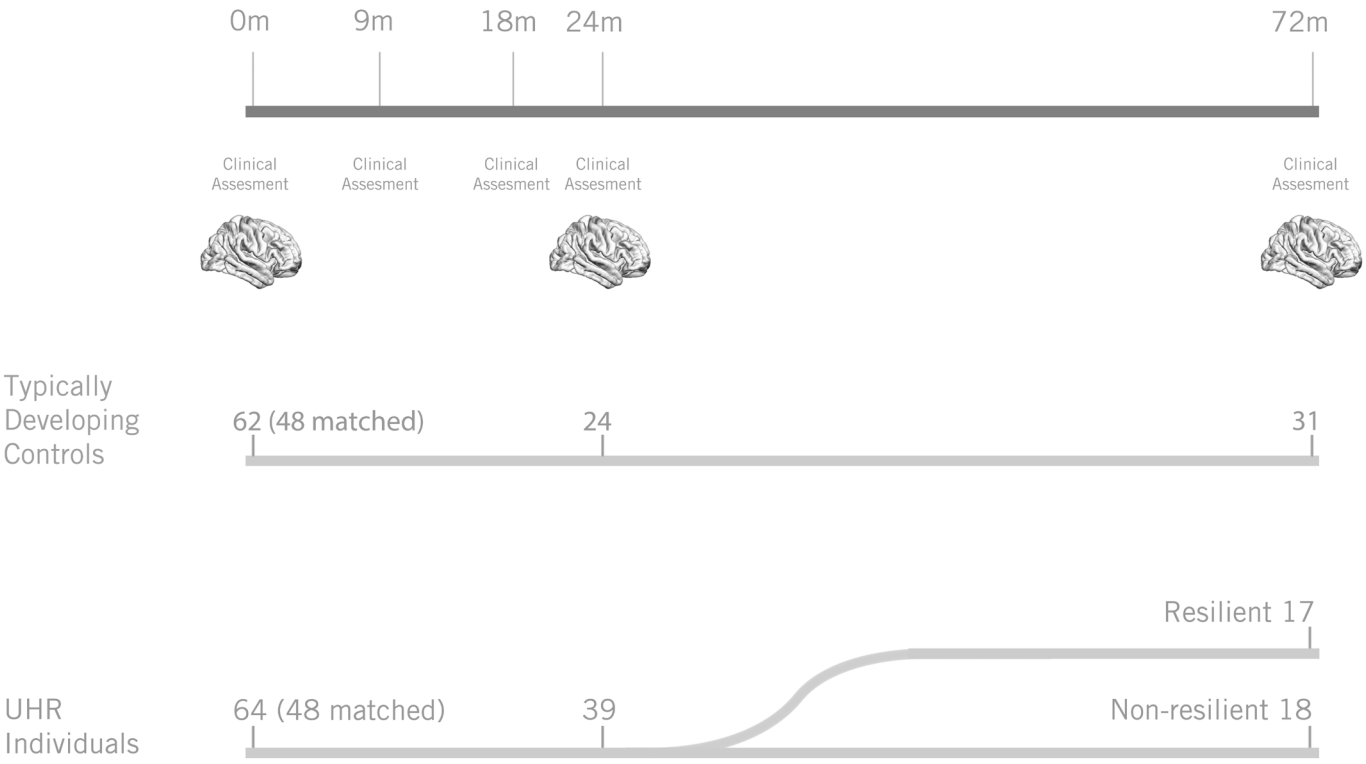

Figure 1 Timeline of the study. Clinical assessments were collected at baseline, 9 months, 18 months, 24 months and 72 months post baseline. MRI scans were assessed at baseline, 24 months and 72 months post baseline. 62 typically developing individuals and 64 UHR individuals were included at baseline, 48 matched pairs were included for further analysis. 24 controls and 39 UHR individuals had at least one follow up scan. Furthermore, 17 individuals met criteria for resilience of good functional outcome in our primary analysis. *16 individuals showed complete remission of UHR criteria and were included in our secondary analysis.

thesis_LW_V3.indb 156

06/06/16 07:38

and number of follow-up scans, resulting in a longitudinal dataset of 48 UHR individuals and 48 typically developing controls that had one, two or three scans, adding up to a total of 225 MRI scans. Participants were aged between 12,2 and 19,6 years at the time of the first MRI scan (Table 1). Follow-up assessments were conducted 9 months, 18 months, 2 years, and 6 years post baseline (range 3,5-8,0 years). The follow-ups at 9 and 18 months included clinical assessments only. For an overview, see Figure 1. We split the UHR group into two groups based on the 6-year follow-up data: 'resilient' and 'non-resilient' subgroups. Resilience was defined in one of two ways and identical analyses were run for each subgrouping. First, resilience was defined by functional outcome using the modified Global Assessment of Functioning (mGAF) scale (Hall 1995). Here, poor functional outcome (non-resilient) was defined as an mGAF score of < 65 and good functional outcome (resilient) as an mGAF score of ≥ 65. The cut off of 65 has been used before (Allen et al. 2014) as the 60–70 range corresponds to 'generally good function with meaningful interpersonal relationships, and some persistent mild symptoms and/or some persistent difficulty in social, occupational, or school functioning' (Hall 1995). A score below 60 indicates 'moderate to severe symptoms and/or moderate to severe difficulty in social, work, or school functioning,' while scores above 70 correspond to 'some transient mild symptoms to absent or minimal symptoms and/or slight to no impairment in social, work, or school functioning'. The second method to define resilient subgroups was determined by complete remission from UHR criteria, as defined by McGlashan and colleagues (McGlashan et al. 2001). Individuals who had converted to psychosis and individuals who still met UHR criteria were classified as non-resilient individuals, whereas those individuals who no longer met UHR criteria and had never experienced psychosis were classified as resilient. Details of both subgroupings can be found in supplemental information S1.

Image acquisition and processing
Acquisition

MRI scans were acquired on a single 1.5-T scanner (Philips, Best, The Netherlands). Whole brain T1-weighted three-dimensional fast field echo scans were made with 1.5-mm contiguous coronal slices of the whole head (256×256 matrix, FoV = 256 mm, echo time (TE) = 4.6 ms, repetition time (TR) = 30 ms, flip angle = 30°).

thesis_LW_V3.indb 157 06/06/16 07:38

Image Processing

Scans were processed and analyzed using FreeSurfer v 5.1.0 software. Technical details of the automated reconstruction scheme of this well-validated software program are described elsewhere. (Dale et al. 1999; Fischl et al. 1999; Carmona et al. 2009) We calculated average volume (mm^3), cortical thickness (mm), surface area (mm^2), and gyrification for the 34 cortical structures in each hemisphere from the Desikan-Killiany atlas (Desikan et al. 2006), as well as cortical thickness and surface area for each lobe and the whole brain, and total gray and white matter volume per hemisphere and the whole brain. Gyrification could not be estimated for 7 scans, because of FreeSurfer processing errors. We also measured the volume of subcortical structures, as well as subcortical gray matter volume and gray and white matter separately for the cerebellum. In order to reduce within-subject variability between scan sessions, the longitudinal analysis processing pipeline of FreeSurfer was used for subjects with more than one scan (Reuter & Fischl 2011). Manual edits were performed as necessary by a rater blind to subject identity and group membership.

Statistical analyses

The lme package in the statistical software package R version 2.14.0 was used (1) to test for between-group differences in the demographic and clinical data and (2) to investigate the effects of age, group and their interaction on brain measures using a linear mixed model. We used a top down selection procedure to test for the best-fit growth model. Two effects were of particularly interest: (1) main effects of group, where differences between groups were present at first assessment and stable over developmental time (range 12-24 years), and (2) group*age interaction effects where the developmental trajectories differed between the groups. Details of the model and selection procedure are provided in supplemental information S2.

Results

Between-group differences in demographic and clinical characteristics

Demographic and clinical characteristics of typically developing controls and UHR individuals are provided in Table 1. Both groups were matched for age, gender and number of scans. Hand preference and intracranial volume did not differ between groups, but IQ

thesis_LW_V3.indb 158 06/06/16 07:38

was lower for UHR individuals than for typically developing controls.

Demographic details of subgroups defined by both operationalisations of resilience are given in Table 2. There was substantial overlap between the two operationalisations: of 17 individuals classified as resilient based on functional outcome, 12 were also classified as resilient based on UHR remission criteria. Of the 16 individuals classified as resilient based on remission, 12 were also classified as resilient based on functional outcome (Table 2). Of the five individuals classified as resilient based on functional outcome but not remission, two had had a psychosis and later remitted with high mGAF scores at 6-year follow-up. The other three still scored in the UHR range for positive symptoms, but reported good functioning (mGAF scores between 70 and 80) at 6-year follow-up. There were no statistical differences in the demographic variables between the two operationalisations of resilience

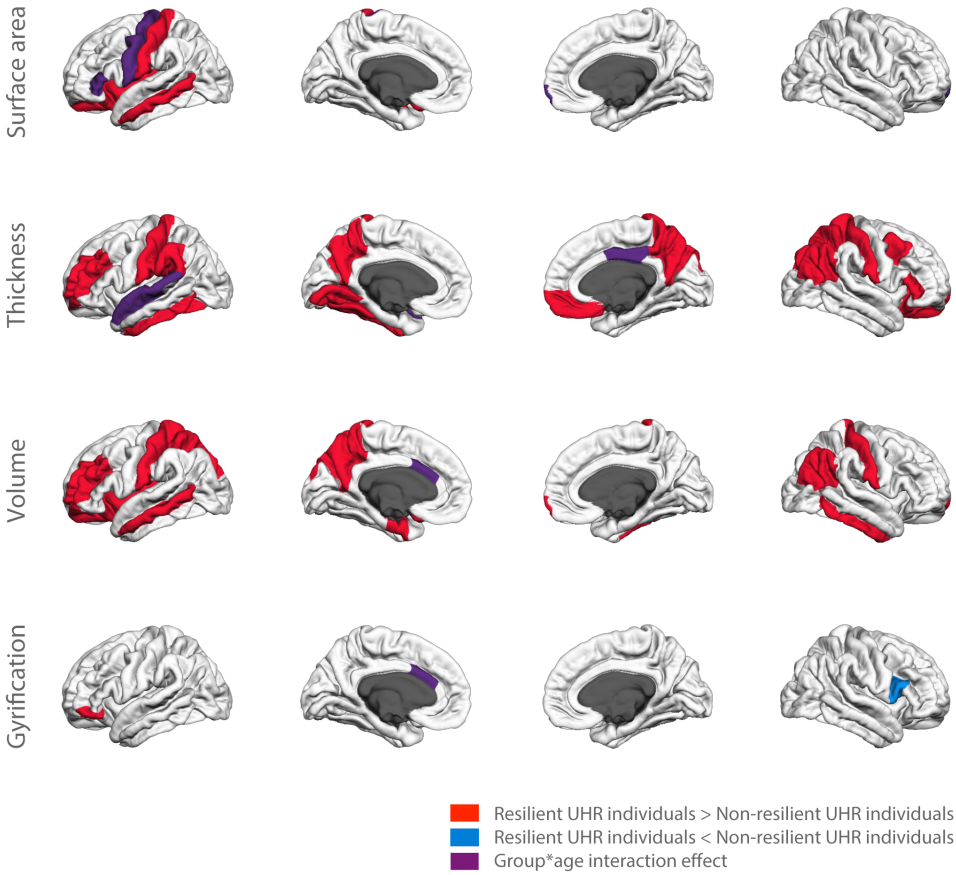

Figure 2 Differences in cortical morphology between resilient and non-resilient UHR individuals

thesis_LW_V3.indb 159 06/06/16 07:38

Table 2 Demographic and clinical data of resilient and non-resilient UHR individuals, based on (1) functional outcome and (2) UHR remission criteria[a]

	(1) Good functional outcome vs. Poor functional outcome			(2) Remission (R) vs. Non-remission (NON-R)		
	good outcome	poor outcome	good vs. poor	R	NON-R	R vs. NON-R
Number of individuals, n (males)	17 (13)	18 (10)	*n.s.*	16 (10)	19 (13)	*n.s.*
Resilient based on remission (n)	12	4		n.a.	n.a.	
Non-resilient based on remission (n)	5	14		n.a.	n.a.	
Resilient based on FO (n)	n.a.	n.a.		12	5	
Non-resilient based on FO (n)	n.a.	n.a.		4	14	
Premorbid IQ, mean (SD)	101.18 (12.89)	103.22 (10.28)	*n.s.*	101.40 (11.78)	102.90 (11.53)	*n.s.*
Age at baseline, years						
Mean (SD)	15.42 (2.20)	15.54 (2.48)	*n.s.*	14.65 (2.00)	16.18 (2.37)	*t = 2.07, p = 0.05*
Range	12.31 - 19.64	12.28 - 19.43		12.28 - 19.32	12.42 - 19.64	
Age at 6-year FU, years						
Mean (SD)	21.34 (2.58)	20.99 (2.32)	*n.s.*	19.99 (2.41)	21.96 (2.27)	*t = 2.29, p = 0.03*
Range	17.88 - 25.79	16.84-24.80		16.84-25.28	17.42 - 25.79	
SIPS/SOPS baseline, mean (SD)						
Total score	21.35 (10.74)	25.06 (11.47)	*n.s.*	21.31 (10.58)	24.89 (11.56)	*n.s.*
Positive symptoms	7.41 (4.53)	8.50 (3.13)	*n.s.*	6.56 (4.39)	9.16 (2.95)	*U = 89.0, p = 0.037*
Negative symptoms	4.24 (4.66)	4.17 (3.67)	*n.s.*	3.62 (3.52)	4.68 (4.59)	*n.s.*
Disorganized symptoms	3.41 (3.30)	5.89 (2.83)	*U = 68.0, p = 0.004*	4.50 (3.65)	4.84 (3.00)	*n.s.*
General symptoms	6.29 (4.33)	6.50 (4.51)	*n.s.*	6.62 (4.77)	6.21 (4.10)	*n.s.*
mGAF baseline, mean (SD)	57.06 (13.57)	56.83 (17.44)	*n.s.*	54.81 (12.15)	58.74 (17.90)	*n.s.*
SIPS/SOPS 6-year FU, mean (SD)						
Total score	11.75 (8.36)	35.11 (14.11)	*U = 20.5, p = <0.001*	13.13 (9.65)	33.89 (15.35)	*U = 38.5, p = <0.001*
Positive symptoms	3.88 (3.59)	10.00 (5.54)	*U = 45.5, p = <0.001*	2.44 (2.37)	11.28 (4.11)	*U = 3.5, p = <0.001*
Negative symptoms	3.88 (3.72)	11.17 (5.79)	*U = 44.0, p = <0.001*	5.69 (4.85)	9.56 (6.64)	*n.s.*
Disorganized symptoms	3.19 (2.74)	7.22 (3.37)	*t = 3.80, p = 0.001*	3.44 (2.90)	7.00 (3.52)	*U = 60.5, p = 0.003*
General symptoms	1.50 (1.59)	6.72 (4.86)	*U = 42.0, p = <0.001*	1.56 (1.59)	6.67 (4.92)	*U = 47.0, p = 0.001*
mGAF 6-year FU, mean (SD)	77.94 (7.30)	47.50 (9.94)	*t = -10.27, p = <0.001*	71.87 (14.13)	54.21 (16.55)	*U = 60.0, p = 0.002*
Psychotropic medication baseline, any			*n.s.*			*n.s.*
No	9	9		7	11	
Yes	8	9		9	8	
Psychotropic medication 6-year FU, any			*n.s.*			*n.s.*
No	13	11		11	13	
Yes	4	7		5	6	

Notes: [a] Subgroups are based on outcome at 6-year FU; outcome was unknown for 13 UHR individuals TDC = typically developing controls; UHR = Individuals at ultra-high risk for psychosis; R = remitter; NON-R = non-remitters; FO = functional outcome; IQ = intelligence quotient; SD = standard deviation; FU = follow-up; SIPS/SOPS = Structured Interview for Prodromal Symptoms / Scale of Prodromal Symptoms; mGAF = Modified Global Assessment of Functioning

thesis_LW_V3.indb 160 06/06/16 07:38

($p > .20$). In clinical terms, both definitions led to statistical improvements on symptom measures at follow-up for resilient versus non-resilient individuals, while there were few differences in symptoms at baseline. The subgroups did not differ in terms of the use of psychotropic medication for either operationalisation (Table 2). We provide results from the more comprehensive operationalisation based on functional outcome in the main paper and provide the results from the operationalisation based on remission from UHR criteria in the supplemental information.

Brain development in UHR compared to typical development

To allow comparison to earlier studies, we first tested for differences in brain development between the all UHR individuals and typically developing controls. In the cortex we found the largest differences for cortical surface area. We primarily observed group*age interaction effects: smaller decreases over developmental time in UHR individuals in frontal and parietal areas compared to typically developing controls. We observed fewer differences in cortical volume, thickness and gyrification. Furthermore, subcortical structures showed larger decreases in UHR individuals over developmental time in hippocampus and thalamus volume, as well as smaller volumes at baseline and larger increases over developmental time in the third and inferior lateral ventricles than typically developing controls. Results are listed in supplemental information S3.

Brain development in resilient versus non-resilient UHR individuals

Main effects of group and group*age interaction effects are shown in Figure 2 and listed in supplemental information S4. Results from the analyses using our secondary operationalization of resilience (remission from UHR criteria) are available in supplemental information S5. These results were largely overlapping with the findings in our primary operationalization criteria (good functional outcome at 6 year follow up).

Stable differences between groups

There were widespread stable differences between resilient and non-resilient UHR individuals (i.e., main effect of group). Resilient individuals showed larger volumes of frontal, temporal and parietal cortex, corpus callosum and nucleus accumbens than

thesis_LW_V3.indb 161 06/06/16 07:38

non-resilient individuals (see supplemental information S4). Furthermore, overall cortical thickness was larger in resilient compared to non-resilient individuals, this was mainly observed in frontal, parietal and temporal lobes. Cortical surface area was also larger in resilient individuals compared to the non-resilient group, this effect was

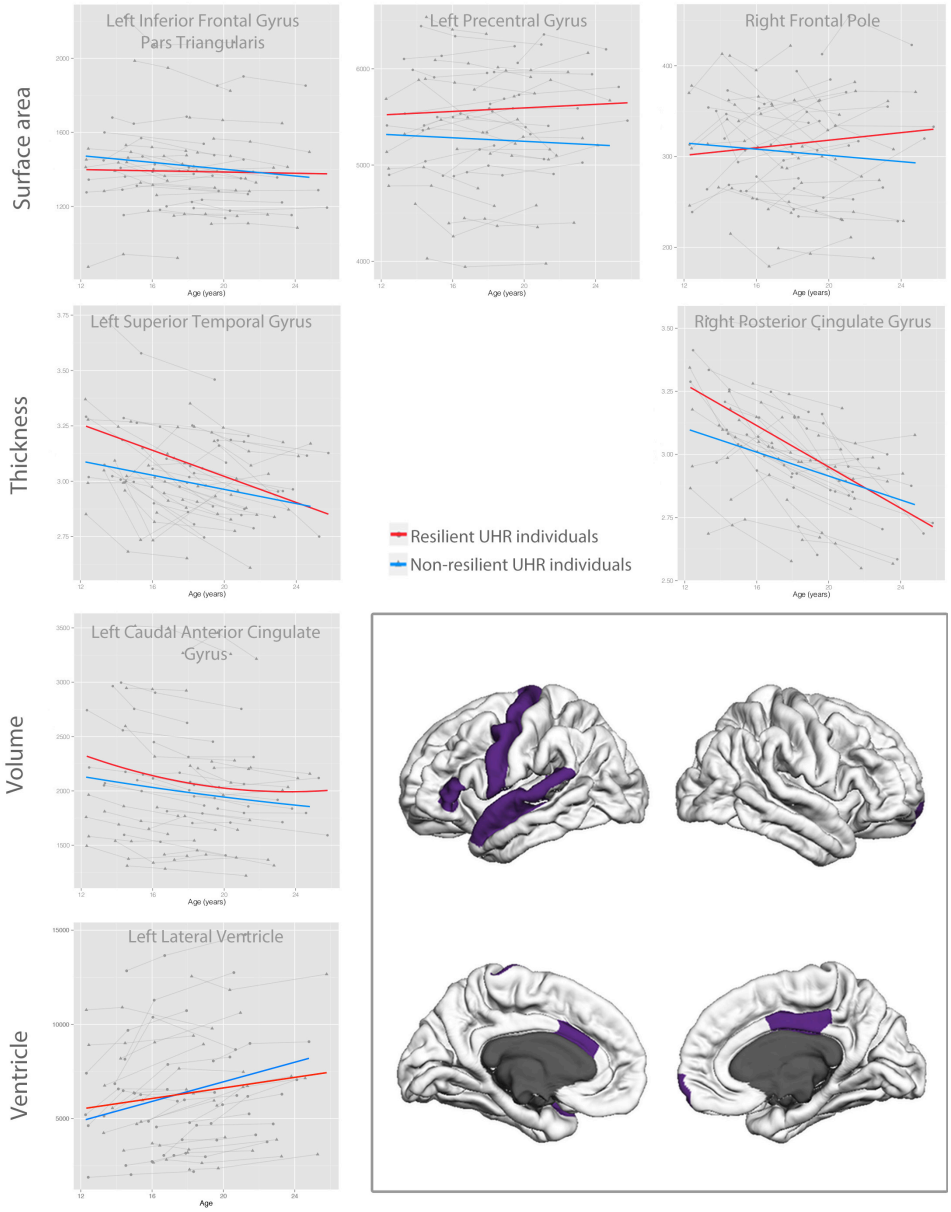

Figure 3 Distinct developmental trajectories between resilient and non-resilient UHR individuals

thesis_LW_V3.indb 162 06/06/16 07:38

predominantly observed in the left hemisphere. In addition, there were three regions that showed group differences in gyrification (see supplemental information S4).

When we compared the above mentioned findings to typically developing controls, we observed that controls fell between the two UHR groups: resilient individuals showed generally larger values than controls, while non-resilient individuals showed smaller values compared to controls. We illustrated this effect for three regions of interest in the supplemental information (S6).

Developmental differences

We also observed differences in developmental trajectories between resilient and non-resilient UHR individuals (group*age interactions; see Figure 3). Resilient individuals showed smaller decrease in volume over developmental time in the anterior cingulate gyrus and smaller increase in the lateral ventricles compared to non-resilient individuals. They additionally had greater decreases in cortical thickness in the superior temporal cortex and posterior cingulate gyrus than non-resilient individuals. Furthermore, resilient individuals showed increases over developmental time in cortical surface area in the precentral gyrus and frontal pole while these regions showed decreasing values in non-resilient individuals. Resilient individuals also showed decreases in gyrification in the anterior cingulate gyrus over developmental time compared to increasing values in non-resilient individuals.

Discussion

We investigated brain development over six years in a matched sample of 48 adolescents at ultra-high risk for developing psychosis and 48 typically developing controls, with up to three MRI scans per individual. Our main goal was to compare brain development between resilient and non-resilient UHR individuals. We operationalized resilience one of two ways: in our primary analysis resilient individuals were operationalized as good functioning at 6-year follow-up, while our secondary analysis is the more traditional operationalization where individuals completely remitted from UHR criteria. We found widespread differences in the volume of frontal, temporal and parietal cortex at baseline that remained stable over development. Furthermore, we observed differences in developmental trajectories of

thesis_LW_V3.indb 163 06/06/16 07:38

cortical surface area between resilient and non-resilient individuals. These were located in frontal regions including the cingulate gyrus. These diverging developmental trajectories may reflect compensatory neural mechanisms in better functioning resilient individuals.

When we compared brain development between all UHR individuals and typically developing volunteers, we observed diverging developmental trajectories for cortical surface area in frontal and parietal regions: typically developing controls showed greater decreases over development than UHR individuals. Furthermore, we found decreases in hippocampus and thalamus volume and increases in the volume of the third and inferior lateral ventricles in UHR individuals that were already present at baseline. These findings are in keeping with other studies on psychosis and UHR (Fusar-Poli et al. 2011, 2012b; Wood et al. 2013; Bois et al. 2014).

We observed four general patterns when we compared developmental trajectories between resilient and non-resilient UHR individuals: First, there were differences that were present at baseline and remained stable over development. These included greater cortical thickness and cortical and subcortical volumes in resilient individuals than non-resilient individuals. Interestingly, when we added the trajectories of typically developing controls in these areas, we found that they fell between those of resilient and non-resilient individuals (see supplemental information S6). Hence, brain volumes of resilient individuals exceeded that of typically developing volunteers, suggesting that greater volume may be protective for worse outcome. Earlier longitudinal studies on brain development in UHR individuals focused on transition to psychosis. Most of these studies showed differences between subgroups of UHR individuals in insular, temporal, parietal and superior frontal regions (Fornito et al. 2008; Sun et al. 2009; Ziermans et al. 2012; Wood et al. 2013). These regions overlap with our results. Our data suggests that these areas may hold promise for predicting, which UHR individuals will get better and which will worsen over time.

A second pattern we observed showed overlapping values at baseline but diverging trajectories with increasing age. Areas showing this pattern included the precentral gyrus, frontal pole, anterior cingulate gyrus and lateral ventricle (see Figure 3). Enlarged lateral ventricles was one of the first brain findings to be reported in

thesis_LW_V3.indb 164 06/06/16 07:38

schizophrenia and is still one of the most consistently reported (Shenton et al. 2001). In our study, the volume of lateral ventricles increased more over development for non-resilient individuals than for resilient ones. The anterior cingulate gyrus showed decreases in volume that stabilized in early adulthood for resilient individuals, whereas it continued to decrease in the non-resilient group. This structure is important for goal-directed behavior and involved in error and conflict monitoring and has often been reported to show changes in structure and function in UHR and schizophrenia (Fornito et al. 2008, 2009; Reid et al. 2010). The stabilization in the resilient group may reflect neural changes as a result of recovery in this group, whereas the continuing loss of volume in non-resilient individuals may reflect their continuing difficulties with cognitive and emotional integration (Fornito et al. 2008, 2009). The left precentral gyrus and right frontal pole showed developmental increases in surface area in resilient individuals compared to slight decreases in non-resilient individuals. Changes in frontal areas have often been associated with UHR and schizophrenia (for review, see Wood et al. 2013). As such, these increases may also represent compensatory mechanisms, related to better functioning in resilience.

The third main pattern was observed for other structures including the posterior cingulate and superior temporal gyrus. These regions showed converging trajectories for cortical thickness; baseline differences disappeared with development. Interestingly, both groups showed decreases over development in cortical thickness in these areas, similar to what is seen in typical development. However, the non-resilient group showed a slower rate of change than the resilient group.

There were also brain areas that differed between UHR individuals and typically developing controls, but not between resilient and non-resilient UHR individuals. These included hippocampus, thalamus and frontal and parietal cortical surface area. These changes are unlikely to be useful for predicting long-term functioning in UHR individuals, as they do not differ between resilient and non-resilient individuals. Rather, they may be related to non-specific UHR risk factors, such as obstetric complications (Stefanis et al. 1999; Wood et al. 2008).

We performed a second analysis where we defined resilience as complete remission

thesis_LW_V3.indb 165 06/06/16 07:38

from UHR criteria. The results from this analysis were similar but noisier (see supplemental information S5). We chose not to present both analyses in the main paper, as there was significant overlap between the groups defined by the two criteria. We presented the results from the operationalisation based on functional outcome as we felt that this definition has the most clinical relevance. The operationalisation based on remission considers only positive symptoms, whereas the one of our primary analysis is based on functional outcome and herewith considers the whole spectrum of functioning.

There are some limitations to this study. First, the sample size is relatively modest, especially for the follow-up analyses on resilience (17 versus 18 subjects for our primary analysis). This is in part related to our matching procedure where we matched for age and gender. Nevertheless, we felt these matching criteria increase the power of our study as previous studies reported on gender differences in indiivudals with UHR and schizophrenia (McGrath et al. 2008; Walder et al. 2013; Cocchi et al. 2014). In addition gender is highly related with brain size and showed differences in developmental trajectories (Lenroot et al. 2007; Wierenga et al. 2014). The limited sample size may be related to the relatively small number of developmental changes observed in the present study. However, longitudinal samples require far fewer participants than cross-sectional studies in order to detect small differences in brain structure (Steen et al.). The power of our longitudinal design is comparable to a cross-sectional dataset including ~ 250 subject per UHR subgroup. Moreover, this is the first study to report up to three MRI scans per individual.

A second limitation is that a large number of UHR individuals were on medication for the duration of this study. This is often the case in UHR studies and the numbers did not differ between subgroups, neither at baseline or follow-up. This suggests that medication did not affect our results related to subgroups of UHR individuals. The lack of a difference between resilient and non-resilient individuals could even be taken to suggest that medication does not play a role in individual outcome.

In conclusion, brain development in resilient individuals that were at UHR for psychosis differs from that of non-resilient individuals. Widespread differences in

thesis_LW_V3.indb 166 06/06/16 07:38

cortical thickness and volume were evident at baseline and remained stable over development, whereas various frontal areas showed diverging developmental trajectories. The differences that were already present at baseline may hold promise for predicting, at an early age, which individuals will recover from their at risk state and who will not. The diverging developmental trajectories of frontal areas may reflect neural changes related to better functional outcome.

thesis_LW_V3.indb 167 06/06/16 07:38

Supplementary information

Supplementary Information S1: Operationalisations of resilience

At 6-year follow up, the UHR group was subdivided into 'resilient' and 'non-resilient' subgroups where resilience was operationalised using functional outcome or defined by UHR remission criteria[1].

The first operationalisation of resilience was based on functional outcome as assessed by the modified Global Assessment of Functioning (mGAF) scale. This is a numerical scale (0 through 90) that rates social, occupational and psychological functioning using a more structured scoring system than the original GAF. It is therefore more resistant to rater bias[2]. Poor functional outcome was defined as an mGAF score of < 65 and good functional outcome as an mGAF score of ≥ 65. This definition of resilience resulted in subgroups of 17 resilient and 18 non-resilient individuals.

For the second operationalisation of resilience, the UHR group was split into two groups based on remission from UHR symptoms. We followed the guidelines by McGlashan and colleagues[1]. As such, subjects were considered to be in remission if they no longer had positive prodromal symptoms at the sub-psychotic level (i.e., the subject had ratings of ≤2 for all the SIPS/SOPS positive symptom items). The group of non-remitters included[1] those individuals who had converted to psychosis (i.e., subjects with a rating of 6 for ≥1 SIPS/SOPS positive items for a period of more than 7 days) and individuals who still met UHR criteria (i.e., subjects with ratings of 3-5 for ≥1 SIPS/SOPS positive items). Chart reviews were used to retrospectively confirm psychotic transition by clinical expert consensus, and subjects were subsequently diagnosed according to the Diagnostic and Statistical Manual of Mental Disorders, Fourth Edition (DSM-IV) guidelines[3]. This definition of resilience resulted in subgroups of 16 resilient and 19 non-resilient individuals.

[1] McGlashan TH, Miller TJ, Woods SW (2001): Structured Interview for Prodromal Syndromes (SIPS) — version 3.0. PRIME Research Clinic, Yale School of Medicine, New Haven. .

[2] Hall RC (1995): Global assessment of functioning. A modified scale. Psychosomatics. 36: 267–275.

[3] American Psychiatric Association (1994): Diagnostic and Statistical Manual of Mental Disorders IV (DSM-IV). Washington DC: American Psychiatric Association. .

thesis_LW_V3.indb 168 06/06/16 07:38

Supplementary Information S2: Linear mixed models

The relationship between age, group and our measures of interest (brain measures) were tested using a linear mixed model and top down selection procedure. This procedure accounts for irregular intervals between measures, missing data and within-subject dependence[-3]. Each dependent measure of the jth individual and kth time-point was modeled as described previously[4]. Several models including main group effects, linear age terms, quadratic age terms, cubic age terms and interaction effects were fit. The full model is represented by the following formula:

$$\text{Measurement}_{jk} = \text{Intercept} + d_j + ß_1(\text{group}) + ß_2(\text{age}) + ß_3(\text{age}^2) + ß_4(\text{age}^3) +$$

$$ß_5(\text{group} * \text{age}) + ß_6(\text{group} * \text{age}^2) + ß_7(\text{group} * \text{age}^3) + e^{jk}$$

The e_{jk} term represents the normally distributed residual error. Each ß represents a parameter estimate; for example the quadratic age effect parameter is represented by $ß_3$. Furthermore, interaction effects of group and age were modeled. The full model was tested against models including linear or quadratic age terms only. Intercept, group and age effects were fixed, while within-subject dependence (d_j) was modeled as a random effect. All possible models were run using mean-centered age terms (age 17.8).

The choice of best model fit was determined in three steps: First, cubic, quadratic and linear age effects were fit for each region of interest (ROI). If the cubic age effect did not reach significance at $p < 0.05$, we stepped down to the quadratic developmental model, etc. Second, we investigated whether the developmental trajectories differed between groups. Hence, a full model containing both main effects of age and group, as well as interaction effects was used. We accepted the full model that allowed for differences in growth trajectories between groups if the interaction term was significant at $p < 0.05$. If that was not the case, the simpler model including main effects of age and group was tested for significance. If the main group effect term was significant, this model was selected as the model that fit best. Otherwise, the model including only age terms was selected as the best model.

[1] Fox J (2002): Linear mixed models—appendix to an r and s-plus companion to applied regression. Relat 10. p 5261.

[2] Ostby Y, Tamnes CK, Fjell AM, Westlye LT, Due-Tønnessen P, Walhovd KB (2009): Heterogeneity in subcortical brain development: A structural magnetic resonance imaging study of brain

thesis_LW_V3.indb 169 06/06/16 07:38

maturation from 8 to 30 years. J Neurosci. 29: 11772–11782.

[3] Shaw P, Malek M, Watson B, Sharp W, Evans A, Greenstein D (2012): Development of cortical surface area and gyrification in attention-deficit/hyperactivity disorder. Biol Psychiatry. 72: 191–197.

Wierenga LM, Langen M, Oranje B, Durston S (2014): Unique developmental trajectories of cortical thickness and surface area. Neuroimage. 87: 120–126.

thesis_LW_V3.indb 170 06/06/16 07:38

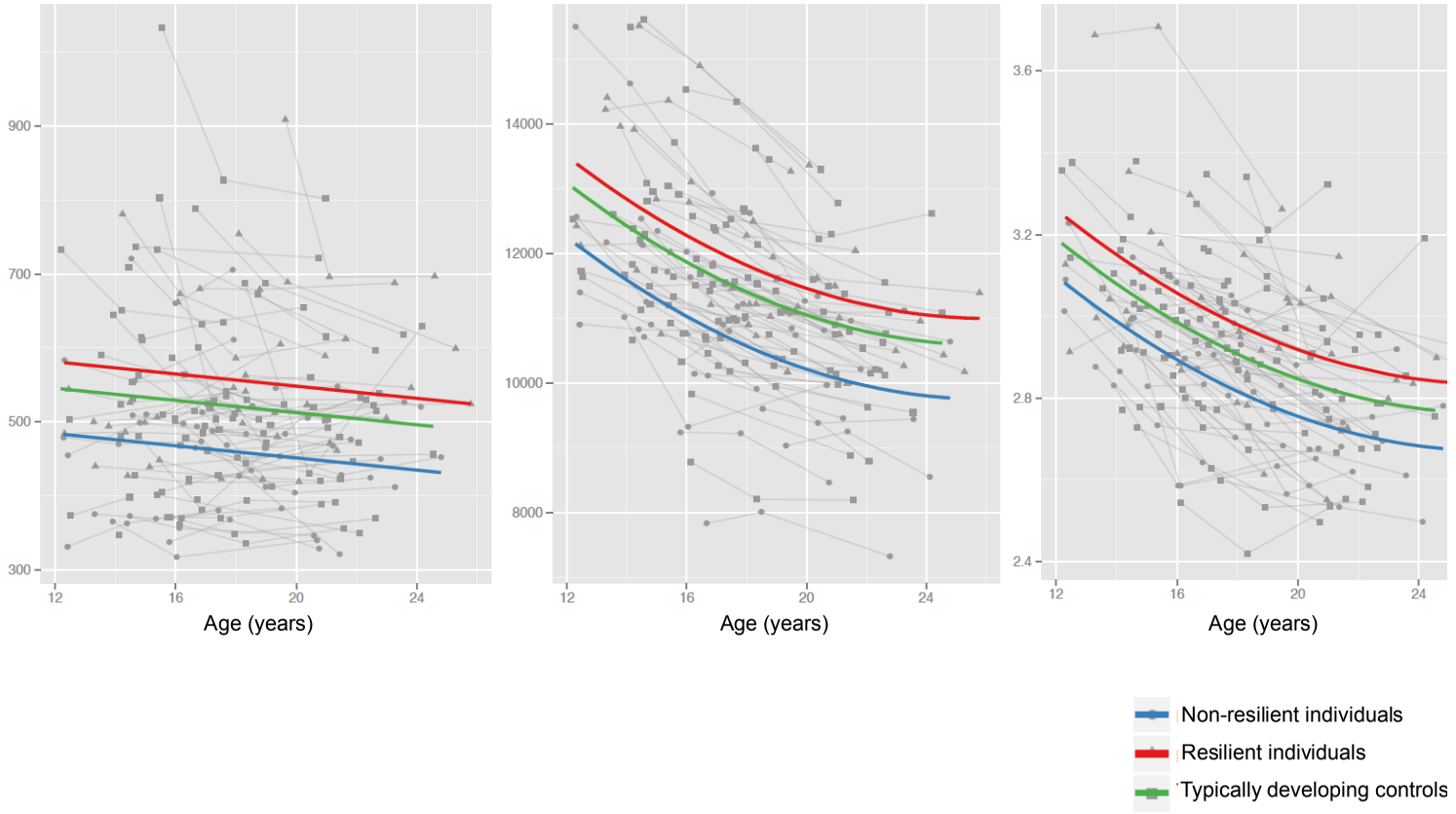

Supplementary Figure 1 Differences in cortical morphology between resilient, non-resilient UHR individuals and typically developping controls

thesis_LW_V3.indb 171 06/06/16 07:38

Supplementary Table 1 Stable and developmental differences between UHR individuals and typically developing controls (TDC) [a]

			Volume			CT			SA			GI		
Region of interest			Growth model	Effect	p	Growth model	Effect	p	Growth model	Effect	p	Growth model	Effect	p
Lobes	Frontal lobe	L							Linear	*Interaction*	0.047			
		R												
	Occipital lobe	L												
		R							Quadratic	UHR < TDC	0.015			
	Total (hemisphere)	L												
		R							Linear	*Interaction*	0.022			
Cortical	Caudal Anterior Cingulate Gyrus	L							Linear	UHR < TDC	0.017			
		R												
	Cuneus	L	Cubic	UHR < TDC	0.014									
		R	Quadratic	*Interaction*	0.010				Quadratic	*Interaction*	0.015			
	Entorhinal cortex	L												
		R				Linear	*Interaction*	0.029						
	Frontal Pole	L												
		R	Cubic	*Interaction*	0.042									
	Fusiform Gyrus	L												
		R							Quadratic	*Interaction*	0.017			
	Isthmus Cingulate Gyrus	L										Linear	UHR < TDC	0.010
		R												
	Lateral Occipital Gyrus	L	Cubic	*Interaction*	0.041									
		R							Cubic	UHR < TDC	0.011			
	Lingual Gyrus	L							Quadratic	*Interaction*	0.021	Linear	UHR < TDC	0.006
		R	Quadratic	*Interaction*	0.043				Quadratic	UHR < TDC	0.045			
	Parahippocampal Gyrus	L												
		R				Linear	UHR < TDC	0.030						
	Inferior Frontal Gyrus - Pars Orbitalis	L										Linear	*Interaction*	0.035
		R	Quadratic	UHR > TDC	0.031									
	Inferior Frontal Gyrus - Pars Triangularis	L	Cubic	*Interaction*	0.021									
		R												
	Pericalcarine Cortex	L	Cubic	*Interaction*	0.043							Linear	UHR < TDC	0.026
		R										Linear	UHR < TDC	0.013
	Postcentral Gyrus	L												
		R							Linear	*Interaction*	0.017			
	Posterior Cingulate Gyrus	L							Linear	*Interaction*	0.023			
		R												
	Precentral Gyrus	L							Linear	*Interaction*	0.021			
		R												
	Precuneus	L										Linear	UHR < TDC	0.032
		R							Quadratic	*Interaction*	0.004			
	Rostral Anterior Cingulate Gyrus	L												
		R							Linear	*Interaction*	0.019			
	Superior Frontal Gyrus	L							Linear	*Interaction*	0.005			
		R												
Subcortical	Hippocampus	L	Quadratic	*Interaction*	0.012									
		R	Cubic	UHR < TDC	0.006									
	Thalamus	L	Quadratic	*Interaction*	0.015									
		R	Quadratic	*Interaction*	0.022									
	Inferior Lateral Ventricle	L	Linear	*Interaction*	0.049									
		R												
	3rd Ventricle	n.a.	Quadratic	UHR > TDC	0.019									

[a] Stable differences are indicated by "</>" whereas developmental differences are indicated by the term "interaction" in bold.

CT = cortical thickness; SA = surface area; GI = gyrification index; L = left; R = right; UHR = individuals at ultra high risk for developing psychosis; TDC = typically developing controls

thesis_LW_V3.indb 172

06/06/16 07:38

Supplementary Table 2 Stable and developmental differences in brain development between resilient (R) and non-resilient (NR) UHR individuals based on functional outcome

			Volume			CT			SA			GI		
Region of interest			Growth model	Effect	p	Growth model	Effect	p	Growth model	Effect	p	Growth model	Effect	p
Lobes	Frontal lobe	L												
		R				Quadratic	R > NR	0.012						
	Parietal lobe	L				Quadratic	R > NR	0.003						
		R				Cubic	R > NR	0.008						
	Temporal lobe	L				Quadratic	R > NR	0.025						
		R												
	Total (hemisphere)	L				Quadratic	R > NR	0.015						
		R				Quadratic	R > NR	0.017						
Cortical	Caudal Anterior Cingulate Gyrus	L	Quadratic	*Interaction*	0.049							linear	*Interaction*	0.049
		R												
	Caudal Middle Frontal Gyrus	L												
		R				Linear	R > NR	0.000						
	Entorhinal Cortex	L	Linear	R > NR	0.005									
		R												
	Frontal Pole	L												
		R	Linear	R > NR	0.033	Linear	R > NR	0.020	Linear	*Interaction*	0.033			
	Fusiform Gyrus	L				Cubic	R > NR	0.011						
		R												
	Inferior Parietal Gyrus	L												
		R	Quadratic	R > NR	0.037	Cubic	R > NR	0.032						
	Inferior Temporal Gyrus	L				Cubic	R > NR	0.031						
		R	Quadratic	R > NR	0.017									
	Insula	L	Quadratic	R > NR	0.025				Linear	R > NR	0.040			
		R												
	Lateral Orbitofrontal Cortex	L	Quadratic	R > NR	0.026				Linear	R > NR	0.023			
		R				Quadratic	R > NR	0.026						
	Lingual Gyrus	L				Quadratic	R > NR	0.046						
		R												
	Medial Orbitofrontal Cortex	L												
		R				Cubic	R > NR	0.005						
	Middle Temporal Gyrus	L	Linear	R > NR	0.030				Linear	R > NR	0.042			
		R												
	Inferior Frontal Gyrus - Pars Opercularis	L												
		R										Linear	R < NR	0.029
	Inferior Frontal Gyrus - Pars Orbitalis	L										Linear	R > NR	0.003
		R												
	Inferior Frontal Gyrus - Pars Triangularis	L							Linear	*Interaction*	0.009			
		R				Quadratic	R > NR	0.004						
	Postcentral Gyrus	L	Quadratic	R > NR	0.005	Quadratic	R > NR	0.011	Quadratic	R > NR	0.041			
		R	Quadratic	R > NR	0.014	Cubic	R > NR	0.001						
	Posterior Cingulate Gyrus	L												
		R				Linear	*Interaction*	0.011						
	Precentral Gyrus	L							Linear	*Interaction*	0.037			
		R												
	Precuneus	L	Quadratic	R > NR	0.003	Quadratic	R > NR	0.001						
		R				Cubic	R > NR	0.023						
	Rostral Middle Frontal Gyrus	L	Quadratic	R > NR	0.026	Cubic	R > NR	0.013						
		R												
	Superior Parietal Gyrus	L	Quadratic	R > NR	0.021									
		R				Cubic	R > NR	0.024						
	Superior Temporal Gyrus	L				Linear	*Interaction*	0.038						
		R												
	Supramarginal Gyrus	L				Quadratic	R > NR	0.005						
		R												
Subcortical	Nucleus Accumbens	L	Quadratic	R > NR	0.019									
		R	Linear	R > NR	0.008									
	Lateral Ventricle	L	Linear	*Interaction*	0.036									
		R												
	CC Anterior		Linear	R > NR	0.018									
	CC Mid Anterior		Linear	R > NR	0.006									
	CC Mid Posterior		Linear	R > NR	0.011									

Stable differences are indicated by "</>" whereas developmental differences are indicated by the term "interaction" in bold.
CT = cortical thickness; SA = surface area; GI = gyrification index; L = left; R = right; R = resilient UHR individuals; NR = non-resilient UHR individuals; CC = corpus callosum

thesis_LW_V3.indb 173 06/06/16 07:38

Supplementary Table 3 Stable and developmental differences between resilient (R) and non-resilient (NR) UHR individuals based on UHR remission criteria

			Volume			CT			SA			GI		
Region of interest			Growth model	Effect	p	Growth model	Effect	p	Growth model	Effect	p	Growth model	Effect	p
Lobes	Frontal lobe	L				Quadratic	R > NR	0.026						
		R				Quadratic	R > NR	0.016						
	Parietal lobe	L				Quadratic	R > NR	0.018						
		R				Cubic	R > NR	0.026						
	Temporal lobe	L				Quadratic	R > NR	0.031						
		R				Quadratic	R > NR	0.003						
	Total (hemisphere)	L				Quadratic	R > NR	0.011						
		R				Quadratic	R > NR	0.007						
Cortical	Banks of the Superior Temporal Sulcus	L				Cubic	R > NR	0.017						
		R												
	Caudal Anterior Cingulate Gyrus	L												
		R										Linear	Interaction	0.015
	Caudal Middle Frontal Gyrus	L				Cubic	R > NR	0.038						
		R	Linear	*Interaction*	0.027	Linear	R > NR	0.009	Linear	*Interaction*	0.001			
	Frontal Pole	L												
		R				Linear	*Interaction*	0.045						
	Fusiform Gyrus	L				Cubic	R > NR	0.007						
		R				Quadratic	R > NR	0.002						
	Inferior Parietal Gyrus	L										Linear	Interaction	0.026
		R												
	Inferior Temporal Gyrus	L												
		R				Quadratic	R > NR	0.006						
	Lateral Orbitofrontal Cortex	L	Quadratic	R > NR	0.015	Quadratic	R > NR	0.034						
		R												
	Lingual Gyrus	L							Linear	R < NR	0.044			
		R												
	Medial Orbitofrontal Cortex	L							Linear	R < NR	0.007			
		R				Linear	*Interaction*	0.043						
	Middle Temporal Gyrus	L				Cubic	R > NR	0.046				Linear	Interaction	0.007
		R												
	Parahippocampal Gyrus	L												
		R				Linear	R > NR	0.021	Cubic	*Interaction*	0.032			
	Inferior Frontal Gyrus - Pars Orbitalis	L				Quadratic	R > NR	0.035						
		R												
	Inferior Frontal Gyrus - Pars Triangularis	L												
		R	Linear	*Interaction*	0.007	Quadratic	R > NR	0.014				Linear	R < NR	0.043
	Posterior Cingulate Gyrus	L	Linear	*Interaction*	0.015	Linear	*Interaction*	0.035						
		R												
	Precentral Gyrus	L										Linear	Interaction	0.033
		R												
	Precuneus	L	Quadratic	R > NR	0.049	Quadratic	R > NR	0.016						
		R												
	Rostral Middle Frontal Gyrus	L				Cubic	R > NR	0.029						
		R	Linear	*Interaction*	0.022							Linear	Interaction	0.002
	Superior Frontal Gyrus	L				Linear	R > NR	0.030						
		R				Linear	*Interaction*	0.017	Linear	Interaction	0.034	Linear	Interaction	0.010
	Superior Parietal Gyrus	L				Quadratic	R > NR	0.027	Linear	R < NR	0.004			
		R							Linear	Interaction	0.038			
	Superior Temporal Gyrus	L										Linear	Interaction	0.012
		R												
	Supramarginal Gyrus	L				Quadratic	R > NR	0.041						
		R	Linear	*Interaction*	0.001	Linear	*Interaction*	0.009				Linear	Interaction	0.011
	Temporal Pole	L												
		R				Linear	*Interaction*	0.002						
	Transverse Temporal Gyrus	L										Linear	Interaction	0.016
		R							Quadratic	Interaction	0.035			
Subcortical	Pallidum	L	Quadratic	R > NR	0.037									
		R												

Stable differences are indicated by "</>" whereas developmental differences are indicated by the term "interaction" in bold.
CT = cortical thickness; SA = surface area; GI = gyrification index; L = left; R = right; R = Resilient UHR individuals; NR = Non-resilient UHR individuals

thesis_LW_V3.indb 174

06/06/16 07:38

References

Allen P, Chaddock CA, Egerton A, Howes OD, Barker G, Bonoldi I, Fusar-Poli P, Murray R, & McGuire P (2014). Functional Outcome in People at High Risk for Psychosis Predicted by Thalamic Glutamate Levels and Prefronto-Striatal Activation. Schizophrenia bulletin 41(2), 429-439.

Bois C, Whalley H, McIntosh A, & Lawrie S (2014). Structural magnetic resonance imaging markers of susceptibility and transition to schizophrenia: A review of familial and clinical high risk population studies. Journal of psychopharmacology 29(2), 144-154.

Carmona S, Proal E, Hoekzema EA, Gispert J-D, Picado M, Moreno I, Soliva JC, Bielsa A, Rovira M, Hilferty J, Bulbena A, Casas M, Tobeña A, & Vilarroya O (2009). Ventro-striatal reductions underpin symptoms of hyperactivity and impulsivity in attention-deficit/hyperactivity disorder. Biological psychiatry 66, 972–977.

Carrión RE, McLaughlin D, Goldberg TE, Auther AM, Olsen RH, Olvet DM, Correll CU, & Cornblatt BA (2013). Prediction of functional outcome in individuals at clinical high risk for psychosis. JAMA psychiatry 70, 1133–1142.

Cocchi A, Lora A, Meneghelli A, La Greca E, Pisano A, Cascio MT, & Preti A (2014). Sex differences in first-episode psychosis and in people at ultra-high risk. Psychiatry research 215, 314–322.

Dale AM, Fischl B, & Sereno MI (1999). Cortical surface-based analysis. I. Segmentation and surface reconstruction. NeuroImage 9, 179–194.

Desikan RS, Ségonne F, Fischl B, Quinn BT, Dickerson BC, Blacker D, Buckner RL, Dale AM, Maguire RP, Hyman BT, Albert MS, & Killiany RJ (2006). An automated labeling system for subdividing the human cerebral cortex on MRI scans into gyral based regions of interest. NeuroImage 31, 968–980.

Fischl B, Sereno MI, & Dale AM (1999). Cortical surface-based analysis II: Inflation, flattening, and a surface-based coordinate system. NeuroImage 9, 195–207.

Fornito A, Yücel M, Dean B, Wood SJ, & Pantelis C (2009). Anatomical abnormalities of the anterior cingulate cortex in schizophrenia: bridging the gap between neuroimaging and neuropathology. Schizophrenia bulletin 35, 973–993.

thesis_LW_V3.indb 175 06/06/16 07:38

Fornito A, Yung AR, Wood SJ, Phillips LJ, Nelson B, Cotton S, Velakoulis D, McGorry PD, Pantelis C, & Yücel M (2008). Anatomic abnormalities of the anterior cingulate cortex before psychosis onset: an MRI study of ultra-high-risk individuals. Biological psychiatry 64, 758–765.

Fusar-Poli P, Bonoldi I, Yung AR, Borgwardt S, Kempton MJ, Valmaggia L, Barale F, Caverzasi E, & McGuire P (2012a). Predicting psychosis: meta-analysis of transition outcomes in individuals at high clinical risk. Archives of general psychiatry 69, 220–229.

Fusar-Poli P, & Borgwardt S (2007). Integrating the negative psychotic symptoms in the high risk criteria for the prediction of psychosis. Medical hypotheses 69, 959–960.

Fusar-Poli P, Borgwardt S, Bechdolf A, Addington J, Riecher-Rössler A, Schultze-Lutter F, Keshavan M, Wood S, Ruhrmann S, Seidman LJ, Valmaggia L, Cannon T, Velthorst E, De Haan L, Cornblatt B, Bonoldi I, Birchwood M, McGlashan T, Carpenter W, McGorry P, Klosterkötter J, McGuire P, & Yung A (2013). The psychosis high-risk state: a comprehensive state-of-the-art review. JAMA psychiatry 70, 107–120.

Fusar-Poli P, Borgwardt S, Crescini A, Deste G, Kempton MJ, Lawrie S, Mc Guire P, & Sacchetti E (2011). Neuroanatomy of vulnerability to psychosis: a voxel-based meta-analysis. Neuroscience and biobehavioral reviews 35, 1175–1185.

Fusar-Poli P, McGuire P, & Borgwardt S (2012b). Mapping prodromal psychosis: a critical review of neuroimaging studies. European psychiatry : the journal of the Association of European Psychiatrists 27, 181–191.

Gogtay N, Nugent TF, Herman DH, Ordonez A, Greenstein D, Hayashi KM, Clasen L, Toga AW, Giedd JN, Rapoport JL, & Thompson PM (2006). Dynamic mapping of normal human hippocampal development. Hippocampus 16, 664–672.

Hall RC (1995). Global assessment of functioning. A modified scale. Psychosomatics 36, 267–275.

Lenroot R, Gogtay N, & Greenstein D (2007). Sexual dimorphism of brain developmental trajectories during childhood and adolescence. Neuroimage 36, 1065–1073.

Maxwell ME (1982). Family Interview for Genetic Studies (FIGS): A Manual for FIGS. Clinical Neurogenetics Branch, Intramural Research Program, National Institute of

thesis_LW_V3.indb 176 06/06/16 07:38

Mental Health, Bethesda, Maryland.

McGlashan TH, Miller TJ, & Woods SW (2001). Structured Interview for Prodromal Syndromes (SIPS) — version 3.0. PRIME Research Clinic, Yale School of Medicine, New Haven.

McGrath J, Saha S, Chant D, & Welham J (2008). Schizophrenia: a concise overview of incidence, prevalence, and mortality. Epidemiologic reviews 30, 67–76.

Miller TJ, McGlashan TH, Rosen JL, Somjee L, Markovich PJ, Stein K, & Woods SW (2002). Prospective diagnosis of the initial prodrome for schizophrenia based on the Structured Interview for Prodromal Syndromes: preliminary evidence of interrater reliability and predictive validity. The American journal of psychiatry 159, 863–865.

Reid MA, Stoeckel LE, White DM, Avsar KB, Bolding MS, Akella NS, Knowlton RC, den Hollander JA, & Lahti AC (2010). Assessments of function and biochemistry of the anterior cingulate cortex in schizophrenia. Biological psychiatry 68, 625–633.

Reuter M, & Fischl B (2011). Avoiding asymmetry-induced bias in longitudinal image processing. NeuroImage 57, 19–21.

Schultze-Lutter F, & Klosterkötter J (2002). Bonn Scale for the Assessment of Basic Symptoms - Prediction list (BSABS-P). Cologne: University of Cologne.

Shenton ME, Dickey CC, Frumin M, & McCarley RW (2001). A review of MRI findings in schizophrenia. Schizophrenia research 49, 1–52.

Simon AE, Borgwardt S, Riecher-Rössler A, Velthorst E, de Haan L, & Fusar-Poli P (2013). Moving beyond transition outcomes: Meta-analysis of remission rates in individuals at high clinical risk for psychosis. Psychiatry research 209(3), 266-272.

Simon AE, Velthorst E, Nieman DH, Linszen D, Umbricht D, & de Haan L (2011). Ultra high-risk state for psychosis and non-transition: a systematic review. Schizophrenia research 132, 8–17.

Sprong M, Becker HE, Schothorst PF, Swaab H, Ziermans TB, Dingemans PM, Linszen D, & van Engeland H (2008). Pathways to psychosis: a comparison of the pervasive developmental disorder subtype Multiple Complex Developmental Disorder and the 'At Risk Mental State'. Schizophrenia research 99, 38–47.

thesis_LW_V3.indb 177 06/06/16 07:38

Steen RG, Hamer RM, & Lieberman JA Measuring brain volume by MR imaging: impact of measurement precision and natural variation on sample size requirements. AJNR. American journal of neuroradiology 28, 1119–1125.

Stefanis N, Frangou S, Yakeley J, Sharma T, O'Connell P, Morgan K, Sigmudsson T, Taylor M, & Murray R (1999). Hippocampal volume reduction in schizophrenia: effects of genetic risk and pregnancy and birth complications. Biological psychiatry 46, 697–702.

Sun D, Phillips L, Velakoulis D, Yung A, McGorry PD, Wood SJ, van Erp TGM, Thompson PM, Toga AW, Cannon TD, & Pantelis C (2009). Progressive brain structural changes mapped as psychosis develops in "at risk" individuals. Schizophrenia research 108, 85–92.

Walder DJ, Holtzman CW, Addington J, Cadenhead K, Tsuang M, Cornblatt B, Cannon TD, McGlashan TH, Woods SW, Perkins DO, Seidman LJ, Heinssen R, & Walker EF (2013). Sexual dimorphisms and prediction of conversion in the NAPLS psychosis prodrome. Schizophrenia research 144, 43–50.

Wierenga LM, Langen M, Oranje B, & Durston S (2014). Unique developmental trajectories of cortical thickness and surface area. NeuroImage 87, 120–126.

De Wit S, Schothorst PF, Oranje B, Ziermans TB, Durston S, & Kahn RS (2014). Adolescents at ultra-high risk for psychosis: long-term outcome of individuals who recover from their at-risk state. European neuropsychopharmacology : the journal of the European College of Neuropsychopharmacology 24, 865–873.

Wood SJ, Pantelis C, Velakoulis D, Yücel M, Fornito A, & McGorry PD (2008). Progressive changes in the development toward schizophrenia: studies in subjects at increased symptomatic risk. Schizophrenia bulletin 34, 322–329.

Wood SJ, Reniers RLEP, & Heinze K (2013). Neuroimaging findings in the at-risk mental state: a review of recent literature. Canadian journal of psychiatry. Revue canadienne de psychiatrie 58, 13–18.

Ziermans T, de Wit S, Schothorst P, Sprong M, van Engeland H, Kahn R, & Durston S (2014). Neurocognitive and clinical predictors of long-term outcome in adolescents at ultra-high risk for psychosis: a 6-year follow-up. PloS one 9, e93994.

thesis_LW_V3.indb 178 06/06/16 07:38

Ziermans TB, Schothorst PF, Schnack HG, Koolschijn PCMP, Kahn RS, van Engeland H, & Durston S (2012). Progressive structural brain changes during development of psychosis. Schizophrenia bulletin 38, 519–530.

Ziermans TB, Schothorst PF, Sprong M, & van Engeland H (2011). Transition and remission in adolescents at ultra-high risk for psychosis. Elsevier B.V. Schizophrenia research 126, 58–64.

thesis_LW_V3.indb 179 06/06/16 07:38

SUMMARY AND GENERAL DISCUSSION

thesis_LW_V3.indb 181 06/06/16 07:38

Summary

Brain development is a dynamic process. Billions of connections between neurons are formed in childhood; by adulthood half of these connections are pruned away, while others remain and get strengthened. This period of plasticity is remarkably prolonged in humans, rendering us able - throughout the course of development - to acquire skills to meet environmental needs. On the other hand it makes us vulnerable, as during windows of plasticity, experiences are more likely to have enduring effects on the brain. If we knew when particular developmental windows occur and we are at our most vulnerable and adaptive, we would be able to design interventions more effectively. Therefore, it is important to learn more about the course and timing of developmental plasticity in the brain. This thesis aims to chart developmental patterns throughout the brain by mapping growth trajectories of both cortical and subcortical structures as well as the connections between them. We include longitudinal data, permitting us to track developmental brain changes within individuals. In addition, we tracked brain development in individuals with ADHD and individuals at ultra high risk for psychosis. These latter studies are included to show how knowledge of atypical brain development can inform us on typical brain development.

The complexity of cortical maturation is underlined in Chapter 2, where we assessed the developmental trajectory of cortical morphometry. We mapped regional patterns of both cortical thickness and surface area and showed that the shape of their developmental trajectories differed regionally. These results emphasize a few important aspects: First, changes in cortical volume are more closely related to cortical surface area than to thickness. Second, cortical surface area showed a later peak than cortical volume and thickness. Thus, surface area is still expanding when volume and thickness are already decreasing. Therefore it is of great importance to study cortical surface area in addition to thickness as otherwise the aspect of cortical expansion might be underestimated. Third, males and females showed widespread differences in cortical surface area, this appeared to be stable over the entire age range. Only a small number of regions showed gender differences in cortical thickness, and two of those showed sexual dimorphic trajectories. Together these results highlight the importance of separately assessing cortical dimensions when studying brain development, as it

thesis_LW_V3.indb 182 06/06/16 07:38

may help to narrow down the search for genetic and environmental factors involved in typical and atypical brain development.

In Chapter 3 we mapped the developmental patterns of subcortical brain structures. The basal ganglia, hippocampus, amygdala and cerebellum all showed volume changes in childhood and adolescence. However the shape of the trajectories varied substantially: most basal ganglia structures showed linear decreases in volume suggesting that a peak in their volume had perhaps already occurred at an early age (<7 years old). The putamen and the caudate showed the largest decrease with age. Thalamus, globus pallidum, hippocampus and amygdala volumes showed nonlinear changes with volume increases in childhood leveling off in adolescence and subsequent decreases. The latest peak was observed in amygdala volume. These results indicate heterogeneous developmental patterns of subcortical brain development, where some structures appear to develop relatively early while others continue to develop into adulthood.

However, none of the regions above operates in isolation. Hence, in order to fully understand brain development it is necessary to study how their interactions develop. In Chapter 4, we observed that maturation of white matter bundles between regions is not uniform throughout the brain: projection fibers (subcortical-cortical connections), commissural fibers (connecting cortical regions between hemispheres) and intra-hemispheric cortico-cortical connections within the occipital lobes showed low rates of change during childhood and adolescence, whereas cortico-cortical connections within and between parietal and frontal projections showed greater rates of change. This suggests that connections between higher order association regions show a more protracted development. We further observed age-related changes in network topology using graph theory. The results showed a decrease in global path length, suggesting information transfer within the network becomed more efficient. In addition, average node strength increased with age as well as mean clustering. This suggests that development is characterized by an increase in network integration together with an increase in specialization of local clusters.

The aim of Chapter 5 was to explore brain development in children with ADHD. In this

thesis_LW_V3.indb 183 06/06/16 07:38

chapter, we studied whether reductions in cortical volume were related to differences in cortical surface area, thickness or both. We assessed these aspects of cortical morphometry in a longitudinal cohort and confirmed smaller overall cortical volume in children with ADHD than their typically developing peers, predominantly in the frontal lobes. Similar to our observations on gender differences in Chapter 2 these reductions in cortical volume were largely related to cortical surface area but not thickness. This suggests that cortical layering was largely preserved in children with ADHD. We found that group differences in volume and surface area were consistent over the entire age range, as we did not find any interaction effects. Possibly these structures were affected at an early age, even prenatally. This hypothesis is discussed in more detail later in this chapter.

In Chapter 6, we studied the development of cortical morphometry in individuals at ultra high risk for psychosis (UHR). On average, UHR individuals had less developmental reductions in cortical surface area than typically developing controls, while the developmental trajectories for thickness were comparable between groups. In addition we found wide spread differences in cortical morphometry between UHR individuals who recovered from their UHR state (resilient individuals) and those who did not (non-resilient individuals). These differences were mostly related to reductions in cortical thickness in the non-resilient group compared to the resilient group and controls. Moreover, resilient individuals had greater cortical thickness than controls, which may reflect a compensatory mechanism. With regard to surface area, resilient individuals showed a general pattern of less tissue loss than non-resilient individuals, predominantly in the left frontal lobe.

thesis_LW_V3.indb 184 06/06/16 07:38

General discussion

In the final part of this thesis, we would like to reflect on some of our findings. Our results on cortical morphometry suggest that different biological mechanisms are involved in the development of cortical thickness and surface area. We will first describe how our findings relate to other studies, followed by a discussion of three leading theories on possible mechanisms involved in these different aspects of cortical morphometry. Next, we discuss neurobiological processes involved in brain development and how they may (or may not) relate to our findings. Furthermore, we will reflect on how our findings on atypical brain development may help us better understand typical brain development and vice versa. In the last part of this chapter we discuss methodological considerations and future directions.

Cortical dimensions

The studies in this thesis support previous findings of continued changes in brain structure throughout adolescence and early adulthood. We showed that the volume of grey matter structures generally follow an inverted U-shaped pattern, with relatively late maturational changes in the frontal and parietal regions and mid-temporal gyrus. Nevertheless there were several nuances compared to these earlier studies that were mainly related to the shape of these trajectories. First, peak total cortical volume as observed in Chapter 2 occurred at an earlier age compared to findings in some studies (Giedd, Blumenthal, & Jeffries, 1999; Raznahan et al., 2011), yet were largely in line with results of other longitudinal studies (Aubert-Broche et al., 2013; Lebel & Beaulieu, 2011; Tamnes et al., 2013). This highlights the importance of taking individual variability in brain development into account. The results in Chapter 2 also showed that the inverted U-shaped pattern of cortical volume was mostly related to developmental changes in cortical surface area rather than cortical thickness. This observation has important implications for the interpretation of neuroimaging findings in the field of typical and atypical brain development. First, cortical growth continues longer into adolescence than can be observed by measuring cortical volume alone. This shows the importance of studying multiple dimensions of the cortex as surface area expansion could be obscured by decreases in cortical thickness if only volume is assessed. Second, the unique developmental patterns of cortical surface area and thickness suggest that different biological mechanisms may be involved in the development of these cortical aspects. This

thesis_LW_V3.indb 185 06/06/16 07:38

is supported by the observation that cortical surface area and thickness are both heritable but driven by different genes (Panizzon, Fennema-Notestine, & Eyler, 2009; Winkler, Kochunov, Blangero, & Almasy, 2010). Third, not only are our findings relevant for typical brain development, they may also have important implications for studies of developmental disorders, as assessing them separately may reveal important information about genetic and environmental factors involved in different phases of development (see Chapters 5 and 6). There are several theories that explain the distinct mechanisms that may be involved in cortical thickness and surface area development. We will discuss three leading theories in the context of our findings: the radial unit hypothesis, the white matter tension hypothesis and the differential growth hypothesis.

The radial unit hypothesis

The radial unit hypothesis of Rakic (1988) states that surface area development but not thickness is dependent on input from its afferent connections. If this is true, the developmental trajectories of cortical thickness and surface area may hold important information on experience versus genetically driven brain maturation.

Support for the radial unit hypothesis comes from studies that show that elimination of input to the cortex reduces the number of mini-columns. When thalamic afferent fibers of area 17 were enucleated prenatally in the macaque brain, surface area was highly reduced at birth, which was related to fewer mini-columns. Interestingly cortical thickness was unaffected. The reduction in number of mini-columns appeared to be related to a reduced total number of neurons, while the number of neurons and synapses per volume remained unaffected.

Further support that surface area is input dependent comes from a study that showed that also postnatal enucleation of input to the visual cortex affected cortical surface area development, albeit in opposite direction. Human adults that were enucleated of the contralateral eye before four years of age, showed increased surface area in the visual cortex. Again, cortical thickness did not show any changes (Kelly, DeSimone, Gallie, & Steeves, 2015). Here increased cortical surface area may be related to changes in the developmental trajectory of the visual cortex. Typical development of the surface area would show a

thesis_LW_V3.indb 186 06/06/16 07:38

pattern of expansion and reduction of individual mini-columns (Buxhoeveden, Lefkowitz, Loats, & Armstrong, 1996). Hence, enlarged surface area in individuals enucleated of the contralateral eye may be related to changes in the developmental trajectory of individual mini-columns.

Together these studies indicate that prenatal activity dependent development may affect the number of mini-columns, while in the postnatal phase experiences may drive the development of individual mini-columns by changing the typical inverted U-shaped developmental pattern of column width. Thus prenatal changes in surface area may affect the number of cortical neurons and synapses, while postnatal changes may be related to altered neural and synaptic density.

If this model is true, this has two important implications for the interpretation of our results. First, typical development of surface area is, at least in part, input dependent and thus reliant on intact afferent connections and spontaneous or experience driven activity in connecting regions. In contrast, the development of cortical thickness may be largely regulated by intrinsic genetic programs. Second, group differences in surface area at birth may refer to a difference in number of mini-columns, while changes in the development of cortical surface area may indicate changes in the development of individual mini-column width.

If we adhere to this line of interpretation, our observations in Chapter 5 of decreased but stable cortical surface area reductions in children with ADHD compared to controls suggests changes in the number of mini-columns and thus that the total number of neurons and synaptic connections may be reduced. This would suggest that the developmental trajectories of individual mini-columns and neural and synaptic density could be relatively preserved. Adolescents at ultra high risk for psychosis showed altered developmental trajectories in surface area in addition to stable reductions, see Chapter 6, which may be related to altered development of mini-column width.

Tension based model

It has also been hypothesized that tension along fiber bundles between cortico-cortical connections may be the driving force for the cortical folding pattern and therefore surface area (Van Essen, 1997). In this model, the developmental increase in surface area and

thesis_LW_V3.indb 187 06/06/16 07:38

cortical folding is considered an evolutionary strategy to minimize axonal length in order to save energy and time during signaling. With increasing brain size, tension along the axons of short-range connections would increase the cortical folding pattern and as a result affect cortical surface area. However, computational models do not seem to support this hypothesis: although axons were found to be under considerable tensions in the developing brain these tensions were mostly observed in subcortical tracts rather than tracts between gyri (Im, Lee, Lyttelton, Kim, & Evans, 2008; Xu et al., 2010). As such, fiber tension may have a modulating effect on cortical folding yet the tension model cannot fully explain the folding patterns observed.

Differential growth model

The differential growth hypothesis postulates that distinct layers of the cortex have differential growth patterns so that faster growth rate of inner layers results in the formation of sulci, while slower growth of inner layers forms gyri (Richman, Stewart, & Hutchinson, 1975). Simulation models showed that this model would induce gyrification similar to the patterns observed in the cortex (Razavi, Zhang, Liu, & Wang, 2015). However, this theory would also suggest that the development of surface area is highly related to cortical thickness development, which is in contrast with our findings.

Although none of the theories above can fully explain our observations, a combination of these theories could do so. Moreover, different mechanisms may be involved in different developmental periods.

Cortical subplate

In addition to the models described, there is another issue that may contribute to developmental changes in cortical morphometry. It has been shown that the grey-white matter border is harder to detect with increasing age in adults. This is thought to be related to myelin formation in the cortical subplate (Westlye et al., 2009). Surface area is typically measured along the white- grey matter border hence, a shift of this border upwards into the cortex would increase estimates of surface area and simultaneously reduce thickness. We cannot directly infer from our results whether this also applies to our findings. However, we did find white matter increases in childhood that were in parallel with cortical thinning and increases in surface area. However, it does not correspond with the surface area decreases

thesis_LW_V3.indb 188 06/06/16 07:38

we observed in adolescence. In addition, the observation that CSF in the subarachnoid space and ventricles increases during typical brain development suggests that the process of cortical gray matter reductions represent some "true" loss of neural elements (Jernigan, Trauner, & Hesselink, 1991).

Neural mechanisms in subcortical development

Unfortunately, relatively little is known about the mechanisms underlying developmental changes observed for subcortical structures (e.g. Chapter 3). Subcortical structures are surrounded by large white matter tracts. As such, increases in myelination could potentially cause similar effects for detecting the grey-white matter border as has been suggested for the cortical subplate. This may partly explain the observed decreases in volume of e.g. striatal structures.

As subcortical structures lack a columnar organization, theories like the radial unit hypothesis do not apply. Rather, subcortical regions are organized in nuclei. Interestingly, some studies have shown regional differences in maturational patterns of subparts within a single brain structure (e.g. Gogtay et al., 2006). Hence, to study constituent parts of subcortical structures is an important next step in understanding the mechanisms involved in subcortical development.

Components of plasticity - the biologist's view

The timing and magnitude of brain development differs per region, where regional grey matter volumes may change by as much as 10% from childhood into adolescence (Giedd et al., 2015; Wilke, Krägeloh-Mann, & Holland, 2007). On a micro-scale, these changes must be tremendous since a $1mm^3$ voxel may contain up to 70 million neurons. Hence, the observed increase in hippocampal volume of almost $1000mm^3$ from childhood into adolescence (see Chapter 3) may reflect changes in trillions of neurons and connections. Although it is currently not possible to directly relate developmental change in MRI to developmental changes in cellular or synaptic anatomy, findings from post mortem research and animal studies may inform us about possible underlying mechanisms involved in our findings. In the next section we will discuss studies on cellular processes that may give rise to the developmental changes observed for grey and white matter voxels.

thesis_LW_V3.indb 189 06/06/16 07:38

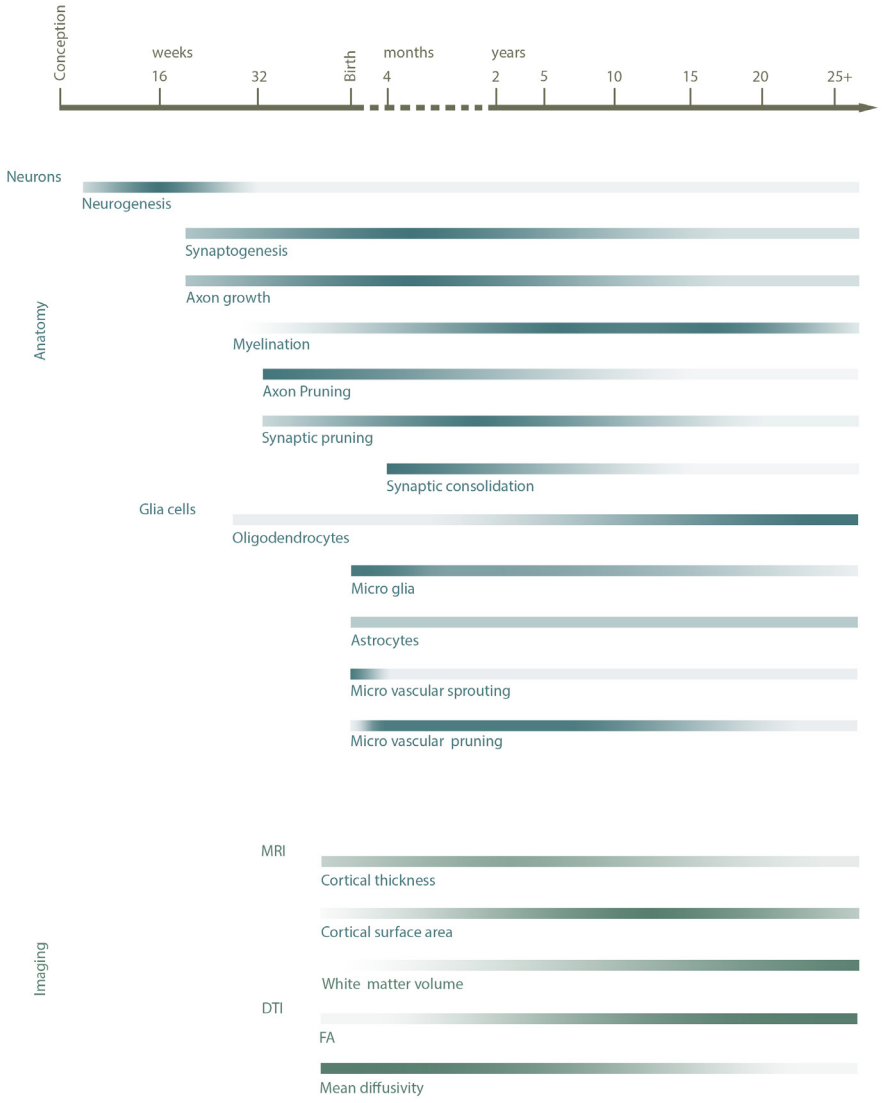

Figure 1 Time line of major neurobiological events in brain development (top) and global neuroimaging observations (bottom). The color intensity of each bar corresponds to the intensity of the event or relative change in tissue type. Modified and adapted from Giedd et al. (1999).

thesis_LW_V3.indb 190 06/06/16 07:38

Grey matter voxels

After birth the number of neurons is believed to be stable across age (with the exception of the hippocampus and olfactory bulb), as such developmental changes in gray matter as observed using MR are unlikely to be related to changes in the number of neural cells (Huttenlocher, 1990; Ghashghaei, Lai, & Anton, 2007). An often-postulated candidate for the volume changes in MRI is changes in synaptic density. Synaptogenesis has been shown to be ongoing throughout the brain, with large rates at an early age (see Figure 1). In early stages of brain development, this process is thought to occur relatively randomly and is therefore hypothesized to be regulated by intrinsic local factors. After two years of age, synaptogenesis has been observed to coincide with synapse elimination. This process of synaptic pruning is thought to be more selective and may be largely experience driven. The rates of synaptogenesis and pruning shifts with age resulting in a net decrease in synaptic density in late childhood, with almost half of the number of synapses eliminated by adulthood (Bourgeois, Goldman-Rakic, & Rakic, 1994; Huttenlocher, 1990). Although these net rates of synaptic density cannot directly be compared to observed changes in the MR signal, they are a popular explanation for the developmental changes observed. However, the total volume that synapses encompass is only a fraction of the total grey matter volume (estimated to be less than 1.5% of cortical volume) and therefore cannot fully explain the marked decreases in cortical volume (up to 10% reductions). Yet, synaptogenesis coincides with many other events. These events include changes in number of dendrites and axons, myelination of subcortical axons, vascular sprouting and pruning, and changes in glia cells (for an overview see Figure 1). Though, the timing and magnitude of these processes differs substantially, they all support connectivity in one way or another. Although we cannot directly compare these neural processes to our MRI findings, the inverted U-shaped developmental trajectories in grey matter structures may hold important information on the timing of plasticity: processes that support synaptogenesis seem to dominate brain maturation before a peak in grey matter volume is observed while synaptic and dendritic elimination seem to co-occcur with decreasing volume rates.

thesis_LW_V3.indb 191 06/06/16 07:38

White matter voxels

In addition to white matter volume measurements, DTI provides contrasts that have proven to be useful in unraveling white matter structure and integrity. However, the interpretation of developmental changes in measures of anisotropy and diffusivity is not always straightforward.

White matter is dominated by myelin content, which plays an important role in conduction velocity along axonal projections. Developmental increases in anisotropy and decreases in diffusivity are generally thought to be related to myelin content, hence changes in these values are thought to support effective communication between distant brain regions. But there are also other candidates for the observed changes in diffusion values, such as changes in fiber organization and axonal packing density (see Figure 2). The later process is a less likely candidate for the observed changes in our age range, as prenatal elongation of axons is dominated by an overgrowth at an early age followed by selective elimination later in life (Price et al., 2006). Hence a net increase in number of axons is questionable.

A limitation with regard to the interpretation of developmental changes in fractional anisotropy (FA) is its sensitivity to crossing fibers: an increase in crossing fibers may reduce the FA signal (see Figure 2). Hence, in areas of crossing fibers an increase in myelination may nevertheless reduce the FA signal. For this reason we chose to use mean diffusivity (MD) over FA as a measure of white matter maturation in chapter 4. Next to axons and myelin, white matter contains approximately 48% astrocytes. Although rarely taken into consideration, astrocytes have been shown to affect values of diffusivity and anisotropy in animal models following injury (see review Concha, 2014). The number of astrocytes has been shown to be relatively stable across development, but it is unknown if and how developmental changes in astrocytic processes may affect diffusion values (O'Kusky & Colonnier, 1982; Walhovd, Johansen-Berg, & Káradóttir, 2014). Given the above we suggest that the observed developmental changes in Chapter 4, are likely to reflect increases in myelination, axon diameter or fiber organization, supporting increases in conduction velocity along fiber bundles.

Taken together, events that are reflected in gray and white matter voxels of the MR signal include facilitation of connectivity on a local level through synaptogenesis, synaptic

thesis_LW_V3.indb 192 06/06/16 07:38

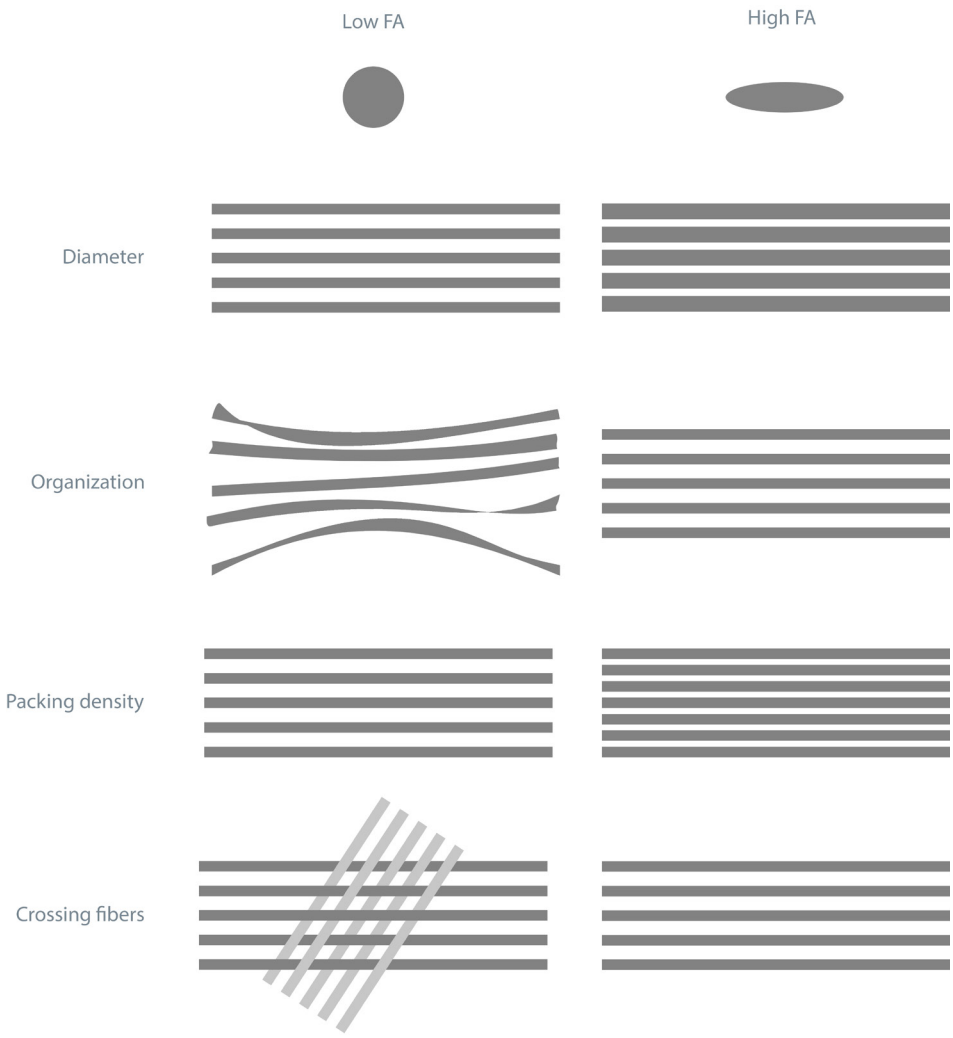

Figure 2 Schematic representation of maturational changes related to FA. Larger FA values are associated with increased fiber thickness, fiber organization and packing density. Note that even if all of the above-mentioned events take place, crossing fibers may reduce FA values (bottom row).

strengthening and pruning, but also global integration through modification of long-distance axons. All of these events promote connectivity and therefore contribute to the formation and fine-tuning of a complex neural network that enables the integration of functionally diverging brain regions. This fine-tuning is a delicate process as adequate timing of these mechanisms is important for healthy brain development.

thesis_LW_V3.indb 193 06/06/16 07:38

Lessons from atypical development

Developmental disorders may offer particular insight into which processes are key in typical brain development. We hypothesized in Chapter 1 that symptoms that emerge at certain ages might be associated with brain regions that show the greatest developmental change during at that age. Hence, developmental disorders that emerge in childhood may be associated with changes in different brain regions than those that emerge in adolescence. Bellow we describe our finding in a childhood onset disorder, ADHD, and an adolescent onset disorder, psychosis.

Surface area in ADHD

In Chapter 5, we observed that children with ADHD showed reductions in cortical surface area while cortical thickness was relatively preserved. This reduction was present at an early age and remained stable over the course of development. In line with the radial unit hypothesis this may indicate that the growth trajectory of each single mini-column is relatively preserved. Rather, the number of mini-columns may be more affected in ADHD and thus prenatal processes may be involved in the observed reduction in surface area. This is in line with the observation that the use of teratogenic substances during pregnancy is related to ADHD. These substances, such as nicotine and alcohol, target progenitor cells that regulate the number of mini-columns during prenatal brain development (Banerjee, Middleton, & Faraone, 2007; Linnet et al., 2003). Further support for this hypothesis comes from the observation that a number of genetic and molecular factors that regulate neuronal proliferation, have also been linked to ADHD (Poelmans, Pauls, Buitelaar, & Franke, 2011; Reif et al., 2011; Rivero et al., 2013). This suggests that the number of neurons and synaptic connections may be reduced in children with ADHD rather than neural and synaptic density.

The reduction in cortical surface area in children with ADHD was most apparent in frontal cortex. As changes in cognitive functioning are already present at an early age in children with ADHD, this may provide important insights for typical development: first it suggests that cortical surface area is related to cognitive functioning. And second it shows that even though these frontal regions mature relatively late, they already play an important role in cognitive functioning earlier in life.

thesis_LW_V3.indb 194 06/06/16 07:38

Brain trajectories in psychosis

Adolescents at ultra high risk for psychosis showed changes in brain structure that were stable with age, as well as changes in developmental trajectories (see Chapter 6). We predominantly found differences in parietal and frontal regions with slower decreases in surface area development in the UHR group than controls. These slower decreases in surface area could point to a delayed or elongated sensitive period. This highlights that the process of surface area reduction in frontal and parietal regions is an important process for healthy brain development.

Subcortical structures showed the opposite pattern: UHR subjects showed steeper decreases in thalamus and hippocampus volume than controls. These faster declines may indicate that sensitive windows in these regions may be shortened and hence these regions may not be fully developed. This suggests that the length and timing of plastic windows is important for typical brain development.

We observed several differences between UHR subjects with good clinical outcome (resilient individuals) and those with poor clinical outcome (non-resilient individuals): first some structures showed stable differences over the entire age range, with larger structures for resilient individuals than non-resilient individuals, which may indicate a compensatory mechanism. Second, some structures, such as the anterior cingulate gyrus, showed similar reductions for both groups at baseline but its volume stabilized in the resilient group while it continued to decline in non-resilient individuals. Third, there were structures including the hippocampus and thalamus that showed reductions in both resilient and non-resilient individuals compared to typical developing controls. Thus, although these regions were reduced in both groups compared to controls these reductions were not exclusively related to transition into psychosis. Nevertheless, they might play an important role in increased risk. This indicates that the balance between regional development rather than the developmental pattern of a single region may be important for clinical outcome.

thesis_LW_V3.indb 195 06/06/16 07:38

Methodological considerations

The studies in this thesis have several strengths, for example the sample sizes are relatively large and the longitudinal approach dramatically increased power: e.g. in order to detect a 5% group difference in whole brain volume with a power of 80%, you would need at least 73 participants per group in a cross-sectional study design, whereas in a longitudinal design 5 subjects per group is sufficient (Steen, Hamer, & Lieberman, 2007). This is particularly important when comparing age groups. The samples in the present thesis therefore have comparable power to cross-sectional studies of more than 1000 participants. Nevertheless, the interpretation of our results or developmental MRI studies in general is challenging for a number of reasons. Below we describe these challenges and how we addressed them.

Subject motion

MRI techniques are sensitive to several confounding effects, such as crossing fibers, partial volume effects, and head motion. The latter is particularly troublesome in developmental research involving children as systematic variations with age and between clinical groups may induce spurious findings. Accounting for the effects of motion is challenging, in particular for diffusion imaging. Movement may cause miss-alignment between images within scanning series. In addition, motion may alter the diffusion value by causing microscopic random movement of water molecules. The first issue can be addressed with standardized realignment algorithms. However, the latter issue is more difficult to control. Yendiki and colleagues (2013) showed that movement is likely to result in an underestimation of FA values; they compared children with autism to typically developing children and showed that group differences in motion partly explained the observed group differences in diffusion values. Not only diffusion images, but also T1 contrasted images have shown to be affected by movement, and this has been linked to underestimation of cortical thickness (Reuter et al., 2015).

One strategy to reduce the effects of head motion was to retrospectively remove outliers either by visual inspection or statistical methods. A study of Ducharme and colleagues (2015) indicated the significance of such outlier removal procedures. They showed that the level of quality control, e.g. the criteria for outlier removal, affected estimates of cortical

thesis_LW_V3.indb 196 06/06/16 07:38

thickness, and hence the observed developmental trajectory. We developed an in-house quality control protocol to reduce the impact of movement on our results: independent trained raters visually inspected all scans and manual edits were applied where necessary. As the effects of micro-movements are not always detectable by visual inspection, we additionally applied a statistical outlier detection procedure. Although this strategy may be somewhat stringent, we felt the magnitude of the problem justified this method.

Adjustment for total brain volume

There is substantial variation in total brain volume between subjects. For example males have on average 10% larger brain volume than females. The interpretation of sexual dimorphisms in subcomponents of the brain is therefore greatly affected by the way this difference is accounted for. An often-used strategy is to use total brain volume (TBV) as a covariate when comparing volume size of structures between groups. However, the interpretation of group differences may vary to a large extent depending on whether total brain volume is co-varied for or not. And hence, finding "true" group differences may be complicated by differences in overall brain size.

Although often used, co-varying for total brain volume may induce spurious findings for several reasons. First, it violates the assumption that the covariate itself should not have any systematic relation between the groups (see e.g. Field, 2009). This has important implications, as observed differences in the covariate between non-randomly assigned groups (e.g. gender) may reflect a group difference that is inherent to group membership (Miller & Chapman, 2001). For example, when comparing 3rd and 4th graders on test performance, an ANCOVA might seem appropriate to test whether groups differ on test performance if they were not different in age. However, 4th graders are inherently not 3rd graders, and there is no way to "control" for that fact by using "age" as a covariate. Rather, the purpose of a covariate is to "remove" variance from the dependent variable to increase statistical power, as is illustrated in the upper part of Figure 3. If the assumption that the covariate should not vary between the groups is violated (e.g. age differs between 3rd and 4th graders) the covariate will not only remove variance from the dependent variable but will additionally alter the group variable (see lower part of Figure 3). This renders the results uninterpretable as it has poor construct validity. Although it may seem reasonable to

thesis_LW_V3.indb 197 06/06/16 07:38

"control" for the differences in total brain volume between genders or clinical groups, there is no reliable statistical way to control for these pre-existing differences between groups.

A second complicating factor of including TBV as a covariate is related to the relation between size and shape. Volume is a three-dimensional measure while thickness and surface area are 1 and 2 dimensional, respectively. Correcting a lower order dimension (thickness) with a higher order one (volume) results in overcorrection. More importantly, thickness increases only slightly with increasing brain size between subjects and even between species while surface area increases to a larger extent with increasing total brain size (Im, Lee, Lyttelton, Kim, & Evans, 2008). Thus, adding total brain volume as a linear covariate would affect data on thickness and surface area differently in smaller compared to larger brains.

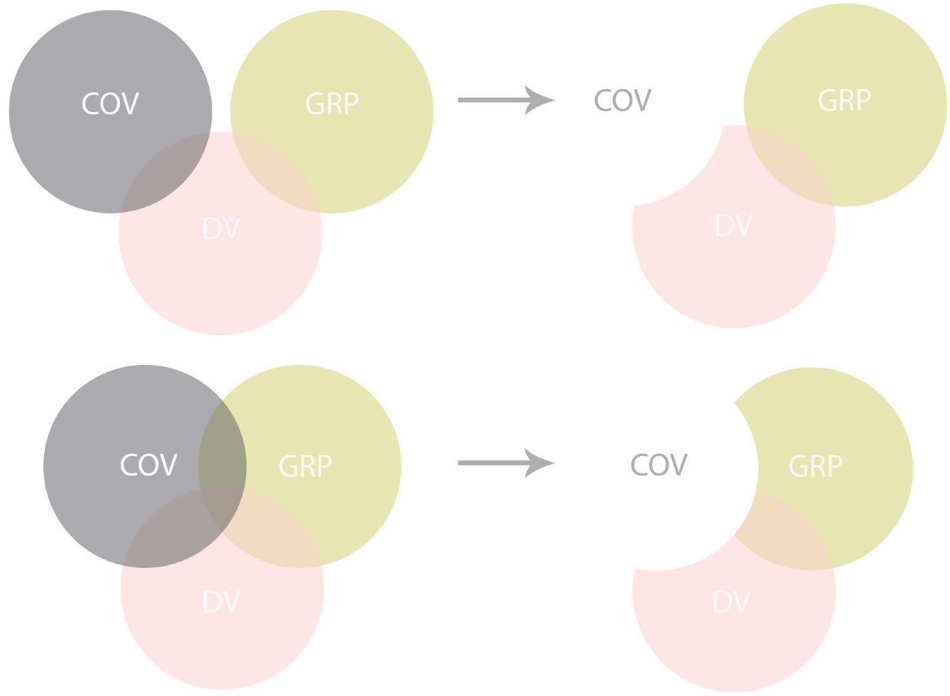

Figure 3 Illustration of the effect of a covariate on group variable. In the top part the covariate does not hold any systematic relation with the grouping variable and herewith successfully reduces variance and herewith increases power. However, as the bottom half illustrates, adding a covariate to the model becomes problematic when it holds any systematic relation with the grouping variable. It not only removes variance from the dependent variable, but will also remove an unknown part of the variation of interest, herewith making results challenging to interpret.

thesis_LW_V3.indb 198 06/06/16 07:38

Third, the relation between TBV and volume differs per region. Thus, the extent of "correction" would differ throughout the brain. Last, TBV shows non-linear change with age and hence would affect a particular volume of interest in a different way at different ages. Thus, especially when investigating developmental aspects of brain morphometry, the interpretation after co-varying for total brain volume is challenging. This does not only apply to comparing genders but also affects the comparison of clinical groups. For example, we showed in Chapter 6 that children with ADHD have smaller total brain volumes than typically developing children. Hence, including TBV as a covariate would have violated the assumption that the covariate did not differ between groups. In sum, the question whether to control for TBV and how requires sufficient consideration.

A matter of scale

In addition to the issues mentioned above, developmental studies in humans are limited by the non-invasive imaging techniques that are currently available. The main limitation is spatial resolution, which means it is currently impossible to detect changes at the neuronal level, or trace - for example - short cortical U-fibers in humans in vivo. It should also be kept in mind that all measures in our studies are derived from reconstructions. The reconstruction algorithms face many challenges, such as crossing fibers or detection of the grey-white matter border. Our results are therefore inherently limited by these factors.

Avenues for future developmental research

The limitations described above highlight the need for independent replication. Unfortunately to date there are only a limited amount of longitudinal samples available. Furthermore, our work and that of others highlights the large inter-individual variability in brain morphology. Little is known about individual variation in brain developmental trajectories and should be the focus of future research. For example, how does the sequential development of brain structures of the average population translate at an individual level? Is the organization of concordant (or discordant) maturation between structures essential for healthy brain functioning? In order to track these differences in developmental trajectories between individuals, large cohorts that follow individuals over a long time period are necessary.

However, by increasing the number of time points, imaging modalities (e.g. T1, DTI,

thesis_LW_V3.indb 199 06/06/16 07:38

genetics), and measures of interest (e.g. 20.000 voxels in an average T1 scan) data complexity also dramatically increases. This gives rise to a new issue: the so-called "big data" problem. The currently available statistical methods and software tools to unravel complex patterns between data types of different modalities are insufficient. Although the resolution of imaging techniques will improve, and datasets will likely become larger and of higher quality, the biggest challenge of the next decade may lie in developing methods that will permit us to uncover the complex patterns of development from such large multimodal datasets.

thesis_LW_V3.indb 200 06/06/16 07:38

Concluding remarks

The complexity of brain development is reflected by the heterogeneous patterns reported. Together with observations of regional non-linear developmental changes, this leads us to conclude that the brain is differently structured and wired in childhood, adolescence and adulthood. Observed rapid changes in grey matter areas and white matter connections during childhood and adolescence suggest that over the course of development the brain shifts from a relatively malleable state into a more stable and efficient one. The results from the clinical studies in Part II of this thesis indicate that changes in regional developmental trajectories may be related to behavioral changes. Therefore, mapping the timing of regional patterns may be informative for unraveling the brain behavior relationship and may help us to understand when the brain is most malleable and adaptive.

thesis_LW_V3.indb 201 06/06/16 07:38

References

Aubert-Broche, B., Fonov, V. S., García-Lorenzo, D., Mouiha, A., Guizard, N., Coupé, P., et al. (2013). A new method for structural volume analysis of longitudinal brain MRI data and its application in studying the growth trajectories of anatomical brain structures in childhood. NeuroImage, 82, 393–402. http://doi.org/10.1016/j.neuroimage.2013.05.065

Banerjee, T. D., Middleton, F., & Faraone, S. V. (2007). Environmental risk factors for attention-deficit hyperactivity disorder. Acta Paediatrica (Oslo, Norway : 1992), 96(9), 1269–1274. http://doi.org/10.1111/j.1651-2227.2007.00430.x

Bourgeois, J.-P., Goldman-Rakic, P. S., & Rakic, P. (1994). Synaptogenesis in the Prefrontal Cortex of Rhesus Monkeys. Cerebral Cortex, 4(1), 78–96. http://doi.org/10.1093/cercor/4.1.78

Buxhoeveden, D., Lefkowitz, W., Loats, P., & Armstrong, E. (1996). The linear organization of cell columns in human and nonhuman anthropoid Tpt cortex. Anatomy and Embryology, 194(1), 23–36.

Concha, L. (2014). A macroscopic view of microstructure: using diffusion-weighted images to infer damage, repair, and plasticity of white matter. Neuroscience, 276, 14–28. http://doi.org/10.1016/j.neuroscience.2013.09.004

Field, A. (2009). Field: Discovering statistics using SPSS - Google Scholar.

Ghashghaei, H. T., Lai, C., & Anton, E. S. (2007). Neuronal migration in the adult brain: are we there yet? Nature Reviews. Neuroscience, 8(2), 141–151. http://doi.org/10.1038/nrn2074

Giedd, J. N., Blumenthal, J., & Jeffries, N. O. (1999). Brain development during childhood and adolescence: a longitudinal MRI study. Nature Neuroscience 2, 861 – 863. doi:10.1038/13158

Giedd, J. N., Raznahan, A., Alexander-Bloch, A., Schmitt, E., Gogtay, N., & Rapoport, J. L. (2015). Child psychiatry branch of the National Institute of Mental Health longitudinal structural magnetic resonance imaging study of human brain development. Neuropsychopharmacology : Official Publication of the American College of Neuropsychopharmacology, 40(1), 43–49. http://doi.org/10.1038/npp.2014.236

thesis_LW_V3.indb 202 06/06/16 07:38

Gogtay, N., Nugent, T. F., Herman, D. H., Ordonez, A., Greenstein, D., Hayashi, K. M., et al. (2006). Dynamic mapping of normal human hippocampal development. Hippocampus, 16(8), 664–672. http://doi.org/10.1002/hipo.20193

Huttenlocher, P. R. (1990). Morphometric study of human cerebral cortex development. Neuropsychologia, 28(6), 517–527. http://doi.org/10.1016/0028-3932(90)90031-I

Huttenlocher, P. R., & Dabholkar, A. S. (1997). Regional differences in synaptogenesis in human cerebral cortex. The Journal of Comparative Neurology, 387(2), 167–178

Im, K., Lee, J. M., Lyttelton, O., Kim, S. H., & Evans, A. C. (2008). Brain size and cortical structure in the adult human brain. Cerebral Cortex, 18(9), 2181–2191. http://doi.org/10.1093/cercor/bhm244

Jernigan, T. L., Trauner, D. A., & Hesselink, J. R. (1991). Maturation of human cerebrum observed in vivo during adolescence. Brain : a Journal of Neurology. http://doi.org/10.1093/brain/114.5.2037

Kelly, K. R., DeSimone, K. D., Gallie, B. L., & Steeves, J. K. E. (2015). Increased cortical surface area and gyrification following long-term survival from early monocular enucleation. NeuroImage: Clinical, 7, 297–305. http://doi.org/10.1016/j.nicl.2014.11.020

Lebel, C., & Beaulieu, C. (2011). Longitudinal development of human brain wiring continues from childhood into adulthood. The Journal of Neuroscience : the Official Journal of the Society for Neuroscience, 31(30), 10937–10947. http://doi.org/10.1523/JNEUROSCI.5302-10.2011

Linnet, K. M., Dalsgaard, S., Obel, C., Wisborg, K., Henriksen, T. B., Rodriguez, A., et al. (2003). Maternal Lifestyle Factors in Pregnancy Risk of Attention Deficit Hyperactivity Disorder and Associated Behaviors: Review of the Current Evidence. American Journal of Psychiatry, 160(6), 1028–1040. http://doi.org/10.1176/appi.ajp.160.6.1028

Miller, G. A., & Chapman, J. P. (2001). Misunderstanding analysis of covariance. Journal of Abnormal Psychology, 110(1), 40–48.

O'Kusky, J., & Colonnier, M. (1982). Postnatal changes in the number of astrocytes, oligodendrocytes, and microglia in the visual cortex (area 17) of the macaque monkey: A stereological analysis in normal and monocularly deprived animals. The Journal of

thesis_LW_V3.indb 203 06/06/16 07:38

Comparative Neurology, 210(3), 307–315. http://doi.org/10.1002/cne.902100309

Panizzon, M. S., Fennema-Notestine, C., & Eyler, L. T. (2009). Distinct genetic influences on cortical surface area and cortical thickness. Cerebral Cortex, 19(11), 2728–2735. http://doi.org/10.1093/cercor/bhp026

Poelmans, G., Pauls, D. L., Buitelaar, J. K., & Franke, B. (2011). Integrated genome-wide association study findings: identification of a neurodevelopmental network for attention deficit hyperactivity disorder. American Journal of Psychiatry, 168(4), 365–377. http://doi.org/10.1176/appi.ajp.2010.10070948

Price, D. J., Kennedy, H., Dehay, C., Zhou, L., Mercier, M., Jossin, Y., et al. (2006). The development of cortical connections. European Journal of Neuroscience, 23(4), 910–920. http://doi.org/10.1111/j.1460-9568.2006.04620.x

Rakic, P. (1988). Specification of cerebral cortical areas. Science (New York, N.Y.).

Razavi, M. J., Zhang, T., Liu, T., & Wang, X. (2015). Cortical Folding Pattern and itsConsistency Induced by BiologicalGrowth. Nature Publishing Group, 1–14. http://doi.org/10.1038/srep14477

Raznahan, A., Shaw, P., Lalonde, F., Stockman, M., Wallace, G. L., Greenstein, D., et al. (2011). How does your cortex grow? The Journal of Neuroscience : the Official Journal of the Society for Neuroscience, 31(19), 7174–7177. http://doi.org/10.1523/JNEUROSCI.0054-11.2011

Reif, A., Nguyen, T. T., Weissflog, L., Jacob, C. P., Romanos, M., Renner, T. J., et al. (2011). DIRAS2 is associated with adult ADHD, related traits, and co-morbid disorders. Neuropsychopharmacology : Official Publication of the American College of Neuropsychopharmacology, 36(11), 2318–2327. http://doi.org/10.1038/npp.2011.120

Reuter, M., Tisdall, M. D., Qureshi, A., Buckner, R. L., van der Kouwe, A. J. W., & Fischl, B. (2015). Head motion during MRI acquisition reduces gray matter volume and thickness estimates. NeuroImage, 107, 107–115. http://doi.org/10.1016/j.neuroimage.2014.12.006

Richman, D. P., Stewart, R. M., & Hutchinson, J. W. (1975). Mechanical mode of brain convolutional development. Science, 189(4196), 18-21

thesis_LW_V3.indb 204 06/06/16 07:38

Rivero, O., Sich, S., Popp, S., Schmitt, A., Franke, B., & Lesch, K.-P. (2013). Impact of the ADHD-susceptibility gene CDH13 on development and function of brain networks. European Neuropsychopharmacology : the Journal of the European College of Neuropsychopharmacology, 23(6), 492–507. http://doi.org/10.1016/j.euroneuro.2012.06.009

Steen, R. G., Hamer, R. M., & Lieberman, J. A. (2007). Measuring Brain Volume by MR Imaging: Impact of Measurement Precision and Natural Variation on Sample Size Requirements. American Journal of Neuroradiology, 28(6), 1119–1125. http://doi.org/10.3174/ajnr.A0537

Tamnes, C. K., Walhovd, K. B., Dale, A. M., Østby, Y., Grydeland, H., Richardson, G., et al. (2013). Brain development and aging: Overlapping and unique patterns of change. NeuroImage, 68, 63–74. http://doi.org/10.1016/j.neuroimage.2012.11.039

Thomas, A. G. (2012). The effects of aerobic activity on brain structure, 1–9. http://doi.org/10.3389/fpsyg.2012.00086/abstract

Van Essen, D. C. (1997). A tension-based theory of morphogenesis and compact wiring in the central nervous system. Nature, 385(6614), 313–318. http://doi.org/10.1038/385313a0

Walhovd, K. B., Johansen-Berg, H., & Káradóttir, R. T. (2014). Unraveling the secrets of white matter – Bridging the gap between cellular, animal and human imaging studies. Neuroscience, 276, 2–13. http://doi.org/10.1016/j.neuroscience.2014.06.058

Wilke, M., Krägeloh-Mann, I., & Holland, S. K. (2007). Global and local development of gray and white matter volume in normal children and adolescents. Experimental Brain Research, 178(3), 296–307. http://doi.org/10.1007/s00221-006-0732-z

Winkler, A. M., Kochunov, P., Blangero, J., Almasy, L., Zilles, K., Fox, P. T., et al. (2010). Cortical thickness or grey matter volume? The importance of selecting the phenotype for imaging genetics studies. NeuroImage, 53(3), 1135–1146. http://doi.org/10.1016/j.neuroimage.2009.12.028

Yendiki, A., Koldewyn, K., Kakunoori, S., Kanwisher, N., & Fischl, B. (2013). Spurious group differences due to head motion in a diffusion MRI study. NeuroImage, 88C, 79–90. http://doi.org/10.1016/j.neuroimage.2013.11.027

thesis_LW_V3.indb 205 06/06/16 07:38

thesis_LW_V3.indb 206 06/06/16 07:38

NEDERLANDSE SAMENVATTING

thesis_LW_V3.indb 207 06/06/16 07:38

Nederlandse samenvatting

De ontwikkeling van de hersenen

De ontwikkeling van het brein is een dynamisch proces. Zo worden er tijdens de vroege ontwikkeling biljoenen verbindingen tussen neuronen gelegd; de synapsen. Vele van deze verbindingen verdwijnen tijdens de kindertijd weer, terwijl andere verbindingen juist verstevigd worden. In volwassenen zijn nog maar de helft van het aantal verbindingen overgebleven die in de kindertijd zijn aangelegd. We denken dat deze dynamische processen bijdragen aan de plasticiteit van het brein. Deze periode van plasticiteit is uitzonderlijk lang bij mensen in vergelijking met andere diersoorten. Het zou kunnen dat dit belangrijk is voor het ontwikkelen van de juiste vaardigheden om ons aan te passen aan een omgeving die snel kan veranderen. Maar die lange periode van plasticiteit heeft ook een keerzijde; het maakt de mens kwetsbaar doordat ervaringen die een mens opdoet tijdens deze zogenaamde plastische periodes een groter en langdurig effect kunnen hebben op het brein. Als we zouden weten wanneer welke structuur in het brein deze periode van plasticiteit doormaakt, zouden we dit kunnen gebruiken om bijvoorbeeld behandelingen gerichter in te zetten.

Een manier om dit te onderzoeken is door het ontwikkelende brein in beeld te brengen met behulp van beeldvormende technieken, zoals Magnetic Resonance Imaging (MRI). Deze techniek heeft het grote voordeel dat het non-invasief is, dit maakt het mogelijk om hersenen van mensen in vivo te bestuderen en de hersenen van hetzelfde individu meerdere malen in verschillende levensfases te onderzoeken. Het doel van dit proefschrift is om met behulp van deze techniek een gedetailleerde beschrijving te geven van ontwikkelingstrajecten van verschillende structuren in de hersenen. Daarbij nemen we de verschillende dimensies (oppervlakte, dikte) van de hersenschors mee, en ook hoe de verbindingen tussen de verschillende hersenstructuren veranderen in kinderen en adolescenten. Om dit goed te kunnen doen is het van groot belang om niet alleen individuen van verschillende leeftijden met elkaar te vergelijken, maar ook om de veranderingen binnen hetzelfde individu in kaart te brengen. De MRI techniek maakt dit mogelijk. We hebben hiervoor gebruik gemaakt van longitudinale datasets waarbij individuen tussen de 7 en 23 jaar oud elke twee jaar zijn onderzocht. Ook waren we geïnteresseerd óf, en zo ja hóe, het brein anders ontwikkelt bij individuen met een ontwikkelingsstoornis. Daarom hebben we in dit proefschrift ook een

thesis_LW_V3.indb 208 06/06/16 07:38

studie opgenomen naar hersenontwikkeling bij kinderen met Attention Deficit/Hyperactivity Disorder (ADHD) en een studie over adolescenten met een verhoogd risico op psychose. De resultaten van deze studies kunnen ons helpen te begrijpen welke leeftijdsgebonden processen belangrijk of zelfs essentieel zijn voor de typische ontwikkeling van de hersenen.

De hersenschors in 4D

De studie beschreven in hoofdstuk 2 brengt de complexe ontwikkeling van de hersenschors, ook wel cortex genoemd, in kaart. Allereerst hebben we de cortex opgedeeld in verschillende gebieden aan de hand van individuele morfologische oriëntatiepunten, zoals de vouwingen in de cortex. Voor ieder gebied zijn de ontwikkeling voor drie dimensies in kaart gebracht door de leeftijdsverandering van zowel dikte als de oppervlakte te meten. Wat blijkt is dat de oppervlakte en dikte van de cortex verschillende ontwikkelingspatronen laten zien. Zo neemt de dikte van de cortex in de leeftijd van 7 tot 23 lineair af terwijl de oppervlakte in sommige gebieden tot de leeftijd van 13 jaar toeneemt alvorens af te nemen. Als je alleen het volume van ieder gebied zou beschouwen, zoals in eerdere studies vaak het geval was, dan zouden deze veranderingen in de verschillende dimensies van de cortex elkaar kunnen uitbalanceren. Hierdoor zou je de groei van de cortex kunnen onderschatten, doordat het zou kunnen lijken dat de cortex bijvoorbeeld niet ontwikkelt of alleen maar afneemt met leeftijd. Ieder hersengebied heeft zijn eigen unieke patroon van oppervlakte- en dikteontwikkeling. De resultaten van deze studie onthullen nog een paar belangrijke principes over de ontwikkeling van de cortex: veranderingen in corticaal volume zijn met name gerelateerd aan veranderingen in corticale oppervlakte en in veel mindere mate aan corticale dikte. Verder observeerden we dat mannen voor veel structuren een groter oppervlakte hebben dan vrouwen terwijl de dikte van de cortex grotendeels gelijk is tussen mannen en vrouwen. Al deze resultaten bij elkaar benadrukken hoe belangrijk het is om corticale dikte en oppervlakte los van elkaar te onderzoeken omdat ze beide andere aspecten van hersenontwikkeling onthullen. Deze resultaten kunnen ons helpen gerichter te zoeken naar welke genetische en omgevingsfactoren een rol spelen in typische en atypische hersenontwikkeling.

thesis_LW_V3.indb 209 06/06/16 07:38

Ontwikkeling van diepe kernen en kleine hersenen

In hoofdstuk 3 brengen we de ontwikkelingstrajecten van de volumes van een aantal hersenkernen in kaart in individuen tussen de 7 en 23 jaar oud. Deze gebieden spelen een belangrijke rol in basale processen van het brein. Zo zijn de basale ganglia (putamen, caudate en globus pallidus) betrokken bij het controleren van bewegingen, motivatie en beloning. De hippocampus staat bekend om zijn centrale rol in geheugenprocessen en is samen met de amygdala onderdeel van het limbische systeem. Dit systeem is onder andere betrokken bij het ervaren van emotie en het emotioneel geheugen. Een andere centrale kern is de thalamus; deze structuur selecteert welke sensorische prikkels naar de hersenschors worden doorgestuurd. Tenslotte hebben we de ontwikkeling van het cerebellum onderzocht, ofwel de kleine hersenen. Deze zijn betrokken bij fijne motoriek. Minder bekend is dat het cerebellum ook een rol speelt in cognitieve processen. Omdat deze processen bij kinderen en adolescenten nog volop in ontwikkeling zijn, is het cerebellum een belangrijke structuur om mee te nemen in ons onderzoek naar hersenontwikkeling. Eerdere onderzoeken laten zien dat deze structuren andere activatiepatronen vertonen in individuen met een ontwikkelingsstoornis, daarom is het van belang om in kaart te brengen hoe deze structuren typisch ontwikkelen. De resultaten laten zien dat al deze structuren veranderen van grootte in de leeftijd van 7 tot 23 jaar. De specifieke patronen van de ontwikkelingstrajecten verschillen echter per structuur: zo nemen de volumes van de basale ganglia af, waarbij de putamen en caudate de grootste afname in volume laten zien. De volumes van de thalamus, globus pallidus, hippocampus en amygdala laten een ander ontwikkelingstraject zien: bij jonge kinderen nemen de volumes toe, terwijl bij oudere kinderen en adolescenten er een afname plaatsvindt. Door dit omslagpunt, of volumepiek, tussen de verschillende hersenstructuren te vergelijken kunnen we misschien iets te weten komen over de relatieve ontwikkelingsfase van iedere hersenkern. Een eerdere volumepiek zou een eerdere ontwikkelingsfase of kortere plastische periode aan kunnen geven. Als dit zo is dan ontwikkelen de basale ganglia zich eerst, gevolgd door de thalamus, dan het globus pallidum, het cerebellum en het langst plastisch blijken de hippocampus en amygdala.

thesis_LW_V3.indb 210 06/06/16 07:38

Verbindingen in het brein

Alle gebieden in de hersenen staan in verbinding met elkaar en vormen zo een geïntegreerd netwerk. Ze worden verbonden door axonen. Hierdoor kunnen hersengebieden die niet direct naast elkaar liggen toch informatie uitwisselen. Dit netwerk zou u kunnen vergelijken met het wegennetwerk van Nederland. De snelheid en hoeveelheid waarmee mensen en goederen zich kunnen verplaatsen tussen plaats A en B is afhankelijk van de kwaliteit van de weg, zo gaat het verkeer een stuk sneller over een 8-baans snelweg dan een landelijke N-weg. U kunt zich wellicht voorstellen dat de grootte van een stad invloed heeft op hoeveel en wat voor soort wegen er naar toe lopen, en omgekeerd kan een goede verbinding er voor zorgen dat een stad goed bereikbaar is en wellicht vaker wordt bezocht. Zo zouden we kunnen zeggen dat we in hoofdstukken 2 en 3 hebben gekeken naar de groei van steden en dorpen; de hersengebieden. Even belangrijk voor het functioneren, maar minder bekend is hoe het wegennetwerk in het brein ontwikkelt. Dit onderzoeken we in hoofdstuk 4 met behulp van diffusie imaging, waarmee we een schatting kunnen maken van waar in het brein zich axonen bevinden en welke gebieden ze met elkaar verbinden. Uit voorgaande onderzoeken blijkt dat bij de geboorte het menselijk hersennetwerk, alle verbindingen en axonen (het wegennetwerk) al aanwezig is. Het is daarom niet waarschijnlijk dat er nieuwe verbindingen aangelegd worden of verdwijnen. Wat wel verandert tijdens de ontwikkeling is de kwaliteit van deze verbindingen. Dat gebeurt met name door myeline, een vetlaagje, dat zich om axonen wikkelt met geregelde tussen-openingen, of knopen. Dit zorgt ervoor dat signalen niet het hele axon af gaan, maar van opening naar opening worden doorgegeven. Een gemyeliniseerde axon kan op deze manier tot wel 300 keer sneller een signaal doorgeven dan een axon zonder myeline. Je zou kunnen stellen dat myeline van een landelijke weg een snelweg kan maken. Hierdoor kan het hele netwerk efficiënter worden.

De resultaten uit ons onderzoek bevestigen dit. Met behulp van zogenaamde “complexe netwerkanalyses” hebben we de leeftijdsverandering in padlengte van het hersennetwerk uitgerekend. Padlengte is de gemiddelde reisafstand tussen twee gebieden. Een afname in padlengte hebben we afgeleid uit de observatie dat diffusie waarden voor veel verbindingen afnamen. Echter de snelheid waarmee deze diffusiewaarden afnemen is zeer verschillend per verbinding. We denken dat verbindingen die niet veel veranderingen meer laten zien

thesis_LW_V3.indb 211 06/06/16 07:38

in deze leeftijdsgroep (7 tot 23 jaar) al bijna uitontwikkeld zijn, terwijl de verbindingen die met grote snelheid groeien nog volop in ontwikkeling zijn. Om er achter te komen welke verbindingen al uitontwikkeld en welke nog volop in ontwikkeling zijn, hebben we alle verbindingen in het brein verdeeld over vier categorieën. Daarbij vonden we dat er niet veel verandering plaats vindt in verbindingen tussen beide hersenhelften en ook niet in verbindingen tussen diepe kernen en de cortex. Wel zijn er grote veranderingen in ontwikkeling te zien in de verbindingen binnen en tussen de kwabben. Daarbij tonen de occipitale en temporale kwab de minste groei, terwijl de verbindingen binnen en tussen de frontale en pariëtale kwabben snel groeien en dus laat ontwikkelen. Dit betekent dus dat het efficiënter worden van het hele breinnetwerk in deze levensfase vooral komt doordat er wordt geïnvesteerd in verbindingen in gebieden die complexe informatie verwerken.

Breinontwikkeling in ADHD

Kinderen met ADHD hebben over het algemeen een kleiner breinvolume. Of dit gerelateerd is aan één of alle dimensies van de cortex is wat we onderzochten in hoofdstuk 5. We hebben daarvoor kinderen, adolescenten en jongvolwassenen met ADHD vergeleken met leeftijdsgenoten zonder ADHD. Een groot deel van deze kinderen hebben we twee of drie keer onderzocht. Onze data bevestigt het kleinere breinvolume bij kinderen met ADHD ten opzichte van kinderen zonder ADHD. Het kleinere volume in de cortex blijkt gerelateerd aan een kleiner oppervlakte van de cortex. De dikte is vrijwel hetzelfde in kinderen met en zonder ADHD. Dit verschil in oppervlakte van de cortex was stabiel over de hele leeftijdsgroep. Dit suggereert dat het verschil al vroeg tijdens de ontwikkeling is ontstaan. Een theorie is dat tijdens de aanleg van de cortex in de prenatale fase er minder neuronen naar de cortex zijn gemigreerd. De resultaten uit deze studie verklaren mogelijk dat er minder neuronale en synaptische verbindingen zijn in de cortex van kinderen met ADHD, maar dat de dichtheid van neuronen en synapsen intact is. De verschillen in corticale oppervlakte tussen kinderen met en zonder ADHD zijn het meest aanwezig in de frontale cortex. Dit onderstreept de belangrijke rol van dit gebied al in de vroege ontwikkeling van het kind.

thesis_LW_V3.indb 212 06/06/16 07:38

Ultra-hoog risico

Niet alleen bij ADHD maar ook bij andere stoornissen zoals angststoornissen, bipolaire stoornis, depressieve stoornis, eetstoornissen, verslaving en psychose worden vaak afwijkingen in de frontale cortex gevonden. De bovengenoemde stoornissen hebben met elkaar gemeen dat ze vaak tijdens de puberteit tot uiting komen; een periode waarin de frontale cortex de meeste groei doormaakt. Een vooraanstaande hypothese is dan ook dat de snelle groei van de frontale cortex in de puberteit een mogelijke aanleiding is voor het tot uiting komen van deze stoornissen. Het is echter niet duidelijk of voordat de symptomen van een stoornis tot uiting komt frontale afwijkingen al aanwezig zijn, omdat deze individuen vaak pas na het tot uiting komen van de stoornis worden onderzocht. Een uitzondering is het onderzoek naar psychose; een psychiatrische aandoening waarbij iemand tijdens een psychotische episode het normale contact met de werkelijkheid kwijt is. Omdat dit één van de meest voorkomende stoornissen is wordt er veel onderzoek gedaan naar het preventief diagnosticeren en behandelen van mensen met een verhoogd risico op psychose. Deze groep wordt gediagnostiseerd aan de hand van "ultra-hoog risico" (UHR) criteria. Deze criteria zijn gebaseerd op het hebben van subklinische symptomen en/of familiaire belasting. Ondanks dat 70% van deze risico groep geen psychose ontwikkelt, is het lange-termijn functioneren van meer dan de helft van deze groep slecht als men rekening houdt met cognitief en sociaal functioneren. Toch herstelt ook een groot deel van de UHR groep van de UHR symptomen en functioneert deze groep op latere leeftijd goed. Het bestuderen van individuen die voldoen aan UHR criteria is dan ook uitermate geschikt om te onderzoeken of er verschillen zijn in de hersenen - met name de frontale cortex – voorafgaand aan het krijgen van een psychose of cognitieve problemen in het algemeen.

De resultaten van deze studie staan beschreven in hoofdstuk 6. We hebben adolescenten tussen de 12 en 18 jaar die voldoen aan UHR criteria zes jaar lang gevolgd. Daarbij zijn tot drie hersenscans van ieder individu gemaakt waardoor we goed kunnen onderzoeken óf en hóe hersenen verschillen tussen individuen die op lange termijn goed en slecht functioneren. Vergeleken met de controlegroep hebben individuen die voldoen aan UHR criteria een langzamere ontwikkeling in corticale oppervlakte. Er zijn weinig verschillen in corticale dikte tussen de groepen. Daarnaast verschillen de individuen die voldoen

thesis_LW_V3.indb 213 06/06/16 07:38

aan UHR criteria en op lange termijn goed functioneren van UHR individuen die minder goed functioneren op lange termijn. De cortex was dikker en de oppervlakte nam minder snel af in UHR individuen die op lange termijn goed functioneerden dan individuen die na zes jaar slecht functioneerden. Dit verschil was het grootst in de linker frontaalkwab. Dus al voordat symptomen van psychose vol tot uiting komen verschillen deze individuen van individuen die op lange termijn goed functioneren. Omdat we hebben gekeken naar cognitief functioneren kan het ook zijn dat een kleiner oppervlakte van de cortex (inclusief frontale gebieden) mogelijk ook algemeen gerelateerd is aan psychopathologie.

thesis_LW_V3.indb 214 06/06/16 07:38

Afsluiting

De resultaten uit de studies beschreven in dit proefschrift onderstrepen de complexiteit van hersenontwikkeling. Elke hersengebied heeft zijn eigen unieke ontwikkelingspatroon, zo zien we bijvoorbeeld dat verschillende dimensies van de cortex in verschillende leeftijdsfases groeien. Ook veranderen de verbindingen tussen de hersengebieden in verschillende fases. De structuur van het brein verschilt dus aanzienlijk tussen kinderen, adolescenten en volwassenen. Elke leeftijdsfase heeft daardoor dan ook zijn eigen unieke functionele mogelijkheden en beperkingen. Snelle groei vertegenwoordigt mogelijk een gevoelige periode. Door de ontwikkelingspatronen in het brein in kaart te brengen kunnen we dus beter begrijpen wanneer die periodes per hersengebied plaatsvinden. Door dit voor zowel typische als atypische ontwikkeling te doen, weten we steeds meer over de relatie tussen hersenen en gedrag en hopen we uiteindelijk bij te dragen aan vroege diagnostiek en het gerichter inzetten van interventies.

thesis_LW_V3.indb 215 06/06/16 07:38

thesis_LW_V3.indb 216 06/06/16 07:38

Acknowledgements - Dankwoord

Dit proefschrift was niet tot stand gekomen zonder de hulp van de kinderen en ouders die deel hebben genomen aan ons onderzoek. Veel dank aan hun inzet en enthousiasme om mee te werken aan deze bijzondere projecten. Daarnaast is dit onderzoeksveld een wereldwijd team effort waarbij vele onderzoekers ons hebben geïnspireerd en de technische mogelijkheden hebben ontwikkeld om dit onderzoek te kunnen uitvoeren. Ik heb tijdens mijn promotie traject het voorrecht gehad te mogen samen werken met een aantal van deze onderzoekers en wil sommigen in het bijzonder bedanken.

Ten eerste wil ik mijn promotor bedanken. Sarah, bedankt voor je adviezen en je rotsvaste vertrouwen. Onze inhoudelijke discussies en je inzichten hebben me geholpen bij het ontwikkelen van mijn ideeën. Vanaf het begin stond je open voor alle nieuwe plannen waarmee ik bij je aan kwam en je hebt me de ruimte gegeven om dingen tot op de bodem uit te zoeken waar dan ook ter wereld. De creativiteit die door deze vrijheid ontstond heeft mij geholpen bij het ontwikkelen van mijn vaardigheden en het plezier in onderzoek doen bevorderd. Ik heb veel van je geleerd.

Marieke, mijn eerste co-promotor, wat voel ik mij gezegend dat ik onder jouw begeleiding mijn grote PhD project ben gestart, een beter begin kan ik me niet voorstellen. Toen leek het einde nog lang niet inzicht en nu is het dan zo ver. Gelukkig ben je al die tijd niet ver weg geweest en heb ik ook na je tijd bij NICHE veel gehad aan onze koffie momentjes.

Bob, co-promotor nummer twee, je bent nauw betrokken geweest bij het afronden van mijn promotie. Je deur staat altijd voor me open en zelfs als ik ver weg zit ben je bereikbaar voor de urgente kwesties. Bedankt voor je inzet om mijn promotie tot een goed einde te brengen.

Jay, what a great journey to start with you in your lab at UCSD. It was great fun going trough all the start up challenges together, of both working at UCSD and a new life in San Diego. The warm welcome by our coworkers at UCSD has been overwhelming, and I couldn't have been more grateful for my wonderful time there. It feels like having a second home away from home. Our meetings have been incredible inspiring and I hope we will continue our collaboration throughout our careers. I am proud to have you on my commitee.

Martijn, door de samenwerking met jou heb ik me met veel plezier bezig kunnen houden

thesis_LW_V3.indb 217 06/06/16 07:38

met complexe netwerk analyses. Daarnaast heb je hebt me gemotiveerd om alles uit mezelf te halen. Bij elke uitdaging kom jij met een vernieuwende blik en creatieve ideeën en weet je de papers naar een hoger level te tillen. Bedankt voor de brainstorm sessies en het mogelijk maken van dit leuke onderdeel van mijn promotie.

Ook bedank ik graag de leden van mijn commissie: Prof. Maja Dekovic, Prof. Eveline Crone, Prof. Marian Joels, Prof. Iris Sommer and Prof. Walter Matthys. Ik ben zeer vereerd dat deze experts uit verschillende vakgebieden bereid zijn geweest het werk in uit mijn thesis te lezen en beoordelen.

The Boys, mijn paranimfen. Branko, wat te gek dat we samen zijn begonnen bij NICHE en een geluk dat we het zo goed konden vinden zodat we ons lief en leed van de afgelopen jaren konden delen. Naast de inhoudelijke sessie met vaak het thema "Ehhh… wat meten we nou eigenlijk?" heb je vele werksfeer verhogende side-experiments geïnitieerd zoals "Who knows the real Branko?". Vincent, jij was een zeer welkome toevoeging, we konden nu ook de experimenten voor 2+ personen uitvoeren. En de twee deling had nu drie mogelijkheden, wat zorgde voor een interessante dynamiek waar we makkelijk een heel proefschrift aan zouden kunnen wijden. En tja jongens, ik blijf bij mijn besluit dat ik jullie allebei evenveel smiley punten moet geven (uitgekeerd in 17 pepernoten), want een betere combinatie aan kamergenoten tijdens de PhD periode had ik me niet kunnen wensen.

Oud-nichers, het zijn er inmiddels zo veel! De geweldige sfeer heeft er voor gezorgd dat ik met veel plezier in het lab heb gewerkt. Nieuwe mensen worden warm opgenomen, iedereen helpt elkaar en er is altijd ruimte voor samenwerkingen en het opzetten van nieuwe projecten. Zo was ik overweldigd dat het hele lab zich zo enthousiast heeft ingezet voor het creativiteitsproject, zonder jullie inzet (als subjecten en testleiders) hadden we dit niet kunnen doen. Juliette, de harde kern van NICHE, zonder data geen onderzoek en dat ook nog eens gebruiksvriendelijk toegankelijk. Het lab was niet zo ver geweest zonder jou. Sarai, zo leuk om een enthousiast berichtje van je te krijgen dat je een nieuwe plek hebt gevonden. Ik moet altijd onwijs lachen om je humor en heb veel respect voor hoe je je weg hebt gevonden in wat je wil. Heel veel succes met je carrière als psycholoog. Patrick, je hebt ons van af het begin flink uitgedaagd goed methodologisch sterk onderbouwd onderzoek te doen. Je altijd enthousiaste en tegelijkertijd kritische houding zorgde voor vele discussie waarbij je vanaf het

thesis_LW_V3.indb 218 06/06/16 07:38

begin ons het gevoel gaf als volwaardige onderzoekers mee te draaien. Veel succes op de UU! Anneke, we hebben zulke leuke gesprekken gehad over wetenschap in de psychiatrie, ik hoop dan ook dat je een plek vindt waar je goeie ideeën terecht komen. Janna, queen of ICA, jouw denksnelheid lijkt soms met lichtjaren voorbij te schieten, dat dat er ook nog eens zo snel uit komt is helemaal indrukwekkend. Bedankt voor de leuke discussies. Sanne de Wit, tof dat we samen een prachtig paper hebben neergezet. Ik ben onder de indruk van hoe jij je voor deze patiënten groep hebt ingezet en je vernieuwende kijk op hoe we onderzoek naar deze groep moeten benaderen. Lizanne, and yet we meet again! Toen je me mailde of ik een plek wist waar je buitenland ervaring op kon doen, wilde ik niets liever dan dat je naar San Diego kwam. En dat heb je gedaan, te gek! Heel veel succes met je volgende buitenland avontuur. Fenny, ook onze paden kruisten weer in San Diego, zo leuk en een onvergetelijke laatste weekend in Californië. Annemieke, jouw keuze om op deze manier een waardevolle bijdrage te leven aan de wetenschap is bewonderenswaardig. Ik hoop dan ook dat je stuk goed terecht komt. Susanne, door jou is het creativiteitsproject zo succesvol verlopen. Je hebt in één stage een heel onderzoek gestart en afgerond, ik had me geen betere stagiaire kunnen wensen. Ik weet zeker dat je een net zo goeie PhD neer gaat zetten. Marieke vd P., ik wist niet dat meedoen aan een quiz en onverhoopt voetbal kijken in de VIP ruimte zo bonding kon zijn. Wat een lol. De vele andere ex-nicher's en stagiaires, Sanne-2, Sanne-3, Alyssia, Hanne, Diana, Julia, Aleks, Michiel, Iris en Laura, Anouk en nog velen onwijs bedankt voor jullie inzet en de gezellige koffie momentjes.

Nichers van nu, Dienke, wat wisselen wij elkaar mooi af het laatste jaar, zo kunnen we samen een werkplek delen. Heel veel plezier in New York, te gek dat je dat doet met je hele gezin. Devon, how wonderful to have a little bit of US in my current room everyday. Its great to have you in the lab and share opinions on scientific and world-wide issues. Chantal, snorkelen & kona brewery, wat een onvergetelijke trip. Heel veel succes met je PhD! Sara, you go on where others stop (including me) in working out the details so important for science. Thank you for starting the FreeSurfer journey with me, i'll never forget the hours of rating brainy-details. Yvonne, dank voor al je hulp bij de dataverzameling, stoer dat je nu deels als zelfstandige werkt veel succes! Tabitha, zo gezellig om jou in het lab te hebben gehad! Veel succes in het WKZ. Miriam, jeej nog een Amsterdammer erbij. Wat een gezelligheid, veel succes met je phd. Caitlin, wat een leuke nieuwe phd aanwinst. Heel veel succes! Dorinde, yes nog een PhDer

thesis_LW_V3.indb 219 06/06/16 07:38

erbij die je liever niet wil laten gaan. Veel plezier in het lab! En ook Anna, Lieke, Irina en Nina en de anderen, bedankt voor jullie werk, lekkere taarten en de gezelligheid.

Dank aan het Dutch Connectome Lab voor de leuke samenwerking. Marcel, zonder jouw werk had ik de mooie netwerk studies niet kunnen doen, dank voor je tijd en werk en de gezellige borrels op de summerschool. Guusje, wat leuk dat we elkaar sinds kort beter leren kennen nu we een kamer delen. Onwijs knap hoe je je wetenschappelijke en klinische carrière combineert. Veel succes! Ook bedankt Ruben, Lianne en Siemon voor de leuke samenwerking.

Ik wil ook graag de andere collega's in het Brain Center Rudolf Magnus en de afdeling psychiatrie bedanken voor inspirerende gesprekken en leuke tijden op congressen en summer schools. In het bijzonder Neeltje, Christiaan, Bas, Matthijs, Rachel, Yumas, Pascal, Marinka, Mireille, Lucija, Annabel, Thalia, Marc, Martijn, Sanne, Mitzy, Lieke, Sven, Florian, Merel, Manabu en Araija. En veel dank aan alle co-authors voor hun bijdrage Prof dr René Kahn, dr. Tim Ziermans, dr. Patricia Schothorst and dr. René Mandel.

And many thanks to my coworkers at UCSD for sharing their scientific expertise, in particular I would like to thank Prof dr. Terry Jernigan, for her scientific insights and efforts, Prof dr. Judd, for giving me this opportunity, Paula, for all help and assistance, Wes and Chase, for their methodological contributions to our work, Hauke, for making data sharing easy, Kuperman for the best coffee at campus, Tim, my dear friend in science and beyond, many thanks for introducing me to UCSD, San Diego and the unforgetable trip to Arizona (that we barely survived). And off course not to forget your dear wife, Robin, keep on surfing, dudette! Also many thanks to Prof Susan Taper and her lab, for the great meetings and sharing your lab spirit at the San Diego breweries, thank you all for your help Ty, Sonja, Abigail, Alejandro, Alyssa, Claudia, Nadia, Norma, Slivia, Tam, Ashley, Erica and Taylor and many others.

Veel dank aan mijn vrienden, die er altijd voor me zijn waar ik ook ben. L'en, ladies zo fijn dat jullie in mijn leven zijn. Lau, ik ben zo blij met mijn tijd bij jou in je huisje en jouw tijd bij mij in San Diego. We hebben dit toch maar even allebei gedaan, trots op ons! Liz, voor de hoognodige ontspanning bij jouw yoga lesjes, de zondag middag koffie sessies of vrijdag avond in de Brandon. Ik vind je onwijs dapper, veel plezier met jouw nieuwe carrière pad. Lenn, ongelofelijk hoe erg ik jou miste in San Diego en blij dat ik je nu weer vaak kan zien. Je bent de meest optimistische doorzetter die ik ken. Geweldig dat je je droom nu waar gaat maken, terug

thesis_LW_V3.indb 220 06/06/16 07:38

het studenten leven in. Eva, jij weet altijd precies de goede dingen te zeggen, veel succes en plezier met weer terug gaan naar het lab. Kim, erlenmeyertje, mijn eerste lab-ervaring was met jou. Wat een lol hadden we toen en vaak nog steeds. Dank voor alle onvergetelijke avonturen in de afgelopen 10 jaar. Evelien, we hebben zo veel reisjes samen gemaakt, met de Wicked Van naar zuid Frankrijk of een road trip naar Palm Springs, wat een heerlijke tijden, en altijd vol grappen en goeie raad, dit jaar veel onwijs fijne zomerse avonturen in Amsterdam. Shanna, dank voor je inzichten op alle levels in het leven het is altijd heerlijk om je over je avonturen te spreken. Nienke, way back in groningen was er eens een restaurant… Fijn dat je daar nu weer woont en ik altijd langs kan komen, bedankt dat je er was tijdens de aller laatste dagen van het afronden van mijn proefschrift. We hebben het op een onvergetelijke manier gevierd. Charlotte, my san Diego girl, onbeschrijfelijk hoe fijn het was dat ik jou daar ben tegengekomen. Heel veel succes met je laatste fase, we gaan het snel vieren in Leuven en/of Amsterdam. Annemarie, wat heerlijk om een Nederlandse bekende in San Diego te hebben en samen te lachen om de Amerikaanse gewoontes zoals moeder-dochter uitjes naar de schietbaan(?!?). En ook Jake, many thanks for beach bbq's and beer tasting. Roemer, wat tof om het San Diego avontuur met jou te delen, surfen bij sunset, midnight cheese cake en exploding kittens. Heel veel plezier de komende tijd daar en ik hoop dat jullie Amsterdam overwegen als je terug komt. Anouk, wat een fun met de gang te volleyballen en SD en LA te verkennen in de weekenden. Heel veel succes met je Post Doc en geniet van je tijd daar.

En ook mijn familie, Mam je bent de sterkste en dapperste vrouw die ik ken, bedankt dat je er altijd voor me bent. Pap, dank voor je enthousiasme over alles wat ik doe. Opa, voor de onvoorwaardelijke steun. Oma, voor de gezellige rummikub sessies. Bert, voor je support. Matthijs, dapper broertje van mij, binnenkort ga jij op avontuur! Heel veel plezier geniet er van. Mads en David wat een vrolijke familie uitbereidingen zijn jullie, mede dankzij Elke, Mirko, Tobias, Marianne. En Job bedankt voor de onvergetelijke dias de los muertos. Succes met je cycling antipodes avontuur.

En tot slot Midas, jij ziet een wereld vol mogelijkheden. Je reageert altijd enthousiast op de plannen die ik heb, ook al betekend dat dat wij elkaar een tijd niet zien. Je bent een enorme steun in het realizeren van mijn dromen. Bedankt dat je op me hebt gewacht.

thesis_LW_V3.indb 221 06/06/16 07:38

LIST OF PUBLICATIONS

thesis_LW_V3.indb 223 06/06/16 07:38

List of publications

This Thesis

Wierenga, L.M., Langen, M., Oranje, B., and Durston, S.

Unique developmental trajectories of cortical thickness and surface area.

NeuroImage 87C, 120–126 (2014)

Wierenga, L.M., Langen, M., Oranje, B., Ambrosino, S., van Dijk, S., and Durston, S., Typical development of basal ganglia, hippocampus, amygdala and cerebellum from age 7 to 24.

NeuroImage 96, 67–72 (2014)

Wierenga, L.M., M.P. vd Heuvel, and Durston, S.

The Development of Brain Network Architecture.

Human Brain Mapping 37(2), 717-729 (2015)

Wierenga, L.M*., de Wit, S.*, Oranje B., Schothorst P.F., Ziermans T.B., Kahn R.S., Durston S. (*authors contributed equally)

Brain development in adolescents initially at ultra-high risk for psychosis: longitudinal changes related to resilience.

NeuroImage Clinical (in press)

Ambrosino, S., de Zeeuw, P., **Wierenga, L.M.**, Sarai van Dijk, and Durston, S.

Cortical Development in Attention-Deficit/Hyperactivity Disorder: What does it teach us about Early Developmental Mechanisms? (submitted)

Bookchapter

Wierenga, L.M., Oranje, B., Durston, S.

Brain and behavioral development Part VIII: Post natal brain development.

The Cambridge Encyclopedia of Child Development, Hopkins, J.B. (ed) Cambridge, U.K.: Cambridge University Press. (in press)

thesis_LW_V3.indb 224 06/06/16 07:38

Other

Wierenga, L.M., Mensen, V.T., van Dijk, S., Rijks, Y., Oranje, B., Mandel, R., Durston, S., Longitudinal development of cortical thickness and surface area in autism spectrum disorder. (submitted)

Wierenga, L.M., vd Heuvel, M.P., Oranje, B., Giedd, J.N., Durston S., Brown, T.T., Jernigan, T. Longitudinal changes in brain network architecture in 4-13 year old children. (in prep)

thesis_LW_V3.indb 225 06/06/16 07:38

ABOUT THE AUTHOR

Lara Marise Wierenga was born on May 10th 1986 in Groningen, the Netherlands. She graduated highschool in 2004 at the HN Werkmancollege in Groningen. She moved to Amsterdam in 2005 to start the bachelor program Psychobiology at the University of Amsterdam. She graduated in 2008 whereafter she joined the research master program Cognitive Neuropsychology at the VU University in Amsterdam. She graduated this master program cum laude with a functional MRI study on neuropsychological reward related instrumental learning in Attention deficit/Hyperactivity disorder. After graduation she worked as a research assistant at the Curium-LUMC in Leiden, where she was invovled in a research project focusing on neuropsychological factors in relation to treatment success in male juvenile offenders. In 2011 she joined the NICHE lab, where she started her PhD project on typical brain development with Prof. dr. Sarah Durston, dr. Marieke Langen en dr. Bob Oranje. Since 2014 she continued her PhD project at the University of California in San Diego supervised by Prof. dr. Jay Giedd and in close collaboration with Prof. dr. Terry Jernigan. Lara will continue her work on typical brain development as a post doctoral-researcher in collaboration with both the UMC Utrecht and UCSD.

thesis_LW_V3.indb 226 06/06/16 07:38